LIFE-EXTENSION OF RC STRUCTURE BY CATHODIC PROTECTION USING ZINC SACRIFICIAL ANODE EMBEDDED IN CONCRETE

ラフディナル, ラーミタ サリ

https://doi.org/10.15017/1785399

出版情報：九州大学, 2016, 博士（工学）, 課程博士
バージョン：
権利関係：全文ファイル公表済

LIFE-EXTENSION OF RC STRUCTURE BY CATHODIC PROTECTION USING ZINC SACRIFICIAL ANODE EMBEDDED IN CONCRETE

コンクリート中に埋設された亜鉛犠牲陽極方式の電気防食による
RC 構造物の長寿命化

RAHMITA SARI RAFDINAL

LIFE-EXTENSION OF RC STRUCTURE BY CATHODIC PROTECTION USING ZINC SACRIFICIAL ANODE EMBEDDED IN CONCRETE

A DISSERTATION

Submitted to
Kyushu University
in partial fulfillment of the requirements
for the degree of
Doctor of Engineering

by

RAHMITA SARI RAFDINAL

DEPARTMENT OF CIVIL AND STRUCTURAL ENGINEERING
GRADUATE SCHOOL OF ENGINEERING
KYUSHU UNIVERSITY
Fukuoka, Japan
August, 2016

ACKNOWLEDGEMENTS

After an intensive period of three years, today is the day: writing this note of thanks is the finishing touch on my dissertation. It has been a period of intense learning for me, not only in the scientific arena, but also on a personal level. Writing this dissertation has had a big impact on me. I would like to reflect on the people who have supported and helped me so much throughout this period.

I would like to express my special appreciation and sincere gratitude to my supervisor Prof. Hidenori HAMADA, for his patience, motivation, enthusiasm, endless encouragement, immense knowledge and guide throughout my three years of research. He always been available to advise me even he is busy with his daily routine work, make him a great mentor. He inspired me about the art of research in long-term performance. Thank you for your kindness and for accepting me three years ago to experience your extensive knowledge in Concrete Engineering.

My thousands of appreciation also goes to Advisory Committee, Prof. Shinichi HINO and Prof. Koji TAKEWAKA for their precious suggestions and insightful comments with regard to improve this research work. Thank you also for letting my defense be a memorable moment.

I would also like to address my thanks to Assoc. Prof. Yasutaka SAGAWA for his worth guidance and valuable advices during my research and writing of this dissertation. Thank you for taking me and laboratory members to the site visit and sit together during JCI preparation. It may look like small but your humble attitude despite your great knowledge in Concrete Engineering really impressed me.

My thankful also goes to Mr. Daisuke YAMAMOTO for his tremendous help, precious friendship during my study and his non-stop help throughout my experimental work. His wonderful skills really lighten the arising problem.

My special gratitude also is dedicated to the Ministry of Education, Culture, Sports, Science and Technology (MEXT) of Japan for providing financial study assistance during my doctoral program in Japan. My grateful acknowledgement

also to Denki Kagaku Kogyo Kabushiki Kaisha (DENKA) for their support by providing the zinc sacrificial anodes in this research.

My appreciation and thank also extends to present and past members of Concrete Engineering Lab for helping me through thick and thin time. Thank you for working together during specimen preparations. Thank you for the memorable technical site visit and laboratory party, great work environment and fun chat. My thankful also goes to Takaya HIGUCHI who actively supported this research.

I would also like to take this opportunity to express the profound gratitude from my deep heart to my beloved husband, my lovely daughter, my beloved mother and father, parent-in-law, my brothers and sisters, and brother-in-law, for their love, wise counsel and sympathetic ear, patience and continuous support during my study in Japan. All of you always there for me.

Finally, there are my friends. We were not only able to support each other by deliberating over our problems and findings, but also happily by talking about things other than just our papers.

Thank you very much, everyone!

Rahmita Sari Rafdinal

Fukuoka, August, 2016.

Specially dedicated to

Rafdinal Ramadhani & Rita Almoenir

Muhamad Budi Saputra

Aisha Hikari Putri

for

the prayers, patience, support, sacrifice, tears and laughter

ABSTRACT

With the aim of restoring the safety and serviceability of reinforced concrete (RC) structures damaged by concrete degradation or steel corrosion, as well as to ensure a reasonable residual service life of such structures, maintenance or repair interventions are necessary. Such repair strategies may include conventional patch repairs and electrochemical treatments. In order to create a protective current flow from patch repair to parent concrete, using a sacrificial anode or galvanic system with zinc as its main material is one advanced repair technology in electrochemical techniques applied to controlling the corrosion of steel.

From the standpoint of performance and durability issues of anodes in patch repair concrete, it is important to evaluate the service life of the zinc anode in its ability to protect steel bars from corrosion damage in order to increase the service life of RC structures as well. However, two points are still unclear: the anode's ability to achieve cathodic protection over a usable distance (throwing power distance) under realistic service conditions, as well as the number of anodes needed to achieve protective levels. Anode life and protective current delivery operating on the boundary of partially-repaired concrete are also unanswered questions. Related to the cathodic protection (CP) system with sacrificial anodes embedded in concrete, some issues were addressed in this study in order to observe the durability and effectiveness of zinc sacrificial anodes to enhance the life-span of RC structures. This dissertation consists of nine chapters.

Chapter 1 explains the background of this study, the problem statement, as well as the significance and contributions of this research. At first, field surveys and experiments were conducted as a preliminary study to observe the conditions of RC structure deterioration after long-term exposure to tropical marine conditions before being repaired by cathodic protection. In evaluating

zinc sacrificial anode utilization to repair RC structures, the most effective length of anodic throwing power under non-homogenous environmental conditions between patch repair concrete and parent concrete were measured. Steel surface conditions (rusted and non-rusted) when applying anodes in patch repair concrete, ambient temperature effects and the service life of anodes were also investigated. Here, the durability and efficacy of zinc sacrificial anodes to protect deteriorated RC beams after long-term exposure were evaluated, offering new contributions in conclusion.

Chapter 2 reviews previous studies on the deterioration of RC structures and the utilization of sacrificial anodes as protection against the corrosion of steel in concrete. Some factors affecting the durability of concrete and sacrificial anodes were clarified. The issues to be addressed in this study were also discussed.

Chapter 3 investigates the deterioration condition of one 77-year-old RC structure, namely an Indonesian port, exposed to severe marine conditions. Field surveys and experimental research by destructive and non-destructive methods were conducted to evaluate the long-term performance of this Indonesian port. Repair strategies for extending the service life of this structure are also presented in this study. The inspection results showed that this Indonesian port's structure, which was exposed to a tropical marine environment over a long period of time, led to serious damage conditions by chloride-induced corrosion. The main damage included broad delamination, spalling, cracking and loss of cross-section of steel reinforcement. The use of a cathodic protection (CP) system as an immediate reactive repair method was proposed as a sustainable long-term remedial option.

Chapter 4 discusses how to identify the effective length of an embedded steel element on partially-repaired concrete protected by sacrificial anodes against macro-cell corrosion in a non-homogeneous chloride environment. Zinc sacrificial anodes were applied to steel bars embedded in patch repair concrete

(non-chloride contamination) in order to deliver protective currents to corroding steel in the parent concrete (with chloride contamination). Based on the criterion of 100 mV CP, zinc sacrificial anode cathodic protection could protect the steel bar at a distance of between 300 mm to 400 mm from the anode's position in the patch repair concrete to the parent concrete with 4 kg/m^3 of chloride content at 350 days of polarization time. Meanwhile, for 10 kg/m^3 chloride content in existing concrete, the applied anode was effective in protecting the steel bar at a distance of up to 260 mm from the patch repair concrete to parent concrete. This means that, for up to one year of exposure time, the higher the chloride content in the existing concrete, the shorter the effective length. Meanwhile, after 2 years of exposure time, commercially available sacrificial anodes are still powerful enough to protect the corroding steel at a distance of up to 260 mm from the anode in the patch repair concrete to the parent concrete.

Chapter 5 presents the effects of steel surface conditions (rusted and non-rusted) on the performance of a zinc sacrificial anode when applied to patch repair concrete (non-chloride contamination). In addition, a study was carried out on how environmental conditions affect the durability of anodes when installed on rusted and non-rusted steel bars. The results of this study show that the protective current of the anode became more active in humid conditions than in dry conditions, due to the high moisture content inside the concrete. Based on the "100 mV decay" CP criterion, protective conditions were achieved on the steel bars connected to a zinc anode with "non-rusted" as an initial condition. Rust on steel surfaces decreases the efficacy of cathodic protection, even if it's embedded in chloride-free concrete, because the rust on the steel bar impedes the current flow from the anode to the steel bar when a zinc anode is applied on it. In conclusion, to protect corroded steel bars in existing concrete (with chloride contamination), a non-rusted rebar condition in the repair concrete (non-chloride contamination) is the most desirable initial condition when a zinc anode is applied.

Chapter 6 investigates the performance of zinc sacrificial anodes to protect steel bars embedded in concrete (chloride and non-chloride contamination) from corrosion under two extreme ambient conditions, namely, freezing temperatures (-17°C, RH 4-5%) and extreme heat (40°C, RH 96-99%). With respect to the protective current density under exposure to high temperatures and after take-out from a hot chamber, it was shown that anodes produce higher levels of current in hot or humid environments, compared to dry and low-temperature conditions. Moreover, anodes age faster in high temperatures than in freezing conditions. It was found that, the higher chloride content in concrete, the higher the possibility of corrosion occurring on steel bars without CP protection which are exposed to freezing temperatures as well as heat. It can be concluded that using anodes in environments of high chloride content with exposure to heat and high humidity is ineffective.

Chapter 7 presents an estimate of the service life of zinc sacrificial anodes (in a short amount of time) by accelerating the current 10 (ten) times higher than initial current of the anode during a polarization time of 70 days. It was possible to predict over 100 years of the service life of zinc sacrificial anodes exposed to air curing conditions at a constant room temperature. By increasing the current demand by 10 times, the service life of anodes is reduced 10 times after 70 days of exposure. This means that the higher the current delivery function of the anode, the shorter the service life becomes. All in all, the current acceleration method enabled us to successfully observe anodic service life in a short time.

Chapter 8 presents the application of zinc sacrificial anodes to repair 40-year old deteriorated RC beams. Two types of deteriorated RC beams, notably the S-type (150x300x2400 mm) and the L-type (200x300x2400 mm), were evaluated in this study. One anode was applied to patch repair concrete in a S-type beam and embedded in the middle of the tensile bar of the beam. Meanwhile, three anodes were attached to a one-tensile bar of a L-type beam in patch repair concrete at a distance of 200 mm from each other. Polymer concrete was cast in

the patch repair area. The test results demonstrate that anodes embedded in S-type and L-type beams fulfill the current criteria needed to protect the steel bar from corrosion, 0.2 to 2 $\mu A/cm^2$. However, due to the high resistance in repair concrete, a trans-passive region occurs on the interfacial zone between the patch repair concrete and parent concrete. With respect to the potential value and conditions on the boundary, it was observed that there was no protection at all in the non-repaired section. This coincides with the depolarization test result. Based on the "100 mV decay" CP criterion in the depolarization test, it was found that applying three anodes at intervals of 200 mm in patch repair concrete is sufficient to polarize one steel bar in the patch repair section only to the protection level. This means that while the life-extension of existing structures is enhanced by increasing the number of anodes embedded in repair concrete and polymer concrete, casting them in repair sections when anodes are applied inside is less effective.

Chapter 9 offers conclusions and recommendations for future research work.

TABLE OF CONTENTS

LIST OF TABLES

LIST OF FIGURES

LIST OF PHOTOS

Chapter 1 GENERAL INTRODUCTION

1.1 Background of Study

Reinforced concrete (RC) is nowadays present in a large part of the infrastructure all over the world. The high compressive strength of concrete combined with the tensile properties of steel makes it a competitive and versatile material suitable for a multitude of applications. Existing structures made of RC include, for instance, bridges, tunnels, harbors, wharfs, dams or off-shore platforms, as well as a wide range of buildings. It is precisely due to this broad variety of applications that reinforced concrete structures are often exposed to extremely severe conditions, e.g., marine environment, freeze-thaw cycles, carbon dioxide, chemical and biological attack, etc.

Corrosion, due to chlorides in sea water and in most of the de-icing salts used to remove ice and snow from the roads, is today regarded as one of the biggest problems affecting the durability of RC structures [1.1]. Corrosion of reinforcing steel is avoided in the first place because it entails the appearance of surface cracks and rust stains giving a bad aesthetic impression. However, if corrosion proceeds, it may lead to a serious loss of the local cross-sectional area of the reinforcing bars and a reduction of the bond between the concrete and the steel, both of which affect the structural behavior of the RC element and which may eventually compromise the stability and safety of the structure. During the last century a number of structural failures have occurred the causes of which have been mainly attributed to corrosion problems [1.2]. And it makes the corrosion of embedded steel in reinforced concrete has become a major problem world-wide and the leading cause of

deterioration in concrete.

Reinforced concrete (RC) structures damaged by concrete degradation or steel corrosion need maintenance or repair interventions aimed at restoring the safety and serviceability of the structure to the required performance level and, in the meantime, providing a reasonable residual service life of structure[1.3]. The repair strategies may include conventional patch repair and electrochemical treatment. One of famous electrochemical techniques applied for controlling corrosion of steel in concrete is by cathodic protection system.

Cathodic protection (CP) is rapidly being accepted as a repair option for steel-reinforced concrete structures deteriorated by steel corrosion caused by chlorides [1.4]. CP has been one of the essential components of the repair and maintenance strategy for RC structures [1.5]. This technique requires the permanent application of a small direct current to protect the steel [1.6]. Since the original adoption of this technology, there have been a number of advances. One of these is sacrificial anode cathodic protection.

Galvanic anodes made of zinc as one of main material of sacrificial anode has some beneficial features such as simple to install, no power supply needed, no wiring or conduit, suitable for all rebar size, quality of patch repair material is not compromised, performance can be easily monitored and no long-term maintenance. However, the anode ability to achieve cathodic protection over a usable distance (throwing power distance) under realistic service conditions and as function of the number of anodes needed are still unclear. Service life of anode and protective current delivery function on the boundary of partially-repair concrete are also indistinct.

Among the challenges that are still to be taken up in CP system embedded in concrete, therefore some issues were address in this study in order to observe durability and effectiveness of zinc sacrificial anode to increase life-extension of RC structure.

1.2 Problem Statement

Small galvanic anodes (“point anode”) are available commercially for casting in

patch repairs, for the intended purposes of forestalling the halo damage effect which normally occurs between patch repair concrete and parent concrete [1.7]. The anodes usually consist of a zinc alloy piece with steel connecting wires, and embedded in mortar disk. Electronic connection to the rebar is necessary for these anodes to work, and it is made by tying the wires to the rebar in the patch. The mortar around zinc alloy is formulated to obtain high pore water pH, increase water retention, or otherwise promote a regime where the formation of a passive film on the alloy is hindered and the alloys stays in an active condition. The mortar may also engineered to mitigate the effect of expansive anode corrosion products.

Point anodes as described above were the subject of development work and commercial production in Europe and all over the world during previous decade [1.8]. The possibility of large scale applications of anode in infrastructure systems brings up several important performance and durability issues needing resolution.

There was also a need to know how the ability of the anode to provide protective current would be degrade with service time and the total amount of protective charge delivered. It was also unknown over how long the corrosion protection effect may be obtained for a given potential-current function of anode, anode age, and especially the number of anodes needed for a given desired effect could be appraised by the potential user.

In this study, field survey was conducted first to observe deterioration condition of RC structure after long-term exposed to marine severe condition as preliminary study before repair system by cathodic protection applied in realistic condition. Furthermore, from the view point of zinc sacrificial anode utilization to repair the RC structure, protective current throwing from zinc sacrificial anode under non-homogenous environment conditions will be evaluated. Steel surface conditions (rust and non-rusted), temperature effect on exposure of zinc sacrificial anode and anode service life were investigated as well. The effectiveness of zinc sacrificial anode to protect deteriorated RC beam after long-term exposure was evaluated to conclude this study.

1.3 Research Significance

Based on the earlier research background, durability and effectiveness of zinc sacrificial anode to increase life-extension of RC structure is the main issue of this research. By throwing power distance observation under realistic service conditions and as function of the number of anodes needed, it will influences the service life of anode to support remaining service life of structure.

Hence, it is expected an implementation design of zinc sacrificial anode cathodic protection in order to protect the steel bar in partially-repair concrete will be obtained from this study and worthwhile for repair process of infrastructures exposed to severe marine condition.

1.4 Contribution of Research and Novelty

The main objective of this study is therefore to evaluate galvanic point anodes, specifically zinc sacrificial point anodes in order to determine their performance and applicability for repair concrete. Based on the needs indicated in previous section, the present observation focus on durability and effectiveness as two key factors deserving attention.

A. Regarding durability

1. Determination of deterioration grade of RC structure after exposed in long term as a basic diagnosis before beginning repairs by point anode.
2. Determine for selected commercially available point anodes the operating potential/current delivery function, and its dependence on relevant service variables and on service time.
3. Establish anode cumulative capacity (total usable protective current delivered) and associated ultimate service life capability.

B. Regarding effectiveness

1. Assess the anode ability to achieve cathodic protection over a usable distance (throwing power distance) under realistic service conditions and as function of the number of anodes needed, so as establish the means of conducting benefits analyses by potential users.
2. Assess the performance of point anodes to protect deteriorated RC

structure after exposed in long term.

3. Develop an implementation design of sacrificial anode cathodic protection of steel bar in concrete.

Up-to-date, many successful achievements were reported by researchers around the world. However, in Asian cases mainly for tropical countries, very rare information on the use of zinc sacrificial point anode to repair and increase the life extension of RC structure elements after exposed in long term can be gathered. Hopefully by conducting this study, it could provide useful and valuable knowledge for construction technology especially for Asian industry.

1.5 Dissertation Outline

Fig 1.1 shows the structure of dissertation outline which consist of 9 (nine) chapters as follows,

Chapter 1 describes the background of the study, its problem statement and limitation of this study.

Chapter 2 reviews the results of previous studies on deterioration of RC structure and utilization of sacrificial anode as corrosion protection of steel in concrete. Some factors affecting durability of concrete and sacrificial anode were viewed. The issues to be addressed in this study were discussed.

Chapter 3 evaluates deterioration condition of RC structure after 77-year-old exposed to severe marine condition. Field survey and experimental research by destructive and non-destructive methods were conducted to evaluate long-term risk of chloride-induced corrosion on open wharf structure. The limitation of documentary information of structure such as no information about concrete strength, cover depth and outline of structure elements become a challenge and a uniqueness of this study to assess the 77-year-old concrete structure accurately. Repair strategies for extending the service life of this structure are also presented in this study.

Chapter 4 contains experimental work and discussion about durability of sacrificial anode in accordance with effective protected length to embedded steel in

partially-repaired concrete under non-homogenous environment. The results were discussed with regards to corrosion monitoring by polarization of steel bar and anodes.

Chapter 5 evaluates performances of zinc sacrificial point anodes under different initial conditions of steel surface (rusted and non-rusted) in partially-repaired concrete. These steel bars were taken from the specimens exposed in severe chloride environment with high temperature for 20 years. The outcomes were examined associated with corrosion measurement by polarization of steel bar and anodes.

Chapter 6 presents the effect of temperature conditions (freeze, high and normal temperature) during exposure against the operating potential/current delivery function of zinc sacrificial point anodes. The concrete specimens without anode were discussed. Freeze temperature keeps in -17°C with relative humidity (RH) 4-5%, hot temperature stores in 40°C and constant room temperature in 20°C RH 96-99%. In this study, a 20-year-old deteriorated (rusted and non-rusted) as same as in Chapter 5 was used too.

Chapter 7 observes the zinc sacrificial anode service life shortly by current acceleration through the impressed current system. Establish anode cumulative capacity (total usable protective current delivered) and associated ultimate service life capability were discussed.

Chapter 8 assess the anode ability to achieve cathodic protection over a usable distance (throwing power distance) under realistic service conditions and as function of the number of anodes needed to protect deteriorated RC beam after exposed to 40 years. Determination of the state of deterioration of RC beam before anode applied, design, implementation, maintenance and control during protection were discussed.

Chapter 9 concludes the results that obtained from Chapter 3 to Chapter 8. From these conclusions, some future works were recommended.

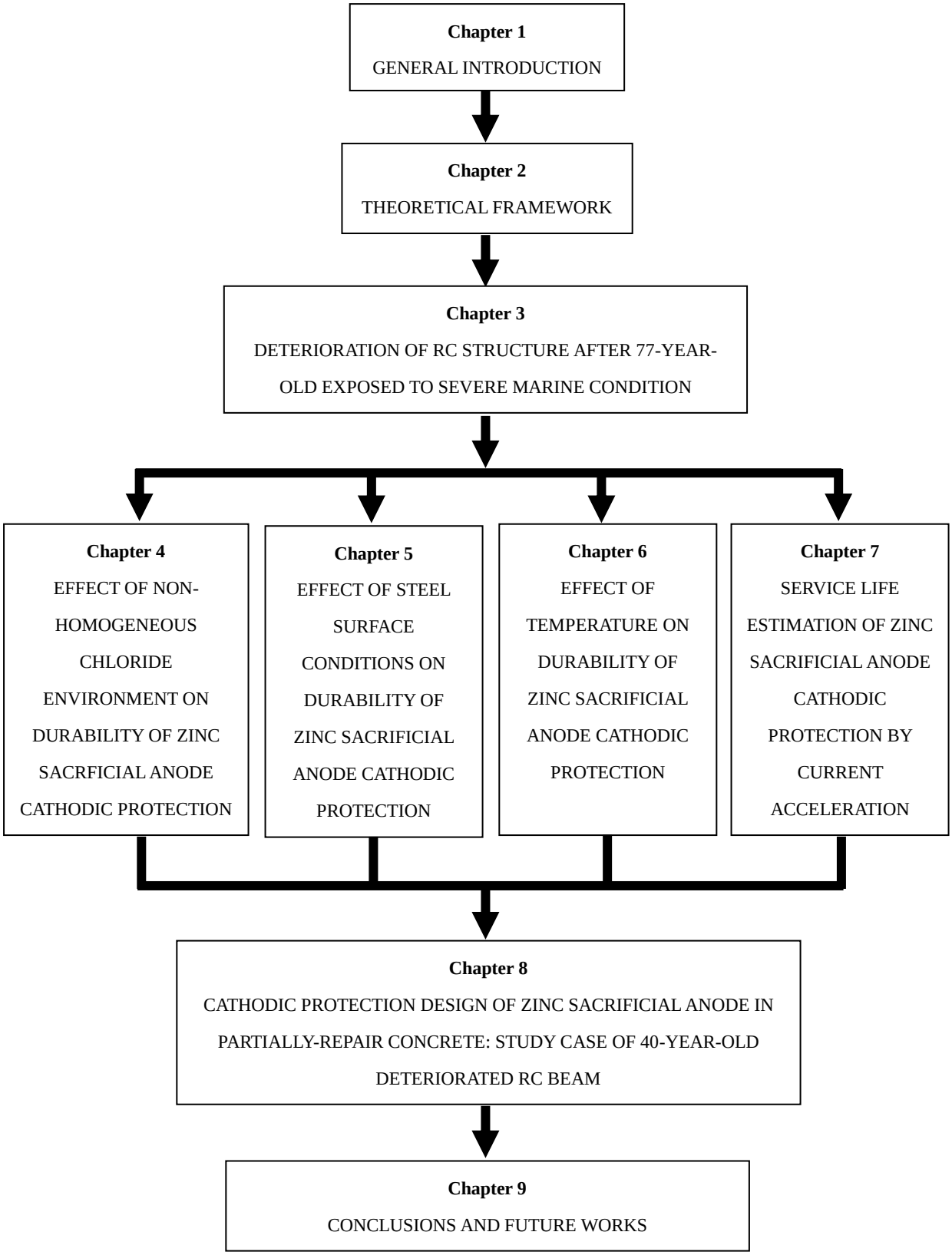

Fig 1.1 Structure of dissertation outline

References

1.1 Hobbs, D., “Concrete deterioration: causes, diagnosis, and minimising risk”. In: International Materials Reviews, 2001, 46.3, pp. 117–144.

1.2 Bertolini, L., Elsener, B., Pedeferri,P., Redaelli, E., and Polder, R., “Corrosion of Steel in Concrete”, 2013, Wiley-VCH Verlag GmBH & Co KGaA.

1.3 RILEM Technical Committee 124-SRC, P. Schiessel (ed), “Draft Recommedation for Repair Strategies for Concrete Structures Damaged by Reinforcement Corrosion”, Materials and Structures, 1994, Vol. 27, pp. 415 – 436.

1.4 Bennet, J., and Turk, T., “Criteria for the Cathodic Protection of Reinforced Concrete Bridge Elements”, Technical Alert, SHRP-S-359, 1994.

1.5 Christodoulou, C., Glass, G. K., Webb, J., Ngala, V., Beamish, S., and Gilbert, P., “ Evaluation of Galvanic Technologies Available for Bridge Structures”, A Report for The UK Highways Agency for Area 9, Sacrificial Anodes in Concrete Repair, Document Reference 9-410414-F-RP-0001, August, 2006, pp. 1-13.

1.6 Pedeferri, P., “Cathodic Protection and Cathodic Prevention”, Construction and Building Materials, 1996, Vol. 10, No. 5, pp. 391-402.

1.7 Bennet, J., and McCord, W., “Performance of Zinc Anodes Used to Extend the Life of Concrete Patch Repairs”, 2006, Corrosion/2006, NACE International, Paper No. 06331.

1.8 Sergi, G., and Page, C., “Sacrificial Anodes for Cathodic Prevention of Reinforcing Steel around Patch Repairs Applied to Chloride-contaminated Concrete”, European Federation of Corrosion Publications, 2001, No. 31, pp. 93-100.

Chapter 2 THEORETICAL FRAMEWORK

2.1 Introduction

In this chapter, several literatures regarding corrosion and deterioration of RC structures are reviewed. Basic information of cathodic protection system is reviewed as well. In addition, the current issues that addressed in this study are discussed in the last section of this chapter.

2.2 Corrosion of Steel in Concrete

In the past, most of the design studies in the literature and research in reinforced concrete assumed that the durability of reinforced concrete structures could be taken for granted. However, many reinforced concrete structures are exposed during their lifetimes to environmental stress (e.g., corrosion and expansive aggregate reactions), which attacks the concrete or steel reinforcement [(2.1), (2.2), (2.3), (2.4), (2.5)]. Corrosion of reinforced steel bars is considered to have been the most famous problem facing structural engineers in the last decade. The corrosion process occurs slowly and propagates with time, so the deterioration rate varies. Corrosion on steel bars affects a structure's safety, which depends on the surrounding environmental conditions that mainly affect the corrosion rate, the location of the member in the building, and the type of the member [(2.6)].

Photo 2.1 shows a clear example of the effect of corrosion on concrete structure deterioration. It shows cracks, spalling and loss of bond between steela and concrete due to corrosions. This reinforced concrete column is a part of structures in Gunkanjima Island, Nagasaki, Japan.

Photo 2.1 Deterioration in a reinforced concrete column

2.3 Passivation or Depassivation

Concrete provides physical resistance to steel reinforcement by acting as a barrier, and chemical corrosion resistance as a result of its high pH. Concrete that is not exposed to any external influences usually exhibits a pH between 12.5 and 13.5 [2.7]. As shown in the Pourbaix diagram (**Fig 2.1**), which defines the range of electrochemical potential and pH for the Fe-H_2O system in an alkaline environment, at potentials and pHs normally found within the concrete, a protective passive layer forms on the surfaces of steel.

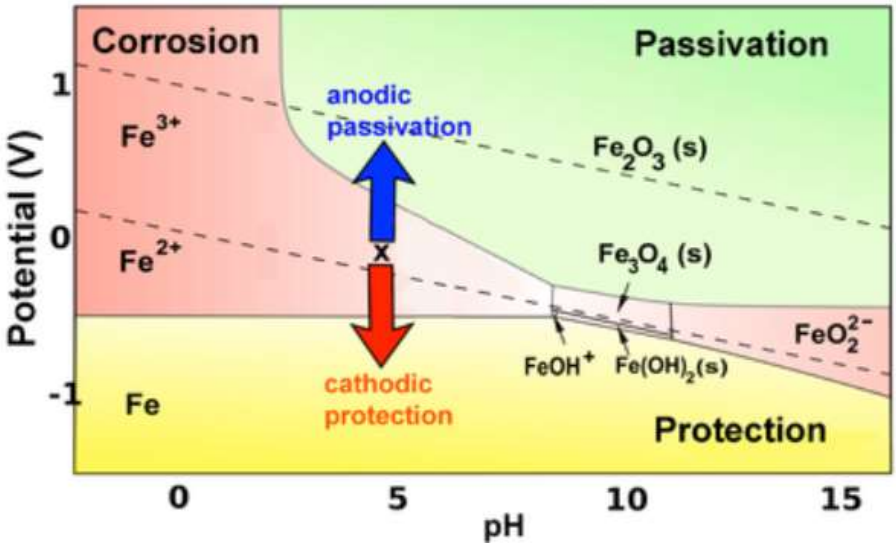

Fig 2.1 Pourbaix diagram for Fe-H_2O at 25°C [2.8]

It is believed that this layer is an ultrathin (<10 nm) protective oxide or hydroxide film that decreases the dissolution rate of steel to negligible levels [2.9]. However the partial or complete loss of the passive layer, known as depassivation, leads to the active corrosion of steel bars. The corrosive products of iron are expansive, and their formation can cause cracking and further deterioration in concrete.

In the yellow part of the diagram in **Fig 2.1**, an active metal such as iron can be protected by a second mechanism, which is to bias so that its potential is below the oxidation potential of the metal. This cathodic protection strategy is most frequently carried out by connecting a more active metal such as Mg or Zn to the iron or steel object (e.g., the hull of a ship, or an underground gas pipeline) that is being protected. The active metal (which must be higher than Fe in the activity series) is also in contact with the solution and slowly corrodes, so it must eventually be replaced. In some cases a battery - the anode of which oxidizes water to oxygen in the solution - is used instead to apply a negative bias.

2.4 The Corrosion Process

After the passive layer is broken down, rust will appear instantly on the steel bar's surface. The chemical reactions are the same in cases of carbonation or of chloride attack. When the corrosion of the reinforced steel bars in concrete occurs, they melt in the void that contains water [2.6]. Corrosion of steel in concrete is an electrochemical process with cathodic and anodic reactions. In the absence of chloride ions and a good quality concrete, the anodic reaction leads to the formation of iron cations as shown in **Eq. (2.1)**:

$$Fe \rightarrow Fe^{2+} + 2e^{-} \qquad (2.1)$$

This reaction is balanced by the cathodic reduction of oxygen, which produces hydroxyl anions according to **Eq. (2.2)**.

$$\frac{1}{2}O_2 + H_2O + 2e^{-} \rightarrow 2OH^{-} \qquad (2.2)$$

The reaction products between anodic and cathodic combine together to build the stability of the passive film on the steel. The stability of this passive film depends on the oxygen availability and the pH value in the interface of

steel/concrete [2.10]. Corrosion start to initiate when the passive film is destroyed due to the presence of chloride ions at the steel-concrete interface.

In the presence of chloride ions, oxygen and water in concrete, they may act as a catalyst by introducing additional anodic reactions are represented in **Eq. (2.3)**.

$$\mathrm{Fe} + 3\mathrm{Cl}^- \rightarrow \mathrm{FeCl_3}^- + 2\mathrm{e}^-$$

followed by $\mathrm{FeCl_3}^- + 2\mathrm{OH}^- \rightarrow \mathrm{Fe(OH)_2} + 3\mathrm{Cl}^-$

or

$$\mathrm{Fe} + 4\mathrm{Cl}^- \rightarrow \mathrm{FeCl_4}^{2-} + 2\mathrm{e}^-$$

followed by $\mathrm{FeCl_4}^- + 2\mathrm{OH}^- \rightarrow \mathrm{Fe(OH)_2} + 4\mathrm{Cl}^-$

or

$$\mathrm{Fe} + 6\mathrm{Cl}^- \rightarrow \mathrm{FeCl_3}^{3-} + 3\mathrm{e}^-$$

followed by $\mathrm{FeCl_3}^{3-} + 2\mathrm{OH}^- \rightarrow \mathrm{Fe(OH)_2} + 6\mathrm{Cl}^-$ (2.3)

These reactions remove ferrous of ferric ions from the steel by forming complex ions with the chlorides then deposited near the anode where they join with hydroxyl ions to form various corrosion products. The chloride ions are released to repeat the process. Secondary reactions may occur due to the expansive products of corrosion. Although the Fe^{2+} and OH^- ions both diffuse into the concrete (from anode to cathode, respectively), the corrosion products form near the anode because the OH^- ions are smaller and more diffuse through the concrete more readily [2.11]. If the supply of oxygen is restricted, ferrous oxides and hydroxides form (**Eq. (2.4**) and **Fig 2.2)**:

$$\mathrm{Fe}^{2+} + 2(\mathrm{OH})^- \rightarrow \mathrm{Fe(OH)_2}$$

or

$$\mathrm{Fe}^{2+} + 2(\mathrm{OH})^- \rightarrow \mathrm{FeO} + \mathrm{H_2O} \quad (2.4)$$

If the oxygen is available, ferric oxides and hydroxides form (**Eq. (2.5)**) [2.11), (2.12)]:

$$2Fe(OH)_2 + \frac{1}{2}O_2 \rightarrow Fe_2 . H_2O + H_2O \quad \text{(red rust)}$$

or $$2Fe(OH)_2 + \frac{1}{2}O_2 + H_2O \rightarrow 2Fe(OH)_3 \quad \text{(red rust)}$$

or $$3Fe(OH)_2 + \frac{1}{2}O_2 \rightarrow Fe_3O_4 + 3H_2O \quad \text{(black rust)}$$

or $$2FeO + \frac{1}{2}O_2 + H_2O \rightarrow Fe_2O_3 . H_2O \quad \text{(red rust)}$$

or $$2FeO + \frac{1}{2}O_2 + 3H_2O \rightarrow 2Fe(OH)_3 \quad \text{(red rust)}$$

or $$3FeO + \frac{1}{2}O_2 \rightarrow Fe_2O_4 \quad \text{(black rust)} \quad (2.5)$$

The preceding chemical reactions show the transformation of steel from ferrous hydroxides ($Fe(OH)_2$), which will react with oxygen and water to produce ferric hydroxides ($Fe(OH)_3$), and the last component, which is the hydrate ferric oxide (rust); its chemical term is $Fe_2O_3.H_2O$. Ferric hydroxide has more effect on concrete deterioration and spalling of concrete cover as its volume will increase the volume of the original steel bars by about two times or more. When iron goes to hydrated ferric oxides in the presence of water, its volume will increase more to reach about 10 times its original volume and will become soft. In this stage, cracks on concrete start until the concrete cover falls; rust, with its brown color, can clearly be seen on the steel bar.

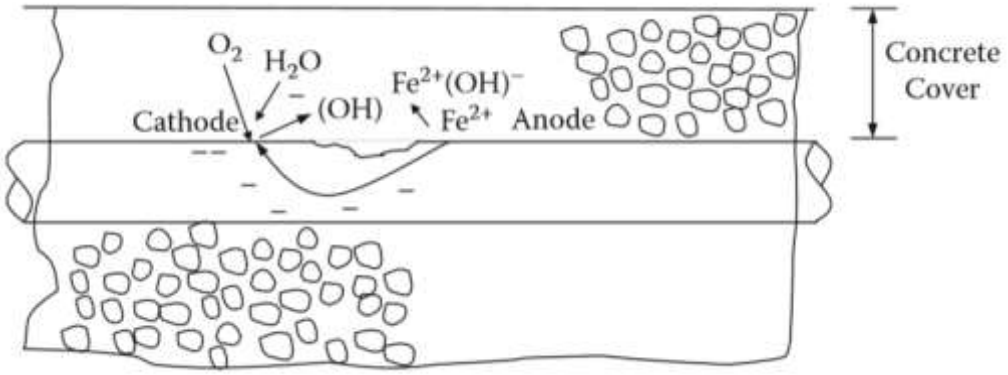

Fig 2.2 Corrosion process on a steel reinforcement surface [2.6]

2.5 Pit Formation

Corrosion in steel bars starts by forming a small pit. After that, the number of pits will increase with time and then the combination of these pits causes a uniform corrosion on the surface of the steel bars. This is obvious in the case of a steel reinforcement exposed to carbonation or chloride effects, as shown in **Fig 2.3**. The pit formation is shown in **Fig 2.4**.

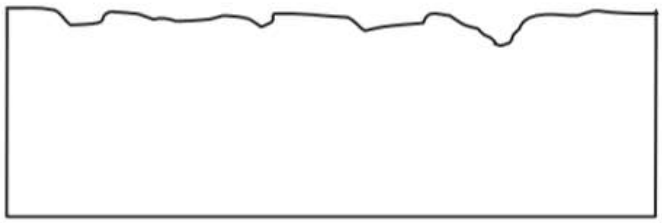

Fig 2.3 Uniform corrosion [2.6]

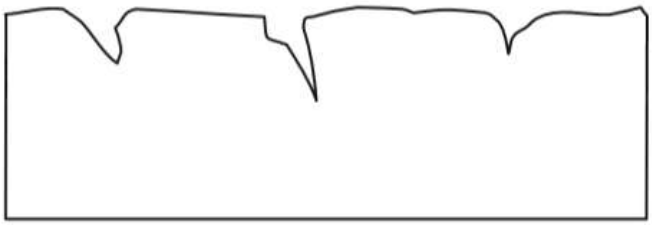

Fig 2.4 Pitting corrosion [2.6]

Many chemical reactions describe the formation of pits and, in some cases, these equations are complicated. But the general principle of pit corrosion is very simple, especially in cases of chloride attacks. In some locations on the steel reinforcement, voids for the cement mortar are present around the steel reinforcement or sulfide is present inside steel bars so that the passive layer is more vulnerable to chloride attack; an electrochemical potential difference attracts chloride ions. Corrosion is initiated and acids are formed as hydrogen from the supplied MnS inclusion in steel and HCl from the chloride ions, if they are present. The following chemical reactions are simple representations of this process:

$$Fe^{2+} + H_2O \Rightarrow FeOH^{+} + H^{+} \quad (2.6)$$

$$MnS + 2H^{+} \Rightarrow H_2S + Mn^{2+} \quad (2.7)$$

Rust may form over the pit, concentrating the acid (H^+) and excluding oxygen so that the iron stays in solution, preventing the formation of a protective oxide layer and accelerating corrosion. We will return to the subject of pitting corrosion later. It is related to the problems of coated reinforcement and to the black rust phenomenon that will be discussed. This corrosion state is characterized by galvanic action between a relatively large area of passive steel acting as cathode and a small anodic pit where the local environment inside the pits has a high chloride concentration and decreased pH value. For pitting to be sustained, it is necessary that a reasonable amount of oxygen should be available to cause polarization of the anode. The average corrosion potential of steel reinforcement has a pitting that is likely to vary between that of the passive state and that of the anodic pitting areas typically in the range of –200 to –500 mV.

2.6 Corrosion Rate

The corrosion process and its shapes have already been described. In this section the corrosion rate of the steel reinforcement will be discussed. The corrosion rate is considered the most important factor in the corrosion process from a structural-safety perspective and in the preparation of the maintenance program for the structure. This factor is considered an economic factor of structural life. When the corrosion rate is very high, the probability of structure failure will increase rapidly and structural safety will be reduced rapidly. The corrosion rate depends on different factors, so if we can control these factors, the corrosion rate will be slow. The corrosion will occur, but it will not cause a serious problem to the structure if the rate is low.

The main factor that affects the corrosion rate is the presence of oxygen, especially in the cathodic zone shown in the previous chemical reactions and in **Fig 2.5**. In a case of no oxygen, the corrosion rate will be slow and different methods are used to prevent the propagation of the oxygen inside the concrete, for example, to take care of the concrete compaction in order to obtain a dense concrete cover so that propagation of the oxygen will be very slow or preventive. Practically speaking, this is an ideal case that cannot happen but that we try to

reach. When we prevent the propagation of oxygen inside the concrete, the oxygen at the steel bars will be less. The difference in volts between anodic and cathodic zones will also be less—an effect on corrosion called "polarization."

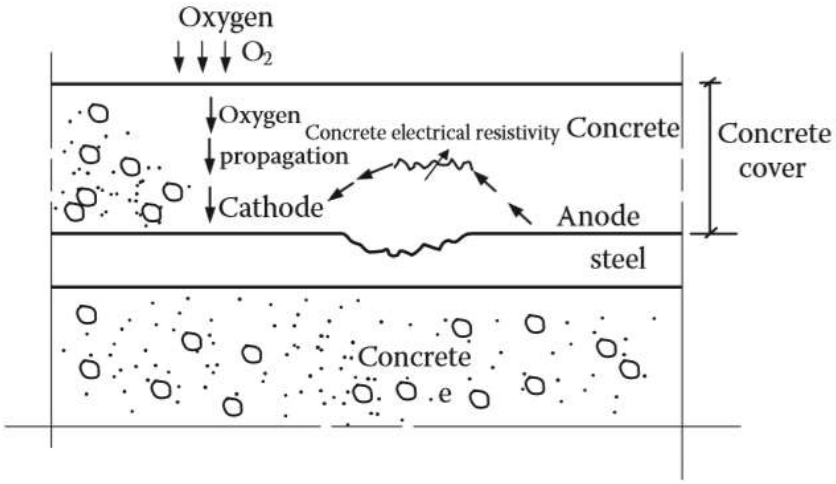

Fig 2.5 Factors affecting corrosion rate [2.6]

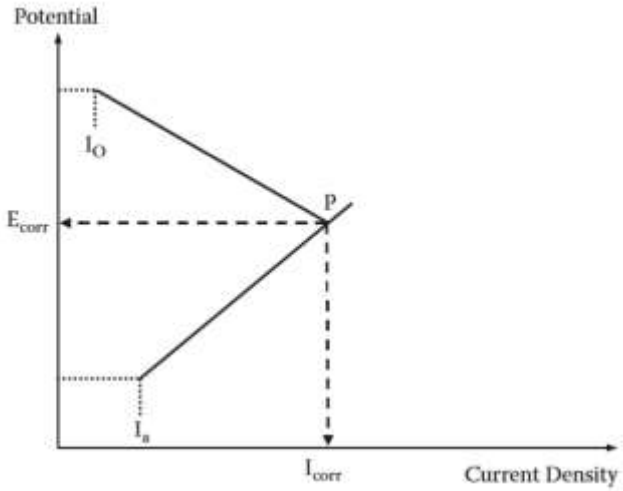

Fig 2.6 Evans diagram for a simple corrosion couple [2.6]

The Evans diagram in **Fig 2.6** shows the polarization curves for separate anodic and cathodic reactions intersecting at point (P), where the mean anodic and cathodic current densities are equal and represent the corrosion rate in terms of a mean corrosion current density, I_{corr}. The electrode potential of the couple at this point is termed the corrosion potential, E_{corr}. The second important factor affecting

the corrosion rate is the moving of the ions inside the concrete voids around the steel reinforcement. If the speed of moving ions is very slight or prevented, the corrosion rate will be very slow also or, in the ideal case, prevented. This case may happen when the concrete around the steel bars has a high resistance to electrical conductivity between anode and cathode.

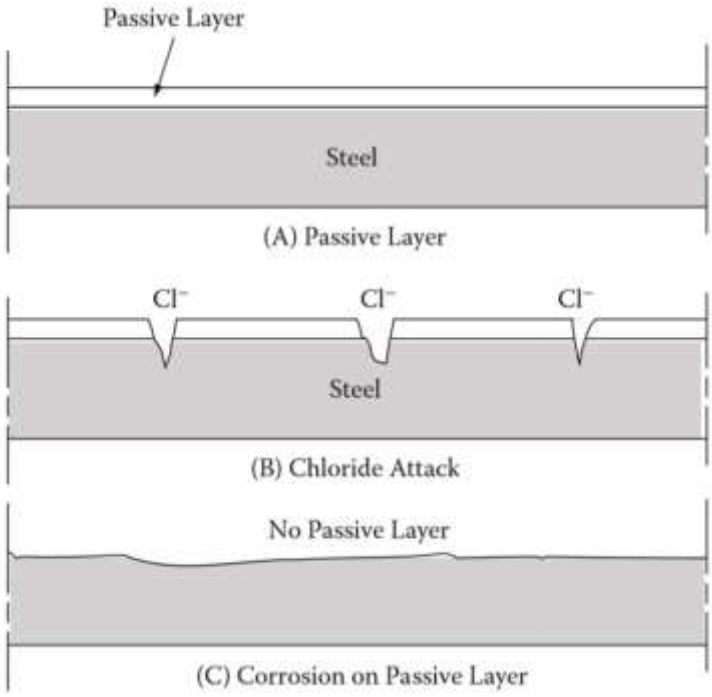

Fig 2.7 Effect of chlorides on demolishing the passive layer [2.6]

The measurement of electrical resisitivity to the concrete surrounding the steel reinforcement can give us an assumption of the corrosion rate and the chemical reaction rate. Another factor can control the corrosion rate because there are different types of metal. One of them is steel reacting with oxygen and forming a layer with 0.01 μm from oxides from the same metal at the surface, if this layer is stable, and protecting it from breaking in any circumstances. The metal is considered protected when it is inside the liquid solution and reduces the melting of ions in the liquid solution surrounding the steel bars so that the corrosion rate will be very slow if this passive layer exists. The corrosion rate will be neglected

and considered zero (shown in **Fig 2.7**). In this case, this layer will be the passive protection layer to the steel reinforcement. The protected passive layer is first responsible for protection from corrosion, and this is obvious in the case of stainless steel. The steel in this case consists of some chromium and nickel and other metals that improve the stability of the protected passive layer. The passive protection layer will be stable if the aqueous solution contains a high quantity of hydroxide ions ($OH^{-)}$. This layer is affected by chloride ions (Cl^{-}) or carbonates reducing the hydroxide in the water solution in the concrete void that will assist in formation of voids and pitting in steel, as shown in **Fig 2.7**. After extensive pitting takes place, they will combine to destroy the passive layer and start the rusting process. In general, the state of corrosion of steel in concrete may be expected to change as a function of time. In attempts to model this time-dependent corrosion behavior, it is convenient to distinguish and understand clearly the following stages:

- During the initiation period, from day 1 of construction until the steel bars have remained passive in the protected layer within the concrete, environmental changes are taking place that may ultimately terminate passivity.
- The corrosion period begins at the moment of depassivation and involves the propagation of corrosion at a significant rate until the third step is reached.
- The final stage is reached when the structure is no longer considered acceptable on grounds of structural integrity, serviceability, or appearance.

2.7 Microcell and Macrocell Corrosion

The corrosion cell may exist as a macrocell or a micro cell [2.12]. The corrosion microcell consists of tiny anodes and cathodes separated by a distance of as small as a micron. The corrosion macrocell consists of anodic and cathodic regions separated by a finite distance of millimeter or meters, as briefly illustrated in **Fig. 2.8**. Corrosion cells, consisting of metallically and electrolytically connected anodes and cathodes, can occur as microcells leading to uniform iron removal

(generalized corrosion) and macrocells causing localized iron removal (pitting corrosion). The detailed definitions are as follows [2.13]:

a) Microcell corrosion, consisting of pairs of immediately adjacent anodes and cathodes, is a type of corrosion in which the anodic reaction is totally supported by the local cathodic reaction;

b) Macrocell corrosion, consisting of spatially isolated anodes and cathodes, is another type of corrosion in which the anodic reaction in the active zone is supported by the cathodic reaction in the passive zone.

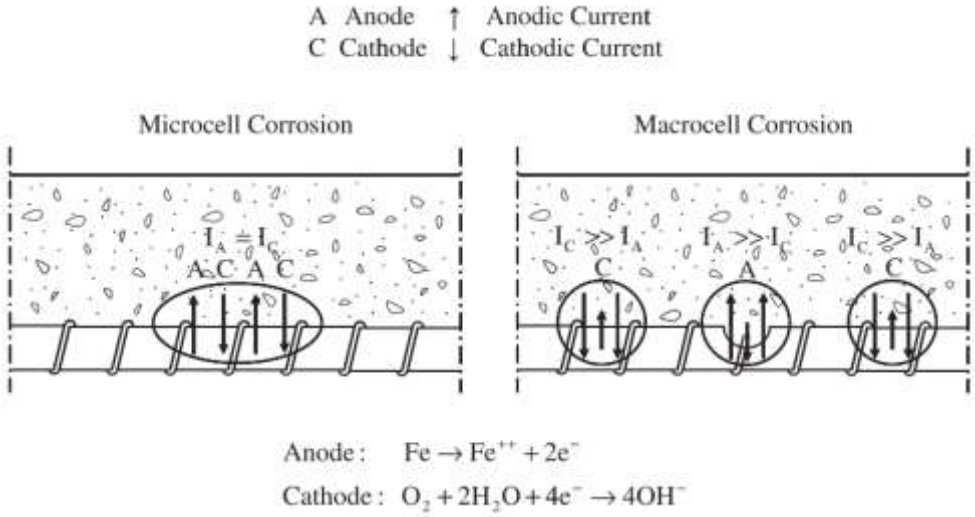

Fig 2.8 Microcell and macrocell corrosion of steel in concrete [2.13]

Macrocell corrosion occurs when an electric current runs through an active and a passive area of steel. It can also occur following a patch repair of reinforced concrete member, when there is a significant difference in chloride concentration between the new patch (chloride free) and its surrounding substrate (chloride contaminated). The corrosion rate may be very high because the passive steel surface in the patched area often shows very positive potentials the effect of which will be a very large driving force. It means the larger the difference in corrosion potential is between these areas the larger the macrocell current becomes. One reason why macrocell corrosion is more severe is that negative ions like Cl^- may migrate to the anode in higher amounts than in microcell corrosion, because

of the high positive potential in this area and the high current. This means that the chlorides can move to the corroded area, and the corrosion may then be accelerated. At the same time the positively charged and dissolved Fe^{2+}, migrate to the cathode zone with less volume expanding corrosion products as a consequence.

Due to the spatially nonhomogeneous concrete properties and the varying environmental conditions within the concrete, the reinforcing steel generally does not corrode uniformly along its whole length. The reinforcing steel bar can be divided into two parts: active zone and passive zone. Actually, anodic and cathodic reactions can coexist in both the active and passive zones. Macrocell corrosion may occur when the active steel is electrically connected to the passive steel. The coupled polarization behavior of macrocell corrosion between the active and passive steel is shown in **Fig 2.9**. The macrocell corrosion current circulating through the concrete between the active steel bar and the passive steel bar generates the ohmic drop (ηohm). Macrocell current density along the steel–concrete interface can be expressed as:

$$i_{mac}^{a} = i_{Fe}^{a} - i_{O_2}^{a} \tag{2.8}$$

for the active steel bar; and for the passive steel bar:

$$i_{mac}^{p} = i_{Fe}^{p} - i_{O_2}^{p} \tag{2.9}$$

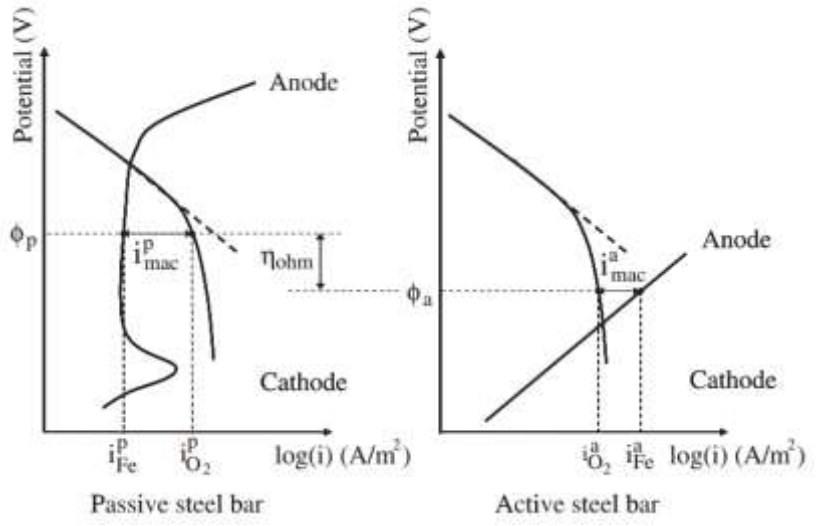

Fig 2.9 Diagram of microcell and macrocell corrosion of steel in concrete [2.14]

2.8 Chloride-induced Corrosion in Reinforced Concrete Structure

One of the most important causes for reinforcing steel corrosion is the presence of chloride ions. They cause localised break-down of the passive film that initially forms on steel as a result of the alkaline nature of the pore solution in concrete [2.15]. Chloride-induced corrosion is a mechanism which has led to premature deterioration of many concrete structures worldwide.

Nowadays, huge amounts of money have to be spent to deal with this deterioration mechanism. The corrosion process is an electrochemical process, which is generally caused by large chloride ion concentrations close to the embedded steel. Permeable concrete allows moisture and chloride ion ingress which will result after some time in corrosion of the reinforcement. Initially a thin protective layer on the surface of reinforcing steel, which inhibits the corrosion of the steel in the beginning, was formed during the cement hydration process.

The passive film is stable by virtue of the high alkalinity of the pore solution, which usually has a pH-value >13. However, the passive layer can be destroyed by the action of chloride ions or when the alkalinity of the environment with regard to the pH value due to carbonation of the cement paste sinks below a pH-value of 9. Beside chloride ions and moisture, the presence of oxygen is necessary to cause corrosion of the steel reinforcement. The most severe conditions in practice are to alternately wetting and drying cycles exposure of concrete members.

Photo 2.2 Chloride-induced corrosion in a marine environment

Therefore, the tidal and splash zones in a marine environment are the areas with the highest risk for chloride-induced corrosion (as shown in **Photo 2.2**). Other sources of chlorides can be de-icing salts, which can generate chloride-induced corrosion on huge concrete surfaces.

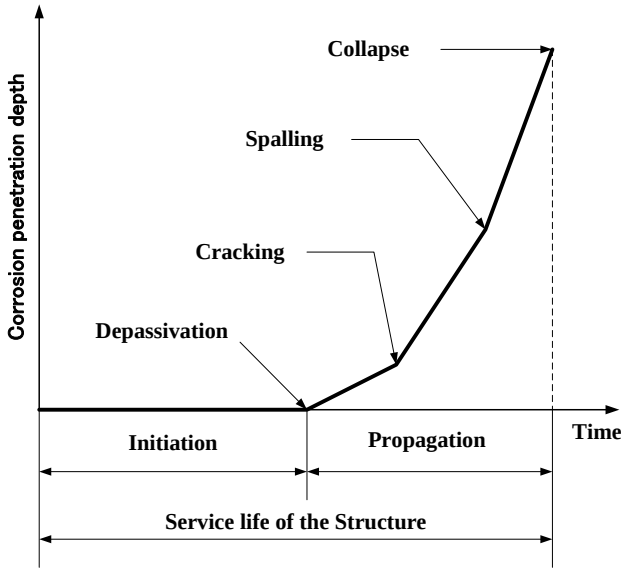

Fig 2.10 Initiation and propagation periods for corrosion in a reinforced concrete structure (From Tuutti's model [2.16])

2.9 Initiation and Propagation of Corrosion

The service life of reinforced concrete structure can be divided in two distinct phases (**Fig 2.10**). The first phase is the initiation phase, in which the reinforcement is passive but phenomena that can lead to loss of passivity, for example, carbonation or chloride penetration in the concrete cover, take place; this phase ends with the initiation of corrosion (the way of defining the initiation of corrosion will be discussed later). The second phase is the propagation phase, which begins when the steel is depassivated (i.e., corrosion initiates) and finishes when a limiting state is reached beyond which consequences of corrosion cannot be further tolerated.

Table 2.1 Defenition of deterioration stages due to chloride attack [2.15]

Stage of deterioration	Defenition	Stage determined by
Initiation stage	Until the chloride ion concentration on the surface of steel reaches the marginal concentration for the occurrence of corrosion (standard value is 1.2 kg/m^3).	Diffusion of chloride ions Initially contained chloride ion concentration.
Propagation stage	From the initiation of steel corrosion until cracking due to corrosion.	Rate of steel corrosion.
Acceleration stage	Stage in which steel corrodes at a high rate due to cracking due to corrosion.	Rate of corrosion of steel with cracks.
Deterioration stage	Stage in which load bearing capacity is reduced considerably due to the increase of corrosion amount.	

Standard Specification for Concrete Structures-JSCE (Part: Maintenance)[2.17] is defined the performance of degradation of structures due to chloride attack as shown in **Table 2.1**. The consequences of corrosion of steel reinforcement involeve several aspects connected with the condition of the structure, such as its esthetic appearance, service-ability, safety and structural performance. The main consequences of corrosion attack are shown in **Fig 2.11**. corrosion is often indicated by rust spots that appear on the external surface of the concrete, or by cracking of the concrete cover produced by the expansion of the corrosion products. The volume of the corrosion products can be from 2 to 6 times greater than that of iron they are derived from, depending on their composition and the degree of hydration.

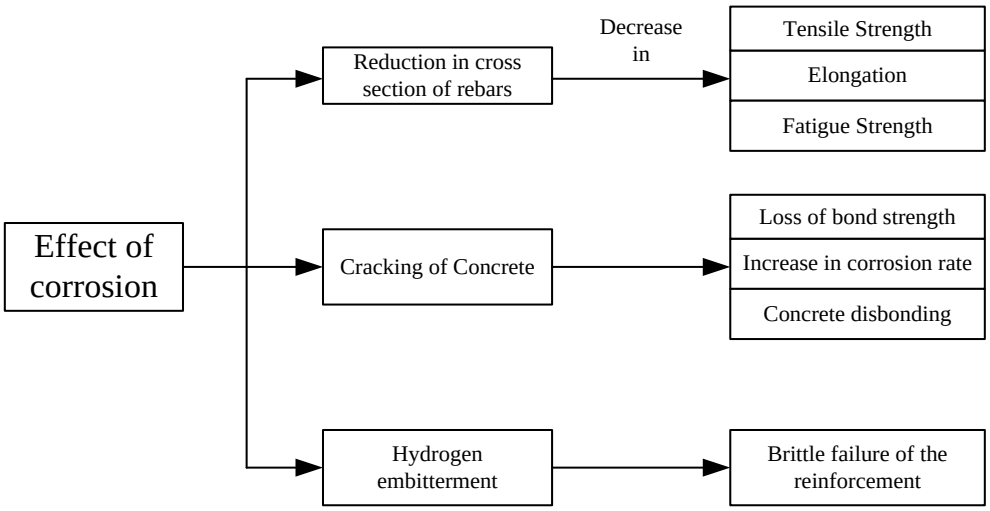

Fig 2.11 Structural consequences of corrosion in reinforced concrete structure

2.10 Cathodic Protection of Steel in Concrete

Cathodic protection (CP) is an electrochemical repair technique that has increasingly been used for the repair of reinforced concrete structures in worldwide. CP is rapidly being accepted as a repair option for steel-reinforced concrete structures deteriorated by steel corrosion caused by chlorides [2.20]. This technique requires the permanent application of a small direct current to protect the steel [2.21].

Principle

The objective of cathodic protection is usually to polarize the reinforcement to an instant-off potential more negative than -850 mV (CSE) [-770 mV (SCE)]. This potential should decay (become less negative) by at least 100 mV from the instant-off potential within 24 hours after the system is disconnected (so called depolarization). With CP, chloride ions slowly migrate away from the reinforcing steel toward the anode. Furthermore, the production of hydroxide ions at the steel surface causes the concrete to revert back to an alkaline state. These factors quickly arrest the corrosion process when current is applied, and allow the passivating film to reform on the surface of reinforcing steel.

Cathodic protection reduces the corrosion rate by cathodic polarization of the reinforcing steel in concrete. The rationale behind cathodic protection is to prevent the reinforcing steel from giving up electrons so that corrosion does not occur. This retention of steel electrons is achieved by supplying the electrons from another source. Consider the corrosion half-cell reactions introduce in **Eq. (2.1)** and **Eq. (2.2)**, if there is an excess of electrons, the rate of the anodic reaction decreases. On the other hand, an excess of electrons will increase the rate of the cathodic reaction. There are two main methods of supplying the electrons: by applying an impressed current or by introducing a sacrificial anode.

Polarization

A simplified graphic representation of a corrosion cell for reinforcing steel in concrete is shown in **Fig 2.13** [2.32]. The electrochemical characteristics of each reaction can be studied by examining the confined half-cell reactions. The resulting polarization, also known as activation polarization, in the absence of other effects, is governed by the following relationship:

$$\eta = a + b(\log I) \qquad (2.10)$$

where

η = activation polarization

a = potential intercept

b = Tafel constant

I = current

The anodic and cathodic half-cells polarize to a common corrosion potential Ecorr. This potential is also called mixed potential because the resulting potential is the combination of the half-cell potentials for the anodic and cathodic reactions. The corrosion current, $I_{corr,}$ is directly proportional to the corrosion rate. I_{corr} and E_{corr} are represented in **Fig 2.12** by the intersection of the anodic and cathodic curves.

Two other types of polarization affect the corrosion of steel in concrete. Cathodic diffusion is associated with concentration polarization by which the rate

of oxygen diffusion through concrete influences the corrosion rate. As shown in **Fig 2.13**, the higher the oxygen diffusion (as shown in Curve 2), the higher the corrosion rate. The other type of polarization is ohmic polarization. Because concrete is not a very conductive medium, the resistance of concrete influences the corrosion rate. As shown in **Fig 2.14**, the higher the resistance, the smaller corrosion rate.

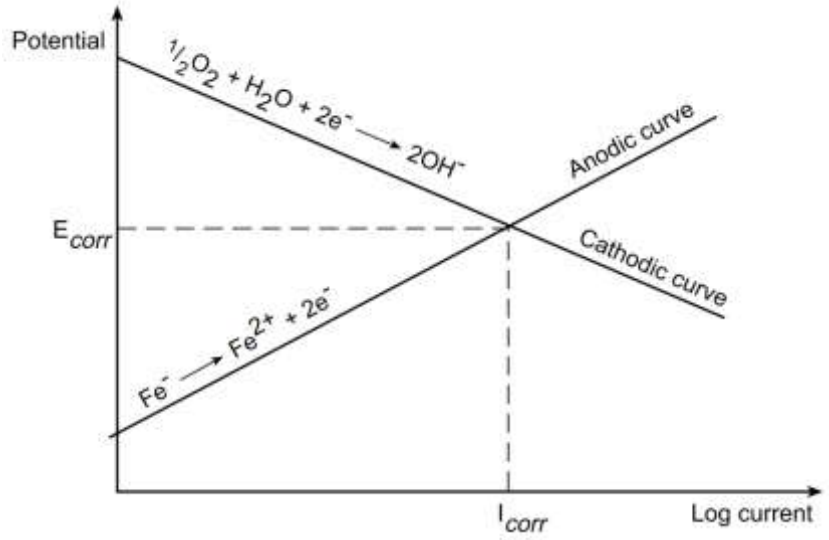

Fig 2.12 Simplified representation of a corrosion cell of steel in concrete [2.30]

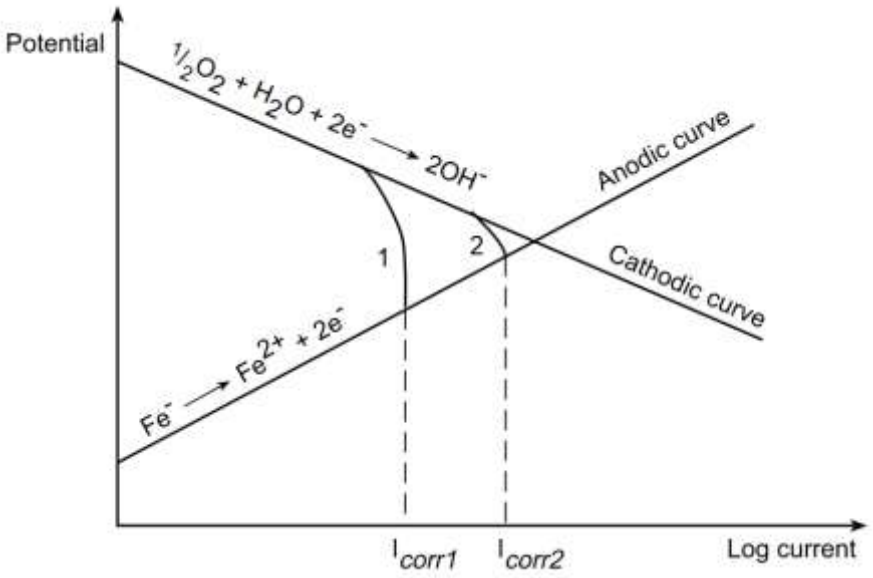

Fig 2.13 Effect of cathodic diffusion on polarization [2.30]

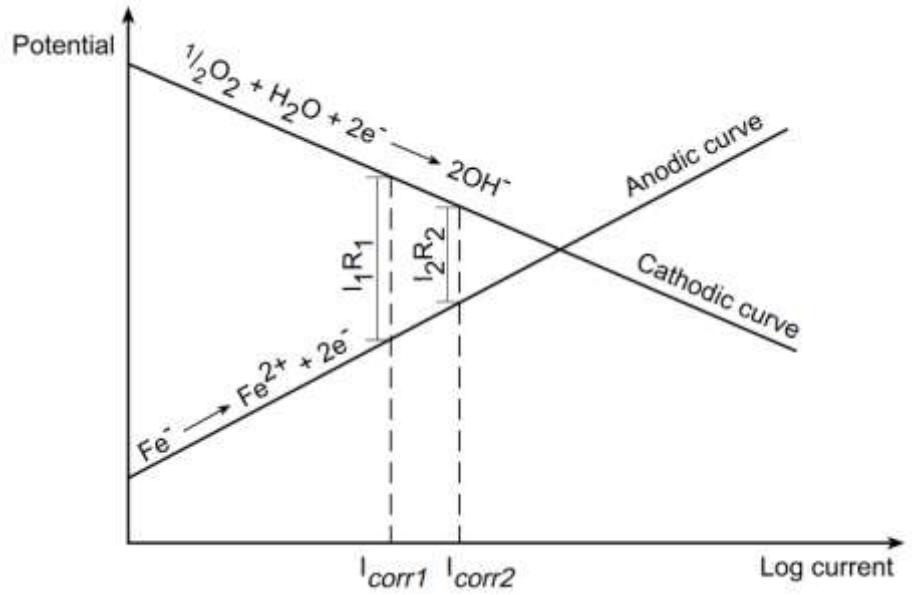

Fig 2.14 Effect of concrete resistance on polarization [2.30]

On a practical level, reinstating corrosion protection in concrete using sacrificial anode cathodic protection does not require perfect repairs; only physical damages need to be repaired, without the need to remove a lot of chloride-contaminated concrete and perfect cleaning of steel [2.21].

The two principal types of cathodic protection systems commonly used are the impressed current cathodic protection (ICCP) and the sacrificial anode cathodic protection (SACP). The direct current (DC) for CP system can be supplied either via mains power in an impressed current CP (ICCP) system or by sacrificial anode CP (SACP) system. In a SACP device, single or multiple anodes distribute the cathodic current to the protected structure [2.22]. The decision on which of the two cathodic protection (CP) systems to use is usually also influenced by a number of factors including but not limited to the condition of the structure, the client's budget and the anticipated life expectancy of the structure following the repairs.

Cathodic protection can work in three stages as shown in **Fig 2.15** [2.22]. Natural corrosion will produce electrons which make a cathodic area as shown in (a). An external supply of electrons can also produce a cathodic reaction for the available amount of oxygen. If the supply of electrons is insufficient, corrosion

may also produce electrons as shown in (b). Full cathodic protection (c) is only achieved where the supply of electrons from an external source is able to react with all the oxygen.

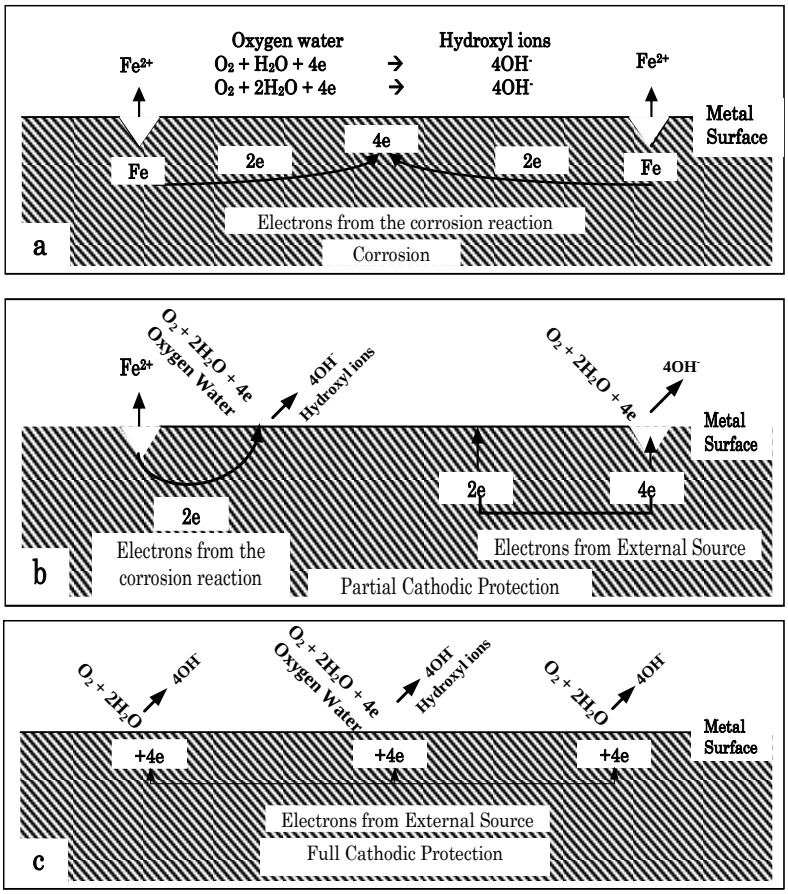

Fig 2.15 Stage of cathodic protection system [2.22]

2.11 Impressed Current Cathodic Protection (ICCP)

In the ICCP, the large electrochemical is formed between an anode and the structure to be protected by a power supply that is controlled by reading a reference electrode close to the structure, as shown in **Fig 2.16**. ICCP is reached by applying a small amount of direct current through the concrete. An anode is usually laid on the concrete surface connected to the positive terminal, and the steel acts as the cathode is connected to the negative terminal of DC power supply. Concrete contains enough pore water to serve as the electrolyte so that when DC is applied, current can flow from the anode to the cathode.

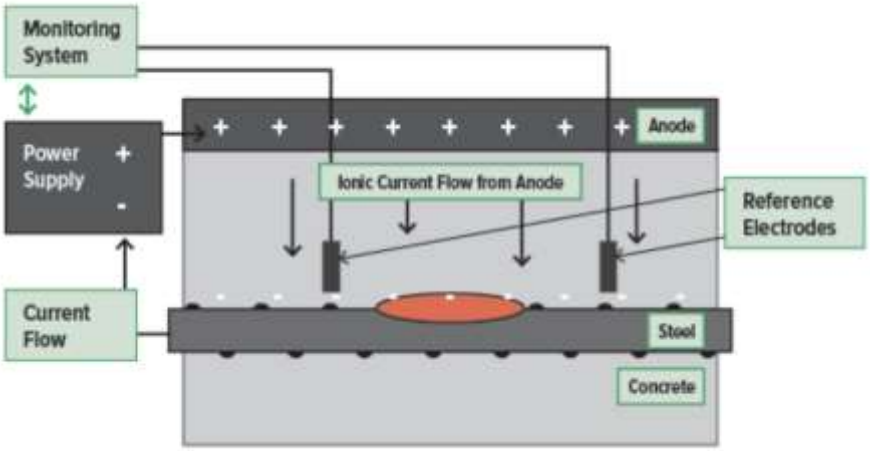

Fig 2.16 Cathodic protection system in ICCP [2.23]

In ICCP systems, a small direct current is passed from a permanent anode to the reinforcing steel. An external power supply needs to be connected between the anode and the steel with appropriate polarity and voltage to prevent the reinforcing steel from giving up electrons. **Fig 2.17** shows an impressed current system schematically and the reactions involved [2.30].

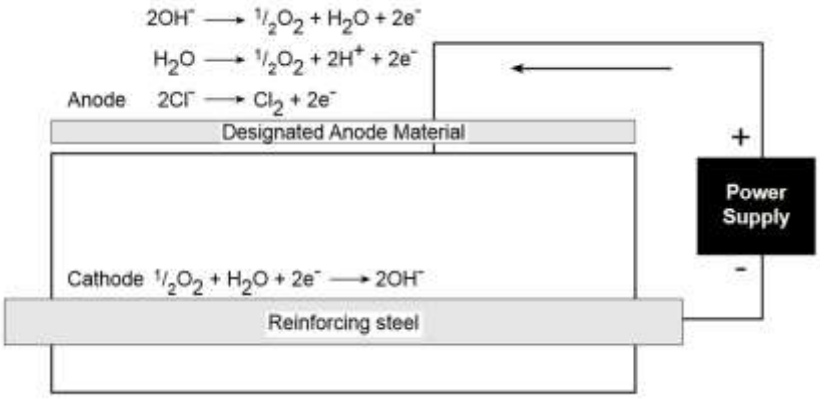

Fig 2.17 Reactions involved in impressed current system [2.30]

If the current applied is enough to stop the anodic reaction from occurring, the only reaction at cathode should be:

$$2e^- + \frac{1}{2}O_2 + H_2O \rightarrow 2(OH)^- \qquad (2.10)$$

If the potential goes too negative, which means the current applied is excessive, the hydrogen evolution reaction can occur.

$$e^- + H_2O \rightarrow H + OH^- \qquad (2.11)$$

The monatomic hydrogen migrates into the steel metal lattice, reducing the strength and resulting in failure under load. This phenomenon is known as *hydrogen embrittlement*. Hydrogen embrittlement is not a problem for conventional reinforcing steel but may be a problem for certain high-strength steels. Caution is justified for cathodic protection installations on structures contain prestressed or post-tensioned steel. Both possible reactions at the cathode, described above, lead to the production of hydroxyl ions, which restore the passivating film broken down by chloride attack. Chloride ions are driven away from the reinforcing steel. Because the chloride ions is negatively charged, it is repelled from the now-cathodic reinforcing steel and moves towards the installed anode.

$$Cl^- \rightarrow Cl^2 + 2e^- \qquad (2.12)$$

Another reaction that occurs at the cathode is the consumption of the hydroxyl ions formed at the cathode to produce oxygen. Water is then oxidized to give rise to hydrogen ions leading to acid etching of the concrete. If the potential gets too negative, the acidification around the anode increases.

$$2OH^- \rightarrow H_2O + \frac{1}{2}O_2 + 2e^- \qquad (2.13)$$

$$H_2O \rightarrow \frac{1}{2}O_2 + 2H^+ + 2e^- \qquad (2.14)$$

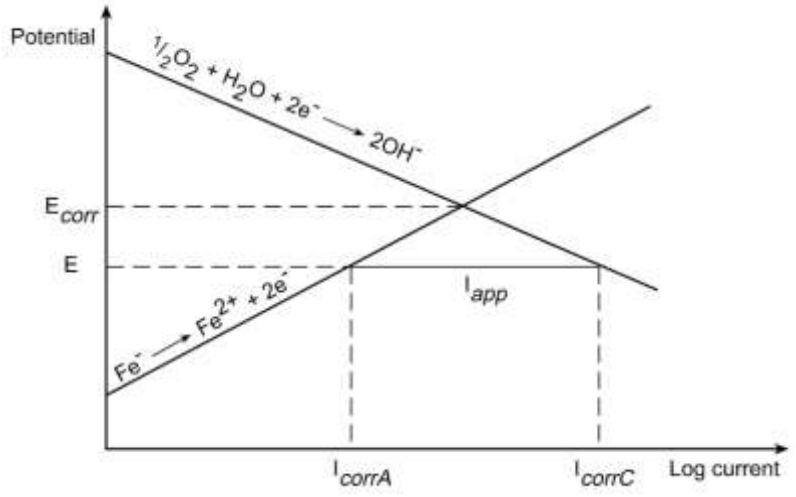

Fig 2.18 Electrochemical principle of impressed current system (2.30)

The electrochemical principle of impressed current cathodic protection

can be explained by polarization curves of the reactions involved. **Fig 2.18** shows the polarization of the two reactions involved. When an electric current is supplied, I_{app}, the potential shifts in the direction from E_{corr} to E owing to the excess of metal electrons supplied at the metal surface [2.31]. The rate of the anodic reaction, corrosion rate, is reduced to I_{corrA}.

The main advantage of ICCP system is its flexibility and durability [2.24]. The current output of the power supply can be adjusted to optimise the protection delivered. Also, ICCP system can be controlled to accommodate variations in exposure conditions and future chloride contamination. The performance of ICCP system is widely determined by the material composition, shape, type and orientation of the anode [2.25]. There are a number of different types of anode that are used in ICCP system for reinforced concrete structure. These include conductive coating, titanium-based mesh in cementitious overlay, conductive overlay incorporating carbon fibres, flame-sprayed zinc and various discrete anode systems. The selection of the anode system must considered environmental conditions, anode zoning, accessibility, maintenance requirements, performance requirements and operating characteristics, life expectancy, weight restriction, track record and costs [2.24].

2.12 Sacrificial Anode Cathodic Protection (SACP)

At the time when the Sacrificial Anode Cathodic Protection (SACP) system is selected, the service life is expected to be shorter than an ICCP system because the anode must consume (sacrificed) to produce the protective current. Hence, if a concrete structure has a relative long life remaining, the SACP may need replacement during the remaining service life of the structure. In general, the life expectancy of a sacrificial anode may be 5-20 years (or longer), and is dependent on the type of material used and the environmental condition [2.326]. Aluminium (Al), zinc (Zn) and magnesium (Mg) are the type of metals that is commonly used for SACP. These metals are also covered with a highly alkaline mortar to improve the long-term performance and dissolution characteristics.

Principles of Operation

Sacrificial cathodic protection, or galvanic protection as it is often referred to, is based on the principal of dissimilar metal corrosion. When two dissimilar metals are connected together, one will tend to act as an anode and will corrode, while the other will form the cathode. The main sacrificial metals used to protect steel in concrete, are aluminum alloys and zinc. These metals are sacrificed in the generation of the protection current. No external power supply is required. Because each element of anode surface acts as its own power supply the anode system does not need to be installed in zones and it is relatively easy to target the system to an area of need. A typical material used is zinc. Such an anode has about 0.5 to 1.0 V available to drive the current to the steel. **Fig 2.19** illustrated about the SACP system for embedded steel in concrete.

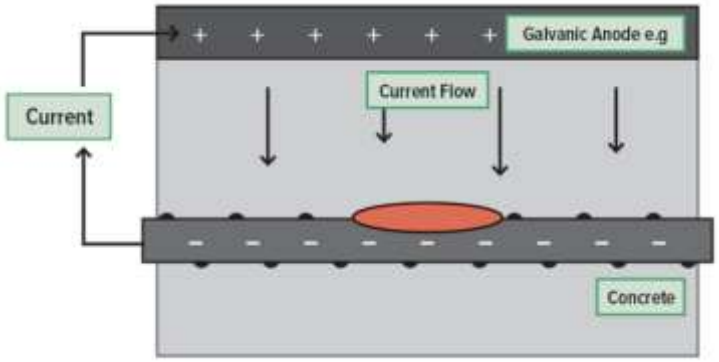

Fig 2.19 Cathodic protection system in SACP [2.23]

The sacrificial anode corrodes preferentially producing electrons. Sacrificial anodes need to be more active than iron to protect the reinforcing steel. Typical anodes are zinc, aluminum, magnesium and their alloys. **Fig 2.20** shows a sacrificial system schematically and the reactions involved.

The reaction at the anode is the consumption of the anode to procedure the electrons that the steel would be otherwise giving up.

$$M \rightarrow M^{n+} + ne^{-} \qquad (2.15)$$

The resistance of the concrete electrolyte is the crucial element to determine whether the use of sacrificial anodes is viable. In cases where the

electrolyte resistance is too high, the effective potential difference between the steel and the anode may not be sufficient to adequately protect the structure. Thus, sacrificial anodes are very common for structures exposed to seawater and to other electrolytes that decrease the concrete resistivity.

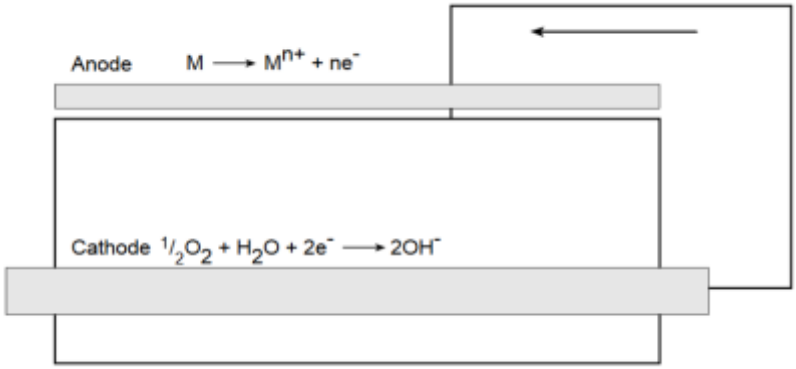

Fig 2.20 Reactions involved in sacrificial anode system [2.30]

The electrochemical principle of sacrificial anode protection can be explained by the polarization curves the reactions involved. **Fig 2.21** shows the polarization of the two reactions involved.

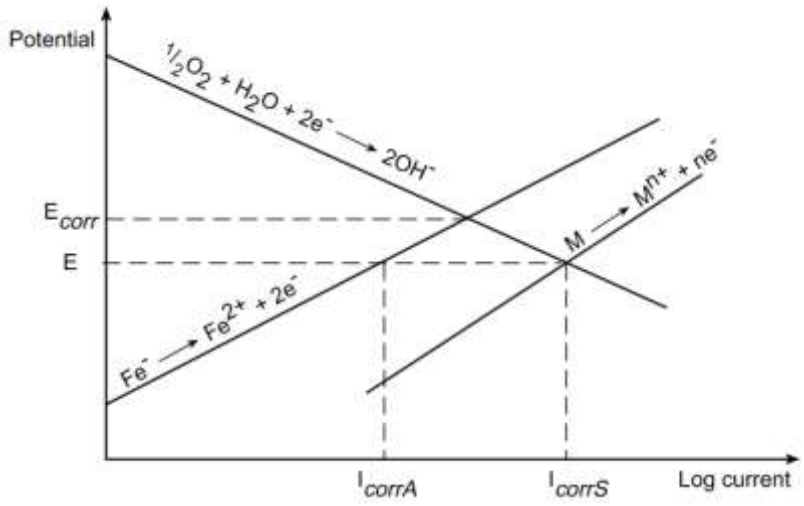

Fig 2.21 Electrochemical principle of sacrificial system [2.30]

When a sacrificial anode is used, the reinforcing steel and the sacrificial anode are polarized to the same potential E. The corrosion rate for the reinforcing steel is

reduced to I_{corrA}. The rate of consumption of the sacrificial anode is given by I_{corrS}.

Sacrificial Anode Type

The application of sacrificial anode CP systems to concrete is relatively new compared to their use in protecting steel in soils and sea water. Issues affecting sacrificial anode system for concrete structures include maintaining the activity of the sacrificial metal, expansive products of metal dissolution and attachment to reinforced concrete structure. The natural alkalinity and density of concrete may cause some sacrificial metals to passivate or prevent the dissipation of the corrosion product and concrete may cause some sacrificial metals to passivate or prevent the dissipation of the corrosion products in the same way that sea water and soils do.

A number of systems have been developed that address these issues and an increasing range of sacrificial anodes is being offered by suppliers. The known sacrificial anode products may be divided into the following types:

1. Metal coatings applied directly to the concrete surface.
2. Sheet anodes attached to the concrete surface.
3. Distributed anodes embedded in a cementitious overlay.
4. Discrete anodes embedded in cavities in the concrete.

Experience of sacrificial anode system on reinforced concrete structure is more limited than impressed current systems. Zinc, thermally applied as a coating to concrete is probably the most widely used galvanic system in the world. These system are not proprietary products and are not promoted by any particular company. In 1990's various surface applied proprietary systems were developed, and from 1999 discrete anode system embedded in cavities in the concrete were introduced to the market. The most widely used systems in the UK are discrete sacrificial anodes that are embedded in holes formed for this purpose and in repair areas in the concrete.

Sacrificial anode products currently known to be available in the UK include thermally sprayed zinc and aluminum, jacketed zinc mesh with a cementitious overlay, adhesive line zinc sheeting and discrete anodes for

embedment in areas of concrete patch repair, discrete anodes for use in cavities formed for the purpose of installing anodes and sacrificial anodes that can be used as both impressed current and sacrificial anodes. Most of these anode systems are proprietary products. Non-proprietary products include thermally sprayed zinc and zinc or aluminum mesh in a porous overly that may be achieving using an air entrained cementitious material that usually contains some chloride as an activating agent. **Photo 2.3** shows typical commercially available of the sacrificial anode.

(a). Sacrificial anode Galvashield XP (b). Sacrificial anode Galvashield F

Photo 2.3 Commercial type of sacrificial anode

Protection Delivered of Sacrificial Anode

The protection delivered by a sacrificial anode system is largely determined by the current output of the anode system and its distribution to the protected steel. The anode current density is approximately 50 times the steel protection current density. In both cases the anodes deliver sufficient current to act in a preventative role (1 to 2 mA/m^2 protection current to the steel on average. The anodes appear to be effective in delivering cathodic prevention current densities).

Long term current output data on sacrificial anode system is limited. The cyclic behavior is evident and is usually attributed to the responsive behavior of

the anode to changing environment condition. The principal environment factor affecting the performance in terms of the protection current delivered to the steel by a sacrificial anode is resistivity which is a function of moisture content, chloride content and temperature. The protection delivered is also a function of current distribution. This effects discrete sacrificial anode assembly's more than distributed surface applied anode assemblies and is discussed in greater detail below.

Factors Affecting Performance of Sacrificial Anode

There are a number of factors affecting the performance of a sacrificial anode system. These are summarized in the **Table 2.2**.

Table 2.2 Summary of factor affecting performance of anode systems applied to reinforced concrete structures [2.12]

Factor	Effect
Charge capacity/ current output	The maximum theoretical life cannot exceed a period determined by the anode charge capacity ad anode current output.
Anode activity/ surface area	Determines protection current output and discrete anodes in particular need a method of anode activation. For alkali activated systems, anode activation is dependent on the quantity of alkali in assembly.
Anode delamination/ adhesion to concrete	Sacrificial anode systems applied to concrete surface in particular are at risk of suffering from delamination and loss of contact with concrete.
Current distribution	Discrete anodes distribute current poorly compared to surface applied anodes but protection can be targeted to the area of need.
Continuing corrosion	Products design for use in a preventative role may fail when trying to arrest an active corrosion process.
Concrete Resistivity	An increase in concrete resistivity reduces the protection current output of a sacrificial anode which limits the protection delivered.

Protection Delivered of Sacrificial Anode

The protection delivered by a sacrificial anode system is largely determined by the current output of the anode system and its distribution to the protected steel. The anode current density is approximately 50 times the steel protection current density. In both cases the anodes deliver sufficient current to act in a preventative role (1 to 2 mA/m^2 protection current to the steel on average. The anodes appear to be effective in delivering cathodic prevention current densities).

Long term current output data on sacrificial anode system is limited. The cyclic behavior is evident and is usually attributed to the responsive behavior of the anode to changing environment condition. The principal environment factor affecting the performance in terms of the protection current delivered to the steel by a sacrificial anode is resistivity which is a function of moisture content, chloride content and temperature. The protection delivered is also a function of current distribution. This effects discrete sacrificial anode assembly's more than distributed surface applied anode assemblies and is discussed in greater detail below.

Sacrificial Anode Service Life

Anode life service primarily determined by anode current output, anode charge capacity, anode utilization and anode efficiency and may be calculated using Faraday's law. In simple terms anode life is given by the useful mA-hours (charge capacity) of the sacrificial metal divided by average output in mA. A current of 1 mA delivered for 50 years is equivalent to a charge of 440 Amp hrs (1 Amp hr = 3.6 kC) the useful charge capacity of an anode system is determined by the anode efficiency and utilization. Longer live may generally be achieved by using more anodes or anodes with high charge capacities that deliver low current densities.

These parameters may be requested from the anode suppliers or obtained from independent tests. Various factors may affect utilization of an anode system. These include the loss of sacrificial anode activities and loss of adhesion of the anode system to the concrete. Loss of adhesion is mainly associated with anode system applied to concrete surfaces and is discussed further below. The level of

anode activity is particularly important in small surface area embeddable discrete anodes which are required to deliver a high anode current density.

For reinforced concrete application, zinc anode has become the most common SACP used presently because several advantages [2.27]:

a. Zinc has high corrosion efficiency i.e. high percentages of the electrons that are discharged when the zinc corrodes are available to protect the steel.
b. As the zinc corrodes, it has a relative low rate of expansion compared to other metals including steel. This makes zinc anodes particularly suitable for application where the anodes are embedded into the concrete structure.
c. Zinc anodes are suitable for use with prestressed and/or post-tensioned concrete because their native potential is not sufficient to generate atoms or cause hydrogen embrittlement in a concrete environment.

The main benefit of SACP is its simplicity and the fact that minimal or no maintenance is required. In SACP system, an external power source is not required to maintain the protective current because directly electrically connected to the steel. This significantly reduces the start-up costs as no provision has to be made to connect to a power supply [2.28]. Also, SACP usually operates below the threshold for hydrogen embrittlement (~ -900 mV vs. CSE) [2.39].

Meanwhile, the major disadvantages of SACP system are the uncertain lifespan of the anodes, and it is dependent on the average current output of the anodes. The amount of current that is generated by SACP is significantly influenced by environmental factors, such as temperature, oxygen content, humidity and also chloride content. In addition, the resistivity of the concrete must be taken into account as the lower driving voltage of the anodes means they may not effective in high resistivity of concrete [2.28].

2.13 Impressed Current versus Sacrificial Anode

The main advantage of sacrificial systems over impressed current systems is that they do not require a power supply. Impressed current systems require more monitoring than sacrificial anode systems. Sacrificial anode systems are, however, limited in the current and voltage that they can produce. For concrete with high

resistivity, as found in atmospheric concrete, the energy output is generally not sufficient to achieve protection. In other environments, such as contact with seawater or seawater splash, protection may be achieved with the use of sacrificial anodes. Impressed current systems provide greater flexibility because current or output can be easily adjusted. While sacrificial anodes corrode, requiring periodic replacement, the service life of the anodes used for impressed current system is usually much longer.

2.14 Effect of Cathodic Protection in Concrete

CP current circulation between an anode and a cathode causes steel polarizes to negative potential, increase the alkanality of concrete and reduction of chloride content at the cathodic area by electrochemical reactions inside the electrolyte.

The negative potential shift can reduce the driving force for the anodic process (thermodynamic effect) and increase or maintain the resistance of the anodic process (kinetic effect) [(2.38)]. The cathodic reactions reduce oxygen content and generate alkalinity on the steel surface, which preventing corrosion because they widen the passive region and depolarize the cathodic process. In the case of passive steel, they hinder local acidification and also interfere with pitting initiation [(2.38)]. In addition, CP current also reduce the chloride concentration on the steel surface by electrophoresis.

The use of CP current in reinforced concrete give not only a benefical effects but also negative effects such as concrete degradation, bond loss and hydrogen embrittlement. These caused by ion migration of sodium (Na^+) and potassium (K^+) towards the concrete-steel interface [(2.39), (2.40)]. Application of a greater CP current can promote hydrogen activity at the concrete-steel interface and the consumption of electron from the corrosion process [(2.41)]. In addition, hydrogen evolution can occur only at potentials more negative than about -950 mV vs. SCE in the case of alkaline environments (pH > 12) [(2.38)]. For these reasons, it is necessary to determine a suitable CP criteria for reinforced concrete structures.

2.15 Performance Criteria of Cathodic Protection in Concrete

The method of CP has introduced to be an effective method to mitigate corrosion of steel in reinforced concrete structures. But, there is still a difference opinion about the appropriate criteria for CP system. A variety of CP criteria have been proposed including using electrode operating potential, potential shift, potential decay, current-potential relationship (E-log*I*), macrocell probes, chloride concentration and a statistical treatment of static potentials [2.33]. Many of these criteria are complex and difficult to apply, and few experimental studies have been conducted to determine the actual effectiveness of the various criteria.

Decay Shift Criteria

After reinforcing steel was installed with the CP system inside the concrete, they were evaluated for when to replace the new anode and measured how long CP could protect steel from corrosion risk. Decay shift can be calculated from off potential deducted by instant-off potential. CP can maintain reinforcing steel from corrosion. The decay shift is more than 100 mV from half-cell potential measurement versus copper/copper sulfate.

The 100 mV depolarization criterion is the most popular criterion currently used for CP system and has been adopted by several codes. This criterion was investigated empirically by Bennett and Mitchell in 1989 [2.34]. In their investigation, the procedure for measuring the instant-off potential (current interruption) and duration of the test is proposed. Also, the effect of temperature, static potential, and steel density was investigated by the test. They recommended that if the chloride concentration is not know, the 100 mV depolarization criterion is reasonable. Although 150 mV should be required if conditions are known to be very corrosive.

NACE SP0290 [2.35] calls for a minimum of 100 mV polarization from native potentials, or 100 mV depolarization from an “Instant Off” reading. The duration of the test can have a clear impact on the values recorded. Per SP0290 the “Instant Off” reading is typically read between 0.1 and 1.0 seconds after the rectifier is interrupted. Readings at times less than 0.1 seconds often include

reactive components that have nothing to do with CP. If one waits more than one second, the observed change will be understated. **Fig 2.22** provides a stylized diagram. Starting on the left with the base potential before CP is applied the polarization is shown, whereby the steel potential is polarized in a negative, cathodic direction. About midway, the rectifier is turned off and the potential shifts in a positive direction. The area between 'CP Off' and 'Instant Off' include IR error and reactive transients resulting from interrupting the CP current. At a point between 0.1 and 1 second is the start of the depolarization.

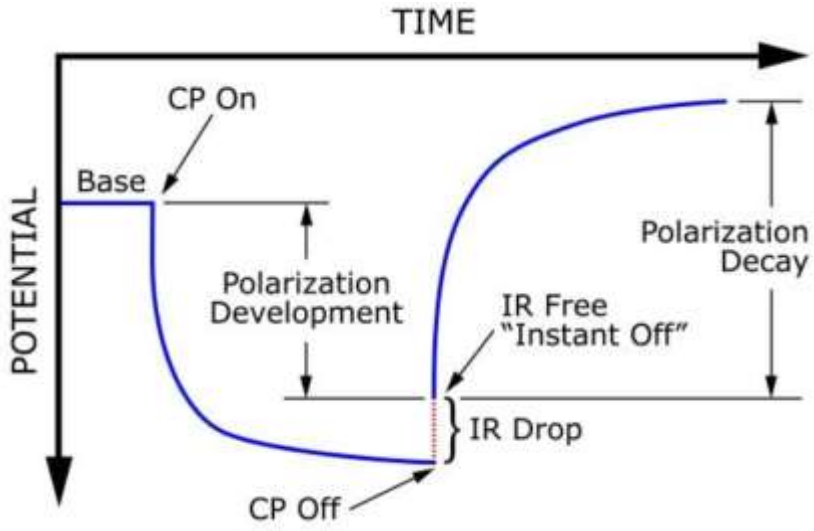

Fig 2.22 Polarization-Depolarization [2.36]

Various researchers have been investigated to determine the effectiveness of this criterion on the corrosion rate of steel in concrete. Funahashi and Young (1992)[2.37] observed the total depolarization needed for complete protection for macrocell and microcell currents under various environments. They discovered that the 100 mV depolarization criterion does not adequate to eliminate both macrocell and microcell corrosion. Takewaka (1993)[2.38] studied the relationship between corrosion weight loss and depolarization value on the 18 concrete blocks with 0.5% chloride by weight of concrete under a dry and wet cycles. Current density level from 0 to nearly 500 mV were used to polarize the steel for eight months. The research results concluded that 100 mV criterion may not sufficient

and that 150-200 mV is necessary to protect the steel under these conditions. Another study was reported by Bennett et al. (1993) [2.39], the amount of polarization needed to control corrosion to an acceptable level was found to be a complex function of many variables. 100 mV of polarization was adequate if chloride concentration was less than 0.26% by weight of concrete. However, at higher chloride concentrations, polarizations up to 150 mV were needed.

The 100 mV decay shift criteria also described as briefly in **Table 2.3**. If potential of CP system is more negative than 850 mV, it means steel is polarized to be in cathodic state and no corrosion will occur. However, in case of reinforcing steel in concrete with a passive state and availability of dissolved oxygen, the application of such criteria has been found to result in very high unneeded current requirement [2.42]. This might be cause premature deterioration of the anode, hydrogen evolution and the loss bond between concrete and steel.

So decay shift criteria is used to determine performance of sacrificial anode cathodic protection system in RC structure.

Table 2.3 Criteria to acceptance of CP [2.29), (2.63]

Test Method	Criteria
ON potential	Negative more than 850 mV potential of steel with CP applied (on potential)
Instant-off potential	Negative more than 850 mV potential of steel with CP applied (instant-off potential)
OFF potential	Negative more than 100 mV potential of steel

E-log I criterion

Several observations have been carried out to understood the effectiveness of the E-log I criterion [2.40), (2.41]. Although these investigations depict the experimental procedure in detail and the effects of variables such as concrete cover, temperature, and moisture content, there is no documentation of the actual effectiveness of this criterion. Bennett and Mitchell (1993)[2.42] observed the current density established by the E-log I criterion. They discoverred that the current density require is higher than that required to achieve 100 mV of polarization. It might that the current density determined by E-log I criterion is sufficient to controlling

corrosion even data not available to support this conclusion. An empirical test method (E-log I) has been developed to determine the steel potential versus applied current relationships in particular cases. As varying levels of current is applied to the steel, the potential E_m can be measured and recorded.

From this data, an E-log I curve can be developed. Over section of the curve close to its natural potential, there should be an almost linear portion from where the relationship between applied current and resulting potential shift can be determined. There should be a change in gradient as the steel moves from anodic to cathodic conditions.

The limitations of this technique are that it is limited to first polarization only and it requires orders of magnitude of applied current. It is therefore quite difficult to determine of the start and end points of the test. It is also difficult to arrange the testing equipment on sites and there remains the possibility of overprotection that can damage to the concrete. It is not generally considered to be a practical-on site test.

The protection current required is taken to be the current at the start of the linear portion of the E-log I curve. Which is sometimes difficult to achieve or detect in real cases.

Current Density Requirement

In real situation, concrete construction attached with many environment such as humidity of air moisture, chloride attached from rain, carbon dioxide gas and other factor that affecting to reinforcing steel inside concrete. Reinforcing steel embedded in concrete exposed in different environment must have different current density requirement too. Efficiency of CP in concrete was described by current density criteria in **Table 2.4**. It is important to determine the amount of protective current or potential difference that required for CP system apply to reinforced concrete structures and to make sure that the anode can provide that current uniformly across the structure.

Table 2.4 Practical CP current density requirements for varying steel conditions [2.36]

Environmental surrounding steel reinforcement	Current density (mA/m^2)
Alkaline, no corrosion occurring, a little oxygen resupply	0.1
Alkaline, no corrosion occurring, exposed structure	1 - 3
Alkaline, chloride present, dry, good quality concrete, high cover, light corrosion observed on the steel	3 - 7
Chloride present, wet, poor quality concrete, medium-low cover, widespread pitting and general corrosion on steel	8 - 20
High chloride levels, wet fluctuating environment, high oxygen level, hot, severe corrosion on steel and low cover	30 - 50

2.16 Issues Addressed in this Study

It is well known, sacrificial anode cathodic protection is one of method to improve the service life of reinforced concrete (RC) structure. Normally, potential difference between conventional patch concrete and parent concrete will accelerate corrosion near the boundary or "ring anode" damage. By sacrificial anode embedded in patch repair concrete with non-chloride contamination in order to protect the steel bar in parent concrete (with chloride contamination) from corrosion, thus "ring anode" will reduced, as illustrated in **Fig 2.23**.

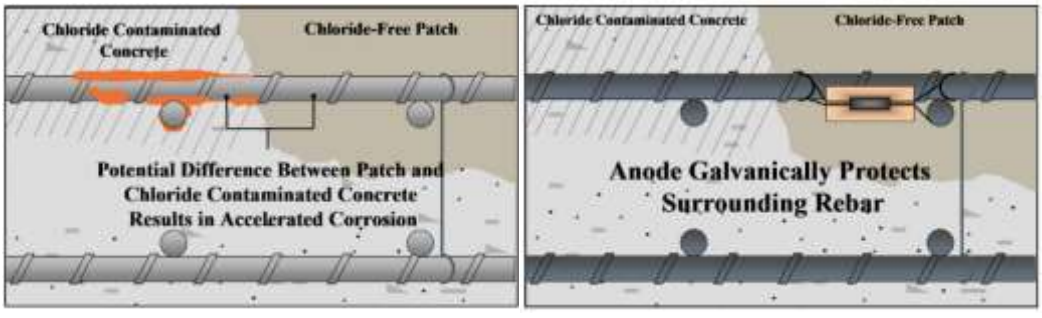

Fig 2.23 Patch repair concrete with and without sacrificial anode

However, sacrificial anode has limitation condition to improve the service life of deteriorated RC structure. Among the challenges that are still to be

taken up in CP system embedded in concrete, therefore some issues were address in this study in order to observe durability and effectiveness of zinc sacrificial anode to increase life-extension of RC structure. First, assessment of RC structure as preliminary investigation before CP applied on it is described in **Chapter 3**. Observations on deteriorated RC structure after 77-year-old exposed to severe marine condition is presented in this chapter.

Furthermore, performances of anode embedded in concrete as corrosion protection from the view point of effective length of protective current of anode in the non-homogeneous chloride environment is presented in **Chapter 4**. Followed by the study on the effect of steel surface conditions when anode installed is described in **Chapter 5**. The effect of temperature towards performance of anode and service life anode were presented in **Chapter 6** and **Chapter 7** respectively.

Finally, in order to observe durability and the effective number of anode to repair 40-year-old deteriorated RC beam, **Chapter 8** will presents an appropriate CP design to increase the service life of RC structure.

References

2.1 Cady, P. D., and R. E. Weyers., "Deterioration Rates of Concrete Bridge Decks", Journal of Transactions in Engineering, ASCE 110(1), 1984, pp. 34–44.

2.2 Kilareski, W. P., "Corrosion-induced deterioration of reinforced concrete - An overview. Materials Performance National Association of Corrosion Engineers, Houston, TX 19(3), 1980, pp. 48–50.

2.3 Mori, Y., and B. R. Ellingwood., "Maintaining Reliability of Concrete Structures. I: Role of Inspection/Repair", Journal of Structural Engineering ASCE 120(3), 1994, pp. 824–845.

2.4 Takewaka, K., and S. Matsumoto., "Quality and Cover Thickness of Concrete Based on the Estimation of Chloride Penetration in Marine Environments. In Concrete in Marine Environment, SP-109, ed. V. M. Malhotra, 1988, pp. 381–400. Detroit, MI: American Concrete Institute (ACI).

2.5 Thoft-Christensen, P., "Advanced Bridge Management Systems", Structural Engineering Review 7(3), 1995, pp. 149–266.

2.6 Mohamed, A.E., "Steel-Reinforced Concrete Structures: Assessment and Repair of Corrosion", Taylor & Francis Group, Boca Raton, 2008.

2.7 Hanson, C.M., "Comments on Electrochemical Measurements of The Rate of Steel in Concrete, Cement and Concrete Research 14, 1984, pp 574 – 584.

2.8 Pourbaix, M., "Atlas of Electrochemical Equilibria in Aqueous Solutions", National Association of Corrosion Engineers, Houston, TX, 1974.

2.9 Carnot, A., Frateur, I., Marcus, P., Tribollet, B., "Corrosion Mechanisms of Steel Concrete Moulds in The Presence of A Demoulding Agent", Journal of Applied Electrochemistry 32, 2002, pp. 865-869.

2.10 Troconis de Rincon, O., et al, "Environmental Influence on Point Anode Performance in Reinforced Concrete," Construction and Building Materials, 22, 2008, pp. 494-503.

2.11 Bertolini, L., Elsener, B., Pedeferri,P., Redaelli, E., and Polder, R.,

"Corrosion of Steel in Concrete", 2013, Wiley-VCH Verlag GmBH & Co KGaA.

2.12 Christodoulou, C., Glass, G. K., Webb., et al, "Evaluation of Galvanic Technologies Available for Bridge Structures", Structural Faults and Repair, 12th International Conference, Edinburgh, UK, 2008, p.11.

2.13 Cao Chong, "Modeling of Interaction between Corrosion-induced Concrete Cover Crack and Steel Corrosion Rate" M. Phil. Thesis, Hong Kong University of Science and Technology, Hong Kong, 2012.

2.14 Cheung, M. M. S., and Cao, C., "Application of Cathodic Protection for Controlling Macrocell Corrosion in Chloride Contaminated RC Structures", Construction and Building Materials 45, 2013, pp. 199-207.

2.15 Montemor, M. F., Simoes, A. M. P., and Ferreira, M. G. S., "Chloride-induced Corrosion on Reinforcing Steel: From The Fundamentals to The Monitoring Techniques", Cement and Concrete Composites 25, 203, pp. 491-502.

2.16 Tuutti, K., "Corrosion of Steel in Concrete", Report 4-82, Swedish Cement and Concrete Research Institute, Stockholm, Sweden, 1982, p. 469.

2.17 JSCE Guidelines for Concrete No. 17, "Standard Specifications for Concrete Structure-JSCE (Part: Maintenance)", 2007.

2.18 Bennet, J., and Turk, T., "Criteria for The Cathodic Protection of Reinforced Concrete Bridge Elements", Technical Alert, SHRP-S-359, 1994

2.19 McArthur, H., D'Arcy, S., and Barker, J. "Cathodic Protection by Impressed DC Currents for Construction, Maintenance and Refurbishment in Reinforced Concrete", Construction and Building Materials Volume 7, Issue 2, 1993, pp. 85-93.

2.20 Hobbs, D. "Concrete Deterioration: Causes, Diagnosis, and Minimizing Risk". In: International Materials Reviews 46.3, 2001, pp. 117–144.

2.21 Pedeferri, P., "Cathodic Protection and Cathodic Prevention", Construction and Building Materials, 1996, Vol. 10, No. 5, pp. 391-402.

2.22 Garcia, J., Almeraya, F., Barrios, C., Gaona, C., Nunez, R., Lopez, I., Rodriguez, M., Martinez-Villafane, A., and Bastidas, J. M, "Effect of

Cathodic Protection on Steel-Concrete Bond Strength Using Ion Migration Measurements", Cement and Concrete Composites, Vol. 34, Issues 2, February 2012, pp. 242-247.

2.23 Chess, P, M., and Broomfield, J, P., "Cathodic Protection of Steel in Concrete and Masonry; Second Edition", Taylor & Francis Group, LCC, CRC Press, Boca Raton, 2014.

2.24 Ngala, V., et al, "The Selection and Use of Cathodic Protection Systems for the Repair of Reinforced Concrete Structures", Construction and Building Materials, 39, 2013, pp. 19-25.

2.25 "Cathodic Protection of Steel in Concrete", Ed. P. M. Chess, E and FN Spon, New York, NY, 1998, p. 187.

2.26 Callon, R., et al, "Selection Guidelines for Using Cathodic Protection Systems on Reinforced and Prestressed Concrete Structures", Corrpro Technical Library, Medina.

2.27 Rajendran, V and Murugesan, R., "Study on Performance of Self Regulating Sacrificial Galvanic Anodes with and without Preconditioning Against Control Specimen and Using Accelerated Corrosion", Asian Journal of Civil Engineering (BHRC), Vol. 14, 2013, pp. 181-199.

2.28 Callon, R., et al, "Selection Guidelines for Using Cathodic Protection Systems on Reinforced and Prestressed Concrete Structures", Corrpro Technical Library, Medina.

2.29 EN 12696, "Cathodic Protection of Steel in Concrete," European Standard, 2000.

2.30 Etcheverry, L., Fowler, D. W., Wheat H, G., and Whitney D. P., "Evaluation of Cathodic Protection Systems for Marine Bridge Substructures", Research Report 2945-1, Center for Transportation Research Bureau of Engineering Research The University of Texas, Austin, December 1998.

2.31 Vaca Cortes, E., "Electrochemical Procedures to Rehabilitate Corroded Concrete Structures", Master's Thesis, The University of Texas, Austin, May, 1993.

2.32 Berkeley, K. G. C., and Pathmanaban, S., "Cathodic Protection of Reinforcement Steel in Concrete", Butterworths & Co. Ltd., 1990.

2.33 Bennett, J. and Broomfield, J. P., "An Analysis of Studies Conducted on Criteria for the Cathodic Protection of Steel in Concrete", NACE CORROSION/97, Paper No. 251, 1997.

2.34 Bennett, J. E. and Mitchell, T. A., "Depolarization of Cathodically Protected Reinforcing Steel in Concrete", NACE CORROSION/89, Paper No. 373, 1989.

2.35 NACE SP0290-07, "Impressed Current Cathodic Protection of Reinforcing Steel in Atmospherically Exposed Concrete Structures", NACE International, Houston, TX, 2007, p. 15.

2.36 Tinnea, J. S., and Tinnea, R. J., "Cathodic Protection Evaluation", Final Report, ODOT Contract PSK28885, Oregon Department of Transportation, Bridge Preservation Unit, Oct 2014, p. 82.

2.37 Funahashi, M. and Young, W. T., "Investigation of 100 mV Shift Criterion for Reinforcing Steel in Concrete", NACE CORROSION/92, Paper No. 193, 1992.

2.38 Takewaka, K., "Cathodic Protection for Reinforced Concrete and Prestressed Concrete Structures", Corrosion Science, Vol. 35, 1993, pp. 1617-1626.

2.39 Bennett, J. E., "Cathodic Protection Criteria Related Studies Under SHRP Contract", Paper No. 323, NACE CORROSION/93, 1993.

2.40 RILEM Technical Committee 124-SRC, P. Schiessel (ed), "Draft Recommedation for Repair Strategies for Concrete Structures Damaged by Reinforcement Corrosion", Materials and Structures, 1994, Vol. 27, pp. 415 – 436.

2.41 Watanabe, H., Hamada, H., Yokota, H., and Yamaji, T., "Long Term Performance of Reinforced Concrete under Marine Environment (20 Year of Exposure Test)", 3rd International Conference on Concrete under Severe Condition, Vancouver, Canada, 2001, pp. 530 – 537.

2.42 Dugarte, M. J. and Sagues, A. A., "Sacrificial Point Anode for Cathodic Prevention of Reinforcing Steel in Concrete Repairs: Part 1 – Polarization Behavior," Corrosion, NACE International, Houston, 70(3), 2014, pp.

303-317.

2.43 Otsuki, N., “A Study of Effectiveness of Chloride on Corrosion of Steel Bar in Concrete,” Report of Port and Harbor Research Institute (PHRI), Japan, 1985, pp. 127-134.

2.44 ASTM C 876-95, “Standard Test Method for Half-cell Potentials of Uncoated Reinforcing Steel in Concrete,” Philadelphia: American Society of Testing and Materials, 1999.

2.45 G.K. Glass, B. Reddy L.A. Clark, “Making reinforced concrete immune from chloride corrosion” , Proceedings of the Institution of Civil Engineers, Constr. Mater, 160, 2007, pp. 155–164.

2.46 Y. Schiegg, M. Büchler, M. Brem, “Potential mapping technique for the detection of corrosion in reinforced concrete structures: Investigation of parameters influencing the measurement and determination of the reliability of the method”, Mat. And Corr. 60, 2009, pp. 79–86.

2.47 G. K. Glass, N. R. Buenfeld, Chloride - induced corrosion of steel in concrete, Prog. Struct. Eng. Mater. 2, 2000, pp. 448–458.

2.48 D.R. Morgan, Compatibility of concrete repair materials and systems, Constr. Build. Mater. 10 (1996), pp. 57–67.

2.49 Concrete Society, Technical Report 22, Non-structural cracks in concrete, Surrey, UK, 2010.

2.50 Concrete Society, Technical Report 54, Diagnosis of deterioration in concrete structures, Surrey, UK, 2000.

2.51 L. Bertolini, M. Gastaldi, M.P. Pedeferri, P. Pedeferri, T. Pastore, Proceedings of the International Conference on Corrosion and Rehabilitation of Reinforced Concrete Structures, Orlando, USA, 1998.

2.52 S. Qian, D. Qu, G. Coates, Galvanic coupling between carbon steel and stainless steel reinforcements, Can. Metall. Q. 45, 2006, pp. 475-484.

2.53 G K Glass, N Davison, A C Roberts, Hybrid corrosion protection of chloride-contaminated concrete, Proceedings of the Institution of Civil Engineers, Constr. Mater. 161, 2008, pp. 163–172.

2.54 L. Bertolini, M. Gastaldi, M.P. Pedeferri, P. Pedeferri, T. Pastore,

Proceedings of the International Conference on Corrosion and Rehabilitation of Reinforced Concrete Structures, Orlando, USA, 1998.

2.55 Denka Guideline for Galvashield XP

2.56 Cicek, V., "Cathodic Protection: Industrial Solutions for Protecting Against Corrosion", John Willey & Sons, Inc., 2013.

2.57 Hobbs, D. (2001). "3rd Concrete deterioration: causes, diagnosis, and minimising risk". In: International Materials Reviews 46.3, pp. 117–144.

2.58 Bertolini, L., Elsener, B., Pedeferri,P., Redaelli, E., and Polder, R., "Corrosion of Steel in Concrete", 2013, Wiley-VCH Verlag GmBH & Co KGaA.

2.59 RILEM Technical Committee 124-SRC, P. Schiessel (ed), "Draft Recommedation for Repair Strategies for Concrete Structures Damaged by Reinforcement Corrosion", Materials and Structures, 1994, Vol. 27, pp. 415 – 436.

2.60 Bennet, J., and Turk, T., "Criteria for the Cathodic Protection of Reinforced Concrete Bridge Elements", Technical Alert, SHRP-S-359, 1994.

2.61 Bennet, J., and McCord, W., "Performance of Zinc Anodes Used to Extend the Life of Concrete Patch Repairs", 2006, Corrosion/2006, NACE International, Paper No. 06331.

2.62 Sergi, G., and Page, C., "Sacrificial Anodes for Cathodic Prevention of Reinforcing Steel around Patch Repairs Applied to Chloride-contaminated Concrete", European Federation of Corrosion Publications.

2.63 Det Norske Veritas (DNV), "Cathodic Protection Design", Recommended Practice DNV-RP-401, 2010, p. 37.

Chapter 3 DETERIORATION OF RC STRUCTURE AFTER 77-YEAR-OLD EXPOSED TO SEVERE MARINE CONDITION

3.1 Introduction

Concrete is the predominant construction type used in critical infrastructure in many countries[3.1]. Moreover, in the last decades it has become well known that the corrosion of reinforcement is the most harmful damage that occures in reinforced concrete (RC) structures. The long-term performance of concrete structures exposed in marine environments has shown that their main cause of deterioration is reinforcement corrosion[3.2), (3.3)].

The deterioration rate of such structures depends not only on the construction processes employed and the composition of the materials used but also on the environment[3.4]. Increases in the changes of temperature and humidity due to a changing climate, especially in the longer term exposed to marine environment, cause an acceleration of deterioration processes due to chloride attack and consequently acceleration in the decline of the safety, serviceability and durability of concrete infrastructure. Tropical environments which are characterized by higher values of temperature and humidity can increase corrosion risks resulting in more widespread corrosion damage and loss of structural safety.

The "great" example of such case happened in the Indonesian Port at Balikpapan city, Indonesia, where the RC structure was exposed to very aggresive

marine enviroment and tropical climate during 77 years. Nowadays, this port still utilized to loading and unloading process. The preliminary inspection performed during the investigations in November 2014 showed that the structure deterioration degree was seriously degraded and in most places at the critical level to have immediate intervention was necessary.

Hence, from the viewpoint of durability of RC structure exposed to tropical marine environment, field and experimental research to evaluate long-term of chloride induced corrosion is very important to conducted to port and harbor facilities. Moreover, this assessment will beneficial as a preliminary diagnosis before repair method is applied [3.5].

Therefore, in this chapter, a durability study of a 77 year-old concrete structure exposed to tropical marine environment and shows severe deterioration due to chloride induced corrosion is present. The limitation of initial documentary information of structure such as no information about concrete strength, cover depth, design drawing, and structure geometry information of structure elements become a challenge and a uniqueness of this study to assess the 77 year-old concrete structure accurately. Countermeasure method to repair and strengthening for extending the service life of this structure is also discussed.

3.2 Research Objective

The objectives of this study is to evaluate the deterioration and durability condition of RC structure after long-term exposed in severe tropical marine environment. To reach the general aim, the following specific objectives have been defined:

- To investigate damage occurs on the port structure elements (beam, slab and pier) under real conditions of seawater attack
- To observe condition of reinforcing steel due to chloride-induced corrosion and chloride ion distribution in concrete
- To observe microstructure condition of steel corrosion products by means of rust
- To propose the remedial recommendations to repair and strengthen the defects on the structure.

3.3 History and Location of the Structure

In this field research, one of the elderly port located at PT. Pertamina (Persero) Refinery Unit (RU) V area in Balikpapan city, Kalimantan Timur Province, Indonesia namely Indonesian Port was investigated. At this region, a typical climate is dominating with dry and rainy season all the time. The location of Indonesian Port is not straight to face to Makassar Strait wave as shown in **Fig 3.1**.

This port was built in 1937 by the Netherlands government. Nowadays, this port used by Pertamina (Perusahaan Pertambangan Minyak dan Gas Bumi Negara), an Indonesian state-owned oil and natural gas corporation. Currently, Pertamina owns six refineries and RU V in Balikpapan is one of them. The Pertamina RU V is Pertamina's second largest refinery and is located in Balikpapan, Indonesia. The refinery began operations in 1984 producing gasoline and other petrochemical products. The refinery is made up of two processing units, the primary unit and a catalytic reforming unit. Current production capacity for this refinery is 260,00 barrels per stream day. The production from this refinery supplies the eastern part of Indonesia. There are eight ports in Pertamina RU V including Indonesian Port as shown in **Photo 3.1**.

Fig 3.1 Indonesian port at Pertamina RU V area in Balikpapan, Indonesia

Photo 3.1 Position of Indonesian Port at Pertamina RU V

Most of Pertamina's port have existed since the 1930s and are still being used until now. Like many refineries, the Pertamina RU V in Balikpapan, Indonesia needs to protect its critical refinery infrastructure from the ravaging effects of a coastal environment and corrosion. **Fig 3.2** shows the climate characterization of Balikpapan. Due to proximity to equator, as same as like all the cities in Indonesia, Balikpapan has a tropical climate characterized by heavy rainfall, high humidity and high temperature all year.

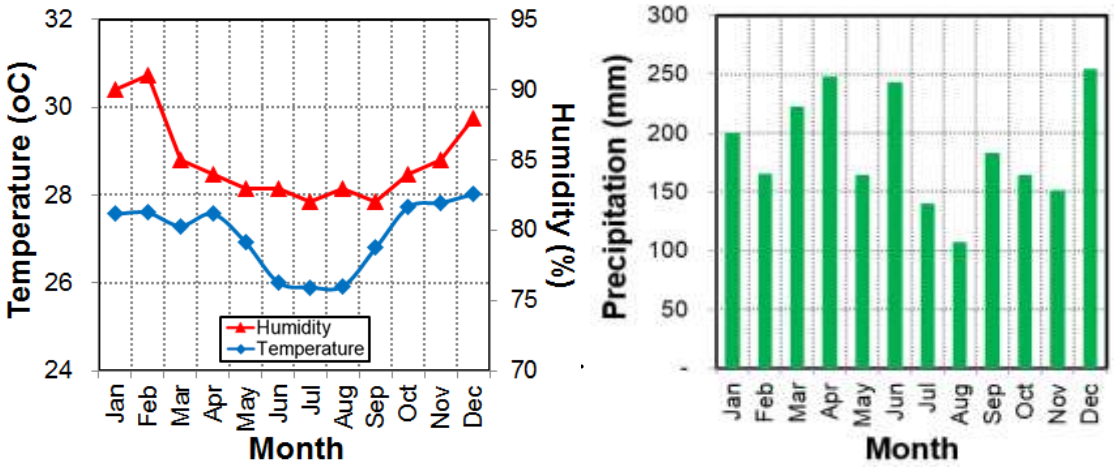

Fig 3.2 Climate characterization of Balikpapan [Source: BMKG, Indonesia]

3.4 Structure Description of the Indonesian Port

As depicted in **Photo 3.2**, this structure has 442 meters in length and has two trestles that connect the port to the land. The trestles lengths are 135 meters and 121 meters. Moreover, there are two warehouse structures which exist on the Indonesian Port to keep maritime equipment.

This structure also has face fender with frame structure type, uses round pipes as material elements and is fitted in parallel and vertical to the jetty **Photo 3.3(a)** shows the fender that is connected to the dock at several places which means it does not take dead load itself but rather transfers it to the pier structure. Originally, this port used trains in its loading equipment process. It can be seen by former lorry trails that are still visible as shown in **Photo 3.3(b)**.

Photo 3.2 The outline of the structure

(a) Face fender structure (b) Former lorry rails

Photo 3.3 Face fender structure and former lorry rails condition

Photo 3.4 Existing load condition

Currently, this port is still used by Pertamina to berth ships with a capacity of 1000-5000 of Dead Weight Tonnage (DWT). The loading and unloading process still continues on going until now as featured in **Photo 3.4**.

3.5 Investigation Method

Site investigation was conducted to assess the actual condition of the Indonesian Port through destructive test by taking core samples and non-destructive test (NDT) namely visual inspection; rebar detection; half-cell potential and carbonation test by Phenolphthalein liquid spray.

Furthermore, laboratory testing was carried out in order to measure chloride ion distribution, apparent diffusion coefficient of chloride ions in concrete and compressive strength test. The microstructures of concrete was also investigated in order to evaluate the pore size distribution by mercury intrusion porosimetry (MIP). In this study, observation of steel corrosion products by means of rust was also observed by Fluorescence Microscope.

In order to simplify the measurement and analyze the data, assessment point in Indonesian Port divided as 2 (two) areas namely area A and B as shown in **Photo 3.5**. The areas A and B are the spots to conduct the visual inspection and measure concrete cover, dimension of structure, rebar position and rebar diameter. The points 1 and 3 are the places where core samples were taken from the eastern and northern side parts of the main beam with dimension 640x1700 mm. Moreover, this beam position faces the ocean wave directly from the eastern and northern parts.

Photo 3.5 Assessment area

In addition, point 2 is the point where the core sample was taken from the upper surface of another main beam with dimension 500x550 mm. These core samples have been used to quantify the level of chloride concentration, apparent diffusion coefficient of chloride ions in concrete, determination of compressive strength, depth of carbonation, half-cell potential measurements and porosity test through MIP as well. The detail of core samples position illustrated in **Fig 3.3**.

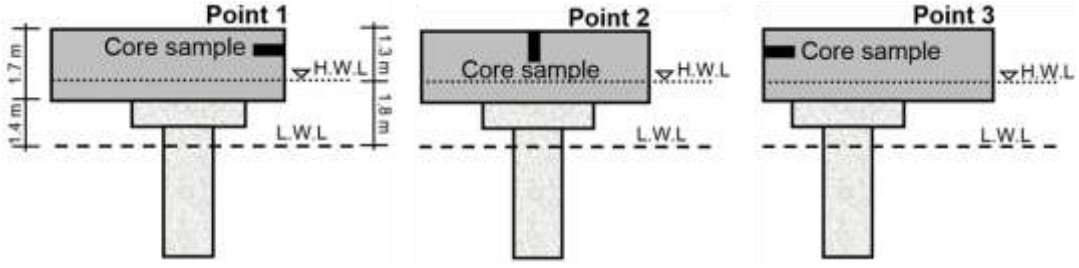

Fig 3.3 Core samples position at point 1, 2 and 3

3.6 Results and Discussion

3.6.1 Visual Inspection

Visual inspection is one of the most versatile and powerful of the NDT methods, and it is typically one of the first steps in the evaluation of a concrete structure. The

result of visual inspection is represented by using the deterioration grade for RC members in a superstructure of an open-type wharf in **Table 3.1**, provided in the Guidelines on Strategic Maintenace for Port Structures [3.5]. Deterioration grades A~D for RC members in all target structures were visually judged according to the criteria.

Table 3.1 Criteria for grading RC members of superstructure in open-type wharf from the view point of reinforcing bars' corrosion

Grade	Criteria
A	Slab: Map cracking (over 50%) Spalling off of concrete cover Heavy rust stain Beam and haunch: Crack along reinforcement with width of larger than 3 mm Spalling off of concrete cover Heavy rust stain
B	Slab: Map cracking (less than 50%) Much rust stain Beam and haunch: Crack along reinforcement with width of less than 3 mm Much rust stain
C	Slab: One directional ccrack or gel extraction Partially extended rust stain Beam and haunch: Vertical crack to longitudinal direction Partially extended rust stain
D	Nothing observed

Photo 3.6 shows about the visual condition of beam and column structures of Indonesian Port at area A in general. It is clearly seen that chipped and corroded reinforcement on the beams has large extent of rust stain and categorized as deterioration grade A. Many wide cracks also occurs and spalling on the concrete cover easily to found especially at the beams elements. The most large extent of spalling of concrete cover were found to beam structures, following by pier head and slab structures.

Photo 3.6 Port damages at area A after 77 years of exposure

Photo 3.7 illustrates the condition of Indonesian Port at area B. It was observed that there was a loss of concrete-cross section a beam with dimension 500x550 mm in the splash zone at B area around 20 cm. This means there was a loss of almost 50% of height section of this beam due to chloride attack and categorized to deterioration grade A for large extent of spalling. Moreover, heavy corroded reinforcement also clearly seen under the slab structures and pier-head of column and categorized to deterioration grade A for heavy rust stain.

Photo 3.7 Typical deterioration of point B after 77 years of exposure

It has also been observed that the western and northern part of the structure which is represented on the point 3 showed a deterioration level higher than that on the eastern and southern structures. This fact is also due to the exposure conditions. Exposure to the sun of the northern structure is fairly higher than that of the others structures. Therefore, it is exposed to higher temperatures, which leads to a quickly drying of the concrete and to a higher access of oxygen to the reinforcement. It is also known that the temperature increases the corrosion stage significantly. The higher relative humidity also causes larger accumulation of chloride in concrete. As an example, the monthly average temperature of an Indonesian port which is located in Balikpapan - Indonesia was reported as gradually above 25ºC for every month with relative humidity ranges between 82% and 91%, as described in **Fig 3.2**.

3.6.2 Dimension of Structure Elements

Due to lack of information about dimension of structure elements, dimensional measurements was conducted. Depth of concrete cover detected approximately 5 cm measured from on the top of beams structure by rebar detection tools. Size of main beam which face the position to the ocean is 640x1700 mm, another main beam under the slab structures is 500x550 mm and secondary beam is 330x400 mm. Futhermore, the pier size are 950x950 mm and 500x500 mm for the prism type and diameter 630 mm for the cylinder type.

3.6.3 Half-cell Potential

Half-cell potential (HCP) mapping for detecting corroding areas on concrete was carried out in this study. The reference electrode of the corrosion analyzing instrument system that used as a measurement tool in HCP as shown in **Photo 3.8** is a $Cu/CuSO_4$ half-cell. The grid was prepared to perform this test as depicted in **Photo 3.9**.

Photo 3.8 Half-cell potential measurement

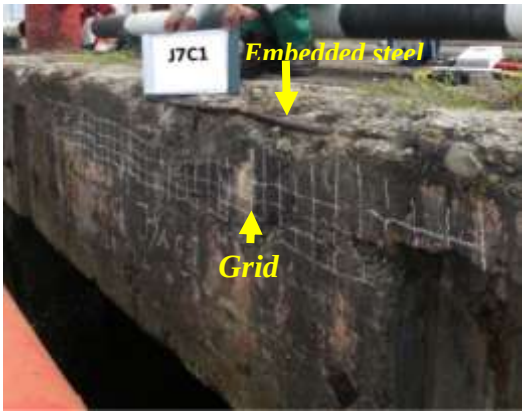

Photo 3.9 Preparation of grid system before half-cell potential measurement

Fig 3.4 shows about potential mapping in 3 measurement areas. The HCP value at the point 1 and 3 were typically in the range of -350 mV to -450 mV in areas where spalling and loss of concrete and steel-cross section had occured. Based on ASTM C876-91:1999, it can be said that there is “a 90% probability of corrosion occuring”. This was also confirmed in visual inspection in which most of the structure elements in this area certainly have been corroded. Meanwhile, potential of steel bar in area point 2 tends to positive direction. It is because location of point 2 is in atmospheric area which more drying than in the beam side of point 1 and 3. The dry condition in concrete will influence the potential value of embedded rebar.

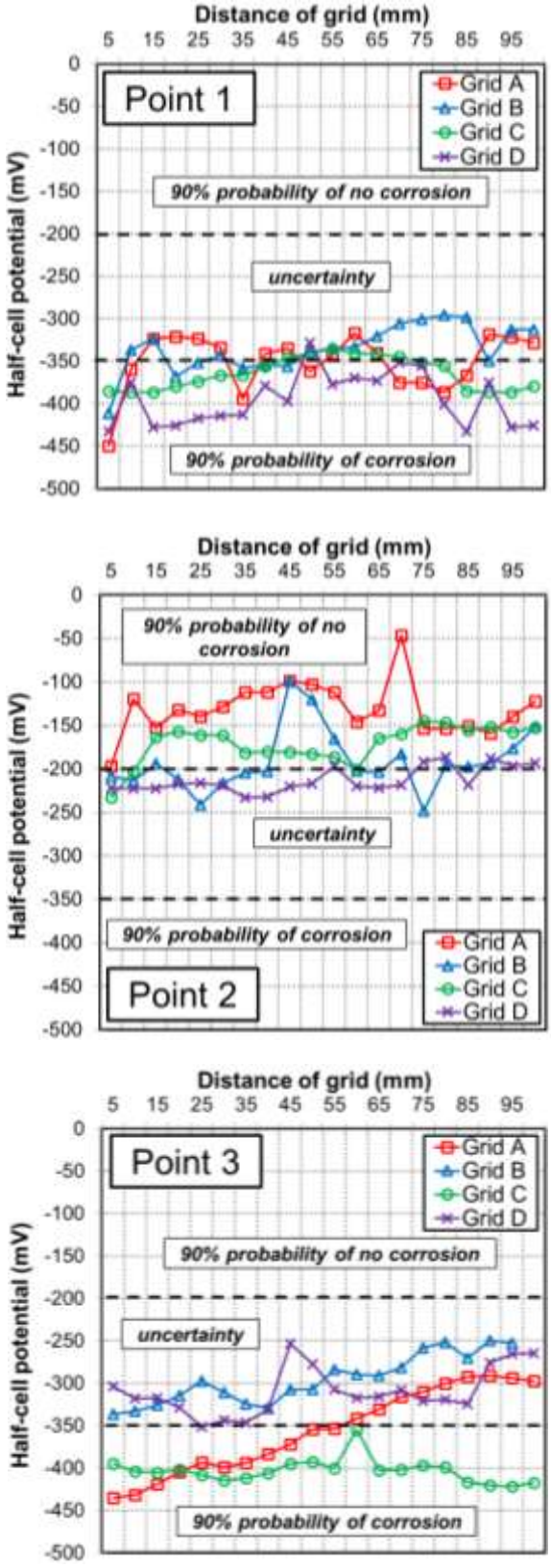

Fig 3.4 Half-cell potential at point 1, 2 and 3

3.6.4 Carbonation Test

Photo 3.10 depicts about the carbonation test conducted at point 1. Carbonation test in this study were carried out by Phenolphthalein liquid spray to the coring sample from point 1, 2 and 3. Carbonation depths were obtained 30 mm, 20 mm and 15 mm for core samples at points 1, 2 and 3 respectively. Therefore, carbonation of concrete was seen to be negligible and hence not likely to have contributed to the corrosion process and spalling of the concrete.

Photo 3.10 Phenolphthalein liquid spray at point 1

3.6.5 Compressive Strength Test

Photo 3.11 illustrates about the compressive strength test to obatin the strength caracteristic of concrete. Coring samples from point 1, 2 and 3 were tested. Regarding the compressive strength, a characteristic value of 29.98 MPa, 31.50 MPa and 27.56 MPa were obtained for the beam structures on the points 1, 2 and 3 as shown in **Fig 3.5**. Due to lack of information about initial condition of compressive strength design of concrete, it cannot be therefore assumed as satisfactory. However, if this characteristic value is compared to the specified strength that is needed for the element structure which is exposed to the marine environment, the values above were seen to be comparatively lower. Concrete in point 1 and point 3 has lower concrete strength than point 2. It was observed that concrete still can support the load bearing capacity even though in severe damage condition.

Photo 3.11 Compressive strength test

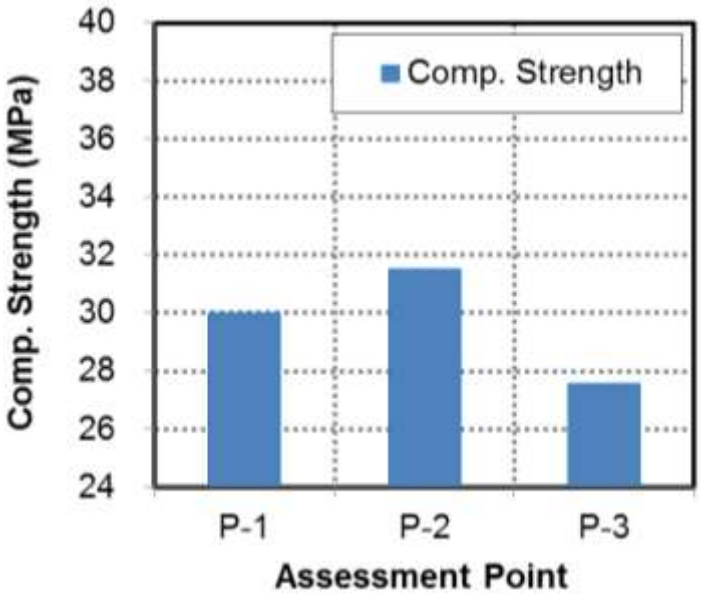

Fig 3.5 Compressive strength result

3.6.6 Chloride Ion Distribution

In order to obtain chloride ion distribution in concrete, chloride ion water solution was made from every coring sample at point 1, 2 and 3 as illustrates in **Photo 3.12**. In addition, it was continued by tittration test. **Fig 3.6** shows the result of chloride

ion distribution for all the point. The chloride concentration levels on the side and top of beam were found to have exceeded the threshold for initiation of corrosion around 1.2 kg/m^3, hence implying that the deterioration of concrete was in the active corrosion or propagation stage. Eventhough chloride level measurements were not carried out under the beams due to difficulty in obtaining samples, the fairly visible and widespread spalling of the concrete indicated that chloride levels on this area would also have exceeded the threshold. Furthermore, regarding the higher of rainfall and the cores location is exposed in a splash zone which wetting and drying cycles due to splash at high tide, so it is susceptible to the chloride washing when raining comes.

Photo 3.12 Process of chloride ion water solution

Based on **Fig 3.7**, the incremental of apparent diffusion coefficient of concrete taken from the structure (Daps) is in line with the increasing of the chloride content quantity inside the concrete. High diffusion coefficient means high chloride ingress into concrete which cause gradual durability loss of concrete.

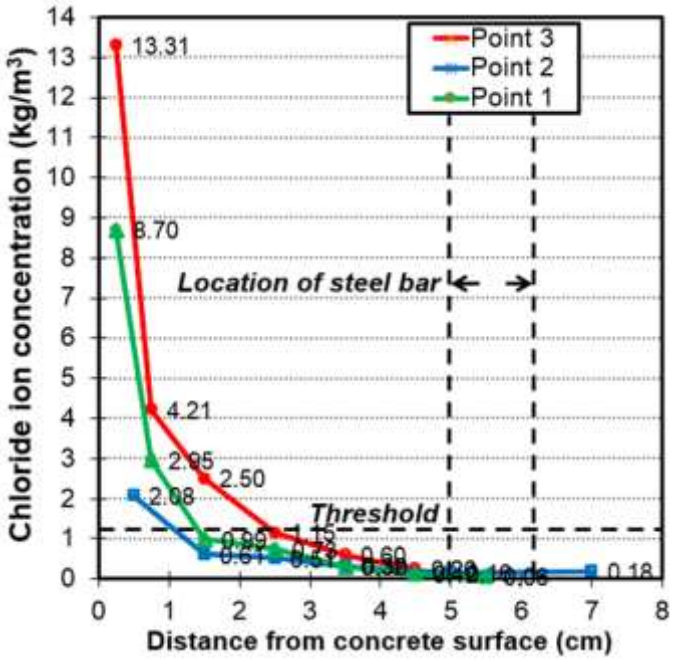

Fig 3.6 Distribution of chloride content in Indonesian Port

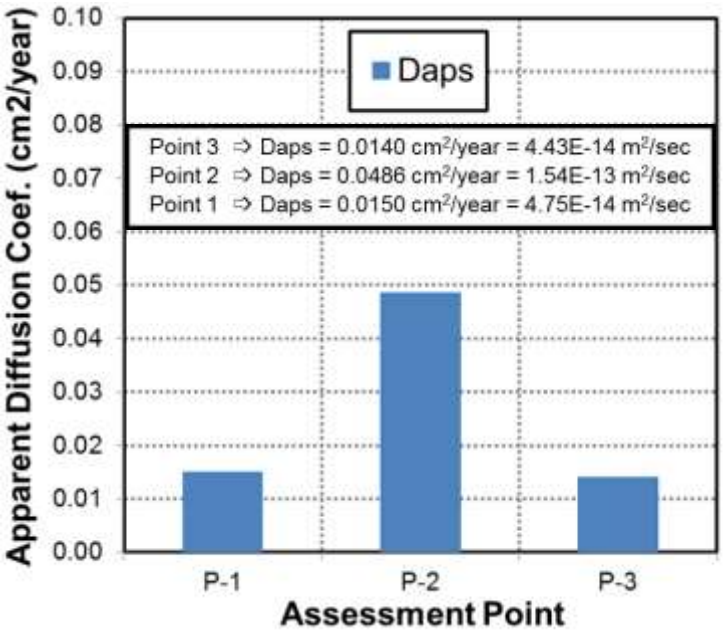

Fig 3.7 Apparent diffusion coefficient (Daps)

3.6.7 Mercury Intrusion Porosimetry (MIP)

The pore structure of concrete was measured by mercury intrusion Porosimetry as shown in **Photo 3.13** below. Total pore volume and pore size distributions of the

concrete collected at 30-40 mm depth of the specimens are shown in **Fig 3.8 (a)** and **(b)**, where porosity and pore size distribution in a certain range exhibit the same trend for all specimens. The concrete durability at point 3 (P-3) has the lower compressive strength value compared to points 1 (P-1) and 2 (P-2). However, the chloride concentrations on the concrete surface, total pore volume and pore size distributions are higher than the concrete at point 1 (P-1) and 2 (P-2).

Photo 3.13 Mercury intrusion porosimetry equipment and testing

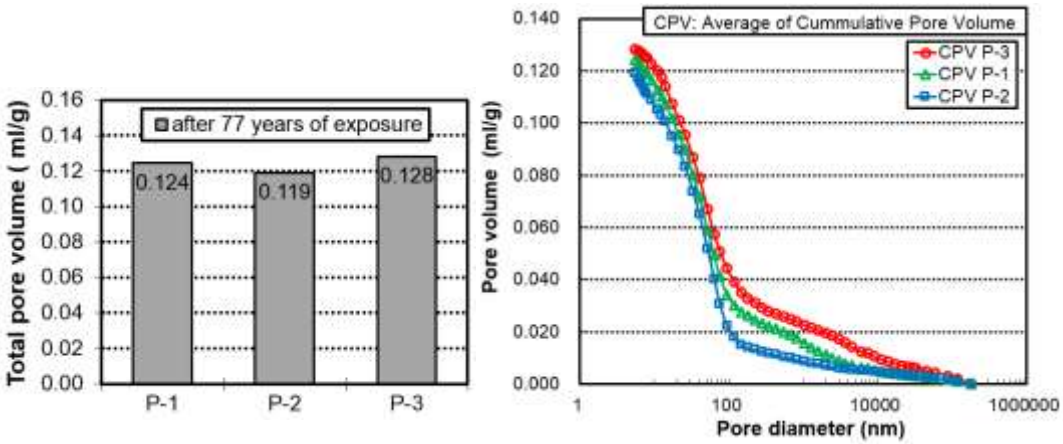

(a) (b)

Fig 3.8 Pore volume (a) and porosity of concrete (b)

3.6.8 Fluoresence Microscope

Corrosion product is composed of two different strata systems, namely micro strata and macro strata. They can be indicators of an environmental condition which has an effect on the corrosion process [3.6]. Flurescence microscope was used to observed these corrosion product. This sample (**Photo 3.14**) was taken at the beam structure on Point 3, as shown in **Photo 3.7(a)**, which already shows a loss of concrete cross-section condition. **Photo 3.15** shows the observation results of flurescence microscope. In these photos, macro strata system was clearly observed. Specifically in photo (a), the space of each layer is in order of "mm".

Photo 3.14 Deteriorated steel in concrete

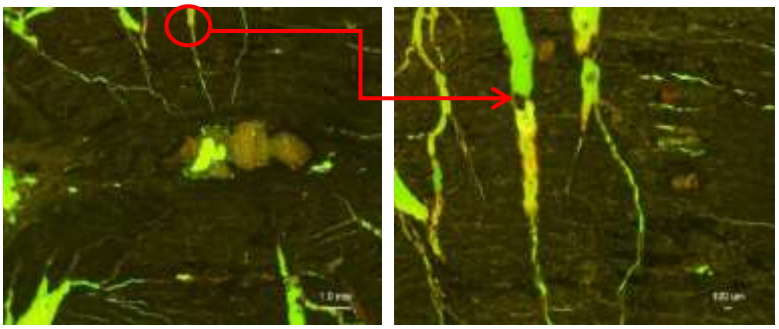

(a) (b)

Photo 3.15 Image by fluorescence microscope

Moreover, a micro size layer whose thickness is in "μm" is also clearly recognized. The layer of macro strata thickness in **Photo3.15 (a)** as certained by 25 of enlarging ratio is from 0.1 mm to 0.80 mm. Furthermore, the micro layer thickness in in **Photo 3.15 (b)** observed by 50 of enlarging ratio is obtained around 50 μm to 260 μm. This state shows that deterioration due to chloride attack in structure exposed at splash zone area can caused a damage in rebar up to layers

corrosion products. Environmental conditions also accelerate this conditions more become worst.

3.7 Service Life Prediction

For the prediction of service life of the structure for initiation of corrosion, the ingress of chloride was considered to be a diffusion process described by Fick's second law diffusion. As can be seen in **Fig 3.9**, on the chloride-ion profile of each the prediction of initiation of corrosion time was featured with respect to the surface chloride ion concentrations (C_{0s}). Initiation phase means the time required for carbon dioxide or chloride ion to penetrate the rebar level and initiate corrosion. Using the measured values of the various parameters such as the higher surface chloride ion concentrations (C_{0s}) around 13.31 kg/m^3 and concrete cover 5 cm, the time to initiation of corrosion time for the beam structure at Point 3 was estimated to be approximately 311 years.

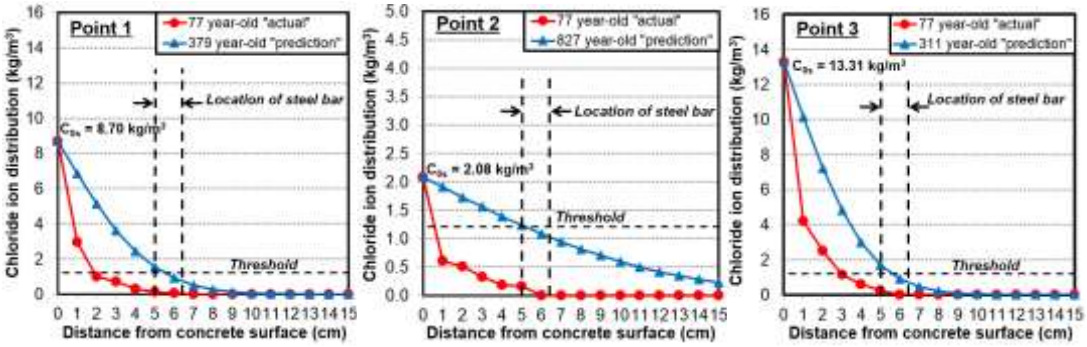

Fig 3.9 Chloride-ion profile in the present and prediction initiation time with respect to the surface chloride ion concentrations (C_{0s})

With the age of the structure being 77 year-old, it could be said the structure is still in its initiation stage. However, finding severe damages in this area through crack, the loss of concrete cross-section, loss of steel-section, spalling and exposed corroded reinforcement shown in the structure is already in the propagation and active corrosion stage. This means the chloride concentration has exceeded the threshold for initiate the corrosion and cracking of concrete cover.

3.8 Remedial Recommendations

Selection of the repair method and area in each member was dependent on the deterioration grade, chloride ion concentration at the surface of steel bar and the scale of deteriorated part [3.5]. The selection flow of repair works for port structure as shown in **Fig 3.10** [3.5].

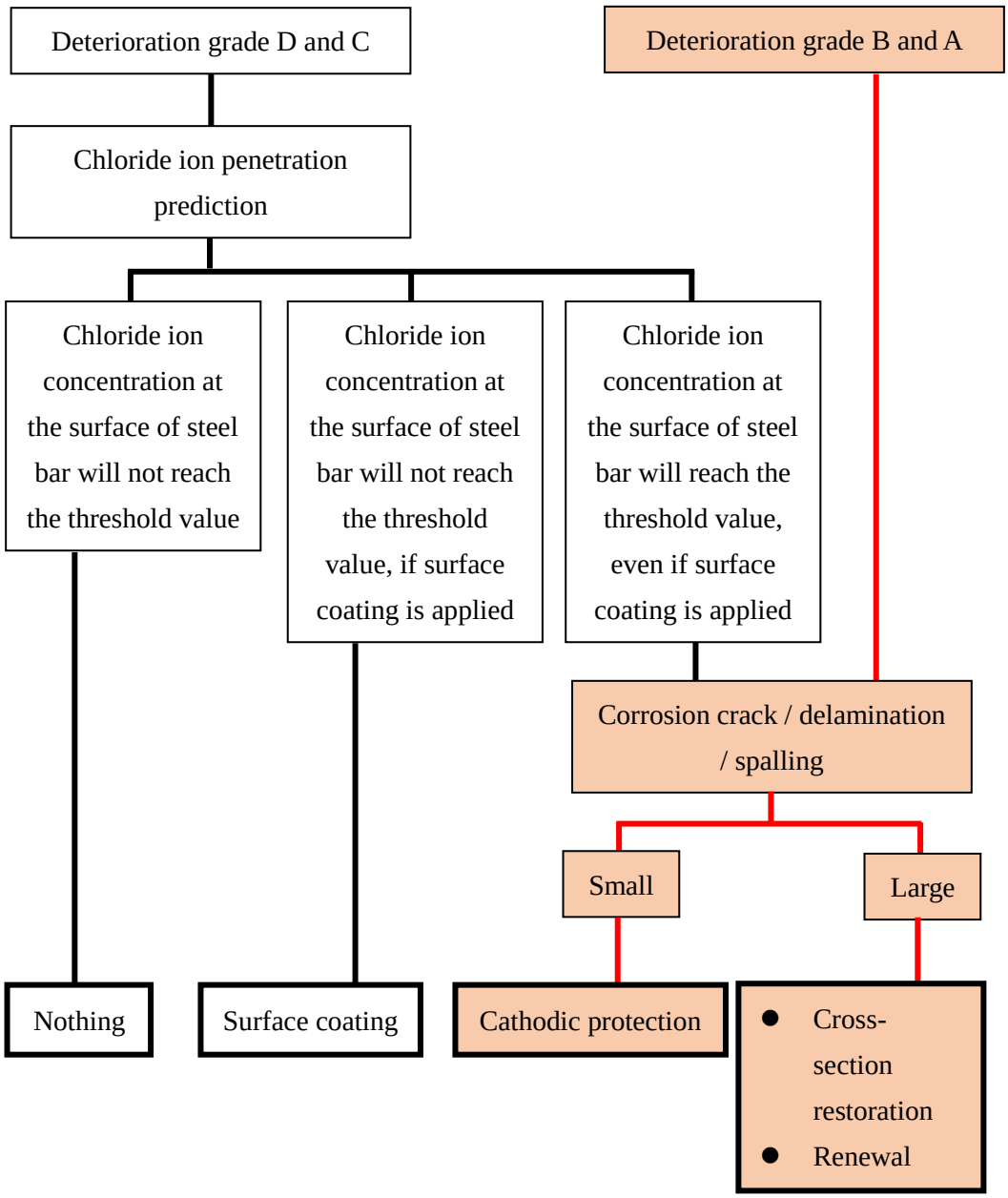

Fig 3.10 Selection flow of repair works based on deterioration grade

The rehabilitation solution for the Indonesian port structure was designed to suitably address the defects observed during the serviceability time. The necessary "immediate reactive" repair methods were proposed to address the defects that merited instant attention. Due to severe damage on structure elements at Indonesian port which has deterioration state as grade A, therefore some repair works based on deterioration grade in **Fig 3.10** (with red highlight) develop as follow:

1. Cross-section restoration for beam and column elements in order to removal deteriorated parts
2. Cathodic protection for suppression of corrosion progress and improvement of load-bearing capacity
3. Delaminated or spalled concrete repairs using the patch repair method,
4. Strengthening the pier by renewal adding new steel piles for improvement of load-bearing capacity

As a sustainable long term remedial option, the use of a cathodic protection (CP) system was proposed as "immediate reactive" repair methods. As part of a proprietary system, sacrificial anodes would be installed on the concrete beam and slab at (a) the boundary of patch repairs to protect against macro-cell corrosion, thereby mitigating corrosion of steel around patch repairs and (b) non-repaired areas which has highly negative potentials to prevent further corrosion of steel reinforcement. Further a galvanic cathodic protection system was proposed for the new steel piles, wherein a zinc point anode would be placed and corrosion would be prevented by providing an electrical current to the affected region. The installation and utilization of a cathodic protection system was seen to be the most economical alternative from a life cycle perspective.

3.9 Conclusions

The assessment of the structures referred to in this study shows that:

1. When defective concrete structures are exposed in long-term period to a tropical marine environment, very high deterioration rates can be developed leading to serious damage conditions and reduced load-carrying capacity of the structure.

2. RC structures in Indonesia have a high risk of steel corrosion in chloride-rich environment because of its proximity to the equator, which has a tropical climate with high humidity and high temperature.
3. The environmental conditions of the tropical marine climate with higher rainfall is vulnerable to the chloride washing on the concrete surface.
4. The inspections carried out showed that the principal mechanism responsible for the extensive deterioration of the structures studied is chloride-induced reinforcement corrosion. This mechanism led to broad delamination, spalling, cracking and loss of cross-section for concrete and steel reinforcement. The macro and micro strata layer on corrosion products are clearly observed due to these severe damages.
5. As a sustainable long term remedial option, the use of a cathodic protection (CP) system was proposed as “immediate reactive” repair methods.

References

3.1 Al-Rabiah, A. R., Rasheeduzzafar., and Baggott, R. "Durability Requirements for Reinforced Concrete Construction in Aggressive Marine Environments", *Marine Structures 3*, 1990, pp. 285-300.

3.2 Costa, A., and Appleton, J. “Case Studies of Concrete Deterioration in a Marine Environment in Portugal”, *Cement & Concrete Composites*, 2002, No. 24, pp. 169-179.

3.3 Castro, P., De Rincon, O.T., and Pazini, E.J. "Interpretation of Chloride Profiles from Concrete Exposed to Tropical Marine Environments", *Cement and Concrete Research*, 2001, Vol. 31, pp. 529-537.

3.4 Ragab, A. M., Elgammal, M. A., Hodhod, O. A. G., and Ahmed, T. E. “Evaluation of Field Concrete Deterioration under Real Conditions of Seawater Attack”, *Construction and Building Materials*, 2016, No. 119, pp. 130-144.

3.5 Port and Airport Research Institute (PARI)., Ocean policy Research Foundation (OPRF)., and Ports and Harbours Bureau, Ministry of Land Infrastructure, Transport and Tourism (MLIT). “Guidelines on Strategic Maintenance for Port Structures”, *ASEAN-Japan Transport Partnership*, 2011, pp. 2- 138.

3.6 Mohamed, T. U., Otsuki, N., and Hamada, H. (2003). "Corrosion of Steel Bars in Cracked Concrete under Marine Environment", *Journal of Materials in Civil Engineering*, ASCE, Vol. 15, No. 5, pp. 460-469.

3.7 Japan Society of Civil Engineers (JSCE). "JSCE Standards on Test Method for Diffusion Coefficient of Chloride Ion in Concrete", *JSCE Guidelines for Concrete*, 2004, No. 2, pp. 21-27.

3.8 Verma, S. K., Bhadauria, S. S., and Akhtar, S. (2013). "Estimating Residual Service Life of Deteriorated Reinforced Concrete Structures", *American Journal of Civil Engineering and Architechture*, Vol. 1, No. 5, pp. 92-96.

3.9 Bertolini, L., Elsener, B., Pedeferri,P., Redaelli, E., and Polder, R., “Corrosion of Steel in Concrete”, 2013, Wiley-VCH Verlag GmBH & Co KGaA

3.10 Hobbs, D., “Concrete deterioration: causes, diagnosis, and minimizing risk”. In: International Materials Reviews, 2001, 46.3, pp. 117–144.

3.11 ASTM C 876-95, “Standard Test Method for Half-cell Potentials of Uncoated Reinforcing Steel in Concrete,” Philadelphia: American Society of Testing and Materials, 1999.

3.12 Y. Schiegg, M. Büchler, M. Brem, “Potential mapping technique for the detection of corrosion in reinforced concrete structures: Investigation of parameters influencing the measurement and determination of the reliability of the method”, Mat. And Corr. 60, 2009, pp. 79–86.

3.13 G. K. Glass, N. R. Buenfeld, Chloride - induced corrosion of steel in concrete, Prog. Struct. Eng. Mater. 2, 2000, pp. 448–458.

Chapter 4 EFFECT OF NON-HOMOGENEOUS CHLORIDE ENVIRONMENT ON DURABILITY OF ZINC SACRFICIAL ANODE CATHODIC PROTECTION

4.1 Introduction

The corrosion of embedded steel in reinforced concrete has become a major problem world-wide. Corrosion prevention and repair of concrete structures will continue to be an important strategy for the rehabilitation of corrosion-damaged structures [4.1]. The repair strategies may include conventional patch repair and electrochemical treatment [4.2].

Nowadays, sacrificial anode as one of cathodic protection system is considered as one of the most effective and widely used electrochemical methods in controlling chloride-induced rebar corrosion. On a practical level, reinstating corrosion protection in concrete using sacrificial anode does not need perfect repairs; only physical damages needs to be repaired, without the need to remove a lot of chloride contaminated concrete and without perfect cleaning of steel. However, as commonly knows, many patch repair or partially-repaired concrete and their surrounding areas have exhibited new corrosion damage after a few months to a year [4.3].

Moreover in some cases, the partial repair causes to generate more local macro-cells corrosion and make the structure deteriorate more rapidly. Macro-cell corrosion with local anode and large cathode mainly occurs in chloride induced corrosion of rebar embedded in concrete and causes very local corrosion damage [4.4]. One of approaches to study the macro-cell corrosion introduced by Miyazato is segmented steel bar [4.5].

Moreover, regardless of the method of partial repair concrete, this situation may eventually create an environment characterized by a non-homogeneous distribution of chloride ions [4.6].

Regarding to the definition of macro-cell corrosion, anodic and cathodic reactions are spatially separated along the reinforcing steel. In the case of segmented-reinforcing steel embedded in concrete, when the corrosion progresses, electronic current travels from element to element through the wire connection. It is supposed that each element only represents either anode or cathode.

Since the length of steel element is different, the possibility of anodic and cathodic reactions occurring in the same element is affected. The longer the length of element is, the possibility becomes larger [4.7]. From the view point of repair method, the effectiveness of anode utilization on partially-repaired concrete is very important to investigate.

In order to contribute to a better knowledge concerning these issues, this study attempts to identify the effectiveness of sacrificial anode with respect to the effective length of embedded steel in partially-repaired concrete can protected by sacrificial anode. The results are discussed with respect to consequences for corrosion monitoring by macro-cell protective and corrosion current density, depolarization and polarization curve of embedded steel and sacrificial anode.

4.2 Research Objective

The aim of the present work is to identify the effective length of embedded steel element on partially-repaired concrete protected by sacrificial anode against macro-cell corrosion under non-homogeneous chloride environment.

4.3 Experimental Outline

4.3.1 Materials and Mix Proportions

Ordinary Portland Cement (OPC) was used in the concrete specimen. Tap water (temperature 20±2°C) was used as mixing water. Sea sand passing 5 mm sieve with density of 2.58 g/cm3 and water absorption of 1.72 % which was less than 3.5% as stated in JIS standard was used as fine aggregate. Meanwhile, crushed stone with 20 mm maximum size was used as coarse aggregate. All aggregates were prepared under surface saturated dry condition. The ratio of fine aggregate to total aggregate volume (s/a) was 0.47. The properties of aggregates and admixtures are shown in **Table 4.1**. In addition, a sacrificial anode with 60 mm in diameter and 30 mm in thickness was used as shown in **Photo 4.1**. Furthermore, the composition of concrete mixing proportions as described in **Table 4.2**.

Table 4.1 Materials properties

Component	**Physical properties**	
Ordinary Portland Cement	Density, g/cm^3	3.16
Fine Aggregate	Density, g/cm^3 (SSD Condition)	2.58
	Water absoption (%)	1.72
	Fineness modulus	2.77
Coarse aggregate	Density, g/cm^3	2.91
AEWR agent	Polycarboxylate ether-based	
AE agent	Alkylcarboxylic	

(b) Appearance of anode

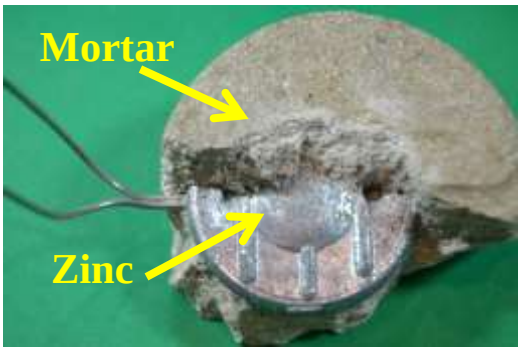

(a) Material of anode

Photo 4.1 Zinc sacrificial anode

Table 4.2 Concrete mix proportions

Material	Existing Concrete		Repair Concrete
	Series N4	Series N10	Series N4, N10
Water-cement ratio (w/c), %	45	45	45
Sand-aggregate ratio (s/a), %	47	47	47
Water, kg/m^3	190	190	190
Cement (B), kg/m^3	422	422	422
Sand, kg/m^3	766	766	766
Gravel, kg/m^3	970	970	970
Chloride, kg/m^3	4	10	-
Additive:			
- AE, mL	B*0.45%		B*0.45%
- AE-WR, gr	2.5mL/kg-B		2.5mL/kg-B

4.3.2 Specimen Geometry

Four concrete specimens with 150x100x795 mm in dimension were prepared in this study to identify the effective length of segmented steel reinforcement element, which is embedded under non-homogeneous chloride environment, namely N41, N42, N101 and N102. Each concrete specimens contained a segmented steel bars connected with sacrificial anode (SCP), a segmented steel reinforcement without connection sacrificial anode (SNCP) and a steel bar without segmented and without sacrificial anode (S) positioned in parallel with an in-between distance of 35 mm.

Three of bars have a clear cover thickness of 30 mm from the bottom surface of specimen. It was also ensured that the segmented steel reinforcement showed no sagging in order to maintain a constant cover thickness along the total exposure length. Series N41 and N101 consist of one segmented rebar 75 mm length in repair concrete. Meanwhile, N42 and N102 consist of two segmented 75 mm length in repair concrete which mean 150 mm in total. The length of the element gradually increases from 75 mm to 100 mm. The detail of the concrete specimen are depicted in **Fig 4.1**.

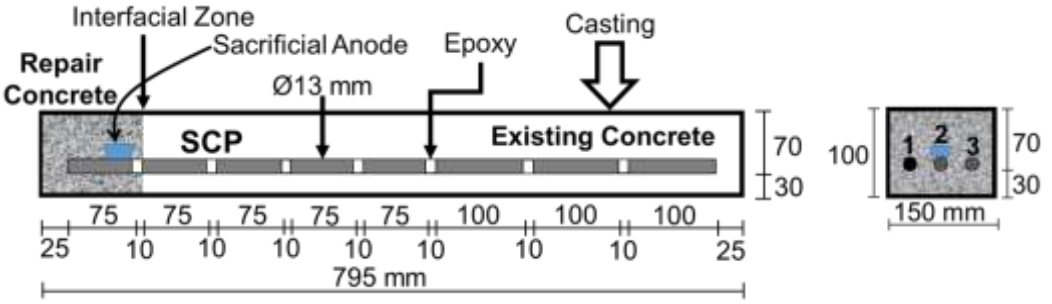

(a) N41 and N101 series geometry

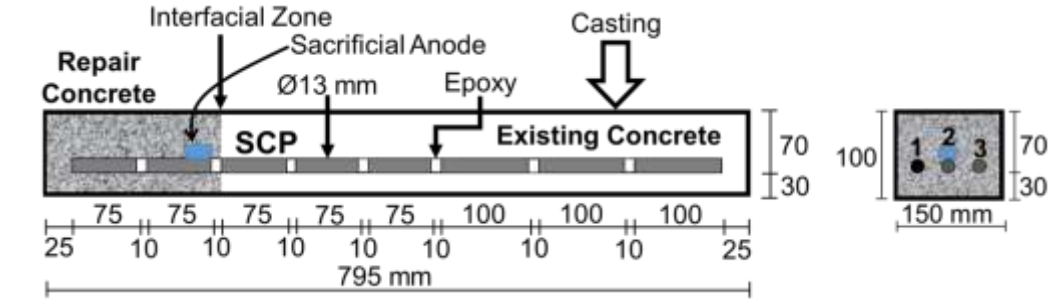

(b) N42 and N102 series geometry

Remark:
1 = S = Single rebar
2 = SCP = Segmented-rebar **with sacrificial anode**
3 = SNCP = Segmented-rebar without sacrificial anode

Fig 4.1 Detail layout of concrete specimen (in mm)

4.3.3 Segmented Steel Bar

A plain steel bar having a diameter of 13 mm was used as segmented and non-segmented embedded steel. There were two types of segmented steel bars with different length of element as shown in **Fig 4.1** and **Table 4.3**.

From the material aspect, the steel bar was separated by steel elements, however on the view of electrical aspect, it was assumed to be continuous by using lead wire connection. At both ends of each element, a 30 cm length lead wire was screwed. The elements were bonded by epoxy resin such that no direct electrical connection exist between the elements except through the wires. The thickness of epoxy layer between two adjacent elements was approximately 10 mm. This condition as described in **Photo 4.2**.

Table 4.3 The number of segmented steel bars

Specimen	Length of Element (mm)	Number of Element (n)	Position in the Concrete	Chloride Content (kg/m^3)
N41	75	1	Repair	-
	75	4	Existing	4
	100	3	Existing	4
N101	75	1	Repair	-
	75	4	Existing	10
	100	3	Existing	10
N42	75	2	Repair	-
	75	3	Existing	4
	100	3	Existing	4
N102	75	2	Repair	-
	75	3	Existing	10
	100	3	Existing	10

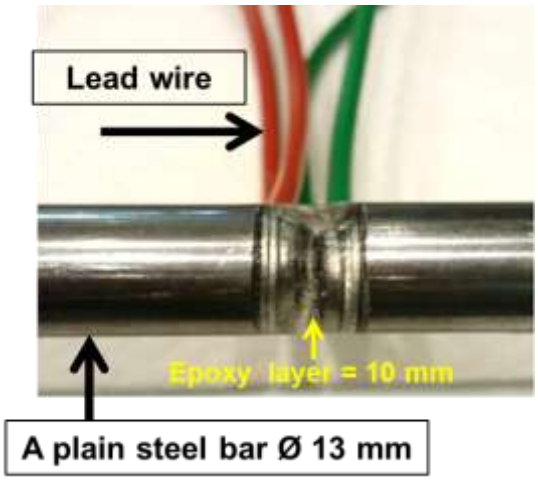

Photo 4.2 Condition of connection on each segmented steel bar

4.3.4 Casting and Curing

Casting of concrete specimens with non-uniform chloride ion concentrations was carried out in two steps. Firstly, casting of existing concrete with chloride contamined in the molds and demolded after 24 hours. After demolding, all specimens were subject to 14 days of sealed curing with wet towels. Secondly,

before placing repair concrete in the molds, sacrificial anode was installed on the steel bar as figures in **Photo 4.3**.

Furthermore, followed by casting the repair concrete, demolded after 24 hours and were kept to 28 days of sealed curing again with wet towels. After 28 days of sealed curing, sacrificial anode connected to lead wires on the segmented steel in repair concrete, so current flows to existing concrete was started. Adjacent steel elements were connected through wires to allow the flow of current. However, these connectors were temporarily disconnected for the purpose of measuring macro-cell and protective currents.

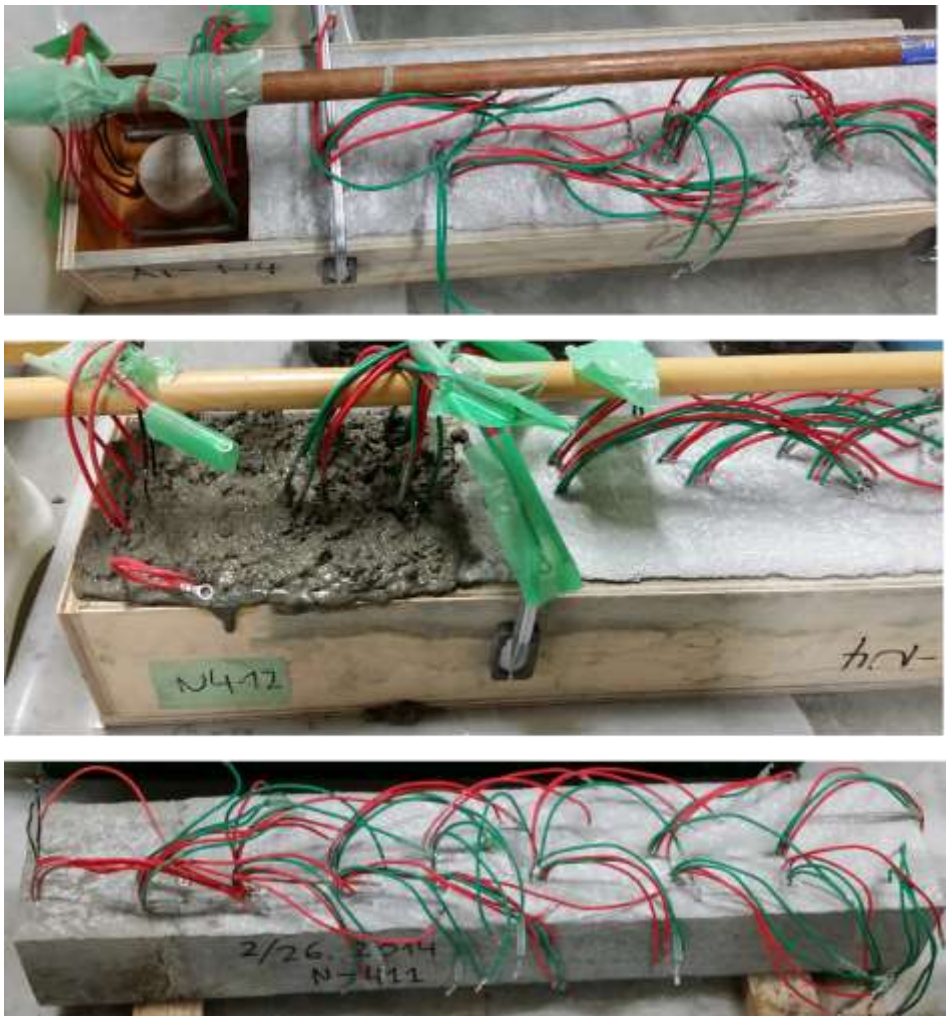

Photo 4.3 Process of casting

4.3.5 Exposure Condition

After existing and repair concrete casting was finished, all specimens were subject to exposure conditions in the form of wet-and-dry cycling. Wet cycle means immersion in 3% NaCl solution through two days followed by five days of dry condition; hence one cycle corresponded to seven days. At the end of dry cycle, measurements were taken weekly. Continuous cyclic exposure condition was maintained throughout.

Photo 4.4 Exposure condition

4.4 Experimental Method

In order to observe performance of segmented steel with sacrificial anode embedded in partial repaired concrete, several electrochemical investigations were conducted. However, this paper focuses on to present about macro-cell corrosion and protection current density, depolarization test and anodic polarization curve testing. Macro-cell corrosion and protective current measurement was carried out periodically once a week at the end of dry cycle by using a data logger. In macro-cell corrosion, a divided steel bar is used to measure the actual macro-cell currents passing through one steel element to the adjacent element as represented in **Fig 4.2**. Depolarization test was regularly carried out by disconnecting the steel bars from sacrificial anodes for 24 hours. In addition, it was continued by anodic-cathodic polarization curve which was conducted in order to determine the conditions of

passivity film of steel bars.

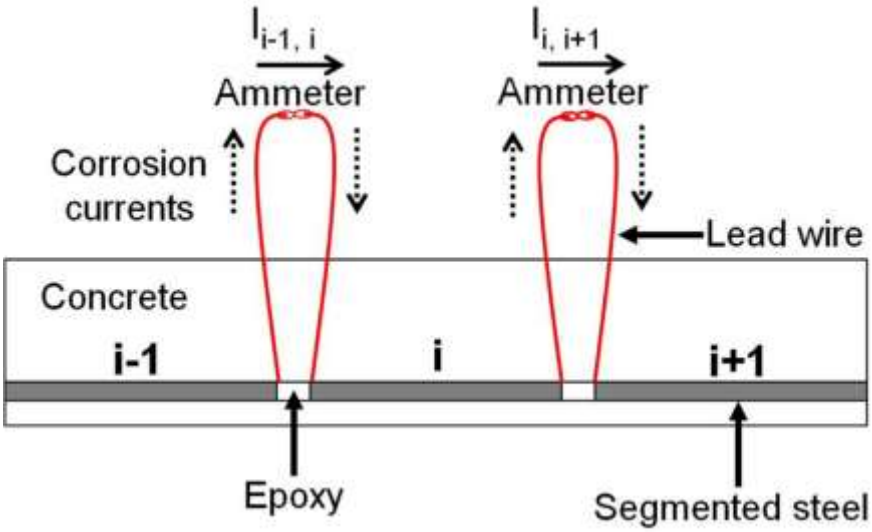

Fig 4.2 Method of macro-cell corrosion current measurement

4.5 Results and Discussions

Compressive strength of concrete at 28 days were 48.00 and 41.70 MPa for 4 and 10 kg/m^3 of chloride content respectively. Moreover, 50.97 and 48.67 MPa at 91 days for 4 and 10 kg/m^3 of chloride content respectively.

4.5.1 Macro-cell Current Density

A. One-steel bar element in repair concrete (N41 and N101)

Macro-cell corrosion current density of specimens with non-uniform chloride concentrations were measured periodically by using zero resistance ammeter as shown in Fig. 2. The following equation was used to calculate the macro-cell current density over a steel element [4]:

$$I_{mac} = \frac{I_o - I_i}{A} \qquad (4.1)$$

where I_{mac} = macro-cell current density of a steel element (μA/cm^2); I_o = outflow current in μA from the steel element; I_i = inflow current in μA to the steel element; and A = surface area of the steel element (cm^2). If the value of I_{mac} is positive, the steel element is defined as an anode, and if negative as a cathode.

The macro-cell corrosion current density on anode at N41 and N101 with one-steel bar element in repair concrete against the distance from edge of repair concrete are present in **Fig 4.3**. Macro-cell corrosion current density is found in relatively early age, and is disappeared in relative later age. This time dependent behavior is observed for both of specimens. The figures also show that macro-cell corrosion was formed coupling between the steel element located at chloride contaminated existing concrete as an anode and other steel elements as cathode. It was also observed that macro-cell corrosion was formed coupling in the boundary between chloride free concrete as an anode and its surrounding chloride contaminated as cathode, in the early age of exposure period.

B. Two-steel bar element in repair concrete (N42 and N102)

Fig 4.4 illustrate the macro-cell corrosion current density on anode at N42 and N102 with two-steel bar element in repair concrete against the distance from edge of repair concrete. In the case of N42, even at 182 days of exposure, macro-cell corrosion was formed coupling in the boundary, and also in the existing concrete. In N102 specimen, at early age of exposure, macro-cell current occurred. In general, both of N42 and N102 specimens show the same tendency with N41 and N101, wherein the macro-cell corrosion current density tends to change over the exposure time at the interfacial zone of non-homogenous chloride environment.

4.5.2 Macro-cell Protective Current Density

A. One-steel bar element in repair concrete (N41 and N101)

The periodic macro-cell protective current density on anode with one-steel bar element in repair concrete against the distance from edge of repair concrete is shown in **Fig 4.5**. It was also observed that protective current still flow up to 672-day from steel bar in patch repair concrete to segmented steel bar in existing concrete. The current flow is ~8 $\mu A/cm^2$ for N41 and ~0.2 $\mu A/cm^2$ for N101 at 672 days of polarization time. It means the throwing current of anode fulfill the cathodic protection current design.

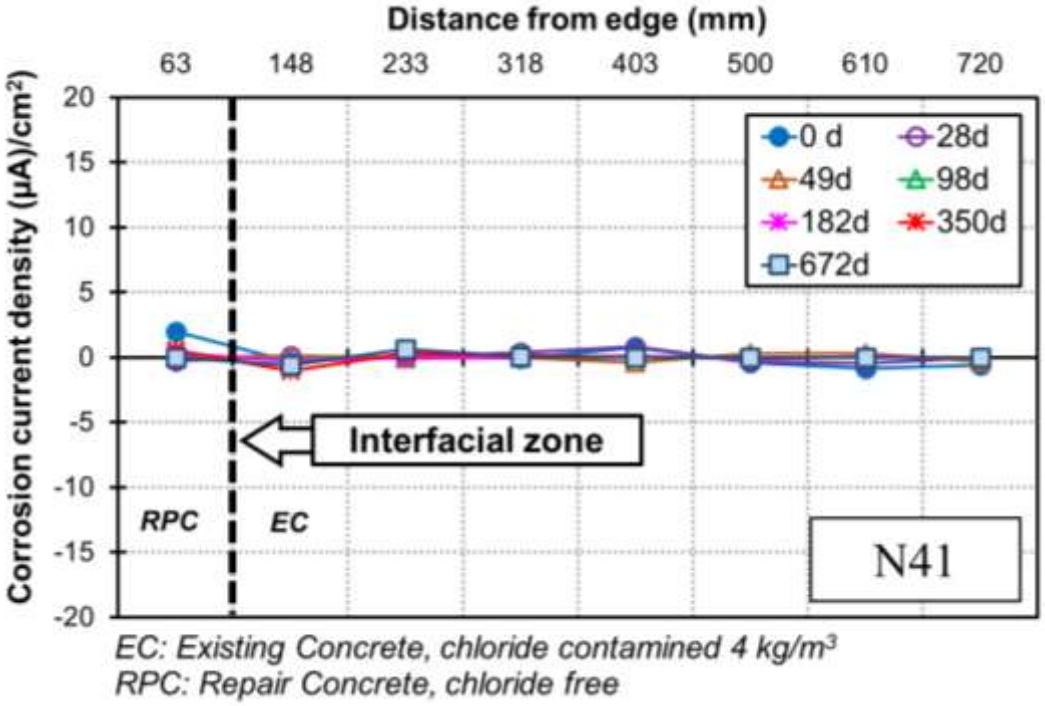

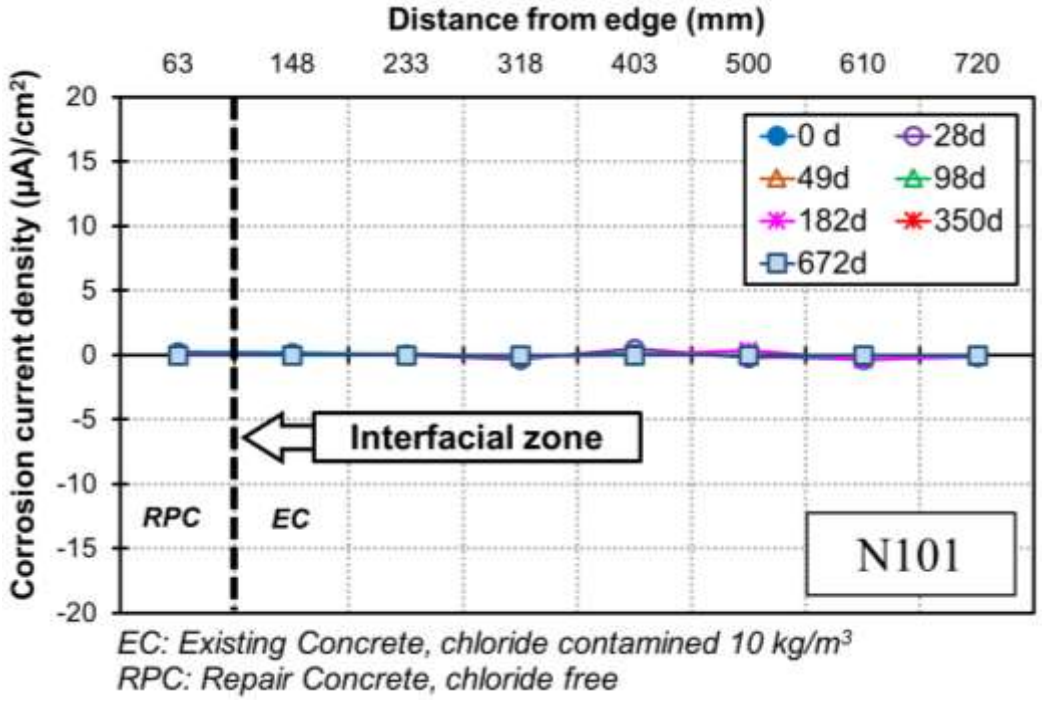

Fig 4.3 Macro-cell corrosion current density on SNCP of N41 and N101

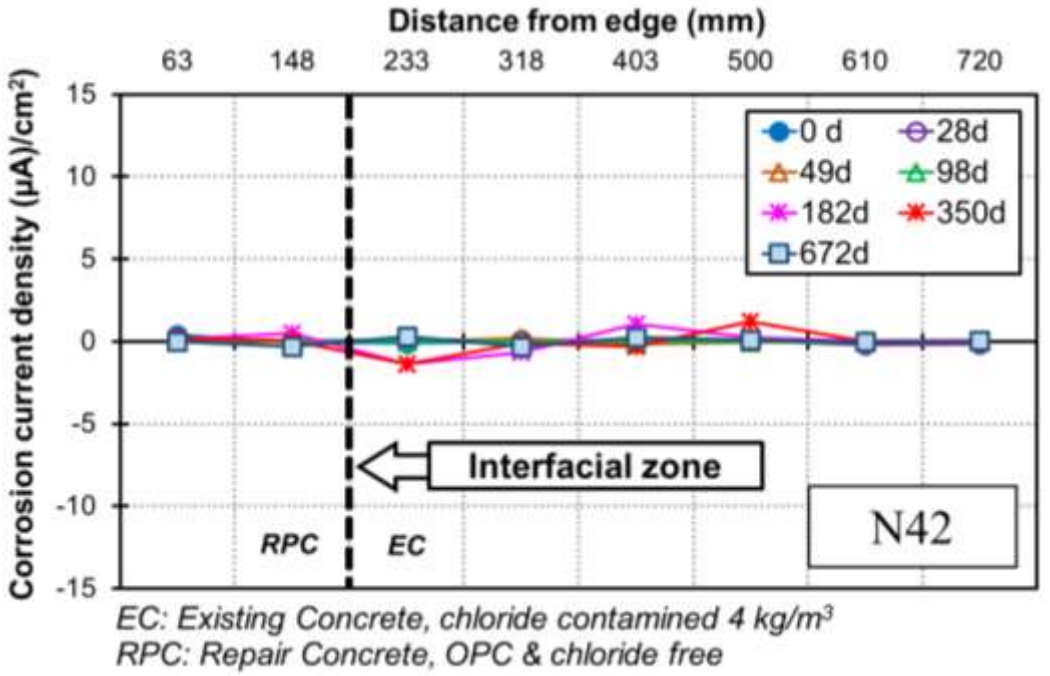

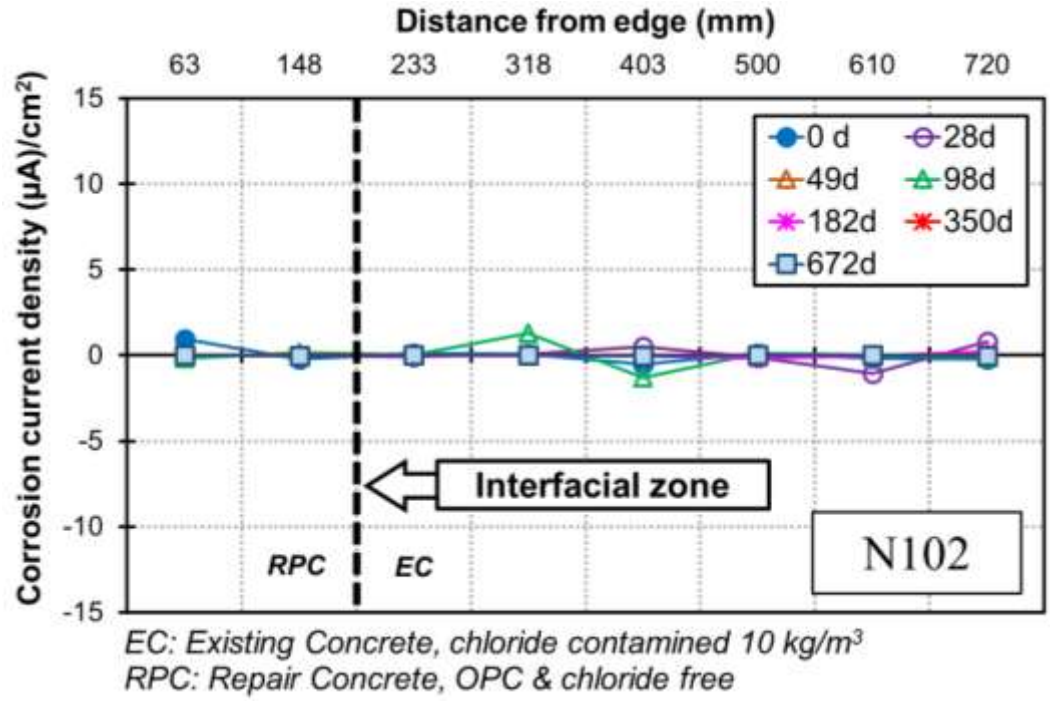

Fig 4.4 Macro-cell corrosion current density on SNCP of N42 and N102

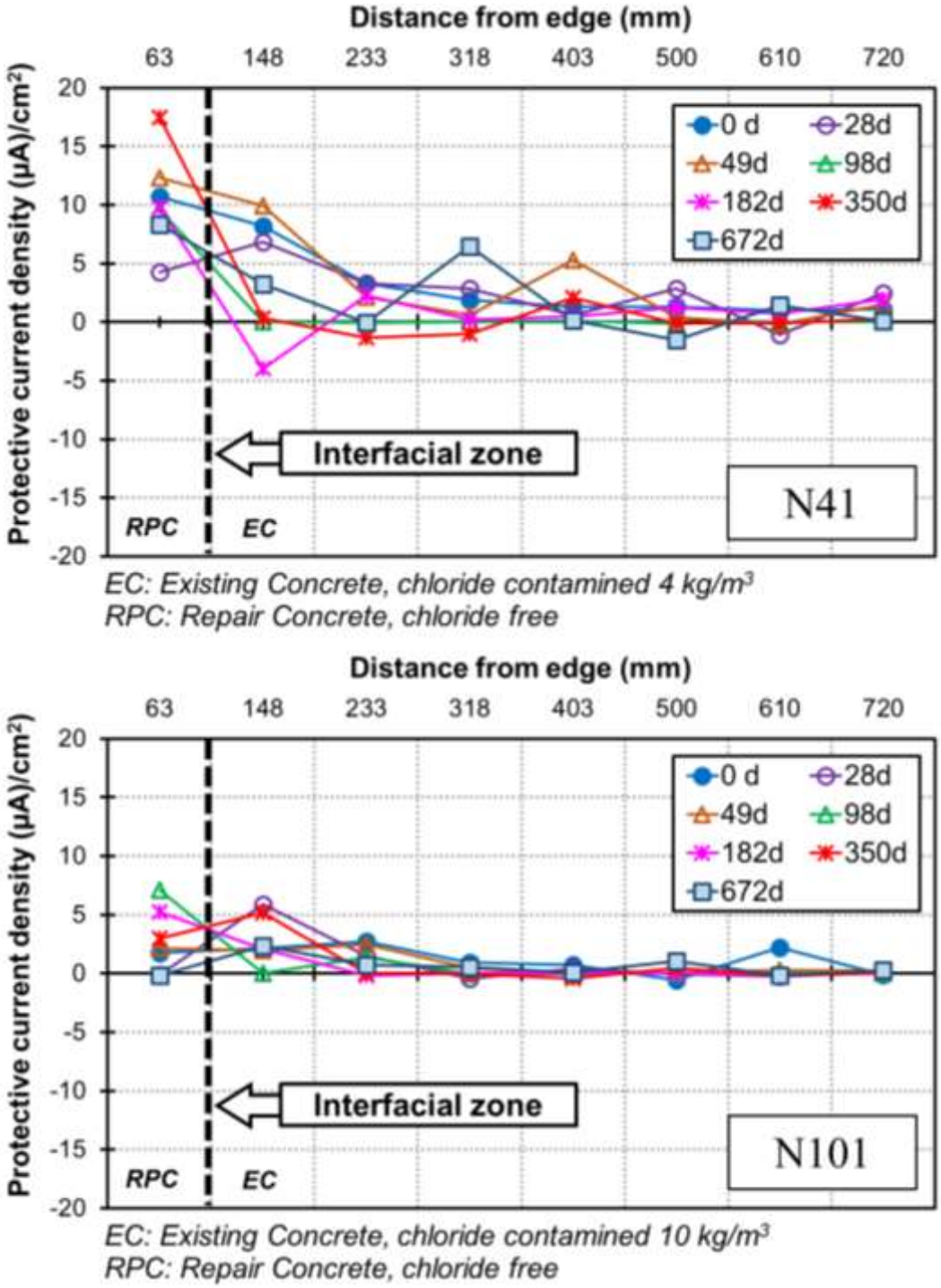

Fig 4.5 Macro-cell protective current density on SCP of N41 and N101

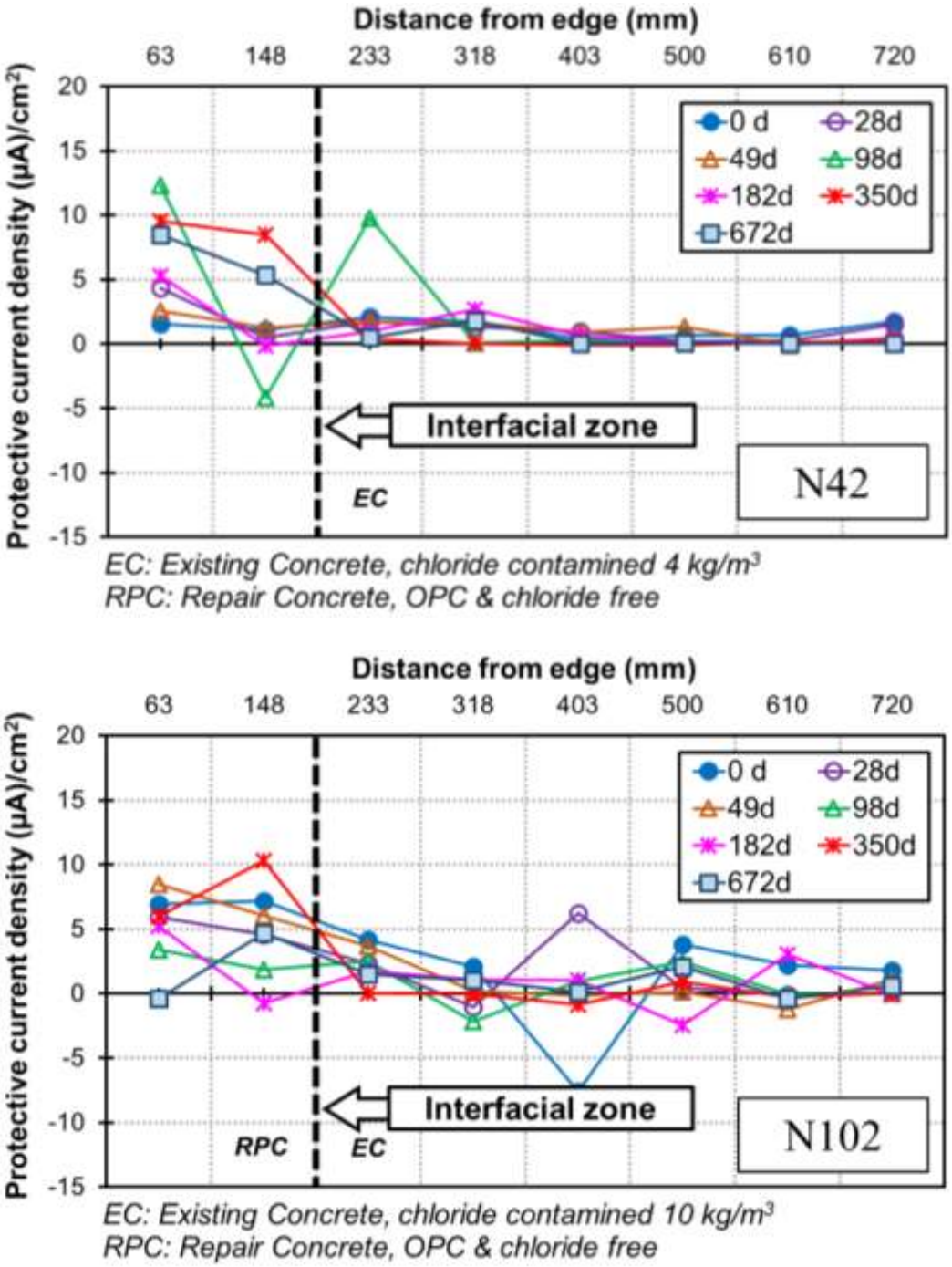

Fig 4.6 Macro-cell protective current density on SCP of N42 and N102

B. Two-steel bar element in repair concrete (N42 and N102)

The periodic macro-cell protective current density on anode with two-steel bar element in repair concrete against the distance from edge of repair concrete is depicts in **Fig 4.6**. It was observed that protective current still flow up to 672-day from steel bar in patch repair concrete to segmented steel bar in existing concrete. The current flow is ~8 $\mu A/cm^2$ for N42 and ~0.39 $\mu A/cm^2$ for N102 at 672 days of polarization time. It means the throwing current of anode fulfill the cathodic protection current design.

4.5.3 Polarization of Steel

A. One-steel bar element in repair concrete (N41 and N101)

Fig 4.7 illustrates about the evolution of instant-off potential of steel bar embedded in N41 and N101 specimen. The data shown that anode polarize steel bar in patch repair concrete of N41 more negative -1000 mV at 672 days of exposure time. Meanwhile, the potential of steel bar increased to noble value at steel bar position around 230 mm from the edge.

Furthermore, anode in N101 also polarize the steel bar in patch repair concrete in protection condition up to 672 days of exposure time. However, this potential value increased to positive direction in the existing concrete.

B. Two-steel bar element in repair concrete (N42 and N102)

Fig 4.8 depicts about the instant-off potential of steel bar embedded in N42 and N102 specimen. The data shown that anode polarize steel bar in repair concrete of N42 more negative -900 mV at 672 days of polarization time. Meanwhile, the potential of steel bar increased to noble value at steel bar position around 310 mm from the edge.

Nevertheless, anode in N102 also polarize the steel bar in patch repair concrete by -700 mV up to 672 days of exposure time. However, this potential value increased to positive direction in the existing concrete as same as like SCP-N41 and SCP-N101.

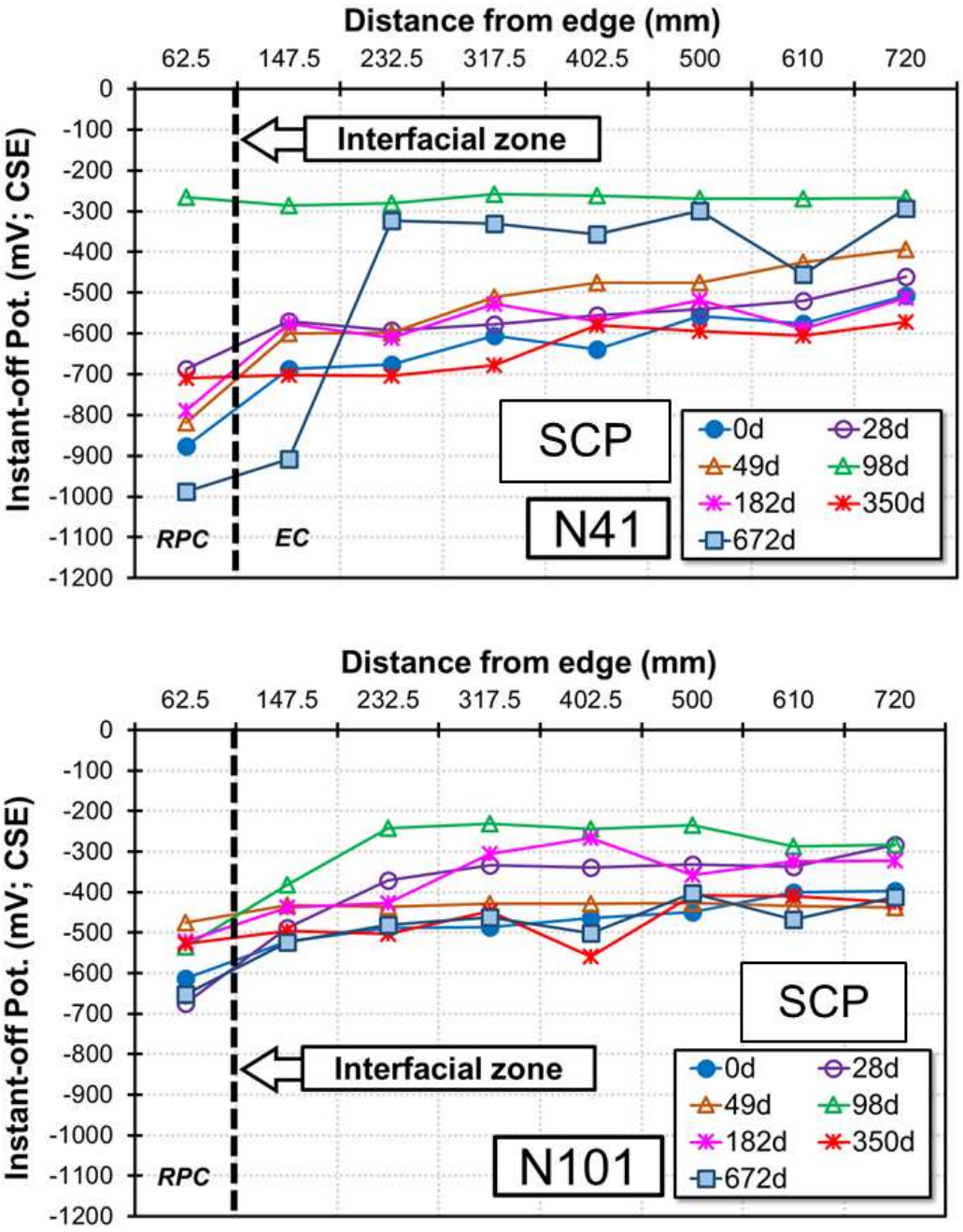

Fig 4.7 Potential of SCP of N41 and N101

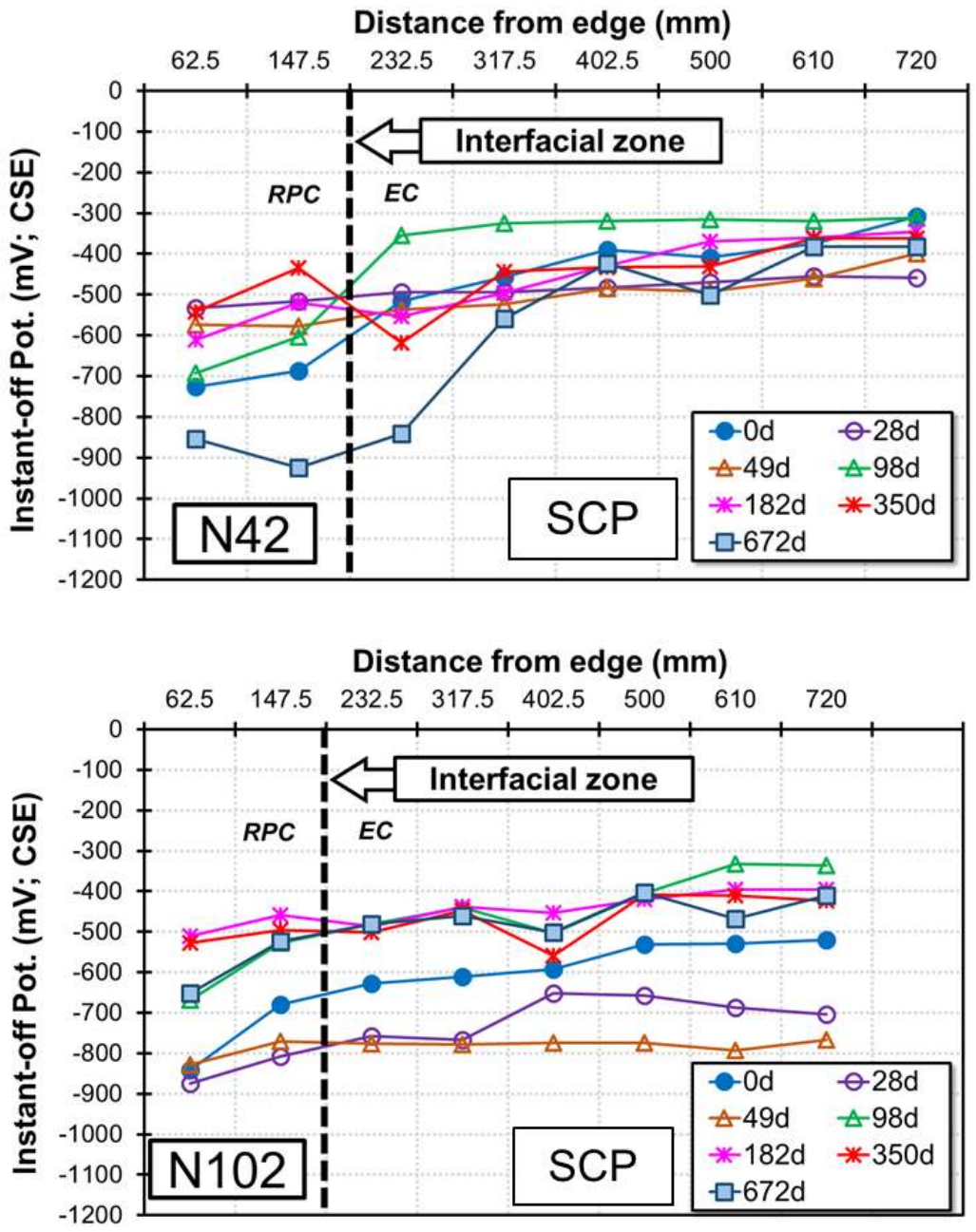

Fig 4.8 Potential of SCP of N42 and N102

4.5.4 Depolarization of Steel Bar

Depolarization tests were regularly carried out by disconnecting the steel bars from the sacrificial anode for 24 hours. Instant off potentials was measured immediately

after disconnection of the sacrificial anodes (E_{off}) and the potential values was measured after 24 hours (E_{off},24h). The commonly used criterion for sufficient protection is 100 mV (the difference of E_{off},24h and E_{off}).

Fig 4.9 illustrates the depolarization test of N41 and N101 on SCP against the distance from edge of repair concrete. Meanwhile, **Fig 4.10** illustrate the depolarization test on SCP at N42 and N102 specimens. From these figures, it was observed that the potential decay decreases as the exposure time increases. The data from **Fig 4.9** shown that potential decay exceed 100 mV for SCP-N41 and SCP-N101 around 403 mm and 318 mm respectively from the edge of specimen at 350 days. Or around 340 mm and 216 mm from the anode position in patch repair concrete for SCP-N41 and SCP-N101 successively. This distance decreased significantly at 672 days of polarization time, reaching 170 mm from the interfacial zone for SCP-N41 and SCP-N101.

Meanwhile, the data from **Fig 4.10** indicates that potential decay exceed 100 mV for SCP-N42 and SCP-N102 around 500 mm and 318 mm respectively from the edge of specimen at 350 days, it means around 440 mm and 260 mm from the anode position in patch repair concrete for SCP-N42 and SCP-N102 successively. This distance fell significantly at 672 days of polarization time for SCP-N42 by reaching 260 mm from the interfacial zone for SCP-N42. However, the effective length for SCP-N102 kept constant by 260 mm with polarization time.

Based on 100 mV CP criterion and as shown in **Fig 4.11**, it was observed that the effective length of embedded steel with sacrificial anode protection and 4 kg/m^3 of chloride content in existing concrete are 340 mm for one-steel bar and 440 mm for two-steel bar from the anode position in patch repair concrete at 350 days of polarization time. Meanwhile, for 10 kg/m^3 chloride content in existing concrete, the effective length from the anode location are 260 mm and 170 mm for one-steel bar and two-steel bar element in repair concrete respectively. It means, up to one-year of exposure time, the higher chloride content in existing concrete, the shorter effective length could be achieved.

Meantime after 672 days of polarization time, the effective length was stand up to 170 mm from the anode position in patch repair concrete for N41 and N101,

in addition around 260 mm for N42 and N102. It means anodic site increases time-dependently in parent concrete mainly for N41, N42 and N101. It was noticed that after two-year of exposure time, effective length of embedded steel element on partially-repaired concrete protected by sacrificial anode against macro-cell corrosion under non-homogeneous chloride environment is 170 mm.

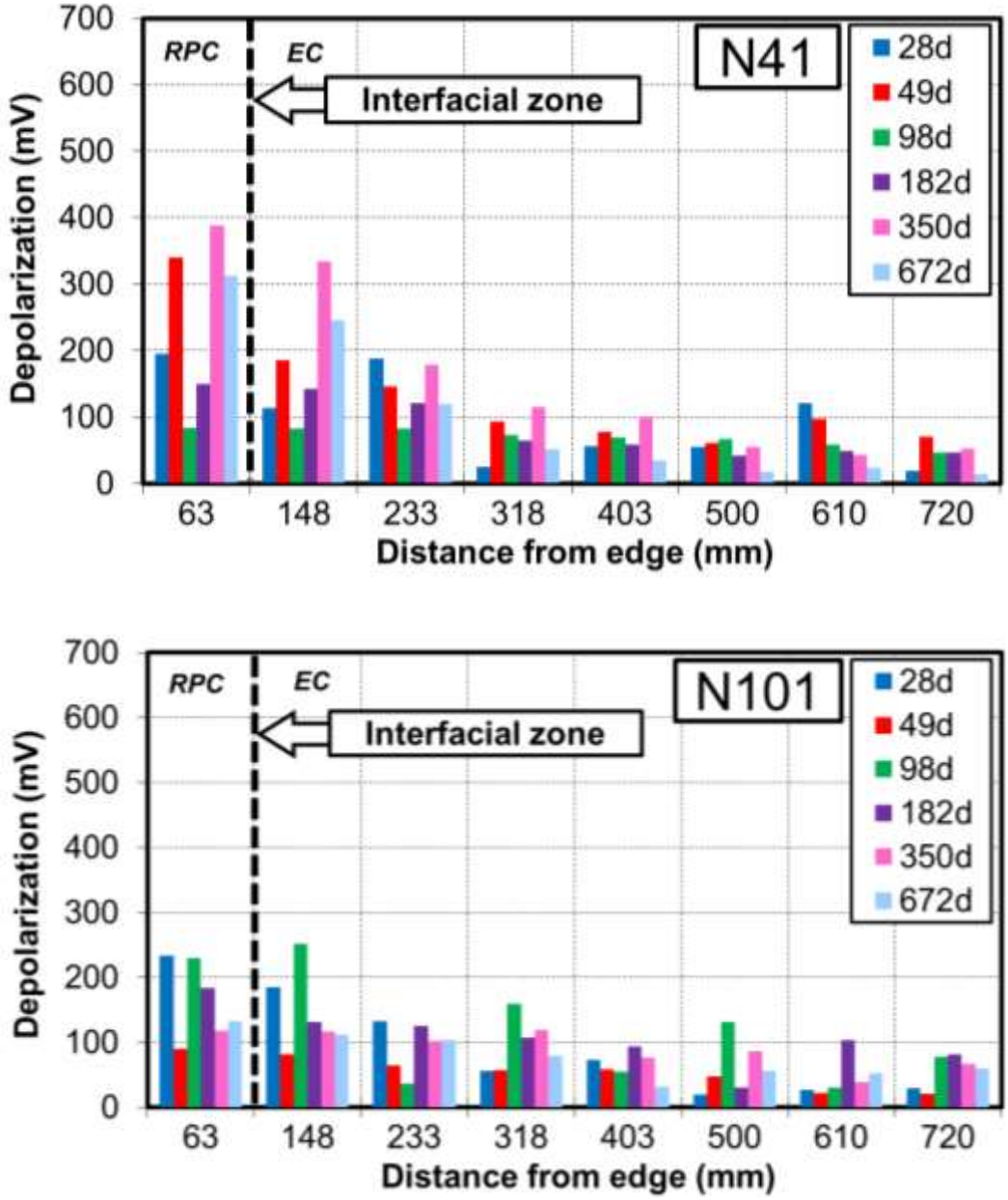

Fig 4.9 Summary of 24-h depolarization test result of steel bar with time for N41 and N101

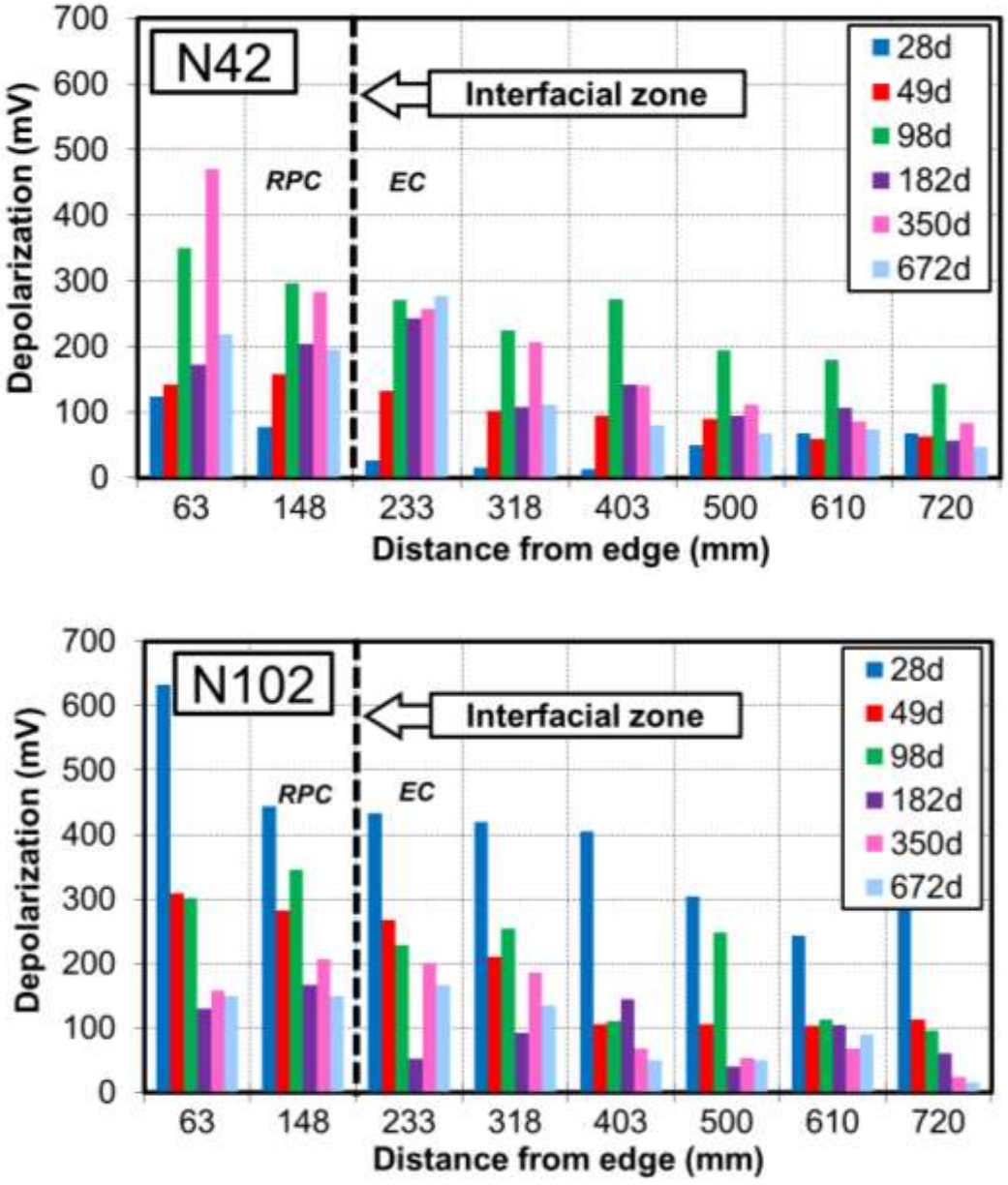

Fig 4.10 Summary of 24-h depolarization test result of steel bar with time for N42 and N102

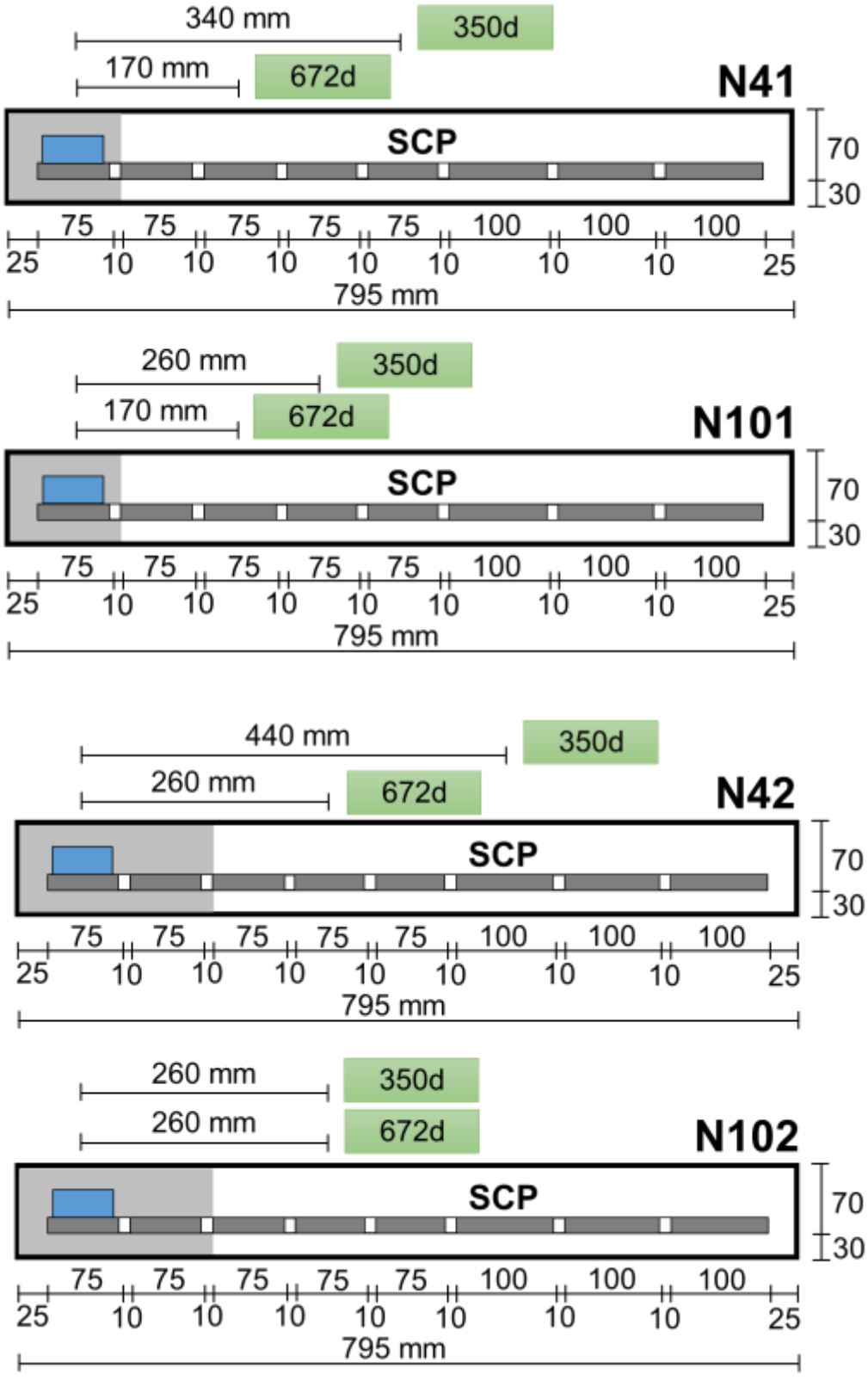

Fig 4.11 Effective length of embedded steel with sacrificial anode protection

4.6 Conclusions

Identification of the effective length on embedded steel element in partially-repaired concrete protected by sacrificial anode against macro-cell corrosion under non-homogeneous chloride environment was presented in this study. From this research, several conclusions can be drawn as follows:

1) From the macro-cell corrosion and protective current density test results, it was observed that macro-cell corrosion was formed coupling in boundary between chloride free concrete as anode and its surrounding chloride contaminated as cathode for all specimens since in the early age of exposure period.

2) Based on 100 mV CP criterion, the effective length of embedded steel with sacrificial anode protection and 4 kg/m^3 of chloride content in existing concrete are 340 mm for one-steel bar and 440 mm for two-steel bar from the anode position in patch repair concrete at 350 days of polarization time. Meanwhile, for 10 kg/m^3 chloride content in existing concrete, the effective length from the anode position is 260 mm for one-steel bar and two-steel bar element in repair concrete respectively. It means, up to one-year of exposure time, the higher chloride content in existing concrete, the shorter effective length could be achieved.

3) Meanwhile after 2-year of exposure time, the utilization of commercially available sacrificial anode is effective to protect the corroding steel around 170 mm to 260 mm from the anode position in patch repair concrete (non-chloride contamination) and parent concrete (chloride contamination concrete).

4) Effective length of anode to protect the steel bar in partially-repair concrete exposed to severe condition (wet-dry cycle) influenced by chloride content of concrete and area of repair concrete.

5) If compare with macro-cell corrosion actual length around 100 mm means that commercially available sacrificial anode is effective to protect the corroding steel

References

4.1 Elsener, B., “Macro-cell Corrosion of Steel in Concrcete–Implication for Corrosion Monitoring”, Cement and Concrete Composites, Vol. 24(1), 2002, pp. 65-72.

4.2 Hung, V.V., Nanayakara, O., and Kato, Y., “Effective Length of Steel Element for Time-Dependent Macro-cell Corrosion”, Seisan-Kenkyu, Vol. 61(4), 2009, pp. 657-660.

4.3 Nanayakara, O., and Kato, Y., “Macro-cell Corrosion in Reinforcement of Concrete under Non-homogeneous Chloride Environment”, Journal of Advanced Concrete Technology, Vol. 7, No. 1, 2009, pp. 31-40.

4.4 Mohammed, T.U., Otsuki, N., and Hamada, H., “Corrosion of Steel Bars in Cracked Concrete under Marine Environment”, Journal of Materials in Civil Engineering, September/October 2003, pp. 460-469.

4.5 Hobbs, D. (2001). “Concrete deterioration: causes, diagnosis, and minimising risk”. In: International Materials Reviews 46.3, pp. 117–144.

4.6 Bertolini, L., Elsener, B., Pedeferri,P., Redaelli, E., and Polder, R., “Corrosion of Steel in Concrete”, 2013, Wiley-VCH Verlag GmBH & Co KGaA.

4.7 RILEM Technical Committee 124-SRC, P. Schiessel (ed), “Draft Recommedation for Repair Strategies for Concrete Structures Damaged by Reinforcement Corrosion”, Materials and Structures, 1994, Vol. 27, pp. 415 – 436.

4.8 Bennet, J., and Turk, T., “Criteria for the Cathodic Protection of Reinforced Concrete Bridge Elements”, Technical Alert, SHRP-S-359, 1994.

4.9 Pedeferri, P., “Cathodic Protection and Cathodic Prevention”, Construction and Building Materials, 1996, Vol. 10, No. 5, pp. 391-402.

4.10 Bennet, J., and McCord, W., “Performance of Zinc Anodes Used to Extend the Life of Concrete Patch Repairs”, 2006, Corrosion/2006, NACE International, Paper No. 06331.

4.11 Sergi, G., and Page, C., “Sacrificial Anodes for Cathodic Prevention of

Reinforcing Steel around Patch Repairs Applied to Chloride-contaminated Concrete", European Federation of Corrosion Publications, 2001, No. 31, P. 93-100.

4.12 Cicek, V., "Cathodic Protection: Industrial Solutions for Protecting Against Corrosion", John Willey & Sons, Inc., 2013.

4.13 G. K. Glass, N. R. Buenfeld, Chloride - induced corrosion of steel in concrete, Prog. Struct. Eng. Mater. 2, 2000, 448–458.

4.14 D.R. Morgan, Compatibility of concrete repair materials and systems, Constr. Build. Mater. 10 (1996) 57–67.

Chapter 5 EFFECT OF STEEL SURFACE CONDITIONS ON DURABILITY OF ZINC SACRIFICIAL ANODE CATHODIC PROTECTION

5.1 Introduction

Chloride-induced corrosion of reinforcing steel in concrete structures creates corrosion products that produce tensile stresses within the concrete and results in cracking and/or delamination of the concrete cover [5.1]. The zone experiencing corrosion maybe patch-repaired by removing the chloride-contaminated concrete there and replacing it with fresh, chloride-free concrete. As a result, the previously active steel in the patch becomes passive and corrosion stops there. However, that transition to the passive condition also elevates the potential of the steel in the patch from its former highly negative value to one that can be several hundred mV more positive, removing the natural cathodic prevention effect initially in place [5.2], [5.3].

The newly lowered value of chloride threshold in the surrounding zone then may be less than the existing local chloride concentration and active corrosion could promptly start [5.4]. This detrimental consequence is called a ring or halo damage around the patch [5.5]. In those cases, prevention may be restored by inserting a sacrificial galvanic anode (e. g., made of zinc, which develops a

highly negative potential) in the patch-repair zone. That anode takes up the function of the previously corroding rebar and prevents corrosion form starting both in the patch area and it's surrounding.

Small galvanic anodes ("point anodes") are available commercially for casting in patch repairs, for intended purposes of forestalling the halo damage effect [5.6]. On a practical level, reinstating corrosion protection in concrete using sacrificial anode cathodic protection in patch repair does not require perfect repairs; only physical damages need to be repaired, without the need to remove a lot of chloride-contaminated concrete and without the need to perfect cleaning of steel. The variability that appears when evaluating anode in such cases stems from the current demand by the rebar assembly, which may sometimes be sustained at high levels for long periods of time, or drop rapidly early in the life of the test depending on the initial condition of the steel surface or small variations in the pore water composition or concrete moisture [5.1), (5.6)].

Accumulation of corrosion products on the steel surface that may impede the passage of ionic current or even promote passivation of the anode surface causing eventually failure to deliver protection [5.1)]. Regarding a thorough cleaning of steel before applying sacrificial anodes, the effect of rust removal on deteriorated reinforced concrete structure before anode application on patch repair has not been clearly reported. From the view point of a thorough cleaning of deteriorated steel surface before cathodic protection (CP) applying on it, the effect of rust removal is important to study.

Therefore, this study attempts to address the issue of steel surface conditions against performance of point anode for controlling corrosion of steel in concrete. According to this aims, zinc sacrificial anode was choose as cathodic protection (CP) system to observe.

5.2 Research Objective

The goal of the present work is to investigate effect of steel surface conditions towards performance of anode in patch repair concrete. To reach the general objective, the following specific aims have been defined:

- To observe the effect of initial condition of embedded steel surface (rusted and non-rusted) towards throwing power of current from point anode.
- To investigate the effect of above condition against environmental change of exposure.

The test result will discussed with respect to polarization behavior of anode and steel bar i.e. instant-off potential, protective current density, potential decay, rest potential, anodic-cathodic polarization curve and corrosion rate.

5.3 Research Outline

Regarding the objectives above, there were 2 (two) types of concrete specimens casted in this study. Variety of specimens based on the steel surface conditions (rusted or non-rusted) in the patch repair concrete. Variety of chloride contamination in existing concrete also considered in this study by 0 kg/m^3 and 10 kg/m^3. Air curing and wet-dry cycle are considered as exposure conditions. The outline of specimen specification as shown in **Table 5.1**.

Table 5.1 Specimens specification for steel surface effect study

Specimen Series	Length of Element (mm)	Initial Condition of Rebar	Position in the Concrete	Chloride Content (kg/m^3)	Cathodic Protection Position
D1	250	Non-Rusted	Repair	-	Yes
	250	Rusted	Existing	10	-
D2	250	Rusted	Repair	-	Yes
	250	Rusted	Existing	10	-

5.3.1 Specimen Preparations

Specimen Design

The geometry of the specimens employed in the present investigation are illustrated in **Fig 5.1**. The beams featured total dimensions of 100×150×580 mm. The reinforcement was positioned to obtain a clear concrete cover of 30 mm at the bottom and sides of the beam whereas the distance between bars was kept at 40

mm. The important point, rusted on steel bar originally achieved before casted in concrete and without corrosion acceleration process.

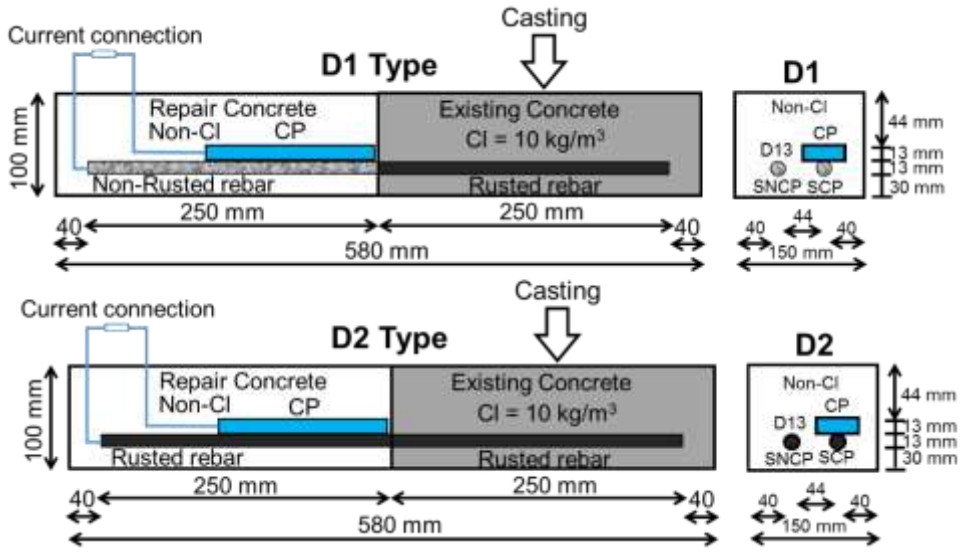

Fig 5.1 Specimen geometry with zinc sacrificial anode embedded in concrete

Anode

A galvanic anode made of zinc as main material and covered by special mortar was used as sacrificial anode. The dimension is 140 mm in length, 45 mm in width and 13 mm in depth, as shown in **Photo 5.1**.

Photo 5.1 Geometry of sacrificial point anode

Steel Bar

In this study, a 20-year-old deteriorated (rusted) reinforcing steel bar with a diameter of 13 mm was used as shown in **Photo 5.2**. These steel bars were taken from the specimens exposed in severe chloride environment with high temperature for 20 years.

Photo 5.2 A 20-year-old deteriorated steel bar used in this study

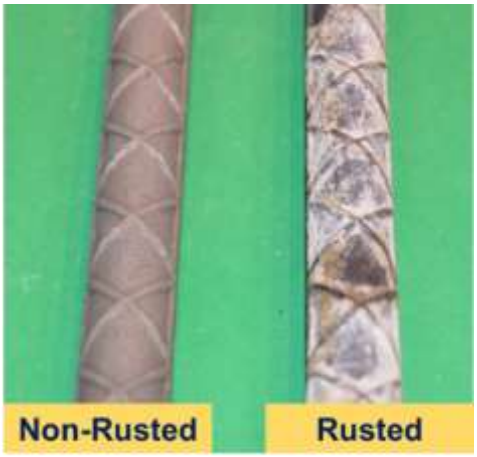

Photo 5.3 Steel bar condition before embedded

Photo 5.4 A 30-cm-long lead was screwed at both ends of each steel element

For non-deteriorated (non-rusted) condition, this rusted rebar was immersed in 10% (weight percentage) diammonium hydrogen citrate solution for 24 hours in 40°C accelerated chamber and then the rust was removed by using steel wire brush as shown in **Photo 5.3**. At both ends of each element, a 30-cm-long lead wire was screwed on as shown in **Photo 5.4**.

Materials and Mix Proportions

The properties of aggregates and admixtures used in this study is shown in **Table 5.2**. Ordinary Portland Cement (OPC) was used as binder and tap water (temperature 20±2°C) was used as mixing water in this study. Washed sea sand passing 5 mm sieve with a density of 2.58 g/cm^3 and water absorption of 1.72 % which was less than 3.5% as stated in Japan Industrial Standard (JIS), was used as the fine aggregate. Meanwhile, crushed stone with a maximum size of 10 mm was used as the coarse aggregate. All aggregates were prepared under surface-saturated dry condition.

Table 5.2 Properties of materials

Component	**Physical properties**	
Ordinary Portland Cement	Density, g/cm^3	3.16
Fine Aggregate	Density, g/cm^3 (SSD Condition)	2.58
	Water absoption (%)	1.72
	Fineness modulus	2.77
Coarse aggregate	Density, g/cm^3	2.91
AEWR agent	Polycarboxylate ether-based	
AE agent	Alkylcarboxylic type	

A concrete mix with a water to cement (w/c) ratio of 0.45 was used for all specimens. Air-entraining agent and water-reducing admixture were added to the cement mass to obtain the slump and air content in all concrete mixes in the range of 10±2.5cm and 4.5±1% respectively. There were two types of concrete mix proportions used for each specimen; namely existing concrete (chloride-contaminated) and repair concrete (chloride-free). In order to accelerate the

corrosion process, chloride ions were deliberately added around 10 kg/m^3 during mixing into the existing concrete. Pure sodium chloride (NaCl) was used as the source of chloride ions. The existing concrete and repair concrete mixture proportions is presented in **Table 5.3**.

Table 5.3 Concrete mix proportions

Material	Existing Concrete	Repair Concrete
Water-cement ratio (w/c), %	45	45
Sand-aggregate ratio (s/a), %	47	47
Water, kg/cm^3	190	190
Cement, kg/cm^3	422	422
Sand, kg/cm^3	766	766
Gravel, kg/cm^3	970	970
Chloride, kg/cm^3	10	0
Additive:	45	45
AE, mL	1900	1900
AE-WR, kg	1.34	1.34

5.3.2 Casting and Curing

The concrete casting process was carried out in two steps. First, the existing concrete was casted and demolded after 24 hours. After demolding, all specimens were subject to 14 days of sealed curing with wetted towels and wrapped with plastic sheet. This was followed by installation of the anode on the steel bar, and repair concrete was casted. They were then demolded after 24 hours and kept for 28 days under sealed curing again with wetted towels and wrapped with plastic sheet as shown in **Photo 5.5**.

After 28 days of sealed curing, the sacrificial anode was connected to the embedded steel in the repair concrete. Adjacent steel elements were also connected to the sacrificial anode through wires to measure the flow of the current. At the ends of steel bar in repair section, a 30cm length lead wire was screwed. The connection of wire and steel bar was covered by epoxy resin in order to avoid the corrosion at the connection. Thickness of epoxy layer was approximately 10 mm.

However, these connectors were temporarily disconnected for the purpose of measuring the instant-off potential, the protective current and depolarization. Silver/silver chloride electrode (Ag/AgCl) is used as reference electrode for potential mapping in this study.

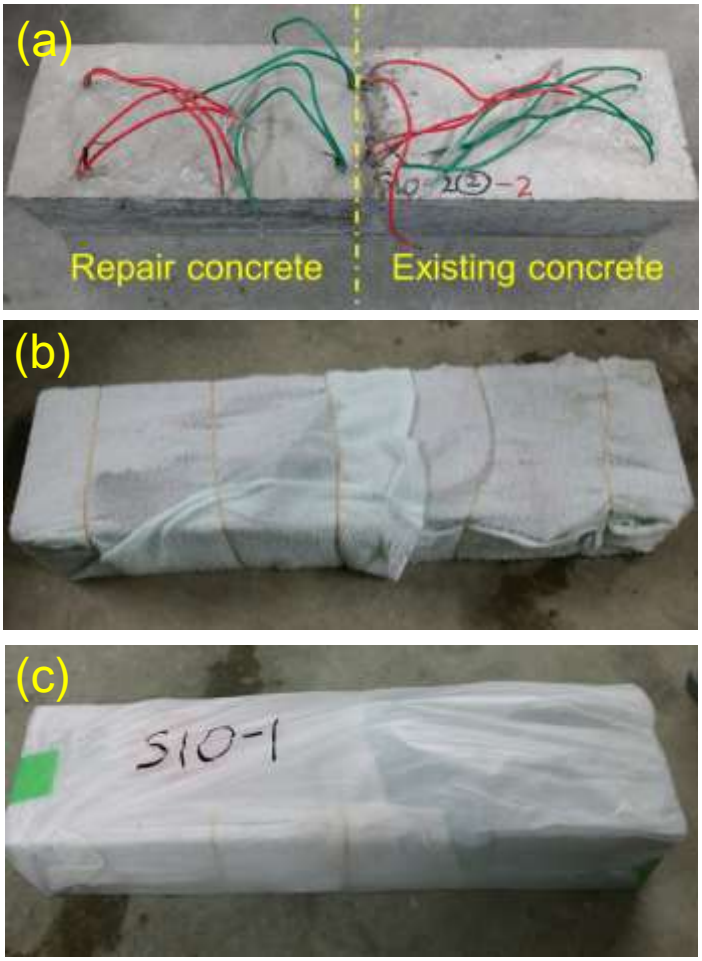

Photo 5.5 Specimen after casted (a), sealed with wetted towel (b) and wrapped with plastic sheet (c)

5.3.3 Exposure Conditions

After the casting of both existing and repair concrete was finished, all specimens were subjected to exposure conditions as illustrated in **Fig 5.2**, in the air curing with a temperature of 20±2°C and a relative humidity of 60%. This environment was kept for 105 days of exposure time. After that, the specimens were moved to the wet-dry cycle condition. The wet cycle involved immersion in a 3% NaCl

solution for two days followed by five days in dry conditions; hence one cycle corresponded to seven days. Measurements were taken weekly at the end of wet cycle.

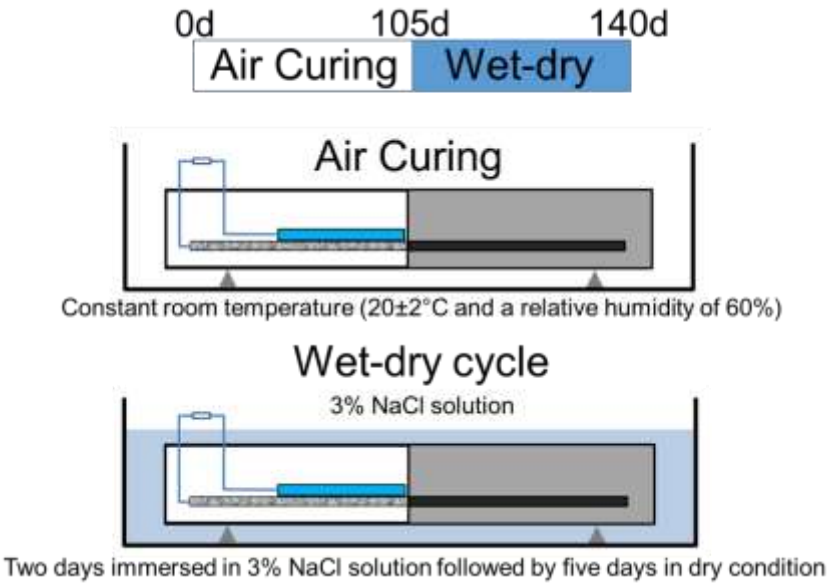

Fig 5.2 Exposure condition in air curing and wet-dry cycle

5.3.4 Corrosion Measurements

In order to observe steel surface effect against durability of zinc sacrificial anode, several electrochemical investigations were conducted in this study. Potential, protective current density, potential decay, rest potential, anodic-cathodic polarization curve and corrosion rate were conducted to D1 and D2 specimens to investigate the polarization behavior of anode and steel bar in concrete. Pre-wetting conducted during 30 minutes before testing and silver-silver chloride used as a reference electrode in this study.

Position of Corrosion Measurements

There are 4 (four) points of measurement on each of repair concrete section and existing concrete section. The first point is starting 50 mm from the interfacial boundary to repair concrete (as point no 1 for repair concrete) and 50 mm from the interfacial zone to existing concrete (as point no 1 for existing concrete). The

measurement point for repair concrete are notice by green dot and red dot for existing concrete as illustrate in **Fig 5.3**. Position for measure potential of steel bars (SCP and SNCP) and anode are point 1, 2, 3 and 4 on each concrete section. However, for measure anodic-cathodic polarization curve, it was conducted on point 1 only. The potential data from point 1 on each section is presented in this report.

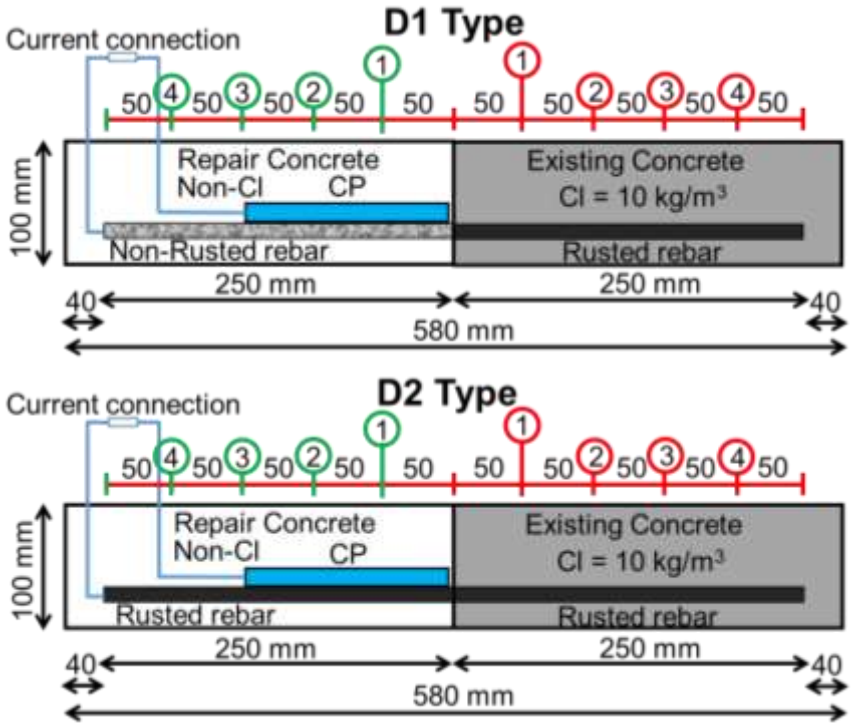

Fig 5.3 Position of corrosion measurements

5.4 Results

In this part, the most relevant results from the experimental programme carried out within this study are presented. Thereafter, the most important observations are highlighted and discussed.

5.4.1 Polarization of Anode

Potential of Zinc Sacrificial Anode

The instant-off potential is measured between 0.1 and 1 second after switching off the protection current in order to remove ohmic drop from the

measured potential. The evolutions of instant-off potentials of anode with polarization time during exposed in air curing and wet-dry condition is shown in **Fig 5.4**. Initially, potentials for anodes in both sets of concrete (CP-D1 and CP-D2) exposed in air curing with constant room temperature were quite negative, ～−1100 mV and ～−930 mV. In 105 days, potential of CP-D2 had stood at ～−380 mV, but by 140 days it almost doubled to ～−690 mV. However, for CP-D1, the protective potential of anode recovered slightly from ～−700 mV at 105 days to ～−750 mV at 140 days. From **Fig 5.4**, it was observed that protective potential of anode in D2 specimen was recovered strongly when the environment change to a humid condition even though still not more negative than anode in D1 over the period of testing.

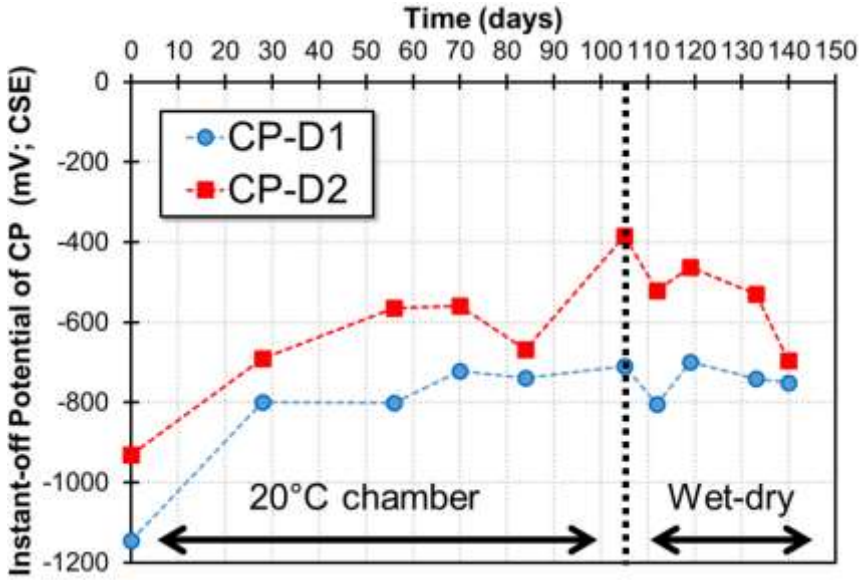

Fig 5.4 Evolution of instant-off potential of anode during 140-day

Protective Current of Zinc Sacrificial Anode

The throwing power of current by anodes to the entire rebar assembly as a function of exposure time is shown in **Fig 5.5**. During exposed to air curing condition, there were a downward trend in the current delivered by CP-D1 and CP-D2. In the beginning, anodes in D1 and D2 delivered the protective current by ～17 μA/cm^2 and ～15 μA/cm^2 respectively. Afterwards, the throwing power of anodes were at its lowest level in 84-day by ～1.72 μA/cm^2 for CP-D1 and ～0.33 μA/cm^2

for CP-D2. After the exposure condition was changed to wet-dry, protective currents generated by anodes increased two times, reaching currents of ～−4.1 μA/cm^2 for CP-D1 and ～−2.19 μA/cm^2 for CP-D2 respectively at the end of test period.

It was noticed that during exposed in dry condition, the level of protective current was within the design limit of cathodic protection between 0.2 – 2 μA/cm^2 as specified in EN 12696 [5.7]. Meanwhile, humid and moisture in wet-dry cycle stimulate the currents generated by anode more than 2 μA/cm^2.

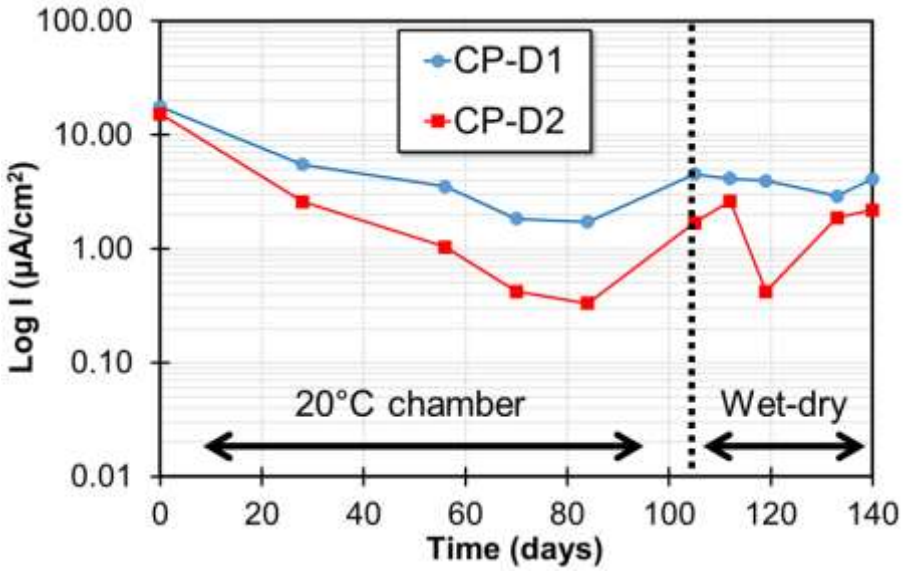

Fig 5.5 Protective current of anode with the function of time

Anodic Polarization Curve of Zinc Sacrificial Anode

Anodic polarization curve testing to anodes in this study were conducted after disconnecting the steel bar from the sacrificial anode for 24 hours. The potential-current delivery function of the anodes applied on non-rusted steel bar (CP-D1) and on rusted steel bar (CP-D2) is presented in **Fig 5.6**.

From 0-day to 84-day, current density of CP-D1 degenerate from ～−13.5 μA/cm^2 to ～−10.7 μA/cm^2. Then after 140-day of exposure time, the current recovered slightly to ～−11 μA/cm^2.

However, the current density of CP-D2 was kept constant ～−11.5 μA/cm^2 for 84 days. Moreover, the current decreased significantly to ～−5 μA/cm^2 at the of test period.

In general, from the anodic polarization curve of zinc sacrificial anode as shown in **Fig 5.6**, it was detected that the activity of anode is gradually decreased with the function of time.

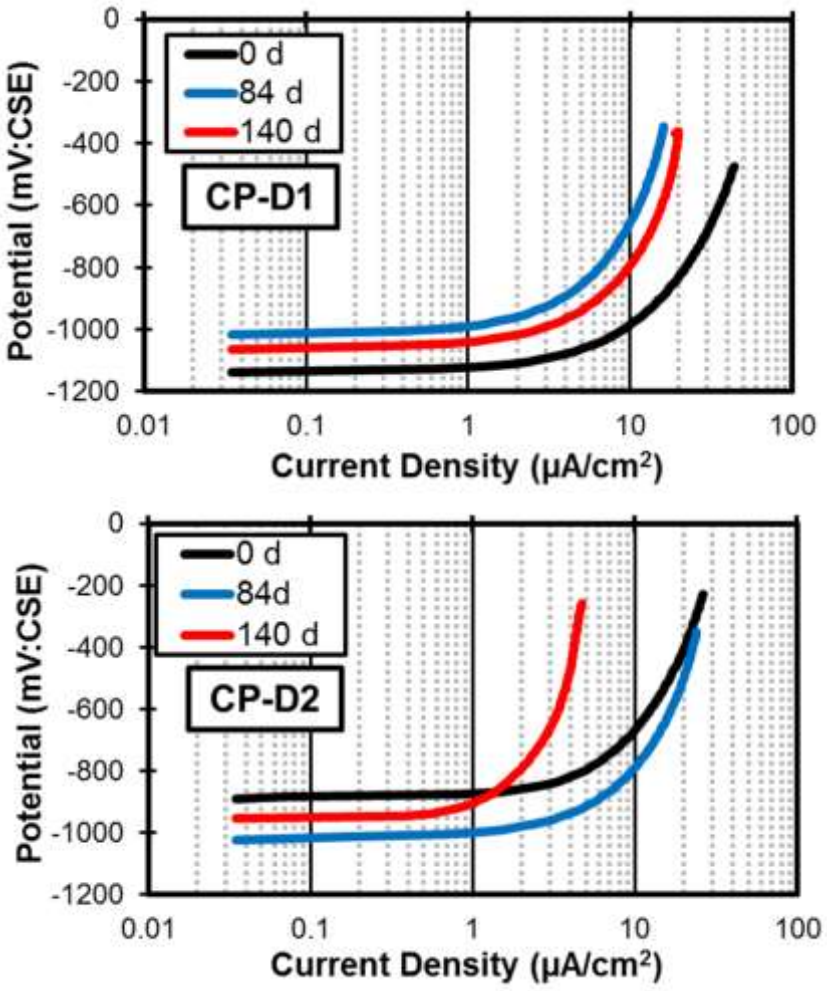

Fig 5.6 Anodic polarization behavior of anodes with the function of time

5.4.2 Polarization of Steel Bar

Instant-off Potential of Steel Bar

The evolution of instant-off potential with time of steel bars (SCP) in patch repair and existing concrete during exposed in two different environments, are shown in **Fig 5.7**. From the data in **Fig 5.**7, it can be seen that potential of SCP-D2 in both set of concrete section more negative than SCP-D1. Between 0-day and 105-day, there were a slight increase to noble value in the potential of SCP-D1 and SCP-D2. However, there were a downward trend to negative direction when the environment change to humid condition for SCP-D1 and SCP-D2 in patch repair concrete as well as in existing concrete. It was observed that anode polarize steel bars in D1 specimen to protection levels.

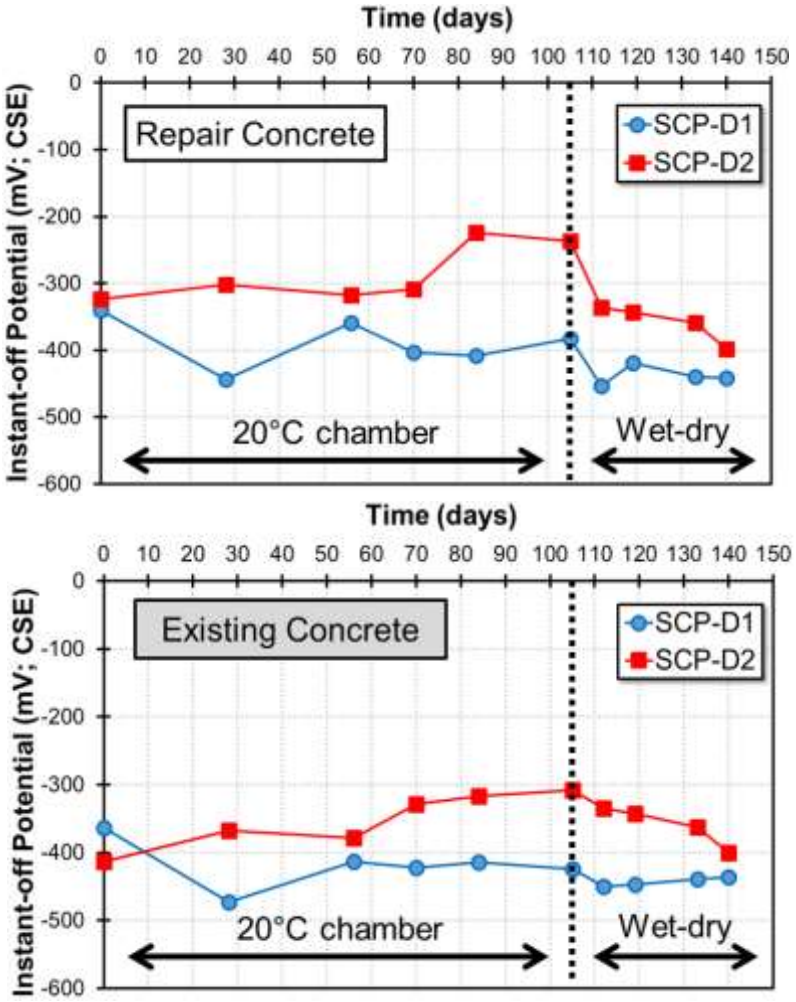

Fig 5.7 Instant-off potential of steel bar in repair and existing concrete

Half-cell Potential of Steel Bar

Half-cell potential of steel bars (SNCP-D1 and SNCP-D2) in patch repair concrete without chloride contamination are presented in **Fig 5.8**. During exposed to 20°C chamber, half-cell potential of SNCP-D2 in repair and existing concrete tends to noble value and SNCP-D1 had a steady potential with the function of time. However, when environment changed to wet-dry condition, between 84-day and 112-day the half-cell potential plunged to ～−410 mV for SNCP-D1 and ～−370 mV for SNCP-D2. It was observed that SNCP-D2 has higher possibility of corrosion to occur compared than SNCP-D1

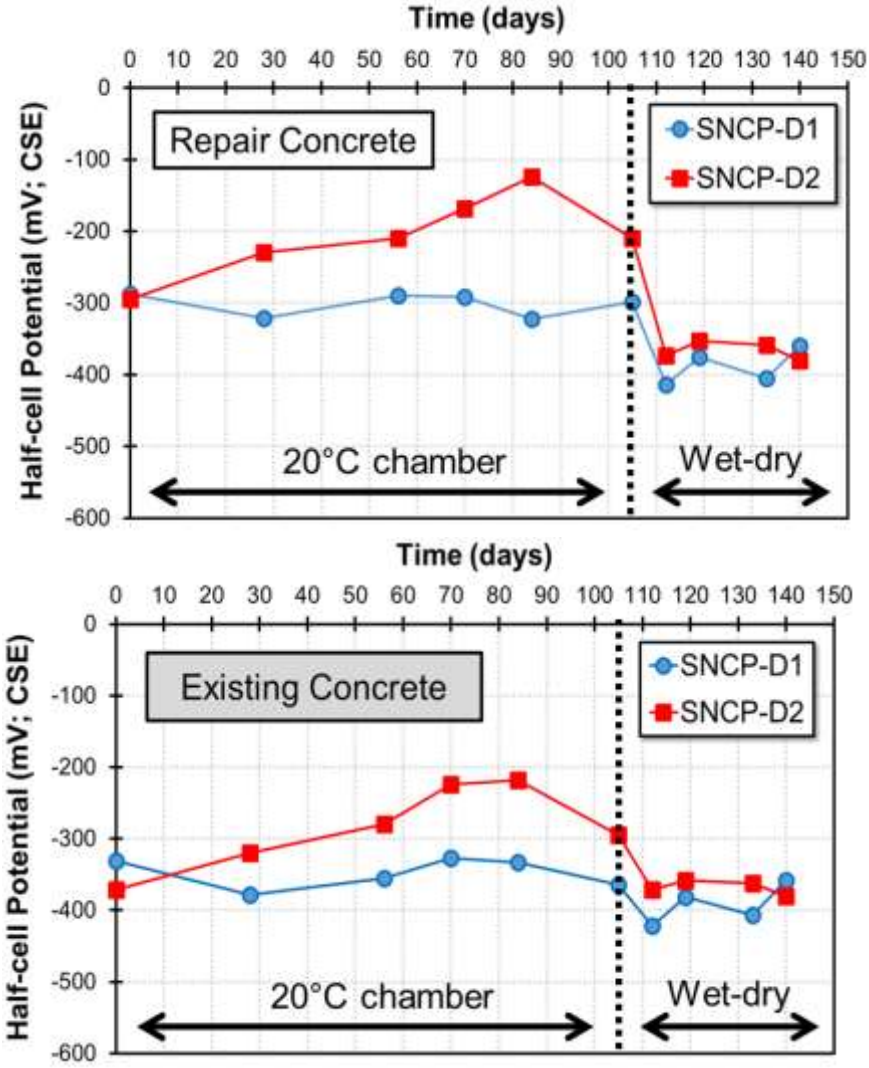

Fig 5.8 Half-cell potential of steel bar in repair and existing concrete

Depolarization of Steel Bar

Potential decay of steel bar in patch repair and existing concrete after disconnecting from the sacrificial anode for 24-hour is presented in **Fig 5.9**. It was observed that potential decay of SCP-D1 exceed 100 mV during exposed to air curing and wet-dry condition with time of polarization. Meanwhile, SCP-D2failed to exceed 100 mV since in the beginning of exposure time. It means anode effective to protect the steel bar only in the patch repair area

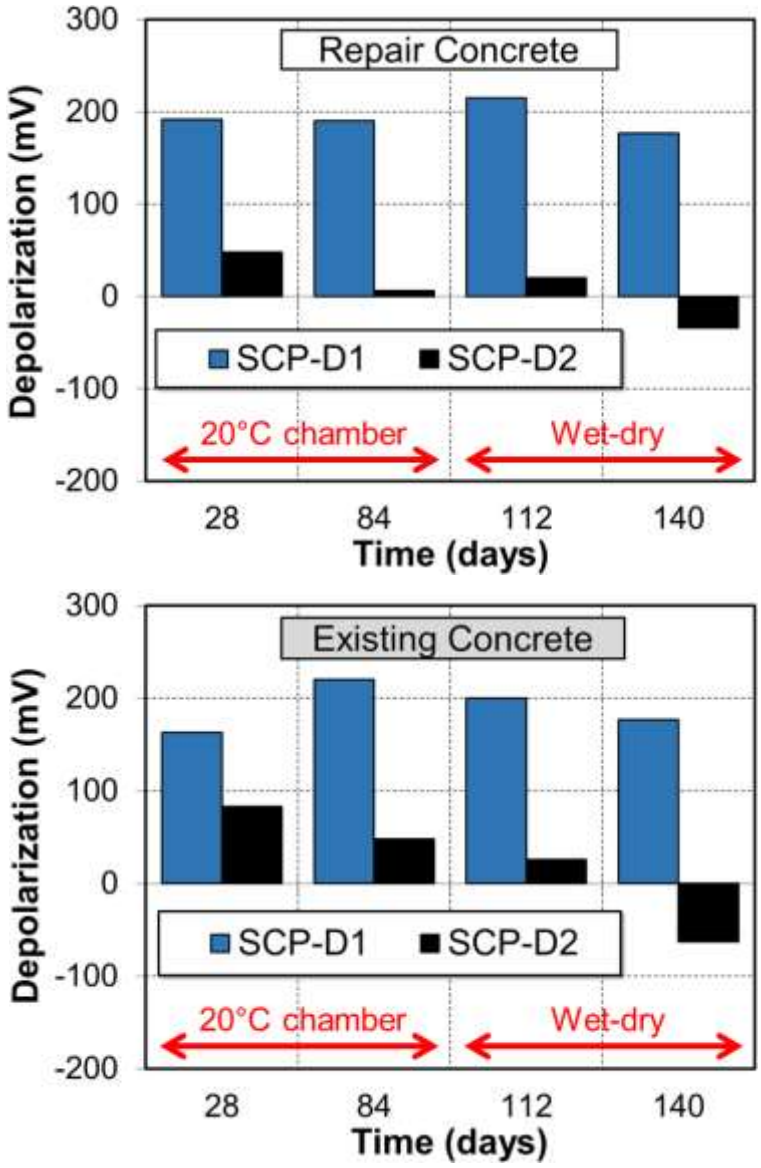

Fig 5.9 Summary of 24-hour depolarization test results

Rest Potential

Fig 5.10 shows about the rest potential or natural potential of anode after disconnected to steel bars by 24-hour. The data shows that natural potential of anode embedded in D1 and D2 at the end of test were ～-1000 mV and ～-900 mV respectively, which is similar to natural potential of Zn alloys. The data also shown that humid condition in wet-dry cycle accelerate potential of anode to negative direction.

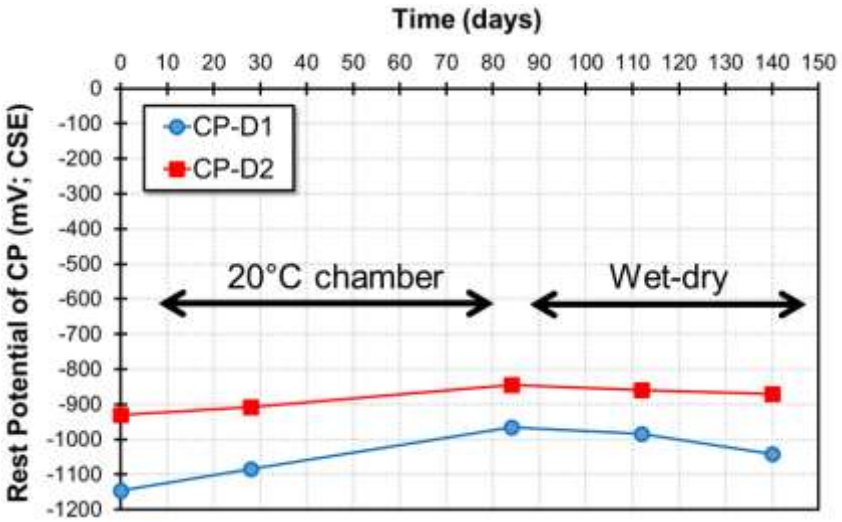

Fig 5.10 Rest potential of anode with time of polarization

Meantime, the line graphs in **Fig 5.11** show about rest potential of steel bars in repair and existing concrete after disconnected with anode 24-hour. The data shows that potential of SCP-D2 within the repair area and non-repaired area increase to positive direction during exposed to 20°c chamber, however, depressed to negative direction ~-400 mV at 140-day of exposure time. Based on corrosion probability per ASTM C876-95 [5.8], it indicates that 90% of corrosion occurs in this area. However, rest potential of SCP-D1 in both of concrete section shown ～-300 mV which indicates uncertainty corrosion occurs in this area. It was noticed that probability of corrosion of steel bar increase during wet and dry condition.

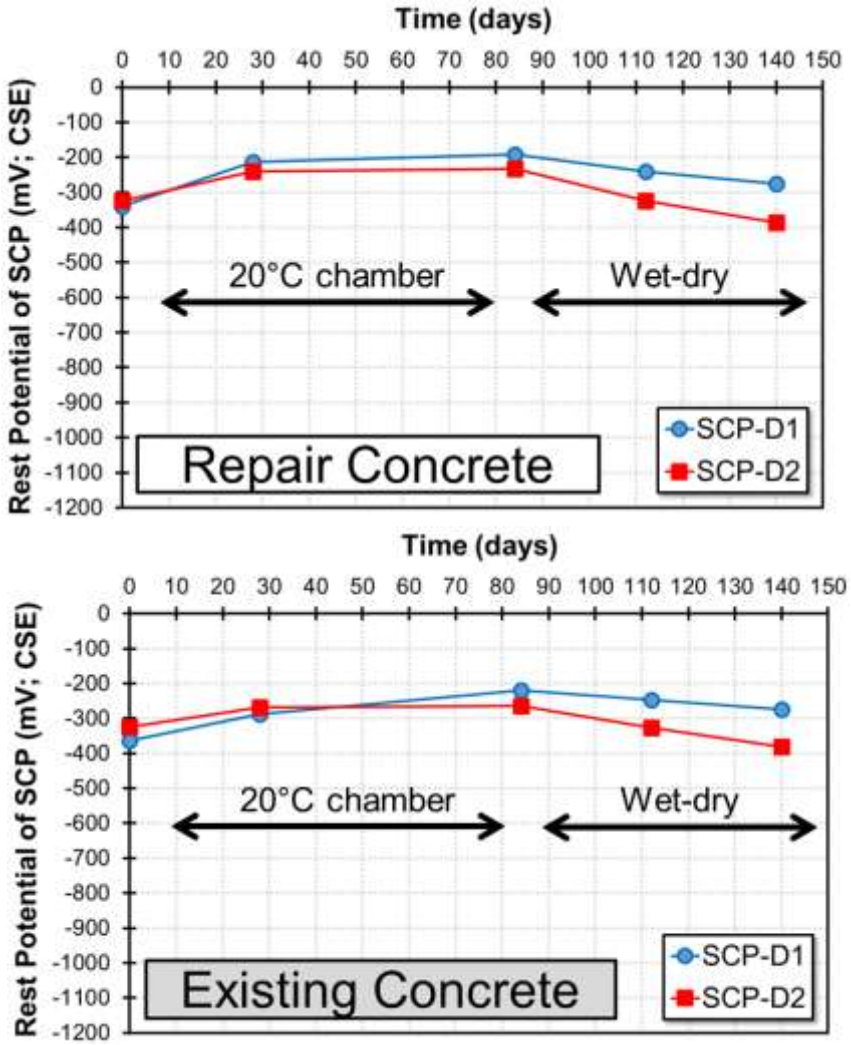

Fig 5.11 Rest potential of steel bar (SCP) with function of time

Anodic-Cathodic Polarization Curve of Steel Bar

The line graphs in **Fig 5.12** and **Fig 5.13** show about potential-current trajectory of SCP-D1 and SCP-D2 with exposure time. Based on the grade of the passivity film of steel bar proposed by Otsuki [5.9], the passivity of SCP-D1 in repair and non-repaired area tend to good condition. However, passivity condition of SCP-D2 in repair area and parent concrete tend to worse condition time-dependently. It mean polarization increases with larger current demand in SCP-D2.

Furthermore, **Fig 5.14** and **Fig 5.15** illustrate about potential-current function of SNCP-D1 and SNCP-D2 with function of time. The data in this graphs

show that there were a downward trend of passivity film of steel bars to worse condition time-dependently.

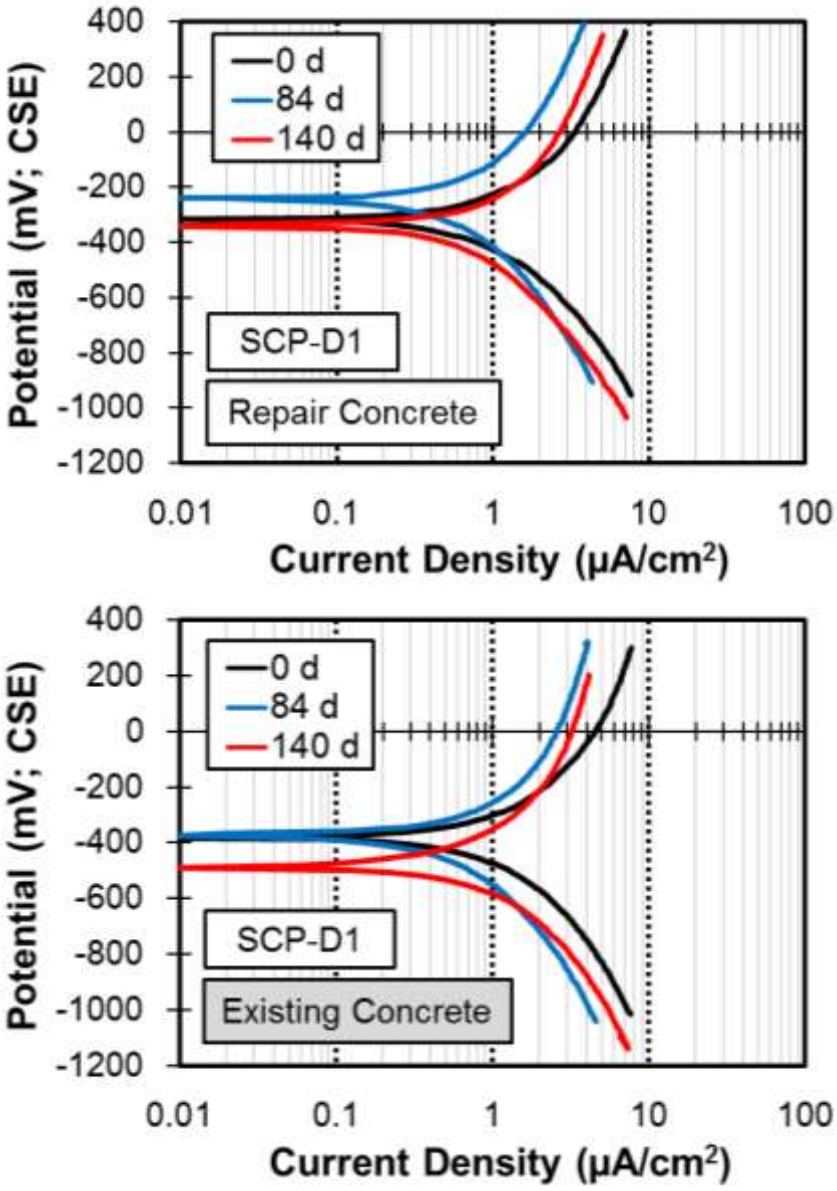

Fig 5.12 Anodic-cathodic polarization curve of SCP-D1

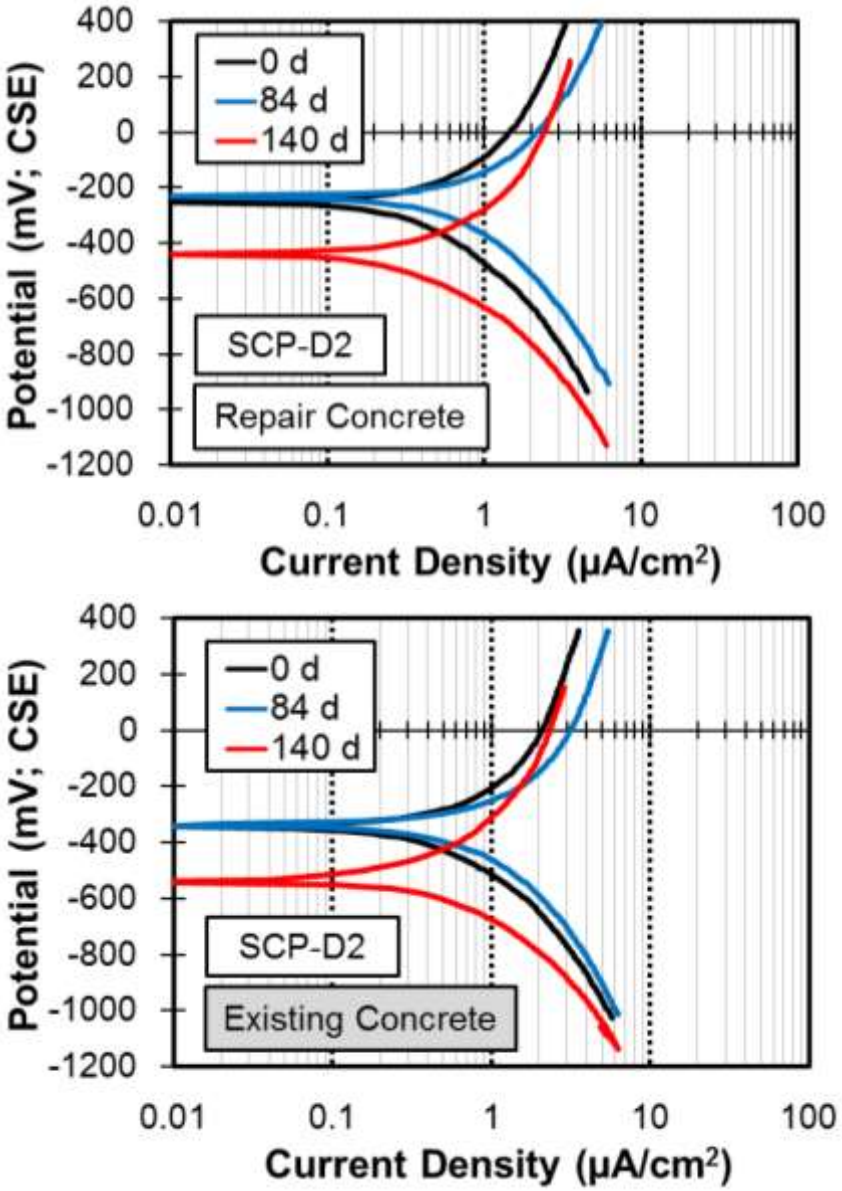

Fig 5.13　Anodic-cathodic polarization curve of SCP-D2

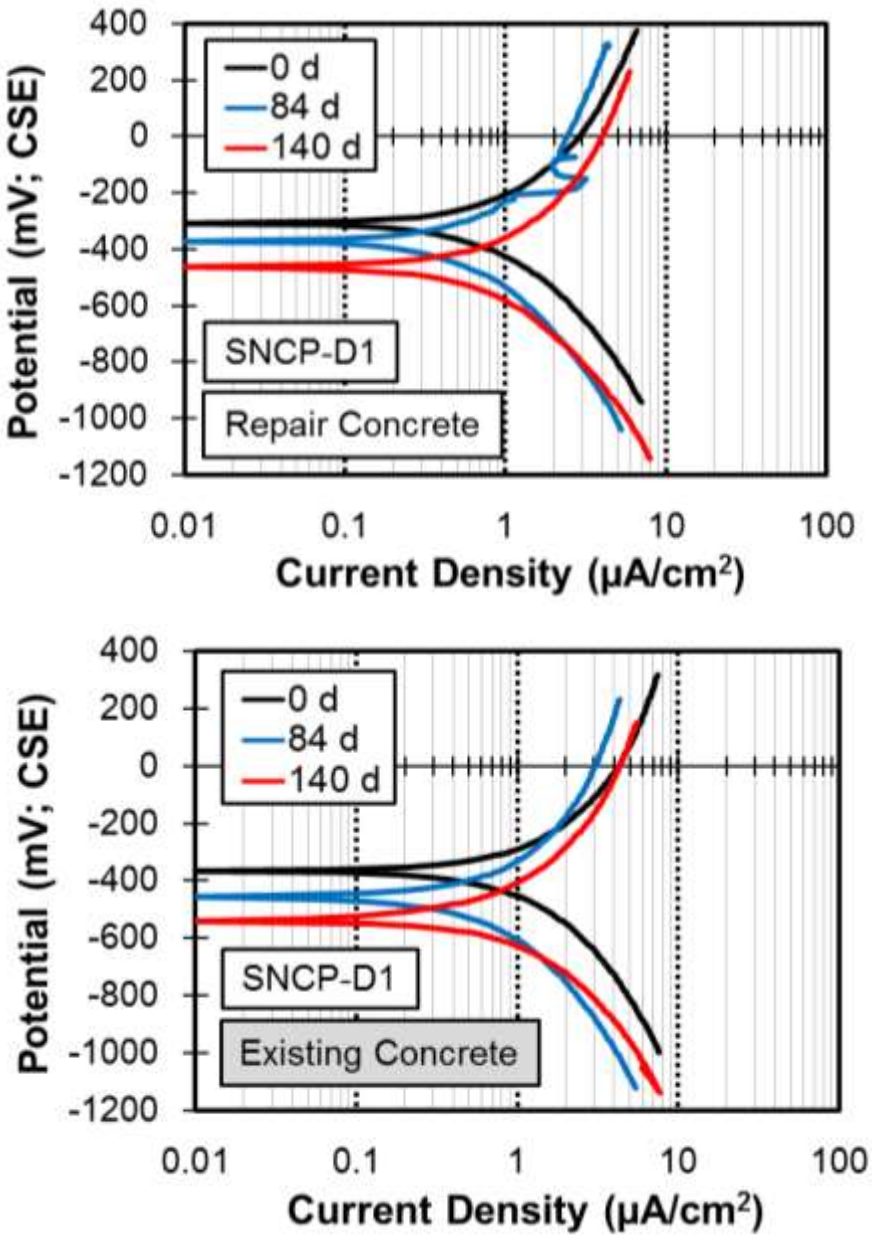

Fig 5.14 Anodic-cathodic polarization curve of SNCP-D1

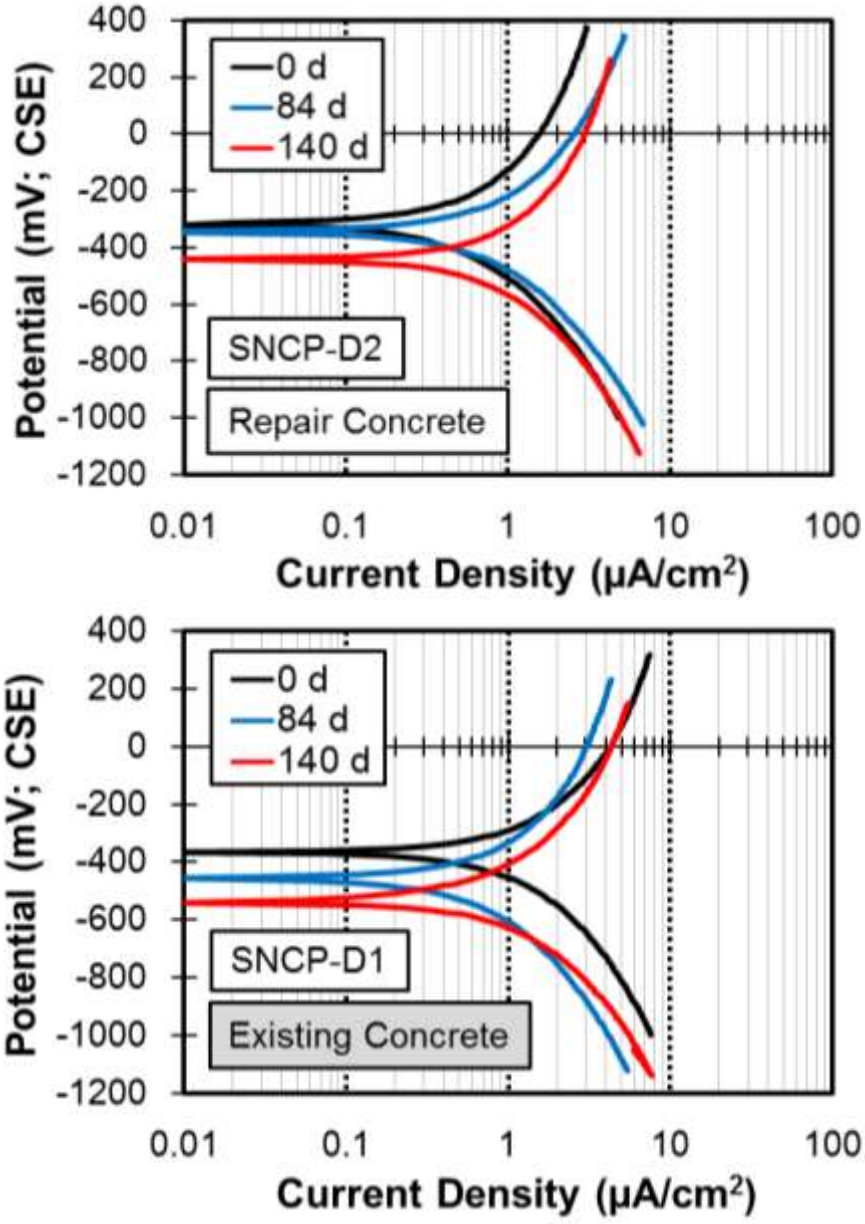

Fig 5.15 Anodic-cathodic polarization curve of SNCP-D2

5.5 Discussions

5.5.1 Effect of Steel Surface

From the polarization results of anode it was obtained information that protective potential of anode was recovered strongly when applied to the steel bar with non-rusted as initial condition. Protective current of anode embedded in non-rusted steel bar successfully to deliver the current to parent concrete, moreover, it is

enough to polarize the steel bars in repair and non-repaired concrete to protection level (as described in depolarization test result). This implies that the sacrificial anode is effective for steel bar with a non-rusted surface in repair concrete even if it is rusted in existing concrete. It may be due to that non-rusted condition gives the protective current flow larger than the rust condition. Anodic polarization curve of anode embedded on the rusted steel surface shown that current delivery were kept constant for long time. It means anode failure to deliver protection because accumulation of corrosion products that may impede the passage of ionic current.

Furthermore, based on the on potential and instant-off potential of steel bar, it was observed that anode active polarize the steel bar with non-rusted surface condition in patch repair concrete to protective levels. Basically, a more negative reading of half-cell potential is generally considered to indicate a higher probability of corrosion. However, this general "rule" may not always be true because of the complexity of today's concrete and repair technologies. This abnormalities can be seen in SNCP-D2 rebar, positive reading on the potential shows that protective layer as a result of rush in the rebar surface protecting the rebar from further corrosion.

5.5.2 Effect of Environmental Change

Potential-current function of anode embedded on non-rusted of steel bar increases to protection criterion when the environment of exposure changed to wed-dry condition. It can be said that potential-current delivery function of the anode with the function of time affected by steel surface condition and moisture level of the concrete.

The same trends also found in steel bar wherein the tendency of polarization increase to protection level when exposed to wet-dry condition. As water increases in capillary pores, oxygen diffusion into concrete is reduced [5.10]. With increasing blockage of oxygen diffusion to the reinforcing steel, the passive film existing on the steel surface becomes unstable and is sometimes eliminated [5.11]. As a result, the corrosion potentials of non-rusted steel bars (SCP-D1) in

repair concrete and rusted steel bars existing concrete was supposed to be more negative than in the specimens SCP-D2 and SCP-D3.It means that potential of the steel bar with the function of time affected by steel surface condition and moisture level of the concrete.

5.6 Conclusions

This study has presented to investigate effect of steel surface conditions towards performance of anode in patch repair concrete. From this research, several conclusions can be drawn as follows:

1. Potential-current delivery function of the anode with the function of time affected by steel surface condition and moisture level of the concrete.
2. Potential of the steel bar with the function of time affected by steel surface condition and moisture level of the concrete.
3. The protective current of the zinc sacrificial anode (CP) became more active in the humid conditions than in dry conditions, due to the high moisture content inside the concrete.
4. Based on the "100 mV decay" criterion, protective conditions were achieved on the steel bars connected to CP with non-rusted as initial condition.
5. Rusted on steel surface decrease the effectiveness of cathodic protection even though embedded in chloride free concrete. Because the rust on the steel bar impede the current flow from anode to the steel bar when CP applied on it.
6. Overall, it can be concluded that non-rusted rebar condition in repair concrete (non-chloride contamination) is the most desirable initial condition when CP is applied on it to protect corroded steel bar in existing concrete (chloride contamination).

References

5.1 Dugarte, M. J. and Sagues, A. A., "Sacrificial Point Anode for Cathodic Prevention of Reinforcing Steel in Concrete Repairs: Part 1 – Polarization Behavior," Corrosion, NACE International, Houston, 70(3), 2014, pp. 303-317.

5.2 Pedeferri, P., "Cathodic Protection and Cathodic Prevention," Construction and Building Materials, 10(5), 1996, pp. 391-402.

5.3 Presuel-Moreno, F. J., Sagues, A. A., and Kranc, S. C, "Steel Activation in Concrete Following Interruption of Long-Term Cathodic Polarization", Corrosion 61, 2005, pp. 428.

5.4 Alonso, C., Castellote, M., and Andrade, C., "Chloride threshold dependence of pitting potential of reinforcements", Electrochemia Acta, Volume 47, Issue 21, 15 August 2002, pp. 3469–3481.

5.5 Christodoulou, C., Glass, G. K., Webb., et al, "Evaluation of Galvanic Technologies Available for Bridge Structures", Structural Faults and Repair, 12th International Conference, Edinburgh, UK, 2008, p.11.

5.6 Sergi, G., "Ten-year results of galvanic sacrificial anodes in steel reinforced concrete", Materials and Corrosion, 62, No. 2, pp. 98-104.

5.7 EN 12696, "Cathodic Protection of Steel in Concrete," European Standard, 2000.

5.8 ASTM C 876-95, "Standard Test Method for Half-cell Potentials of Uncoated Reinforcing Steel in Concrete," Philadelphia: American Society of Testing and Materials, 1999.

5.9 Otsuki, N., "A Study of Effectiveness of Chloride on Corrosion of Steel Bar in Concrete," Report of Port and Harbor Research Institute (PHRI), Japan, 1985, pp. 127-134.

5.10 Arup, H., "Steel in Concrete", Electrochemistry and Corrosion Newsletter 2, 1979, p. 8.

5.11 Funahashi, M., and Bushman, J. B., "Technical Review of 100 mV Polarization Shift Criterion for Reinforcing Steel in Concrete", Corrosion, May 1991, pp. 376-386

5.12 Song, G., and Shayan, A. "Corrosion of Steel in Concrete: Cause, Detection and Prediction", ARRB Transport Research Ltd, Australia, 1998.

5.13 Alhozaimy, A., Hussain, R. R., Al-zaid, R., and Al-Negheimish, "Coupled Effect of Ambient High Relative Humidity and Varying Temperature

Marine Environment on Corrosion of Reinforced Concrete", Construction and Building Materials, 2012, No. 28, pp. 670–679.

5.14 Takewaka, K., "Cathodic Protection for Reinforced Concrete and Prestressed Concrete Structures," Corrosion Science, Vol. 35, 1993, pp. 1617-1626.

5.15 G K Glass, N Davison, A C Roberts, Hybrid corrosion protection of chloride-contaminated concrete, Proceedings of the Institution of Civil Engineers, Constr. Mater. 161, 2008, pp. 163‑172.

5.16 L. Bertolini, M. Gastaldi, M.P. Pedeferri, P. Pedeferri, T. Pastore, Proceedings of the International Conference on Corrosion and Rehabilitation of Reinforced Concrete Structures, Orlando, USA, 1998.

Chapter 6 EFFECT OF TEMPERATURE ON DURABILITY OF ZINC SACRIFICIAL ANODE CATHODIC PROTECTION

6.1 Introduction

The design of a sacrificial anode ("point anode") system should consider the type and location of anodes in order to achieve sufficient and durable protection. It is because the current generated from a sacrificial anode is directly related to the environment that it is placed. Anodes in wet or humid environments will typically produce higher levels of current and distribute it to the reinforcement that needs to be protected [6.1].

All the processes involved in corrosion (i.e., anodic and cathodic electrochemical reactions, transport of aggressive species to steel surface, accumulation of corrosion products on the steel surface or departure from the interface of steel/concrete, and ionic flow through concrete) can be influenced by temperature [6.2]. Regarding the environment conditions of point anode application, the effect of temperature of exposure site when it's applied has not been clearly reported. Therefore, this study attempts to address these issues in order to examine the influence of temperature on the behavior of point anode for controlling corrosion of steel in concrete using electrochemical measurement. According to

this aims, zinc sacrificial anode was choose as cathodic protection (CP) system to observe.

6.2 Research Objective

The aim of the present work is to investigate performance of zinc sacrificial anode to protect steel bar in concrete from corrosion under two extreme of ambient conditions, namely, freeze temperature (-17°C, RH 4-5%) and hot temperature (40°C, RH 96-99%). To reach the general aim, the following specific objectives have been defined:

- To study how the extreme temperature influence corrosion initiation and propagation to steel bar under CP protection and without CP protection in concrete.
- To observe the effect of chloride content in concrete towards throwing power of current from point anode under exposed to extreme temperature.

The test result will discussed with respect to polarization behavior of anode and steel bar i.e. on potential, instant-off potential, current flow and current density, potential decay, rest potential, anodic-cathodic polarization curve and corrosion rate.

6.3 Specimen Preparation and Testing

Regarding the objectives above, there were 8 (eights) concrete specimens casted in this study comprises 4 (four) specimens with anode embedded in concrete with variety of chloride contamination considered in by 0 kg/m^3 and 10 kg/m^3. The outline of specimen specification as shown in **Table 6.1**.

6.3.1 Specimen Design and Materials

The geometry of the specimens employed in the present investigation are illustrated in **Fig 6.1**. The beams featured total dimensions of 100×150×290 mm and were reinforced with two D13-steel bars. The reinforcement was positioned to obtain a clear concrete cover of 30 mm at the bottom and sides of the beam whereas the distance between bars was kept at 40 mm.

Moreover, a galvanic anode made of zinc as main material was used as sacrificial anode. The dimension is 140 mm in length, 45 mm in width and 13 mm in depth, as shown in **Photo 6.1**.

Table 6.1 Specimens specification for temperature effect study

Specimen ID	Chloride Content (kg/m^3)	Initial Rebar Condition	Exposure Condition
CL0-F	0	Non-rusted	Freeze (-17°C, RH 4-5%)
CL0-H	0	Non-rusted	Hot (40°C, RH 96-99%)
CL10-F	10	Non-rusted	Freeze (-17°C, RH 4-5%)
CL10-H	10	Non-rusted	Hot (40°C, RH 96-99%)

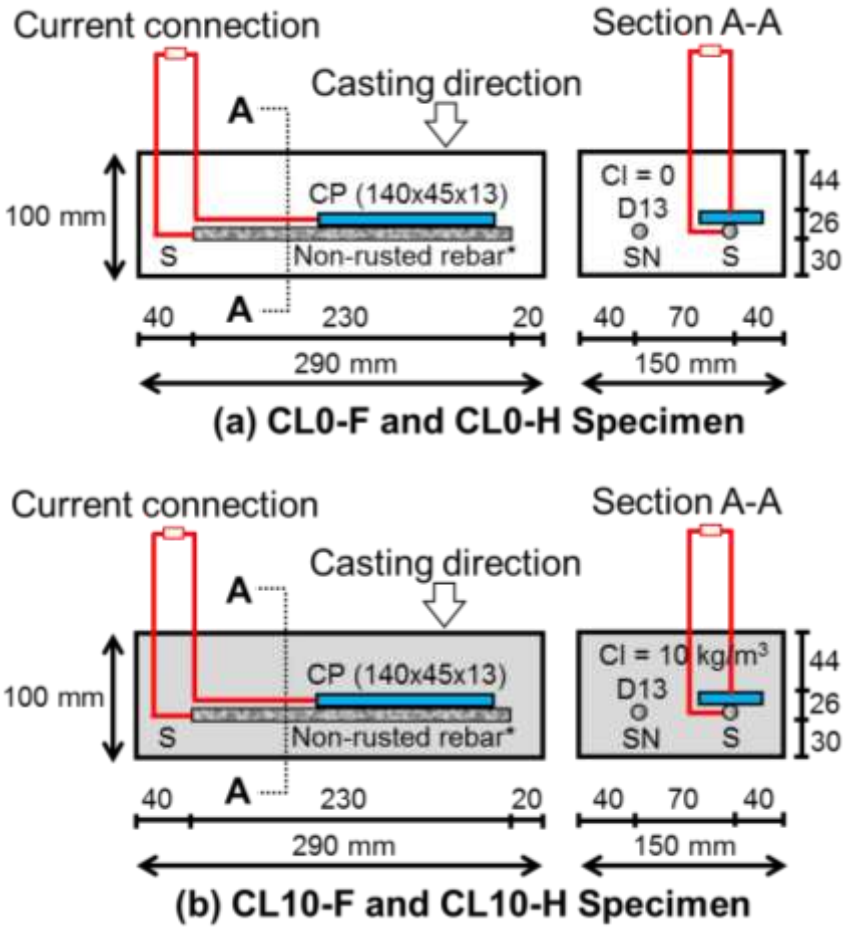

Fig 6.1 Specimen geometry with zinc sacrificial anode embedded in concrete

Photo 6.1 External appearance of zinc sacrificial point anode

Ordinary Portland Cement (OPC) was used as binder and tap water (temperature 20±2°C) was used as mixing water in this study. Washed sea sand passing 5 mm sieve with a density of 2.58 g/cm^3 and water absorption of 1.72 % which was less than 3.5% as stated in Japan Industrial Standard (JIS), was used as the fine aggregate. Meanwhile, crushed stone with a maximum size of 10 mm was used as the coarse aggregate. All aggregates were prepared under surface-saturated dry condition. The properties of aggregates and admixtures are shown in **Table 6.1**.

Table 6.1 Properties of materials

Component	**Physical properties**	
Ordinary Portland Cement	Density, g/cm^3	3.16
Fine Aggregate	Density, g/cm^3 (SSD Condition)	2.58
	Water absoption (%)	1.72
	Fineness modulus	2.77
Coarse aggregate	Density, g/cm^3	2.91
AEWR agent	Polycarboxylate ether-based	
AE agent	Alkylcarboxylic type	

6.3.2 Mix Proportions

The concrete was designed with a water to cement (w/c) ratio of 0.45 and the ratio of fine aggregate to total aggregate volume (s/a) of 0.47. Air-entraining agent and water-reducing admixture were added to the cement mass to obtain the slump and air content in all concrete mixes in the range of 10±2.5cm and 4.5±1% respectively.

In order to accelerate the corrosion process, chloride ions were deliberately added around 10 kg/m^3 during mixing into chloride-contaminated concrete. Pure

sodium chloride (NaCl) was used as the source of chloride ions. The concrete mixture proportions of concrete are shown in **Table 6.2**.

Table 6.2 Mixture proportions of concrete specimens

Material	
Water-cement ratio (w/c), %	45
Sand-aggregate ratio (s/a), %	47
Water, kg/cm^3	190
Cement, kg/cm^3	422
Sand, kg/cm^3	766
Gravel, kg/cm^3	970
Chloride, kg/cm^3	0 & 10
Additive:	
• AE, mL	1900
• AE-WR, kg	1.34

6.3.3 Steel Bar

In this study, a 20-year-old deteriorated (rusted) reinforcing steel bar with a diameter of 13 mm was used as shown in **Photo 6.2**. These steel bars were taken from the specimens exposed in severe chloride environment with high temperature for 20 years.

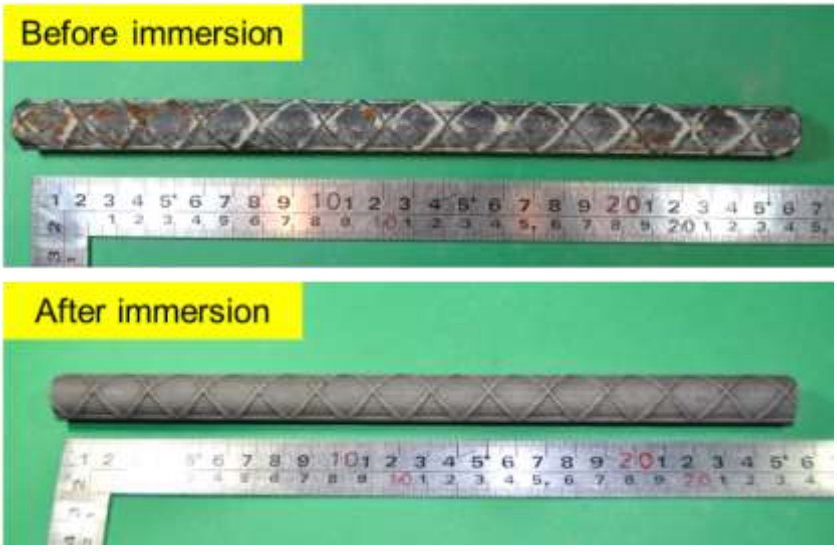

Photo 6.2 A 20-year-old deteriorated steel bar used in this study

For non-deteriorated (non-rusted) condition, this rusted rebar was immersed in 10% (weight percentage) diammonium hydrogen citrate solution for 24 hours in 40°C accelerated chamber and then the rust was removed by using steel wire brush. At both ends of each element, a 30-cm-long lead wire was screwed on.

6.3.4 Casting and Curing

The beam specimens were cast in plywood formwork. Before the concrete casting process conducted, tide the anode to steel bar (S). After 24-hour of concrete casting process finished, the formwork was removed and the beams wrapped with wetted towel and plastic sheets.

Thereafter, all specimens were stored (in wrapping) at room temperature for 28 days. After 28 days of sealed curing, the zinc sacrificial anode was connected to adjacent steel elements (S) in order to throwing protection current. However, these connectors were temporarily disconnected for the purpose of measuring the instant-off potential, the protective current and potential decay during switch-off 24h in depolarization test.

6.3.5 Exposure Conditions

After curing, specimens were stored separated in freeze chamber, high temperature chamber and constant room temperature chamber. The freeze, high and constant room temperature chamber condition as shown in **Photo 6.3 Photo 6.4** and **Photo 6.5**. Freeze chamber was kept temperature in -17°C with relative humidity (RH) 4-5%, high temperature chamber maintained in 40°C and RH 96-99%, and for constant room chamber was kept temperature in 20°C with RH 60%.

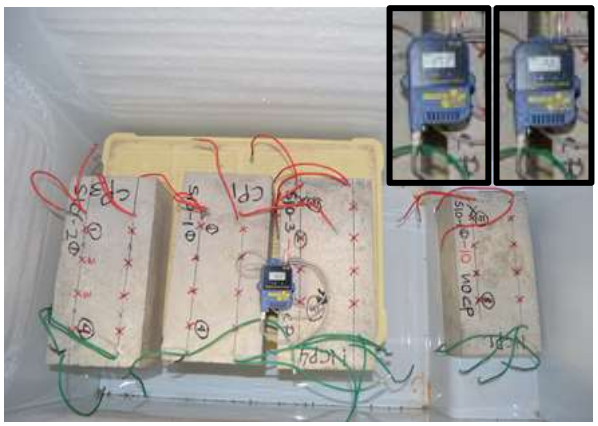

Photo 6.3 Freeze temperature (-17°C and RH 4-5%) chamber

Photo 6.4 High temperature (40°C and RH 96-99%) chamber

6.3.6 Corrosion Measurements

In order to observe performance of zinc sacrificial anode to protect the steel from corrosion in concrete under extreme temperature conditions, several electrochemical investigations were conducted in this study. **Table 6.2** represents about the type of electrochemical testing conducted to CL0 and CL10 specimens to investigate the polarization behavior of anode and steel bar in concrete.

All measurements were conducted in constant room temperature chamber. Specifically for specimens with anode embedded in concrete, the step of measurement illustrated in **Fig 6.3**. From **Fig 6.3**, it can be seen that current monitoring were conducted first before specimens taken out from the freeze and

hot chambers (**Photo 6.6**), then specimens were stored in constant room temperature chamber for pre-wetting during 30 minutes and continued by each of testing. **Photo 6.7** depicts about condition during pre-wetting, potential measurement and potentiodynamic polarization or anodic-cathodic polarization curve measurement. The measurement was conducted with silver/silver chloride electrode after 1 hour of pre-wetting. Then measured value was converted to the potential of the copper/copper sulphate electrode (CSE) at 25°C.

Table 6.2 Type of corrosion measurements on CL0 and CL10 specimens

Test Item	CL0	CL10
Half-cell potential	○	○
On potential	○	○
Instant-off potential	○	○
Protective current	○	○
Potential decay (after switch off 24h)	○	○
Rest potential	○	○
Polarization behavior of anode	○	○
Anodic polarization curve of anode	○	○
Anodic-cathodic polarization curve of steel bar	○	○
Corrosion rate	○	○
Visual inspection of anode	X	X

Remark; ○: Tested, X: Not tested

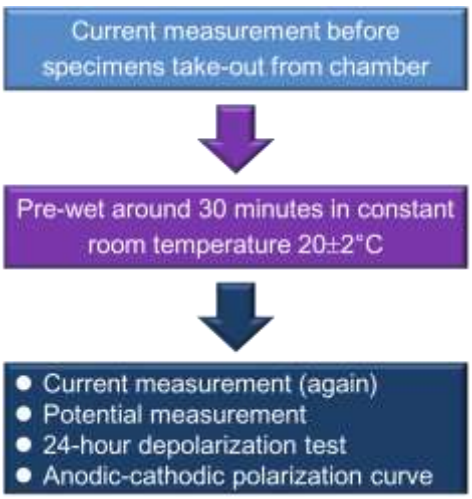

Fig 6.2 The step of measurement towards CL0 and CL10 specimens

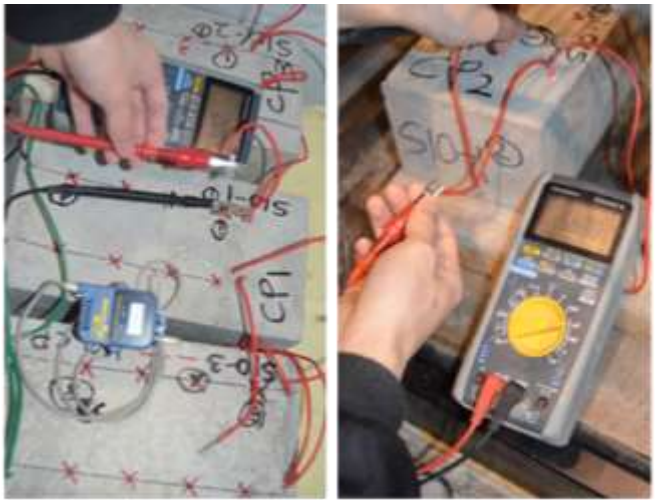

(a) Freeze chamber (b) Hot chamber

Photo 6.5 Current measurement before specimens take-out from freeze and high temperature chamber

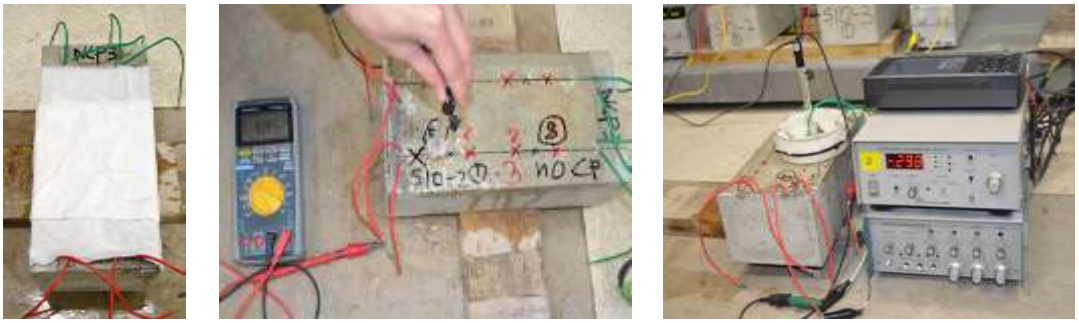

(a) Pre-wet (b) Potential (c) Polarization curve

Photo 6.6 Condition of pre-wet, potential mapping and potentiodynamic polarization

6.4 Results

In this section, the most relevant results from the experimental programme carried out within this study are presented. Thereafter, the most important observations are highlighted and discussed.

6.4.1 Polarization of Anode

Potential of Zinc Sacrificial Anode

In **Fig 6.4**, the results from on potential and instant-off potential measurement of anodes embedded in chloride-contaminated concrete and free-chloride concrete

"after" exposed to freeze and high temperature is presented. "After" means potential of anode measured 30 minutes since take-out from chambers.

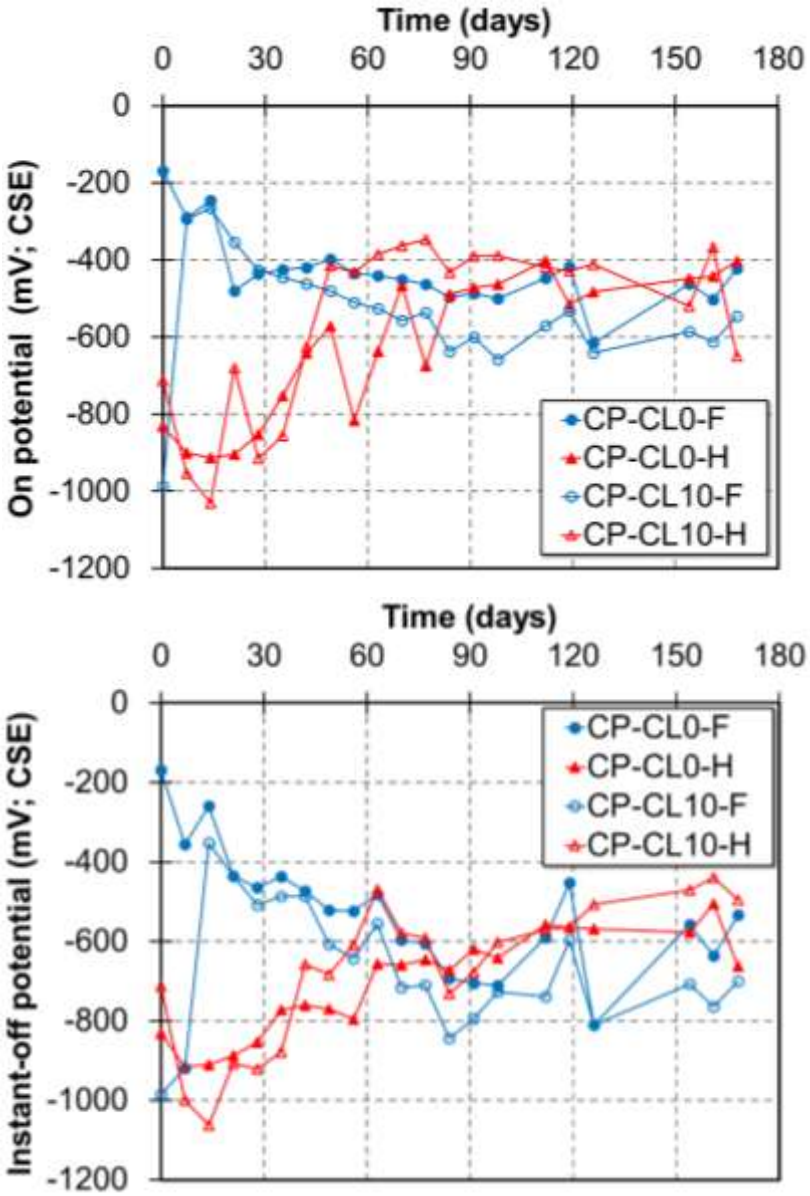

Fig 6.3 On potential and instant-off potential of anodes embedded in concrete with and without chloride contamination exposed to freeze and hot environments

Initially, the data shown that on potential of anode embedded in concrete with and without chloride contamination (CP-CL10-H and CP-CL0H) exposed to hot temperature were quite negative, ～−700 mV and ～−800 mV respectively. However, after 28-day until 49-day, potential of anodes increased gradually to

noble values. Anode embedded in free-chloride (CP-CL0H) and chloride-contaminated concrete (CP-CL10-H) showed a relatively slow increasing on potential trend with time, reaching average potentials of ～−400 mV and ～−600 mV respectively at the end of test period.

Furthermore, for anode exposed in freeze condition, on potential of anodes embedded in both type of concrete decreased gradually to negative direction with time. It was showed a steadily slow decreasing potential trend with time, reaching average on potentials of ～400 mV and ～500 mV for anode embedded in free (CP-CL0-F) and chloride-contaminated concrete (CP-CL10-F) respectively at the end of test period. Anode embedded in concrete with chloride contamination and exposed under zero degree Celsius (CP-CL10-F) has higher on potential compare than anode casted in free-chloride concrete (CP-CL0-F). The evolutions of anode instant-off potentials with time for both sets of concrete (chloride-contaminated concrete and free-chloride concrete) exposed in for freeze and high temperature is shown also in **Fig 6.4**. In the beginning, potentials for anodes in both sets of concrete (CP-CL0-H and CP-CL10-H) exposed in hot environment condition were quite negative, ～−700 mV and ～−800 mV. Then, the potential increased at a much slower rate to positive direction, reaching on average a plateau at ～−400 mV and ～−600 mV after about 168 days.

Meanwhile, anode in both sets of concrete exposed in freeze environment stayed at more negative potentials from 0-day until 84-day of the test period. Afterwards, instant-off potential showed a steadily slow increasing potential trend noble value with time, reaching average on potentials of ～500 mV and ～700 mV for anode embedded in chloride free (CP-CL0-F) and chloride-contaminated concrete (CP-CL10-F) respectively at the end of test period.

Protective Current of Zinc Sacrificial Anode

The current delivered by the anodes to the entire rebar assembly as a function of exposure time is shown in **Fig 6.4**. From **Fig 6.4 (a)** it can be seen that protective current from anode in concrete without chloride contamination (CP4-CL0-H) during exposed to hot condition soared to 21 $\mu A/cm^2$ at 21-day and reaching a

peak at 26 μA/cm^2 after about 42 days. Then, current plunged to 6 μA/cm^2 at 49-day and decayed gradually until to 1 μA/cm^2 at the end of test.

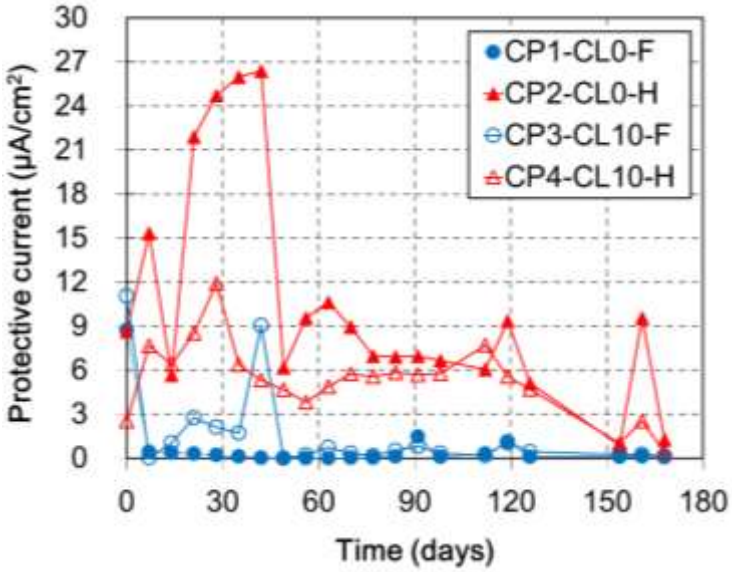

(a) Before take out from chamber

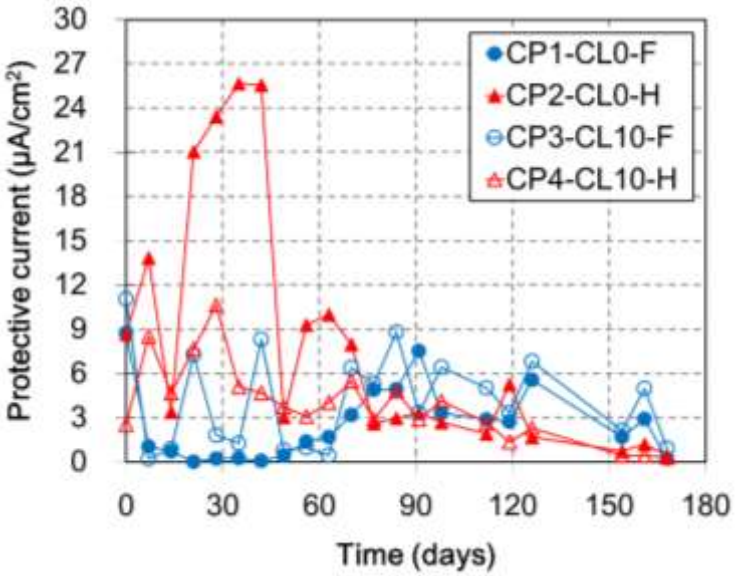

(b) After take out from chamber

Fig 6.4 Protective current of anode before and after take out from freeze and hot chambers

Meantime, the protective current throwing from anode embedded in concrete with chloride contamination (CP4-CL10-H) during exposed in 40°C

chamber shown lower than anode in concrete without chloride contamination over much of the test period, reaching 0.4 $\mu A/cm^2$ at the end of test.

In contrary, for all of anodes exposed to frost condition (CP1-CL0-F and CP3-CL10-F), there were bottoming out of current delivered by anode from 7-day of exposure time until at the end of test period.

Fig 6.4 (b) illustrates the evolutions of delivered current from anode after take out from each chambers, pre-wet for 30 minutes and stored in constant room temperature during measurement process. For anodes from high temperature chamber, current development shown the same trend with current delivered during delivered in hot chamber. It was reaching 0.3 $\mu A/cm^2$ and 0.4 $\mu A/cm^2$ for CP2-CL10-H and CP4-CL10-H at the end of test.

However, for anodes from freeze chamber, current trends were increased gradually from 7-day to 84-day. Afterwards, there was a downward trend in the current evolutions of anodes embedded in CP1-CL10-F and CP1-CL0-F, reaching 0.2 $\mu A/cm^2$ and 0.9 $\mu A/cm^2$ for respectively at the end of test period.

It is noted that during exposed in high temperature, anode throwing power much higher than in freeze temperature condition but lower during stayed in constant room temperature chamber. Vice versa for anode which exposed in freeze condition.

6.4.2 Polarization of Steel Bar

Potential of Steel Bar

Fig 6.5 describes about potential development of steel bar with CP connected (S) time-dependently during on and instant-off condition exposed to freeze and high temperature condition. On potential and instant-off potential of steel bar with CP connected (S) embedded in concrete with (S-CL0-F) and without (S-CL10-F) chloride contamination exposed to frost condition gradually decreased to negative direction from the beginning of exposure time until at the end of test. Notably for steel bar embedded in chloride-contaminated concrete, it has potential more negative than steel bar embedded in concrete without chloride contamination.

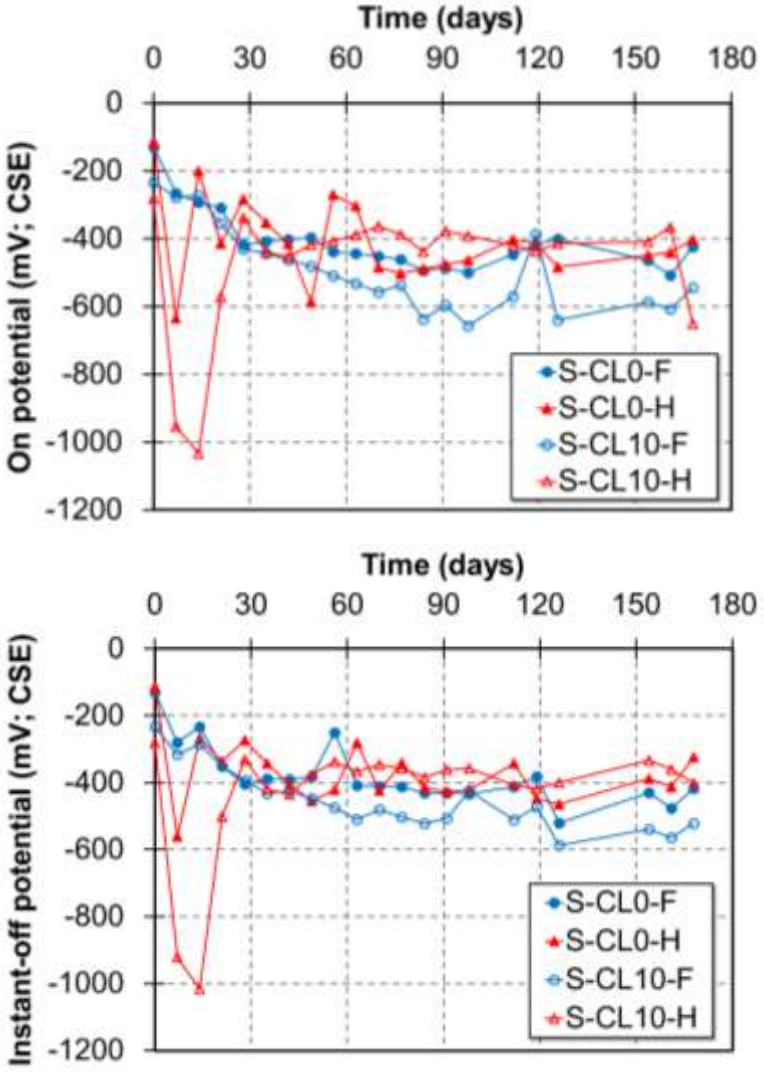

Fig 6.5 On potential and instant-off potential of steel bar embedded in chloride-contaminated and free-chloride concrete exposed to freeze and hot environments

Meanwhile, on potential of steel bar with CP connected (S) in chloride-contaminated concrete (S-CL10-H) exposed to high temperature condition between 7 and 14 days plunged to ～−900 mV and ～−1000 mV. However, it soared to ～−500 mV and ～−300 mV at 21-day and 28-day. After 28 days of test period, on potential of S-CL10-H decreased gradually in negative direction. The same trend were occurred to instant-off potential condition wherein protective condition.

In general, the on potential and instant-off potential of steel bar with CP embedded in chloride free concrete exposed to frost and high temperature (S-CL0-

H) were an overall downward trend to negative value during the period of test as shown in **Fig 6.5**.

It was observed that steel bar connected to CP exposed to freeze condition (S-CL0-F and S-CL10-F) decrease gradually to negative potential during on and instant-off potential than steel bar connected to CP exposed to hot condition (S-CL0-H and S-CL10-H).

Half-cell Potential of Steel Bar

In **Fig 6.6**, evolutions of half-cell potential of steel bar without CP connected (SN) exposed to freeze and high temperature is presented. Half-cell potential of steel bar embedded in chloride-contaminated concrete exposed to hot environment (SN-CL10-H) during on and instant-off shown ~-450 mV over much the period of test. Moreover, half-cell potential of steel bar embedded in chloride-contaminated concrete exposed to freeze environment (SN-CL10-F) fell gradually to more than ~-400 mV over much the period of test. Based on probability of corrosion on ASTM C876-91, condition both of steel bar indicate greater than 90% probability corrosion occurs.

Meanwhile, there was an overall downward trend of on and instant-off potential for steel bar embedded in chloride free concrete exposed to frost condition (SN-CL0-F) between ~-200 mV to ~-350 mV during the period of exposure time. It shown uncertain corrosion condition on this steel bar. Whereas the half-cell potential of steel bar embedded in chloride free concrete exposed to hot condition (SN-CL0-H) stayed steadily less than ~-200 mV and indicate greater than 90% no corrosion occurs.

It was observed that steel bar disconnected with CP embedded in chloride contamination and exposed to hot condition (SN-CL10-H) has the greater opportunity for corrosion occurs followed by SN-CL10-F, SN-CL0-F and SN-CL0-H respectively as the lowest probability.

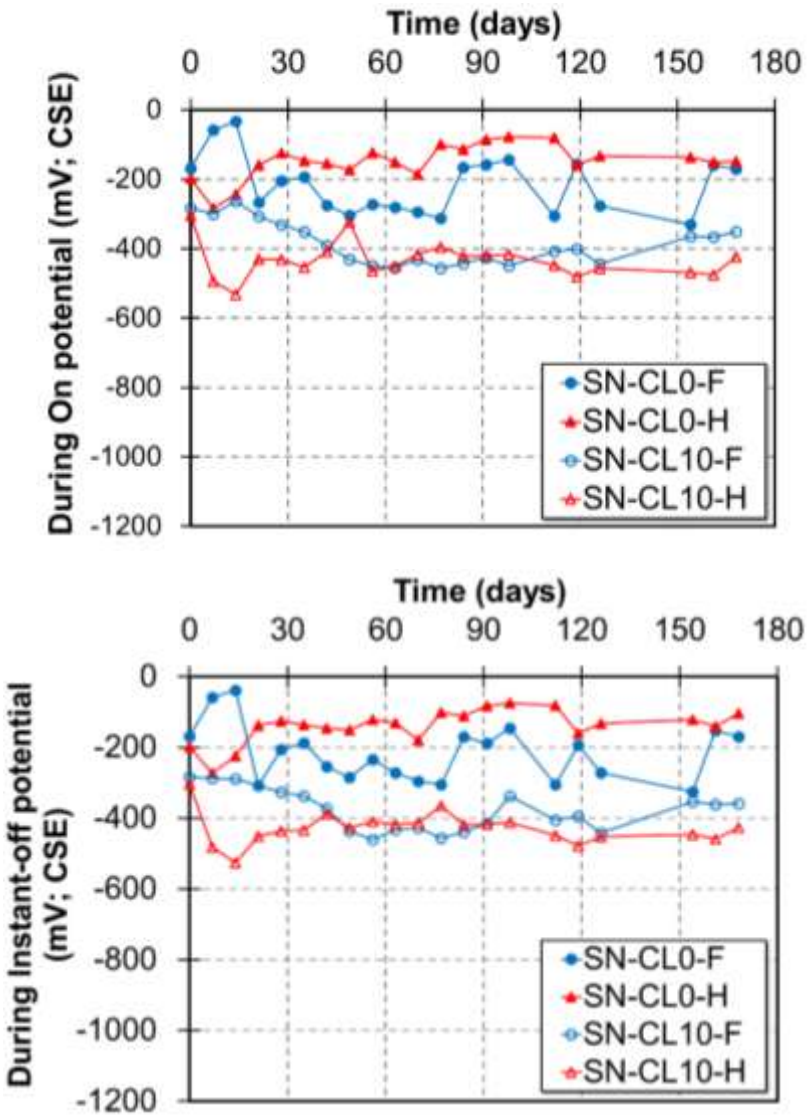

Fig 6.6 Half-cell potential of steel bar embedded in chloride-contaminated concrete and free-chloride concrete exposed to freeze and hot environments during on potential and instant-off potential

Twenty-four-hour Depolarization Test

In order to evaluate the effectiveness of CP in concrete, depolarization test was conducted by disconnecting the steel bar (S) from the sacrificial anode for 24 hours. Twenty-four-hour depolarization test results of the steel bars are shown in **Fig 6.7(a)** for specimens exposed to freeze temperature and high temperature.

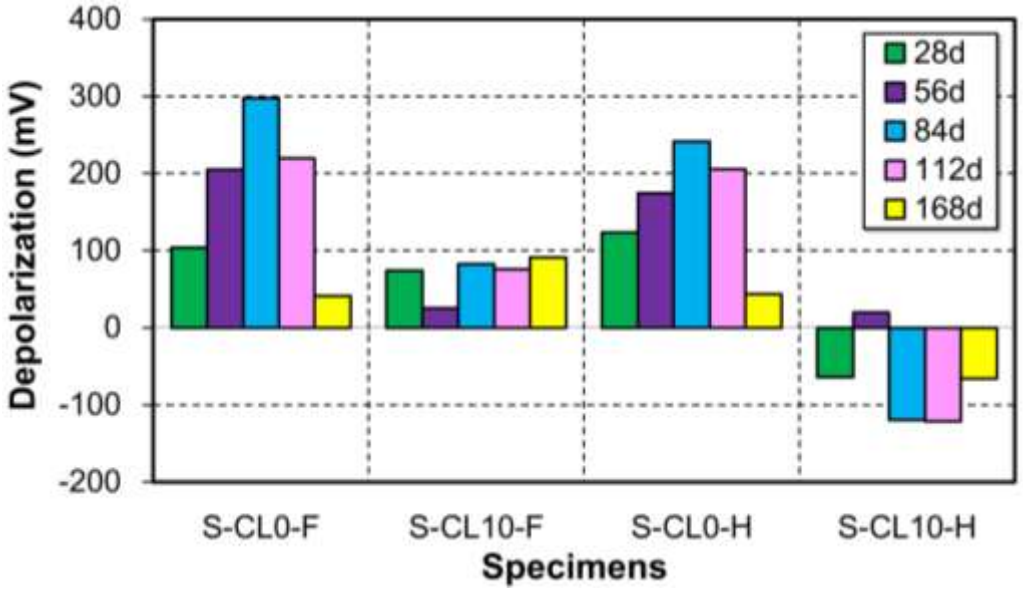

Fig 6.7 Summary of 24-h depolarization test result of steel bar with time

After disconnection for 24-hour, the extent of depolarization increased markedly exceeding 100mV for steel bar embedded in concrete without chloride contamination exposed to frost condition (S-CL0-F) and hot condition (S-CL0-H) from 0-day until 112-day of test period. However, the potential decay fell dramatically to ~-41mV and ~-43 mV for S-CL0-F and S-CL0-H respectively at 168-day.

Furthermore, after disconnection for 24-hour, the extent of depolarization of steel bar embedded in concrete with chloride contamination exposed to frost condition (S-CL10-F) increased steadily up to ~-90 mV at 168 days. Meanwhile, the depolarization level achieved was poor for S-CL10-H until at the end of test.

It is noted only steel bar embedded in concrete without chloride contamination exceed 100 mV criterion of cathodic protection.

Rest Potential

The bar charts in **Fig 6.8** illustrates about the rest potential or natural potential of steel bars and anode embedded in concrete with and without chloride contamination exposed to frost condition after disconnected each other by 24-hour.

.

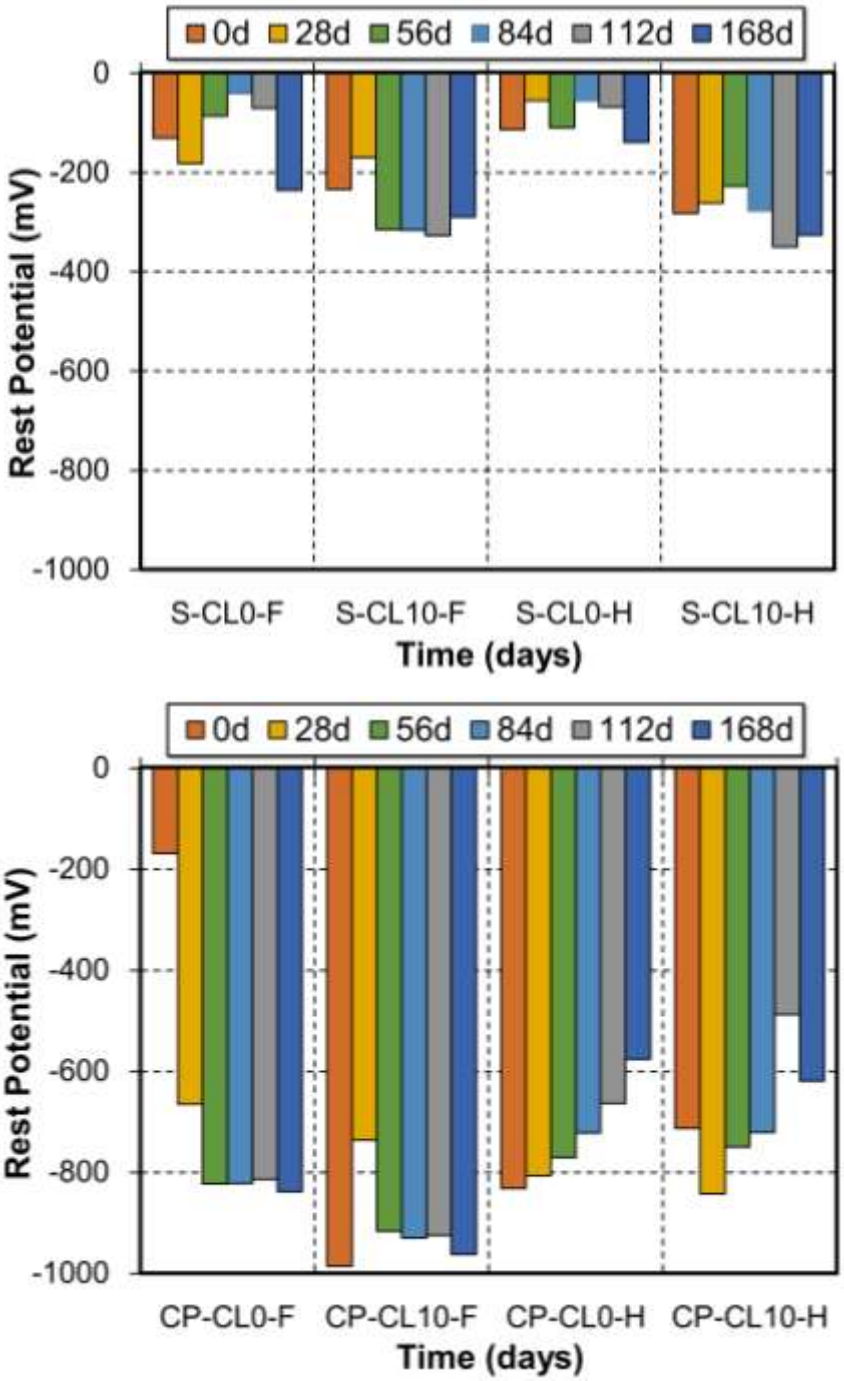

Fig 6.8 Rest potential of steel bar and anodes embedded in free-chloride and chloride-contaminated concrete exposed to hot condition

The data in **Fig 6.8** shows that natural potential of anode exposed to freeze condition and embedded in concrete with chloride contamination (CP-CL10-F) decreased gradually to more than ~-850 mV vs CSE time-dependently, which is

similar to natural potential of Zn alloys [6.3]. Meanwhile, for CP-CL0-F, there was a bottoming out of the rest potential between 56-day and 168-day of exposure time.

Furthermore, there were an upward trend to positive direction, ~-850 mV vs CSE, for natural potential of anode embedded in chloride-free and chloride-contaminated concrete which exposed to hot condition. It was observed that anode exposed to freeze condition will maintain potential of anode approach to natural potential of Zn alloys.

The data in **Fig 6.8** also shows that natural potential of steel bars embedded in concrete without chloride contamination exposed to frost and hot condition (S-CL0-F and S-CL0-H) depressed to positive direction, reaching ~-230mV for S-CL0-F and ~-130mV for S-CL0-H at 168 days of exposure time. Based on corrosion probability per ASTM C876-95 [6.4], it indicates no corrosion occurs in this steel bars.

Meanwhile, the natural potential of steel bars embedded in concrete with chloride contamination exposed to frost and hot condition (S-CL10-F and S-CL10-H) increased gradually and reaching a peak value up to ~-320mV for S-CL10-F and ~-340mV for S-CL10-H at 112 days of exposure time. But these value fell slightly to ~-280mV for S-CL10-F and ~-320mV for S-CL10-H at 168 days of exposure time.

It is noted during open circuit 24 hours in constant room, anode that initially exposed in freeze temperature still had protective potential over ~-800 mV. Meanwhile, the rest potential of steel bars shown lower than ~-350mV

Anodic Polarization Curve of Anode

The potential-current trajectory of the anodes exposed in frost condition measured at 24 hours after switch off is presented in **Fig 6.9**. As can be seen that current of anode embedded in chloride free concrete (CP-CL0-F) increased markedly from ~2 $\mu A/cm^2$ at 0-day to ~3 $\mu A/cm^2$ at 168-day. Meanwhile, the activity of anode embedded in chloride-contaminated concrete (CP-CL10-F) is remarkably increased, current of anode rose significantly with fluctuations from ~2 $\mu A/cm^2$ at 0-day to ~10 $\mu A/cm^2$ at 168-day of test period.

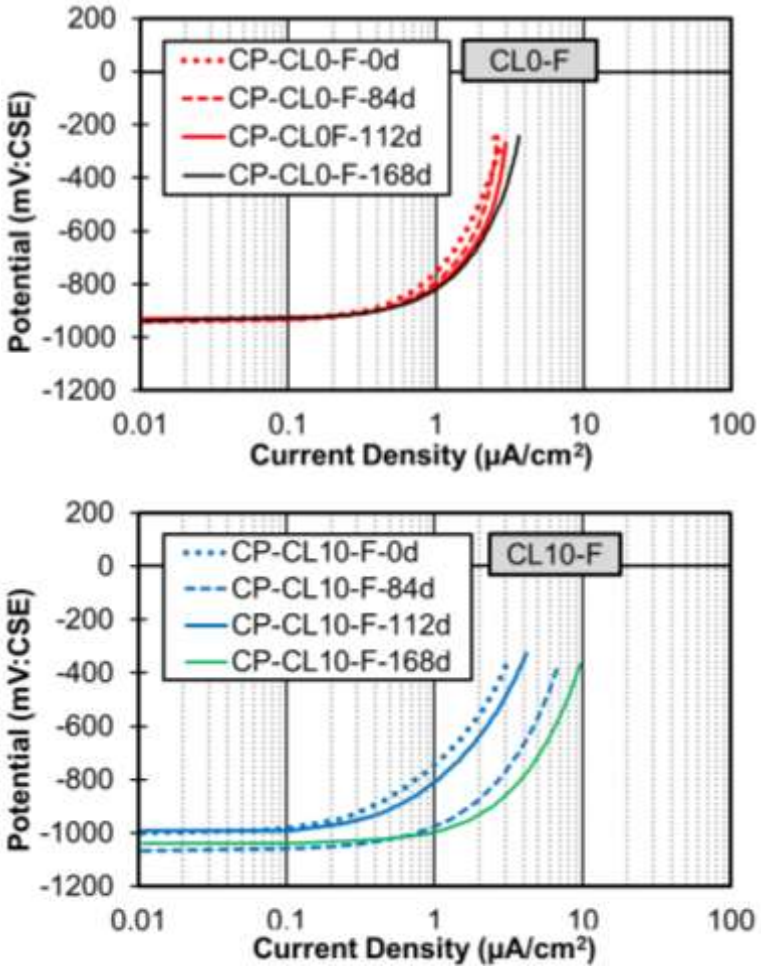

Fig 6.9 Anodic polarization behavior of anodes embedded in free-chloride and contaminated concrete exposed to freeze condition

Nevertheless, performance of anodes exposed to hot environment decreased gradually with the function of time as shown in **Fig 6.10**. It was fell off from ~2 μA/cm^2 at 0-day to ~0.7 μA/cm^2 at 168-day for CP-CL0-H, and from ~2 μA/cm^2 at 0-day to ~0.5 μA/cm^2 at 168-day for CP-CL10-H.

It was observed that there were an increasing anodic polarization with anode age for anode exposed in freeze temperature. Meantime, the curves in **Fig 6.10** reflect significant performance derating with the function of anode aging for anode exposed to hot condition.

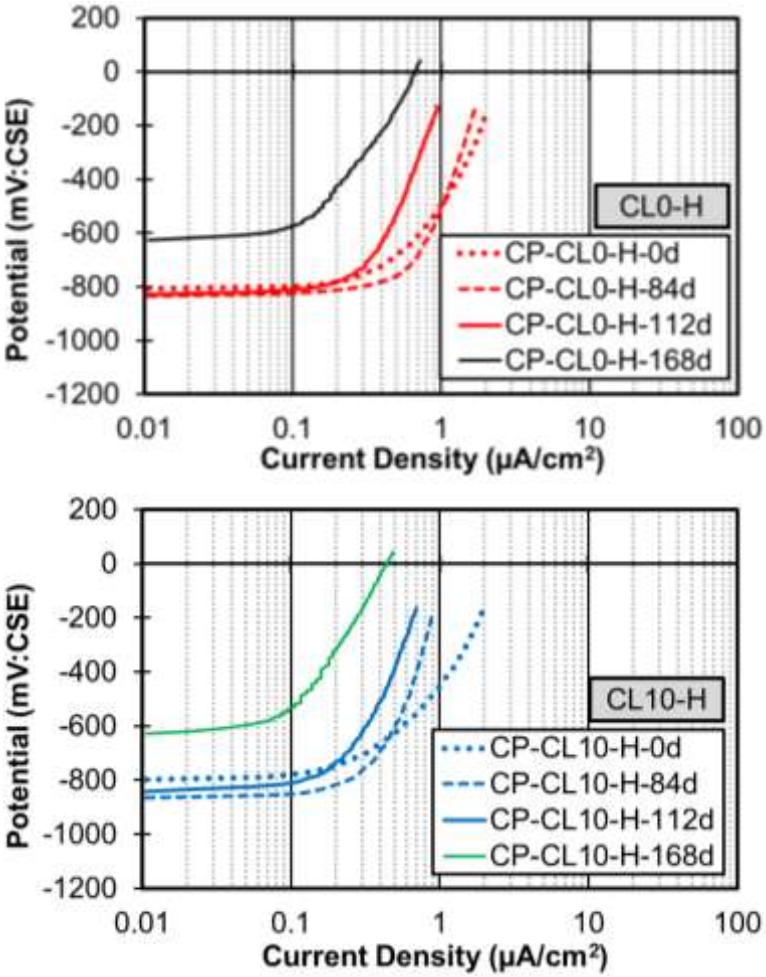

Fig 6.10 Anodic polarization behavior of anodes embedded in free-chloride and contaminated concrete exposed to hot condition

Anodic-Cathodic Polarization Curve of Steel Bar

Anodic-cathodic polarization curve of steel bar connected with anode (S) exposed to freeze temperature is presented in **Fig 6.11**. It shows that current density and cathodic polarization curve of steel bar (S-CL0-F and S-CL10-F) became larger with the function of time. Based on the grade of the passivity film of steel bar proposed by Otsuki [6.5], it is noted that the grade passivity of steel bars and level of O_2 on the steel bar exposed to freeze condition becomes worse over the test period.

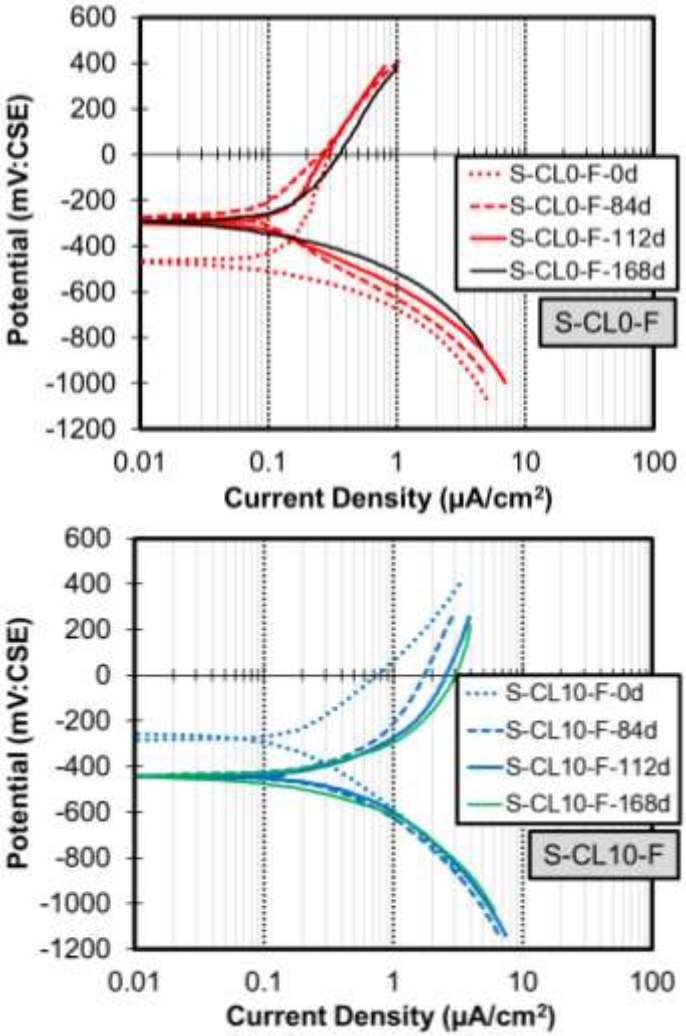

Fig 6.11 Anodic-cathodic polarization behavior of steel bar connected with anode (S) embedded in free-chloride and chloride-contaminated concrete exposed to freeze condition

The line graphs in **Fig 6.12** show about anodic-cathodic polarization curve of steel bar exposed to hot temperature during 168 days. It shows that current density of steel bar recovered slightly for S-CL0-H but the level of O_2 indicates becomes worse. Vice versa condition for S-CL10-H. The current density of these steel bar became larger with the level of O_2 which indicates decreased slightly over the test period

From the **Fig 6.11** and **Fig 6.12**, it can be seen that the grade of the passivity film of steel bar (S) embedded in concrete with chloride contamination exposed

to hot condition and freeze condition indicate tends to become worse with the function of period.

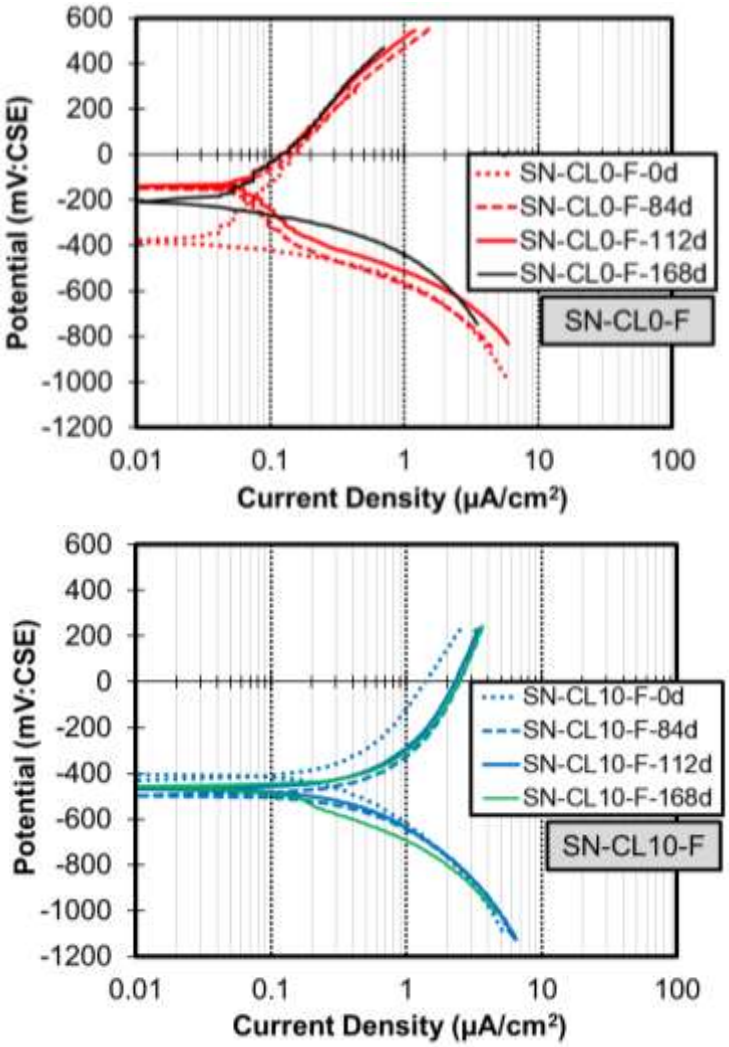

Fig 6.12 Anodic-cathodic polarization behavior of steel bar without connected to anode embedded (SN) in free-chloride and contaminated concrete exposed to freeze condition

The line graphs in **Fig 6.13** show about anodic-cathodic polarization curve of steel bars embedded inn concrete with and without chloride contamination exposed to hot temperature from 0-day until 168-day. It was observed that the grade of the passivity film of S-CL-0-H and S-CL-10-H indicate tends to become worse with the function of test period.

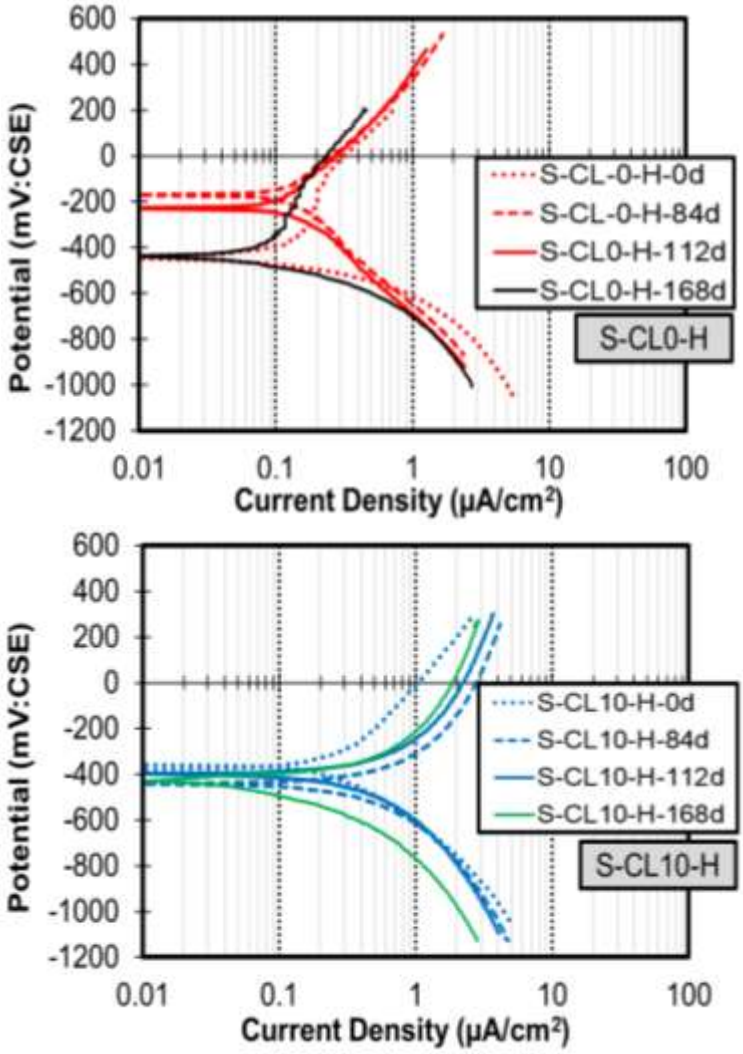

Fig 6.13 Anodic-cathodic polarization behavior of steel bar connected with anode (S) embedded in free-chloride and chloride-contaminated concrete exposed to hot condition

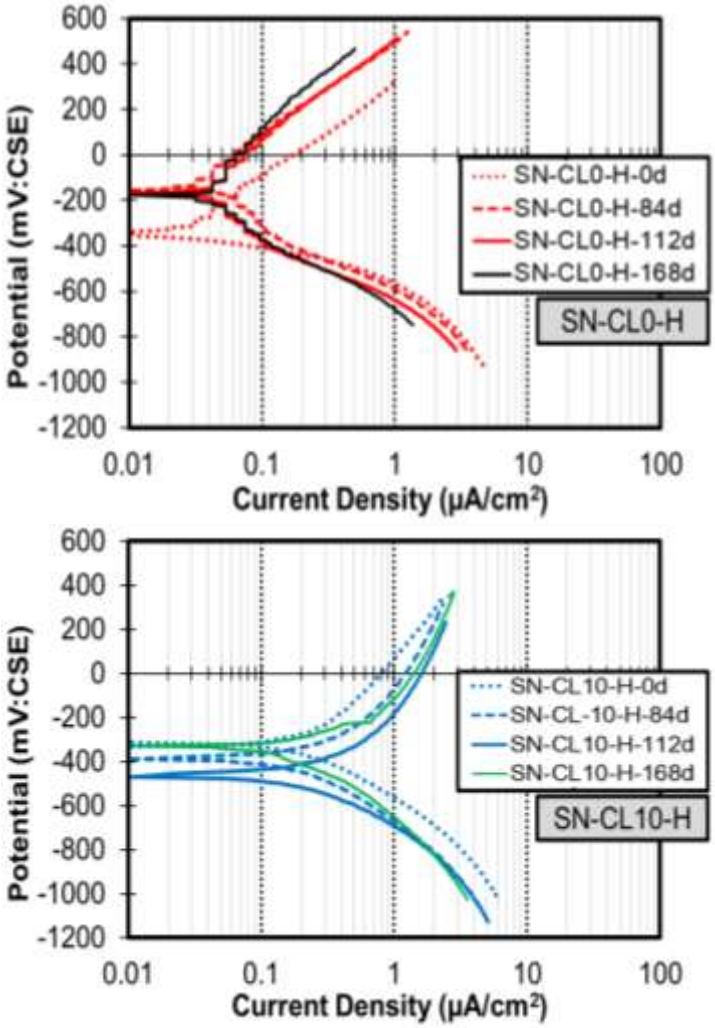

Fig 6.14 Anodic-cathodic polarization behavior of steel bar without anode connection (SN) embedded in free-chloride and contaminated concrete exposed to high temperature condition

Fig 6.14 illustrates about the passivity grade condition and level of O_2 of the steel without anode connection (SN) embedded in concrete exposed to high temperature condition. The data show that current density and level of O_2 of steel bar embedded in concrete without chloride contamination (S-CL0-H) became smaller during period of test. Meanwhile, for S-CL10-H, the passivity of steel bar became worse during 112 days but recovered slightly at 168 days with reduced markedly the level of O_2 on the steel surface over the period of the test.

From the **Fig 6.13** and **Fig 6.14**, it can be notice that the grade of the passivity film of steel bar (SN) embedded in concrete with chloride contamination

expose to hot condition and freeze condition as well indicate tends to become worse with the function of period.

Corrosion Rate of Steel Bar

Corrosion rate of steel bar exposed to freeze condition during open-circuit in constant room temperature is presented in **Fig 6.15**. The data from bar charts in **Fig 6.15** show that corrosion rate in concrete with chloride contamination is higher than in concrete without chloride contamination.

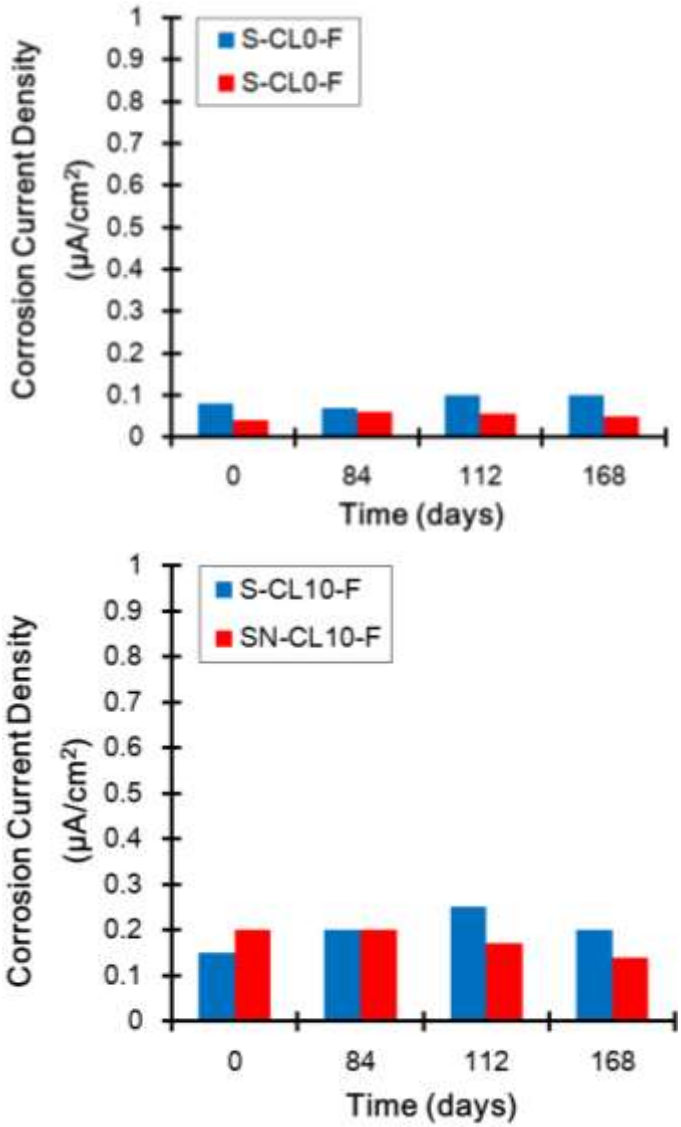

Fig 6.15 Corrosion rate of steel bars exposed to freeze condition

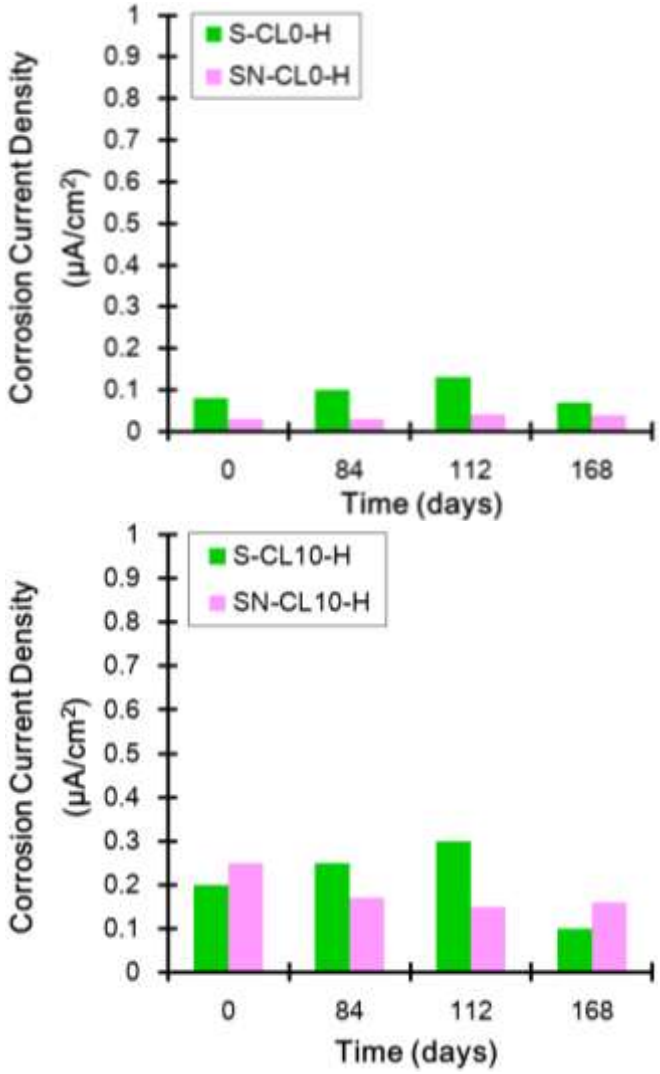

Fig 6.16 Corrosion rate of steel bars exposed to hot condition

Fig 6.16 shows about condition of the corrosion rate of bar embedded in concrete and exposed to high temperature. Steel bar embedded in concrete with chloride contamination has corrosion rate higher than in chloride free concrete. At the end of test of steel bar without CP connection (SN-CL10-H) and embedded in concrete with chloride contamination, has the higher corrosion rate than S-CL10-H.

6.5 Discussions

6.5.1 Effect of Temperature against Anode Performance

There was a downward trend to negative direction for potential of anode embedded in concrete with and without chloride content exposed to freezing

condition. Meanwhile, anode exposed to hot condition increase gradually to positive direction with the function of polarization time. It means aging of anode is faster in high temperature condition than in freeze condition. This observation is in good agreement with the protective current condition during anodic polarization test.

However, it is noted that during exposed in high temperature chamber, anode throwing power much higher than in freeze temperature chamber but lower during stayed in constant room temperature chamber. Vice versa for anode which exposed in freeze condition. It means that anodes produce higher levels of current in wet or humid environments compare than in dry conditions.

Even though deliver small current, but anode exposed in frost condition could polarize steel bars to protection level during on and instant-off condition. In addition, based on the potential decay data during depolarization test, it was observed that anode embedded in concrete without chloride contamination exposed to low and high temperature could polarize the steel bar exceed 100 mV of CP criterion. It means non-chloride contamination in concrete make anode effective to deliver the current and polarize the steel bar even though exposed to frost and hot temperature.

6.5.2 Corrosion Risk

Based on half-cell potential data, it was observed that steel bars embedded in chloride contamination and exposed to hot condition has the greater opportunity for corrosion occurs. Furthermore, steel bar under CP protection shown that trans-passive region occurs on steel bar under hot temperature exposure due to increment of steel bar potential no noble value. This observation is in good agreement with the natural potential of steel bar after disconnected from CP during 24-hour and passivity condition from anodic-cathodic polarization curve.

In addition, corrosion current density from Tafel`s slope extrapolation also shown that corrosion rate in concrete with chloride contamination is higher than in concrete without chloride contamination.

6.6 Conclusions

In this chapter, effect of temperature against performance of point anode to protect steel bar corrosion is presented. Thus, based on the results of experimental study, several conclusions can be drawn as follows;

1. Anode produce higher levels of current in wet or humid environments compare than in dry conditions.
2. Aging of anode is faster in high temperature condition than in freeze condition. This observation is in good agreement with the protective current condition during anodic polarization test.
3. Non-chloride contamination in concrete make anode effective to deliver the current and polarize the steel bar even though exposed to frost and hot temperature.
4. The higher chloride content in concrete, the higher possibility of corrosion occurs on the steel bar without CP protection which exposed in freeze and high temperature.
5. Anode is not effective to be used in high chloride content and exposed to high temperature with high humidity.

References

6.1 Dugarte, M., and Sagüés, A. A., "Galvanic Point Anodes for Extending The Service Life of Patched Areas upon Reinforced Concrete Bridge Members", Contact No. BD544-09, Final Report to Florida Department of Transportation, 2009, pp. 1-113.

6.2 Song, G., and Shayan, A. "Corrosion of Steel in Concrete: Cause, Detection and Prediction", ARRB Transport Research Ltd, Australia, 1998.

6.3 Dugarte, M. J. and Sagues, A. A., "Sacrificial Point Anode for Cathodic Prevention of Reinforcing Steel in Concrete Repairs: Part 1 – Polarization Behavior," Corrosion, NACE International, Houston, 70(3), 2014, pp. 303-317.

6.4 ASTM C 876-95, "Standard Test Method for Half-cell Potentials of Uncoated Reinforcing Steel in Concrete," Philadelphia: American Society of Testing and Materials, 1999.

6.5 Otsuki, N., "A Study of Effectiveness of Chloride on Corrosion of Steel Bar in Concrete," Report of Port and Harbor Research Institute (PHRI), Japan, 1985, pp. 127-134.

6.6 Alhozaimy, A., Hussain, R. R., Al-zaid, R., and Al-Negheimish, "Coupled Effect of Ambient High Relative Humidity and Varying Temperature Marine Environment on Corrosion of Reinforced Concrete", Construction and Building Materials, 2012, No. 28, pp. 670–679.

6.7 Cicek, V., "Cathodic Protection: Industrial Solutions for Protecting Against Corrosion", John Willey & Sons, Inc., 2013.

6.8 Hobbs, D. (2001). "3rd Concrete deterioration: causes, diagnosis, and minimising risk". In: International Materials Reviews 46.3, pp. 117–144.

6.9 Bertolini, L., Elsener, B., Pedeferri,P., Redaelli, E., and Polder, R., "Corrosion of Steel in Concrete", 2013, Wiley-VCH Verlag GmBH & Co KGaA.

6.10 RILEM Technical Committee 124-SRC, P. Schiessel (ed), "Draft Recommedation for Repair Strategies for Concrete Structures Damaged

by Reinforcement Corrosion", Materials and Structures, 1994, Vol. 27, pp. 415 – 436.

6.11 Bennet, J., and Turk, T., "Criteria for the Cathodic Protection of Reinforced Concrete Bridge Elements", Technical Alert, SHRP-S-359, 1994.

6.12 Pedeferri, P., "Cathodic Protection and Cathodic Prevention", Construction and Building Materials, 1996, Vol. 10, No. 5, pp. 391-402.

6.13 Bennet, J., and McCord, W., "Performance of Zinc Anodes Used to Extend the Life of Concrete Patch Repairs", 2006, Corrosion/2006, NACE International, Paper No. 06331.

6.14 Sergi, G., and Page, C., "Sacrificial Anodes for Cathodic Prevention of Reinforcing Steel around Patch Repairs Applied to Chloride-contaminated Concrete", European Federation of Corrosion Publication.

6.15 L. Bertolini, M. Gastaldi, M.P. Pedeferri, P. Pedeferri, T. Pastore, Proceedings of the International Conference on Corrosion and Rehabilitation of Reinforced Concrete Structures, Orlando, USA, 1998.

6.16 S. Qian, D. Qu, G. Coates, Galvanic coupling between carbon steel and stainless steel reinforcements, Can. Metall. Q. 45, 2006, pp. 475-484.

6.17 G K Glass, N Davison, A C Roberts, Hybrid corrosion protection of chloride-contaminated concrete, Proceedings of the Institution of Civil Engineers, Constr. Mater. 161, 2008, pp. 163‑172.

6.18 L. Bertolini, M. Gastaldi, M.P. Pedeferri, P. Pedeferri, T. Pastore, Proceedings of the International Conference on Corrosion and Rehabilitation of Reinforced Concrete Structures, Orlando, USA, 1998.

Chapter 7 SERVICE LIFE ESTIMATION OF ZINC SACRIFICIAL ANODE CATHODIC PROTECTION BY CURRENT ACCELERATION

7.1 Introduction

In this chapter, the life-time of zinc sacrificial anode against corrosion protection of steel bar embedded in concrete is studied. It is now recognized that cathodic protection (CP) of concrete reinforcing steel is necessary to ensure long term integrity of the structure. The CP system must be designed to provide the required current to every part of the structure for the required design life.

The protection delivered by a sacrificial anode as one of method in CP system is largely determined by current output of the anode system and its distribution to the protected steel [7.1), (7.2), (7.3)]. This requires determining anode size, weight, number and distribution to supply current for the design life of the structure [(7.4), (7.5)]. Thus, anode life is primarily determined by anode current output, anode charge capacity, anode utilization and anode efficiency. Longer lives may generally be achieved by using more anodes or anodes with high charge capacities that deliver low current densities.

Nowadays, anode service lifetime is one of among the challenges that are still to be taken up in CP system. However, to observe anodes during service life

will take a long time and long term performance anode data is so limited nowadays. Therefore, this study was carried out in order to observe the zinc sacrificial anode service life shortly with respect to current acceleration through the impressed current system.

7.2 Research Objective

The purpose of this study is to observe service life of the zinc sacrificial anode shortly with respect to current acceleration through the impressed current system. In order to reach the general aim, the following specific objectives have been defined as follow:

1. To observe the anode efficiency and anode capacity by increasing the current 10 times higher than initial current condition of anode
2. To investigate service life of anode expose to constant room temperature

Additionally, to support the general aim and specific objectives above, it is observe also the condition of anode embedded in concrete under circumstances; without bar assembly and without current acceleration, which has purpose as follows:

3. To investigate the effect of chloride contamination in concrete against durability of anode itself
4. To observe the effect of humidity condition towards polarization of anode

Therefore, to simplification discuss this chapter, we marking the specimen to obtain objective no. 3 and 4 as Type A specimen, objective no. 1 and 2 as Type B specimen.

7.3 Experimental Methodology

Type A Specimen

The specifications for type A is shown in **Table 7.1**. Two types of commercial zinc sacrificial anode namely XP-type and F-type were used to find the most effective anode in terms of the protection to the concrete rebar.

There are 4 (four) conditions where set up for type A specimens as follows:

1. CL1 which the XP-type of anode embedded in contaminated-chloride
2. NCL1 which XP-type of anode embedded in free-chloride concrete

3. CL2 which F-type anode embedded in concrete with chloride content
4. NCL2 which F-type anode embedded in concrete without chloride content

Table 7.1 Specifications for Type A specimen

Specimen ID	Length of Specimen (mm)	Cathodic Protection System	Type of Anode	Chloride Content (kg/cm^3)
CL1	290	Zinc Sacrificial Anode	XP	10
CL2	290	Zinc Sacrificial Anode	F	10
NCL1	290	Zinc Sacrificial Anode	XP	0
NCL2	290	Zinc Sacrificial Anode	F	0

Type B Specimen

The setting out for type B is describe in **Table 7.2**. In addition, there were 2 (two) types of acceleration method proposed in this acceleration process as shown in **Table 7.3**; accelerate current from anode to one-steel bar (CA1) and accelerate current from anode to two-steel bar (CA2).

Table 7.2 Specification for Type B specimen

Specimen ID	Length of Steel Bar (mm)	Initial Condition of Steel Bar	Chloride Content (kg/m^3)	Cathodic Protection System	Type of Anode
CA1	250	Non-Rusted	10	Zinc Sacrificial Anode	F
CA2	250	Non-Rusted	10	Zinc Sacrificial Anode	F

Table 7.3 Detail of current acceleration conditions

Specimen ID	Initial Current (mA)	Accelerate 10 times (mA)	Remark
CA1	0.07	0.7	CP connected to one-steel bar
CA2	0.056	0.7	CP connected to two-steel bar

Originally, the initial current for CA1 and CA2 specimens are 0.07 mA and 0.056 mA. However, for the acceleration propose the current was adjust to 0.7 mA

for both specimens. The position of the anode is the same for both condition. Current flow from CP to steel bar in CA1 was delivered to one-steel bar only. Meanwhile in CA2, current throwing interrelated with two-steel bar.

7.4 Experimental Outline

7.4.1 Materials

Ordinary Portland Cement (OPC) and tap water (temperature 20±2°C) were used as mixing water in this study. Washed sea sand passing a 5 mm sieve with a density of 2.58 g/cm^3 and water absorption of 1.72% which was less than 3.5% as stated in JIS standard were used as the fine aggregate.

Meanwhile, crushed stone with a maximum size of 10 mm was used as the coarse aggregate. All aggregates were prepared under surface-saturated dry condition. The properties of aggregates and admixtures are shown in **Table 7.4**.

Table 7.4 Properties of materials

Component	**Physical properties**	
Ordinary Portland Cement	Density, g/cm^3	3.16
Fine Aggregate	Density, g/cm^3 (SSD Condition)	2.58
	Water absoption (%)	1.72
	Fineness modulus	2.77
Coarse aggregate	Density, g/cm^3	2.91
AEWR agent	Polycarboxylate ether-based	
AE agent	Alkylcarboxylic type	

There were 2 (two) types of commercial anode used in this study; XP and F type. A galvanic anode made of zinc as main material was used as sacrificial anode. XP-type anode has dimension 60 mm in diameter and 30 mm in thickness. In addition, F-type anode has dimension 140 mm in length, 45 mm in width and 13 mm in depth, as shown in **Photo 7.1** and **Photo 7.2** successively.

Photo 7.1 Zinc sacrificial anode XP-type

Photo 7.2 Zinc sacrificial anode F-type

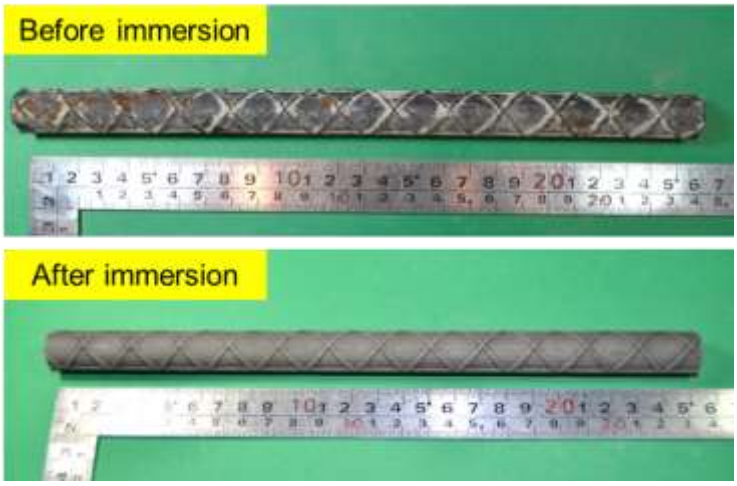

Photo 7.3 A 20-year-old deteriorated steel bar used in this study

7.4.2 Steel Bar

In this study, a 20-year-old deteriorated (rusted) reinforcing steel bar with a diameter of 13 mm was used as shown in **Photo 7.3**. Then, this rusted rebar was immersed in 10% (weight percentage) diammonium hydrogen citrate solution for 24 hours and then the rust was removed by using steel wire brush to obtain non-deteriorated (non-rusted) condition. These steel bars were taken from the specimens

exposed in severe chloride environment with high temperature for 20 years.

At the ends of steel bar in repair section, a 30cm length lead wire was screwed. Adjacent steel elements were also connected to the sacrificial anode through wires to measure the flow of the current. The connection of wire and steel bar was covered by epoxy resin in order to avoid the corrosion at the connection. Thickness of epoxy layer was approximately 10 mm. However, these connectors were temporarily disconnected for the purpose of measuring the instant-off potential, the protective current and potential decay in depolarization test.

7.4.3 Mix Proportions

The concrete mixture proportions of concrete are shown in **Table 7.5**. A concrete mix with a water to cement (w/c) ratio of 0.45 was used for all specimens. The ratio of fine aggregate to total aggregate volume (s/a) was 0.47. Air-entraining agent and water-reducing admixture were added to the cement mass to obtain the slump and air content in all concrete mixes in the range of 10±2.5cm and 4.5±1% respectively.

Chloride-contaminated concrete were casting for CL and CA series. Meanwhile, free-chloride concrete was casting for NCL series. In order to accelerate the corrosion process, chloride ions were deliberately added around 10 kg/m^3 during mixing into chloride-contaminated concrete. Pure sodium chloride (NaCl) was used as the source of chloride ions.

Table 7.5 Mixture proportions of CL, NCL and CA series

Material	CL1, CL2	NCL1, NCL2	CA1, CA2
Water-cement ratio (w/c), %	45	45	45
Sand-aggregate ratio (s/a), %	47	47	47
Water, kg/m^3	190	190	190
Cement (C), kg/m^3	422	422	422
Sand, kg/m^3	766	766	766
Gravel, kg/m^3	970	970	970
Chloride, kg/m^3	10	0	10
Additive per m^3:			
- AE, mL	19	19	19
- AE-WR, gr	1.34	1.34	1.34

7.4.4 Specimen Geometry

Four concrete specimens for CL and NCL series and two concrete specimens for CA series with the dimensions of 290 mm in length, 150 mm in width and 100 mm in depth were prepared in this study. CP positioned in the center of specimen with the cover thickness of 30 mm from the bottom surface of the specimen in CL and NCL series. Furthermore, each concrete specimens in CA series contained two steel bars with a diameter of 13 mm, same surface conditions and positioned parallel to each other with an intermediary distance of 40 mm and the cover thickness of 30 mm from the bottom surface of the specimen. The details of the concrete specimens for CL, NCL and CA series are illustrated in **Fig. 7.1** and **Fig. 7.2** respectively.

Fig 7.2 (a) and **Fig 7.2 (b)** shows the specimen design for CA1 and CA2 specimens. There were zinc sacrificial anodes (CP) with F-type embedded in concrete. For CA1, CP connected to one-steel bar (remark as S). However, CP connected to both steel bar in concrete (remark as S and SN) for CA2 specimen.

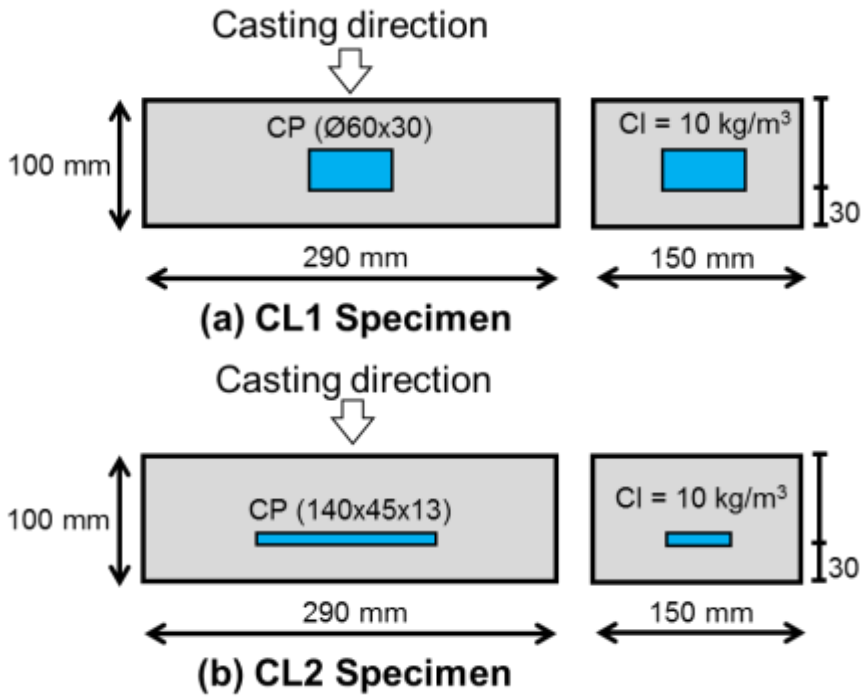

Fig 7.1 Detailed layout of concrete specimens with zinc sacrificial anode only embedded in concrete

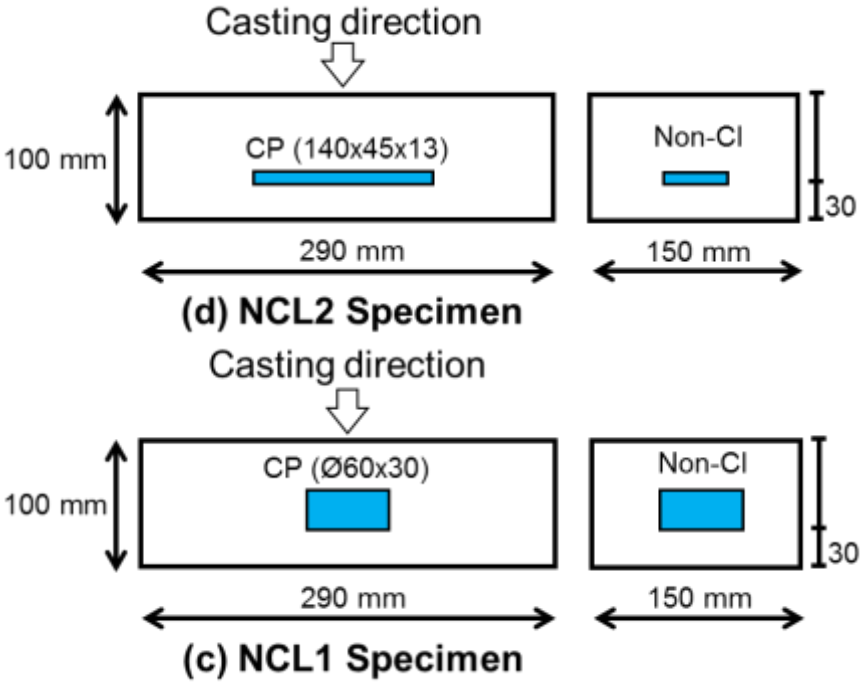

Fig 7.1 Detailed layout of concrete specimens with zinc sacrificial anode only embedded in concrete (Continued)

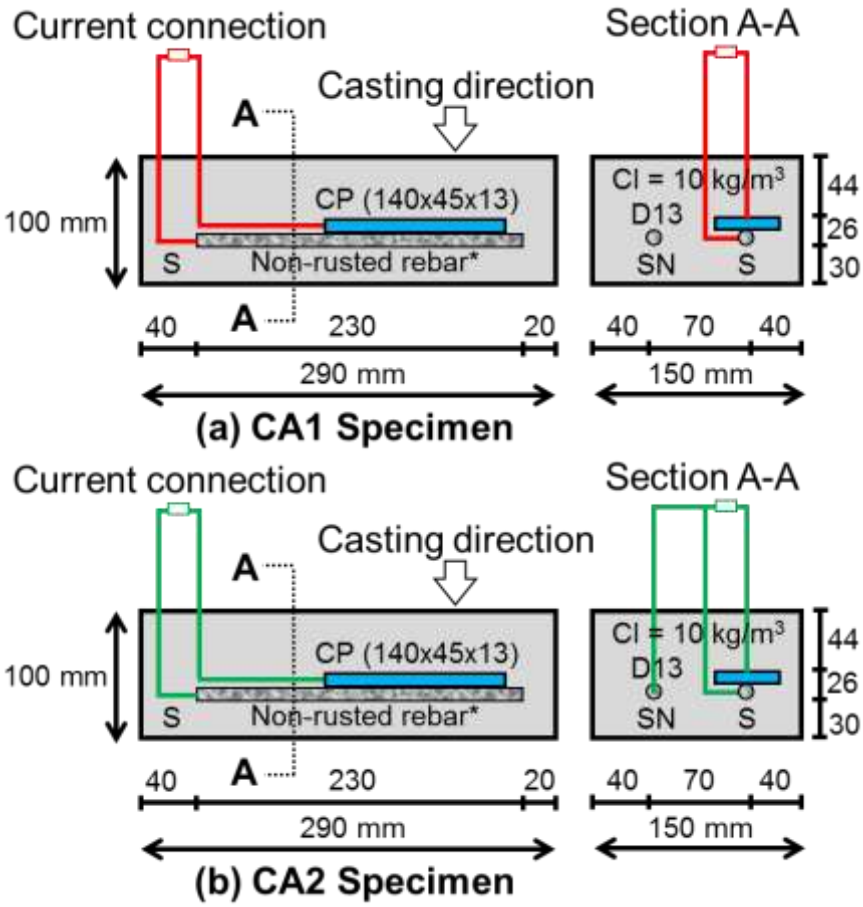

Fig 7.2 Detailed layout of concrete specimens with acceleration current type A

7.4.5 Casting and Curing

After casting of concrete and demolding, all specimens were subject to 28 days of sealed curing with wet towels. After 28 days of sealed curing, the sacrificial anode was connected to the embedded steel-S for CA1; S and SN for CA2. Silver/silver chloride electrode (Ag/AgCl) is used as reference electrode for potential mapping in this study and convert to Copper/copper sulphate electrode (CSE) with temperature consideration.

7.4.6 Exposure Condition

After the casting finished, all specimens were subjected to exposure conditions, in the air curing with a temperature of 20±2°C and a relative humidity of 60%. This environment was kept for 84 days of exposure time for CL and NCL specimens. After that, the specimens were moved to the wet-dry cycle condition. The wet cycle involved immersion in a 3% NaCl solution for two days followed by five days in dry conditions; hence one cycle corresponded to seven days. CL and NCL specimens has been 28 times in cycles. Measurements were taken weekly at the end of wet cycle. The exposure condition of Cl and NCL series as can be seen in **Photo 7.4**.

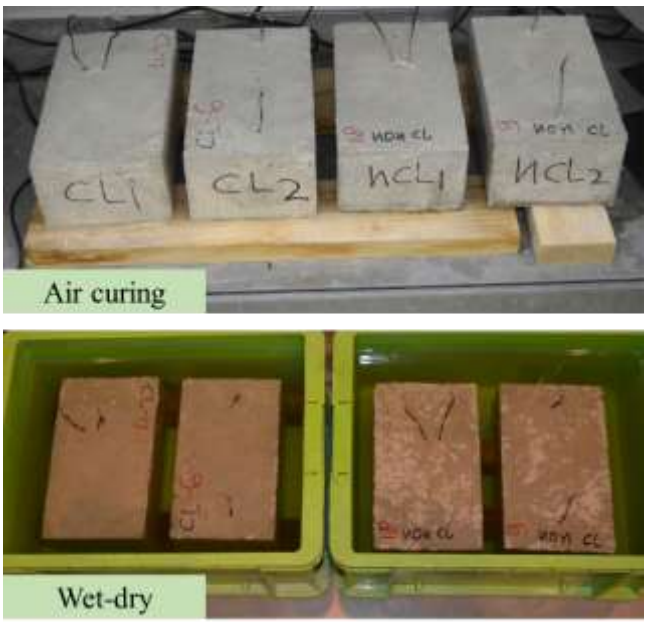

Photo 7.4 Exposure conditions of CL and NCL specimens

However, for CA specimens, after the casting was finished, all specimens were placed in the air curing with a temperature of 20±2°C and a relative humidity of 60% from 0 day until 70 days of exposure time. **Photo 7.5** below shows about exposure condition of CA1 and CA2 specimens in the air curing with a temperature of 20±2°C and a relative humidity of 60%. In addition, **Fig 7.3** show about scheme of acceleration current in CA1 and CA2 by impressed current cathodic protection system.

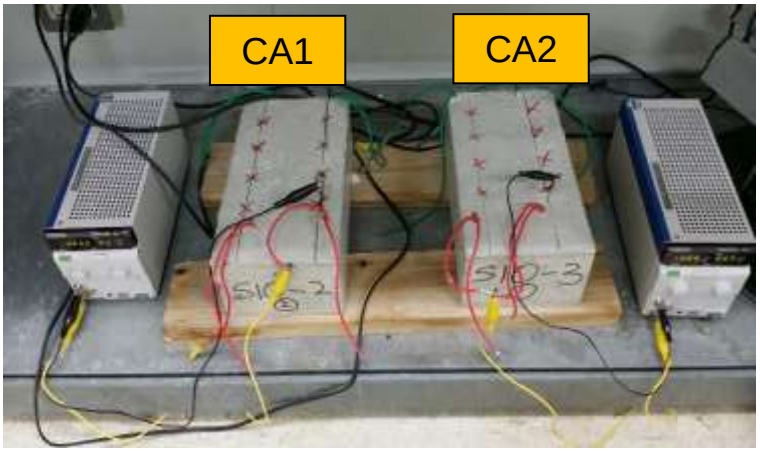

Photo 7.5 Exposure conditions of CA specimens

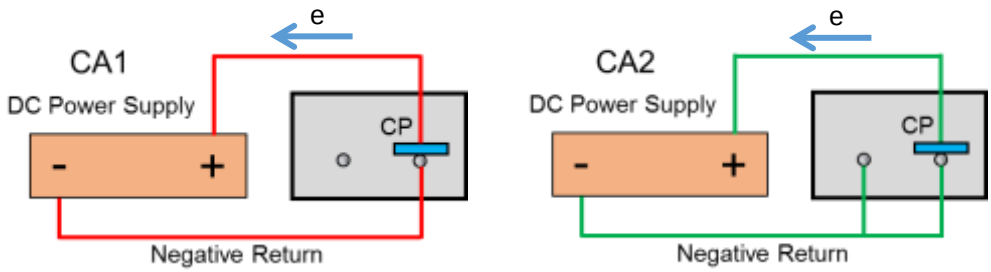

Fig 7.3 Scheme of cathodic protection systems in CA1 and CA2

7.4.7 Monitoring System

Table 7.6 represents, the type of electrochemical testing conducted to CL, NCL and CA specimens in order to monitoring the polarization behavior of anode and steel bar in concrete. For CL and NCL specimens, due to just anode only embedded in concrete, type of testing focused on polarization behavior of anode and anodic polarization curve of anode.

Meanwhile for CA specimens, the type of monitoring system consist of half-cell potential, on potential, instant-off potential, protective current, potential decay during depolarization test, rest potential, polarization behavior of anode, anodic polarization curve of anode, anodic-cathodic polarization curve of steel bar, corrosion rate by extrapolation from Tafel slope at anodic-cathodic polarization curve.

Table 7.6 Electrochemical testing on CL, NCL and CA specimens

Test Item	CL specimen	NCL specimen	CA specimen
Half-cell potential	X	X	○
On potential	X	X	○
Instant-off potential	X	X	○
Protective current	X	X	○
Potential decay (after switch off 24h)	X	X	○
Rest potential	X	X	○
Polarization behavior of anode	○	○	○
Anodic polarization curve of anode	○	○	○
Anodic-cathodic polarization curve of steel bar	X	X	○
Corrosion rate	X	X	○
Visual inspection of anode	X	X	○

Remark; X: Not tested, ○: Tested

7.5 Results and Discussion of CL and NCL Specimens

7.5.1 Potential of Zinc Sacrificial Anode

Fig 7.4 describes about development of anode potential with time during open circuit for both sets of zinc sacrificial anode namely XP-type and F-type. The data show that during exposed in the air curing with a temperature of 20±2°C and a relative humidity of 60%, potential of anodes embedded in chloride-contaminated concrete and chloride-free concrete rose gradually to noble value throughout this period.

In contrast, after the exposure conditions changed to wet-dry cycles, the potential of both sets anode fell significantly to the negative direction, due to the change in moisture and oxygen content in the concrete. After 280 days of exposure time, potential of XP-type anode embedded in chloride-free concrete (NCL2) has potential more than -1000mV with respect to $Cu/CuSO_4$ (CSE) and following by potential of F-type anode embedded in chloride-free concrete (NCL1), XP-type anode and F-type anode embedded in chloride-contaminated concrete respectively.

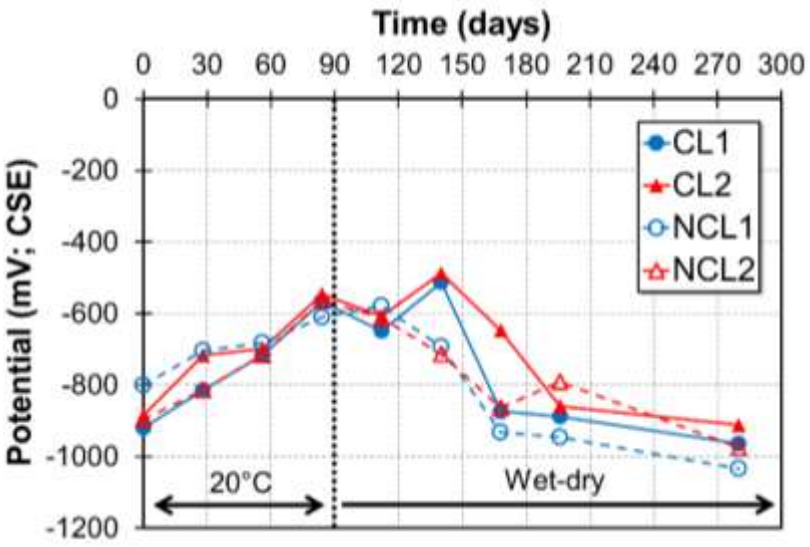

Fig 7.4 Anode potential (off potential) evolution with time for both sets of anode embedded in chloride-contaminated concrete and chloride-free concrete during exposed to air curing and wet-dry conditions

It was observed that moisture and humidity of environment generates protective potential from anode more cathodically polarizes than in dry condition. From this it can be said that the potential value of the sacrificial anode was also affected by the moisture level of the concrete.

7.5.2 Anodic Polarization Curve of Zinc Sacrificial Anode

Fig 7.5 shows, the potentiodynamic polarization measurement result or anodic polarization curve of anodes during open circuit from 0-day until 280-day of exposure time.

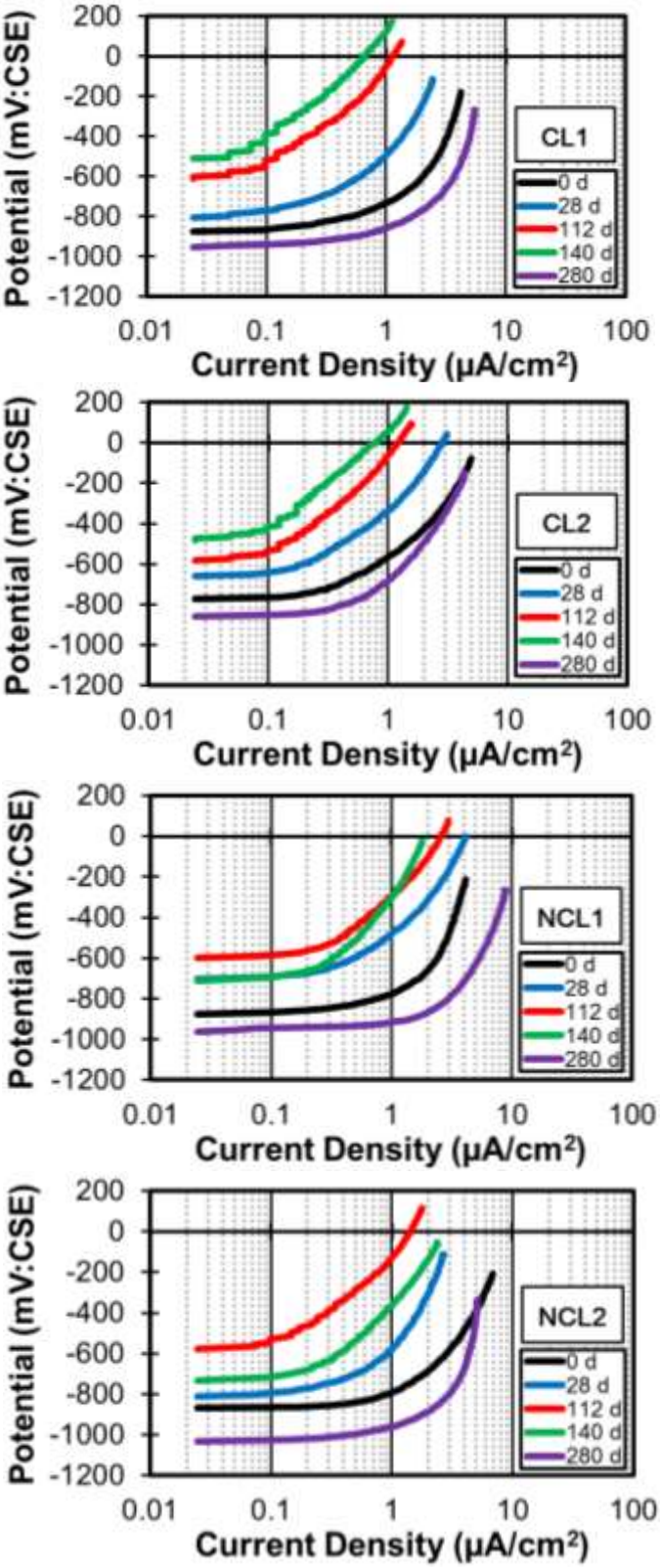

Fig 7.5 Anodic polarization behavior of both sets of anode embedded in chloride-contaminated concrete and chloride-free concrete during exposed to air curing and wet-dry conditions

From **Fig 7.5** it was observed that current density of zinc sacrificial anodes embedded in chloride-contaminated concrete (CL1 and CL2) fell gradually during exposed to air curing and transition phase from air curing to wet-dry cycles. However, the current density of anodes increased markedly from 1 $\mu A/cm^2$ to 5.5 $\mu A/cm^2$ for CL1 and from 1.5 $\mu A/cm^2$ to 3 $\mu A/cm^2$ for CL2 after 28 of cycles.

The same condition was observed for zinc sacrificial anodes (NCL1 and NCL2) embedded in chloride-free concrete from 0 day to 112 days of exposure time. Nevertheless, after 140 days or 20 cycles, the anodes starting to provide larger protection current. Potentiodynamic scans show that XP-type anode embedded in chloride-free concrete (NCL1) provide current density around 9 $\mu A/cm^2$ and 5 $\mu A/cm^2$ for F-type anode (NCL2) after 28 cycles or 196 days after put in wet-dry condition. Protective potential also rose significantly to more than -850 mV with respect to CSE (CP criterion) around -962 mV, -861 mV, -961 and -1032 mV for CL1, CL2, NCL1 and NCL2 at 280 days. This difference because of the moisture content inside the concrete during wet-dry conditions.

It means that protective potential and protective current from anodes achieved when concrete in humid condition. High moisture content accelerate the zinc sacrificial anode more active to provide large protection current.

7.6 Results and Discussion of CA Specimens

7.6.1 Anode Polarization

Protective Current of Anode

The protective current delivered by the anodes to the entire rebar assembly as a function of exposure time is shown in **Fig 7.6** for both sets of current acceleration specimens namely CP-CA1 and CP-CA2. Current at 0-day measurement indicates the initial current before acceleration. For anode with acceleration current connected to one-steel bar, the protective current fell dramatically from anodic site to cathodic side at 28 days of exposure time. It means that throwing power of anode with 10 times higher of current acceleration to one-steel bar up to 20 days was successfully protected the steel-bar.

On the contrary, for anode with acceleration current connected to two-steel

bar (CP-CA2) fell steadily to cathodic site since acceleration initiate to anode embedded in concrete. It means that anodes fail to throw the protection current by this acceleration method.

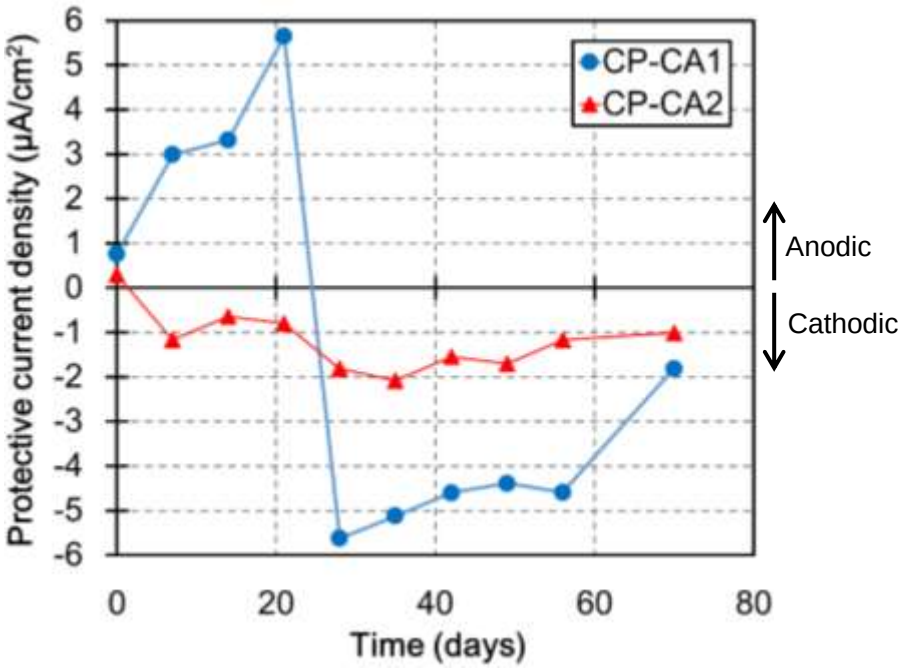

Fig 7.6 Protective current evolution with time for anodes with both sets of current acceleration method

Potential of Anode

The evolution of on potential and instant-off potential of anode with acceleration current connected to one-steel bar (CP-CA1) and two-steel bar CP-CA2) are presented in **Fig 7.7**. The data from **Fig 7.7** shows that on potential and instant-off potential varies with polarization period. In the beginning of exposure, on potential soared to ~1200 mV for CA1 and ~2000 mV for CA1. Afterwards, on potential reached a peak to ~2300 mV at 42 days for CA1. Meanwhile, on potential of CA2 was at its highest level to ~2500 mV in 28 days.

Furthermore, potential of CA1 and CA2 decreased dramatically to negative direction, reaching less than ~-600 mV during instant-off condition as the function of polarization period. However, it was indicates that anode difficult to polarize the steel bar because protective potential of anode less than acceptance performance of

cathodic protection, -850 mV, over much of test period.

From **Fig 7.7** it was observed that current acceleration stimulate the protective potential tends to noble values during on and instant-off.

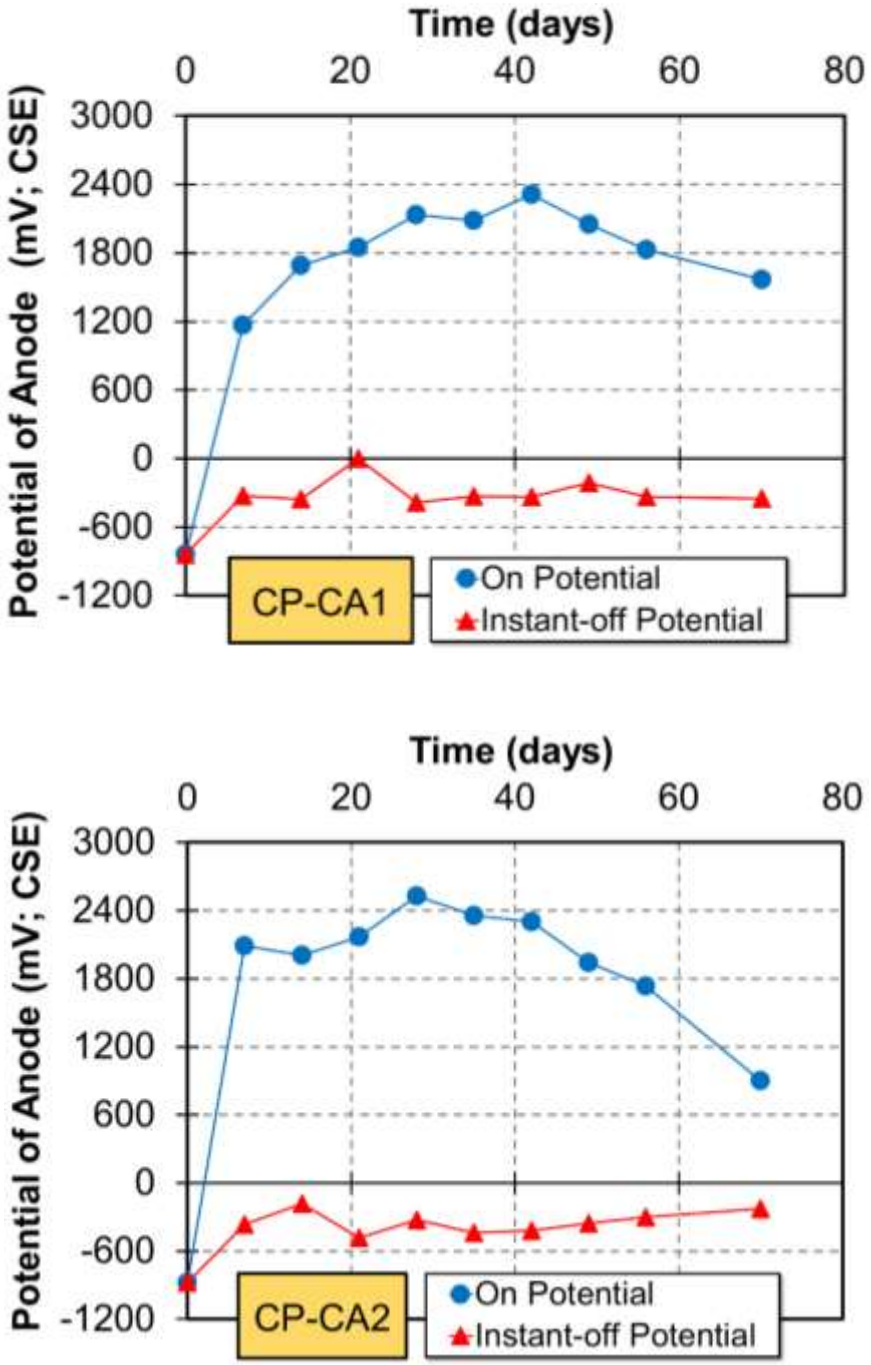

Fig 7.7 Anode potential (on potential and instant-off potential) evolution with time for anodes embedded in chloride-contaminated concrete with both sets of current acceleration method

Anodic Polarization Curve of Zinc Sacrificial Anode

Fig. 7.8 describes the anodic polarization curve of sacrificial anode in CA1 and CA2 series measured after anode the switch off by 24 hours. It was observed that the current density of CP-CA2 gradually decreases time-dependently from 0 day to 70 days of exposure time. Meanwhile, for CP-CA1, current density fell gradually from ~2 μA/cm^2 at 0-day to ~0.95 μA/cm^2 at 70-day of test period. However, the current density of CP-CA1 increased markedly to ~1 μA/cm^2 at 70-day.

It was observed that there were an increasing anodic polarization with anode age for anode in CA1. Meantime, the curves in **Fig 7.8** reflect significant performance derating with the function of anode aging for anode in CA2.

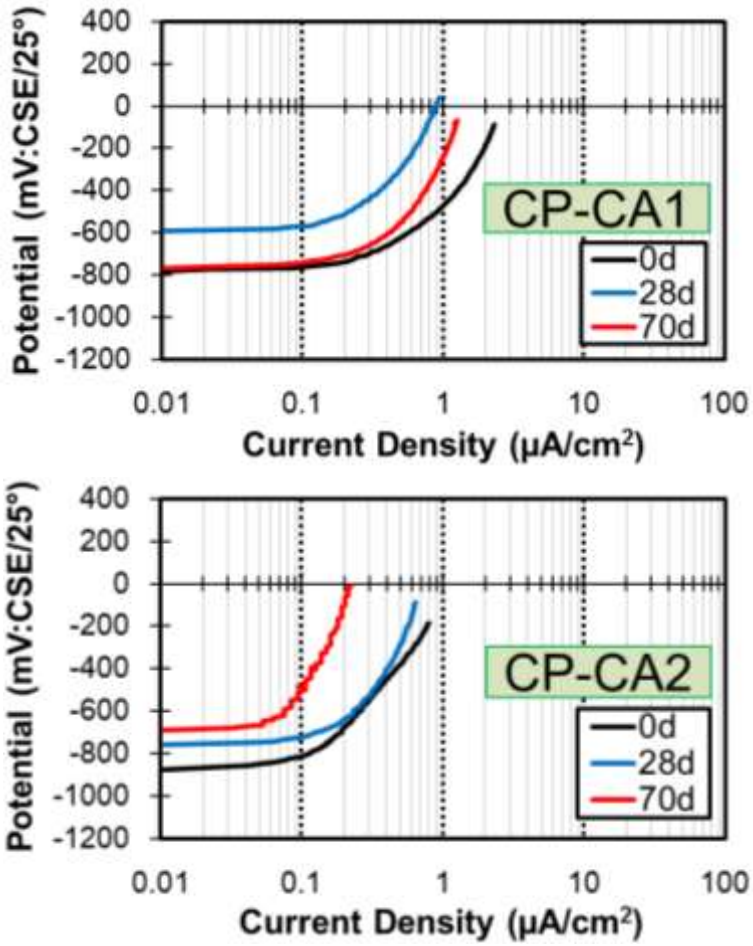

Fig 7.8 Anodic polarization behavior of anodes embedded in chloride-contaminated concrete exposed to air curing conditions after

7.6.2 Rebar Polarization

Potential of Steel Bar

Potential of steel bar connected to CP (S-CA1, S-CA2 and SN-CA2) during current acceleration with polarization time is presented in **Fig 7.9**. On potential of steel bar connected to CP (S-CA1) with 10 times current acceleration decreased with fluctuations to more negative during polarization time. In 28-day of exposure time, on potential reached a peak ~-1000 mV. However, potential of steel bar increased to noble value during instant-off condition. During 70-day of exposure time, there were an upward trend to noble value in the on potential and instant-off potential of S-CA1, reaching ~-550 mV and ~-800 mV respectively. It was observed that on potential of S-CA1 ~-200 mV to ~-400 mV more negative than instant-off potential. In general, it was indicates S-CA1 cathodically protected because protective potential of steel bar shown in the range of acceptance performance of cathodic protection -850 mV.

Furthermore, potential of S-CA2 during on and instant-off signified decreased gradually from o-day until 21-day of polarization time. In 21-day of exposure time, on potential and instant-off potential of S-CA2 reached a peak at ~-780 mV and ~-580 mV respectively. Afterwards, both of potential condition increased gradually to noble value between 28-day and 70-day of exposure time. It was noticed that S-CA2 in the trans-passive region which leading to damage in the passive protective films and resulting mostly in pitting-corrosion as protective potential of steel bar shown increased to positive direction.

Meanwhile, on potential of SN-CA2 fell gradually to ~-750 mV after 28 days of polarization period. But, this trends rose gradually to positive direction until at the end of test. There was a plateau in the instant-off potential of SN-CA2 between 0-day and 56-day. Afterwards, instant-off potential rose significantly to noble value at 70-day of exposure time. As same as like S-CA1 and S-CA2, this steel bar also indicates failed polarize by anode at 70-day of polarization period.

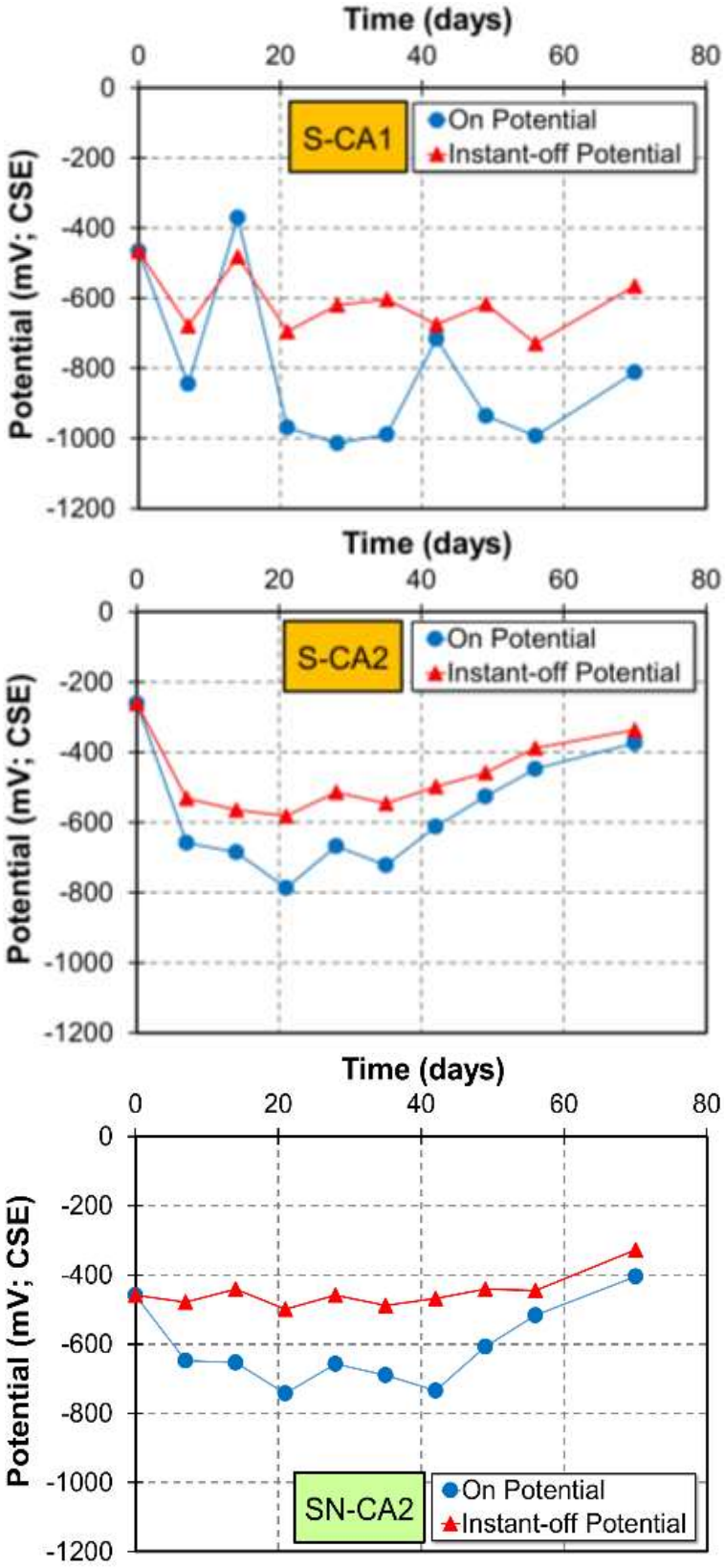

Fig 7.9 Potential of steel bar connected to CP (S and SN) vs time for both sets of current acceleration method

Half-cell potential of steel bar without CP connection (SN-CA1) is shown in **Fig 7.10**. There was a downward trend to negative direction between 0-day and 70-day of exposure time. Half-cell potential of steel bar during on and instant-off condition of CP decreased gradually to more than -400 mV vs CSE from 35-day until 70-day of exposure time, which indicates the 90% probability of corrosion according to ASTM C 876-95. The line graphs of half-cell potential indicates that stray current of anode not enough to protect the steel bar from corrosion.

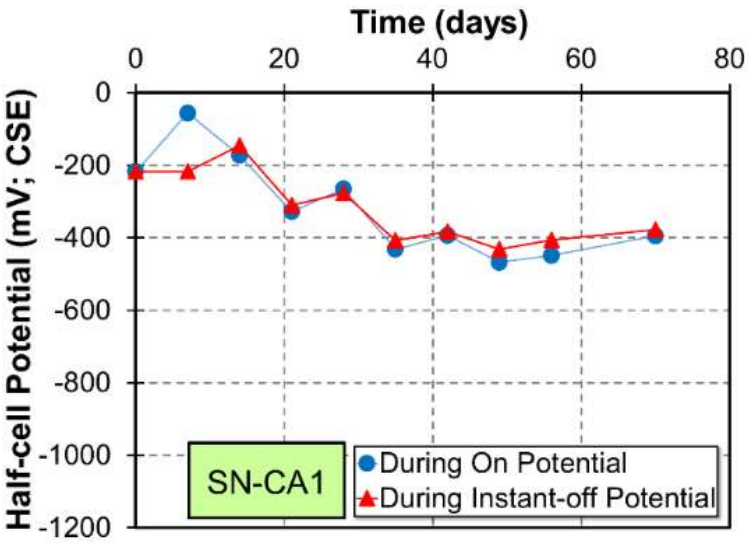

Fig 7.10 Half-cell potential of steel bar without connected to CP vs time

Depolarization of Steel Bar

In order to verify the protection conditions in reinforced concrete structures, the "100 mV" decay criterion was carried out in this study by measure the potential decay after switching off the current during 24-h. In addition, 100 mV depolarization criterion was used to demonstrate the effectiveness of CP.

Fig 7.11 summarizes the depolarization measurement results for different condition of acceleration method and aging times evaluated. It was observed that active steel bars (S-CA1, S-CA2 and SN-CA2) for both sets of current acceleration method exceed of 100 mV decay criterion during the first month of polarization period. However, after 70 days, only S-CA1 surpass the 100 mV decay criterion. Meanwhile, passive rebar (SN-CA1) failed to achieve appreciable levels of

polarization since in the beginning of polarization period. It is indicates that anode effective to protect the steel bar in the CA1 condition.

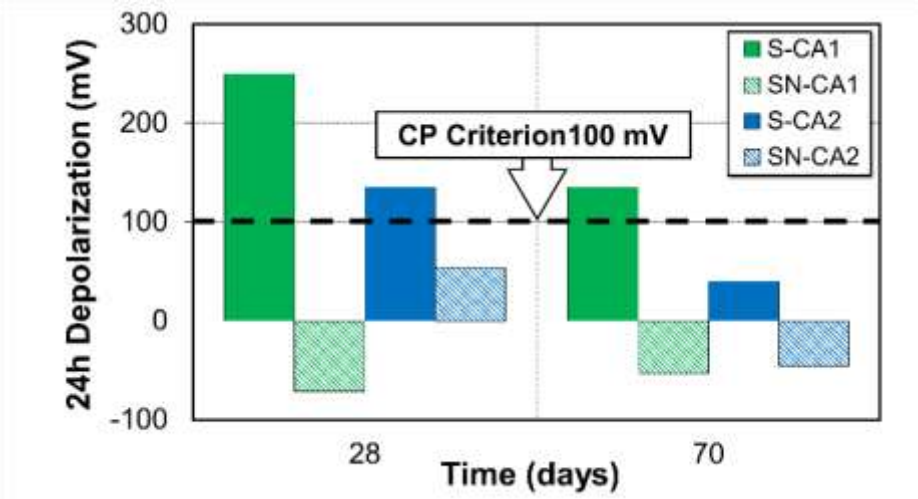

Fig 7.11 Summary of 24-h depolarization test result of steel bar with time

Rest Potential

Fig 7.12 shows the rest potential values of steel bar and anodes after 24h switch-off 24h in depolarization test. The natural potential of zinc anodes decreased moderately less than -850 mV vs CSE with time as shown in **Fig 7.12**. It is due to the low humidity condition which decrease the protective potential of anode.

As can be seen in **Fig 7.12**, the natural potential of active steel bars (S and SN in CA2) embedded in chloride-contaminated concrete with CP current acceleration which connected to this both steel-bar shown less steadily less than -850 mV during polarization period. However, S-CA1 indicates increased to more negative direction from 28-day until 70-day of exposure period which implies protection is going on. And for SN-CA2, the potential denotes probability of corrosion increased to occur. During depolarization process, development of current flow over 24h switch-off were monitored as illustrates in **Fig 7.13**. From **Fig 7.13**, it can be seen that current flow decreased gradually to initial current 0.7 mA after 24h.

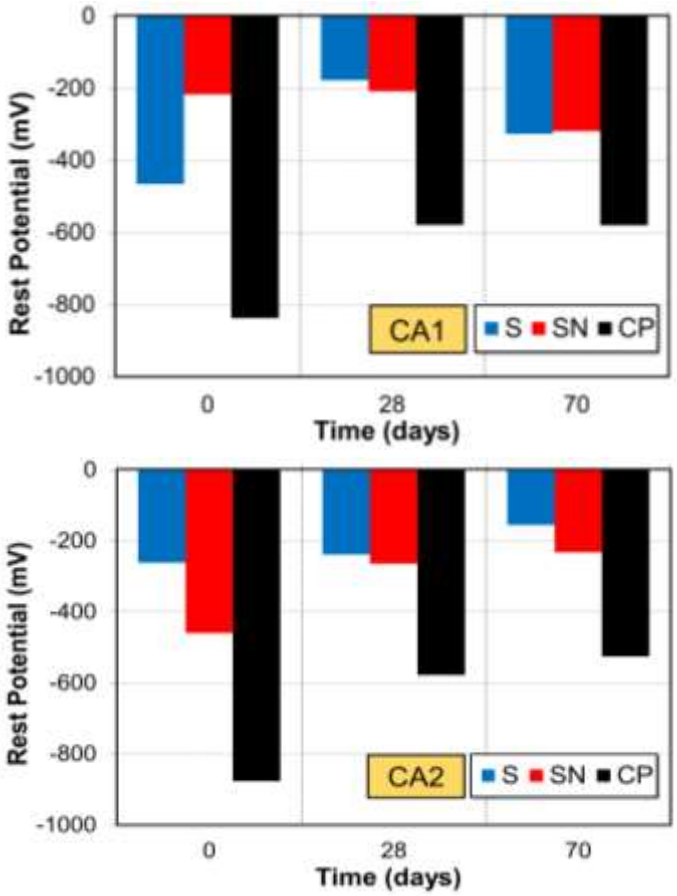

Fig 7.12 Rest potential of steel bar and anodes after switch-off 24h

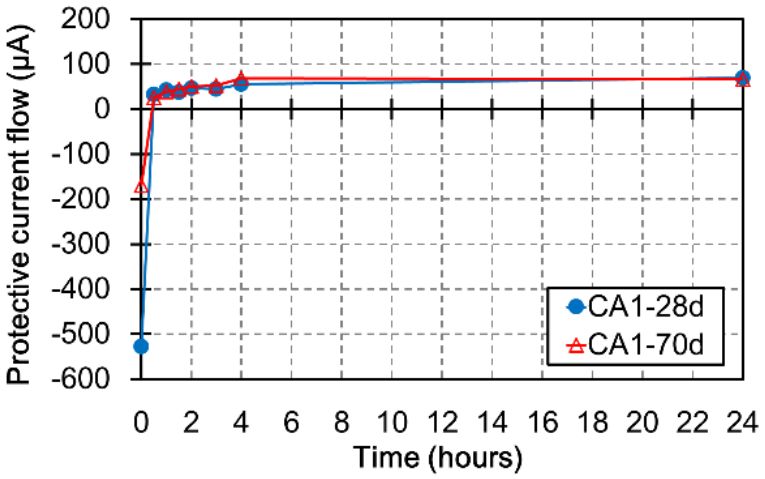

Fig 7.13 Current flow during 24h of depolarization test for both sets of current acceleration method

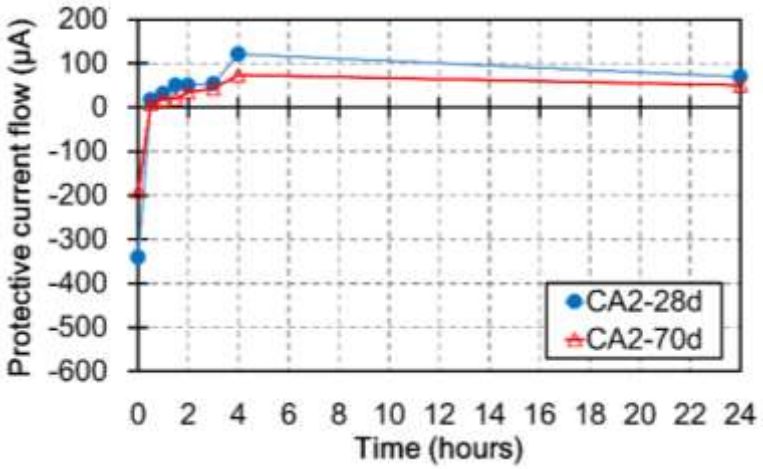

Fig 7.13 Current flow during 24h of depolarization test for both sets of current acceleration method (Continued)

Anodic-Cathodic Polarization Curve of Steel Bar

Fig 7.14 shows the change with time in the anodic and cathodic polarization curves of steel bars (S-CA1, SN-CA1, S-CA2 and SN-CA2). While the change with time in the cathodic polarization behavior of all rebar is small, the anodic polarization can be assessed as having increased, resulting in enhanced passivation except the steel bar without CP connected (SN-CA2) which anodic polarization having decreased at 70-day. This is presumed to be an effect resulting from the environment improvements of steel surface, namely, the rise in pH and decrease in Cl^- concentration of the steel surface due to the supply of protection current. According to the results of this experiment, current acceleration 10 times higher from initial condition resulted in the enhancement of passivation and increased anodic polarization resistance.

Corrosion Rate of Steel Bar

Measurement of corrosion rate in this study was carried out by the open-circuit corrosion rate (corrosion rate in the absence of protection). **Fig 7.15** shows there was a downward trend of corrosion rate for steel bar under CP protection (S-CA1, S-CA2 and SN-CA2) versus time. Meanwhile, corrosion rate of steel bar without CP (SN-CA1) shown increased moderately in corrosion activity. It means that protection current from anode contribute to enhancement of passivation.

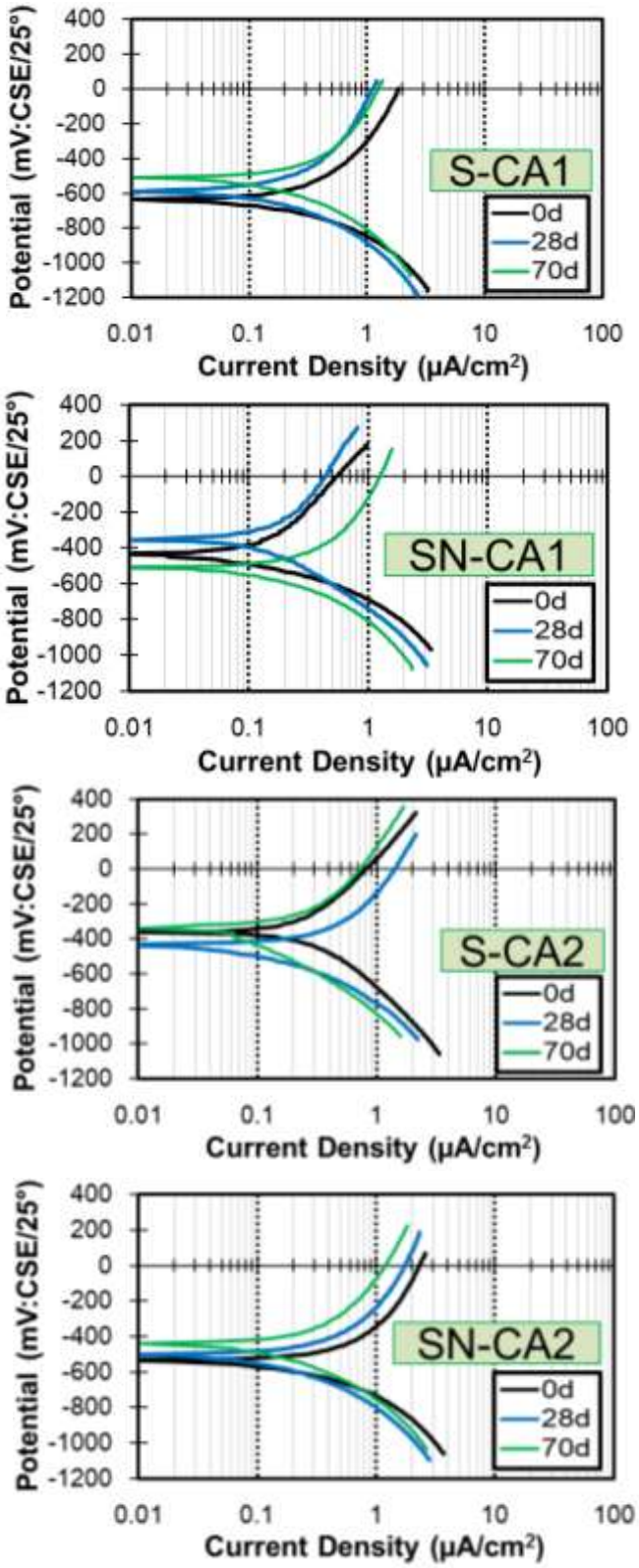

Fig 7.14 Anodic-cathodic polarization curve of steel bars embedded in chloride-contaminated concrete exposed to air curing conditions after switch-off during 24h in depolarization test

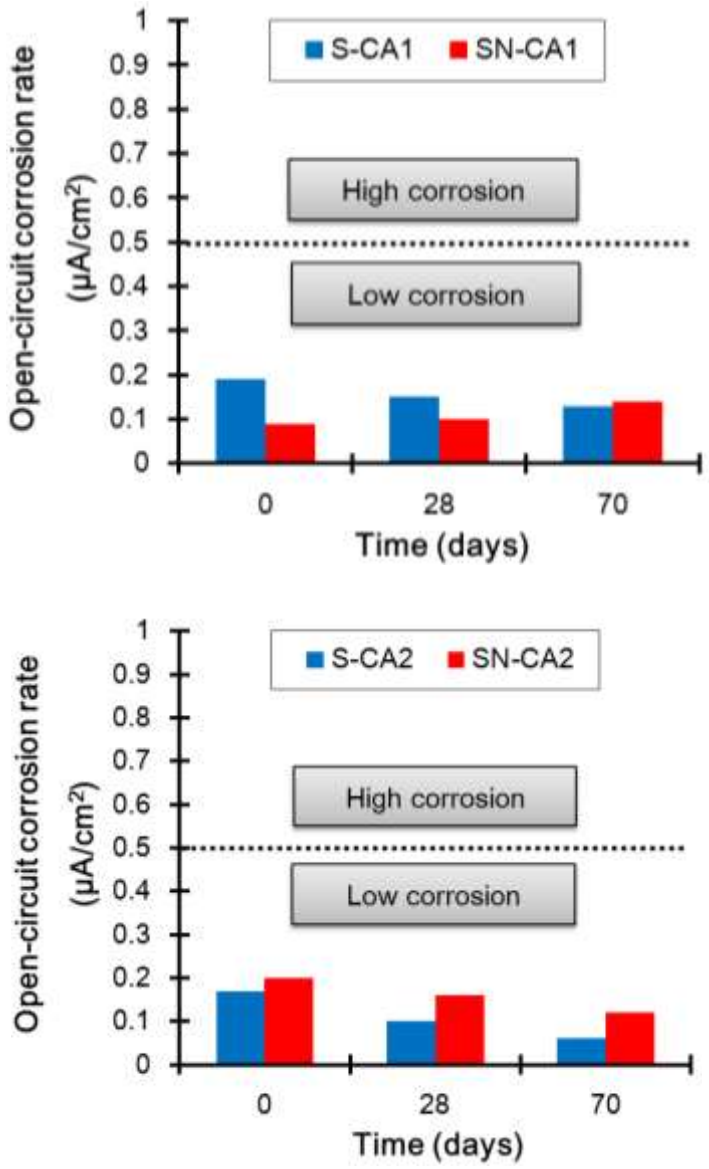

Fig 7.15 Corrosion rate based on corrosion current density from Tafel's extrapolation of potentiodynamic curve

Visual Observation of Steel Bar

Visual observation of steel bar at the end of test are shown in **Fig 7.16**. It was observed that during 70 days in polarization time with 10 times current acceleration by impressed current, there is no corrosion occurs on the steel bar. It is due to the CP current reduced the corrosion rate of steel bars and also due to the effect of exposure condition in air curing with constant temperature during hydration process, which strongly influences the hydroxide ion concentration in the pore solution.

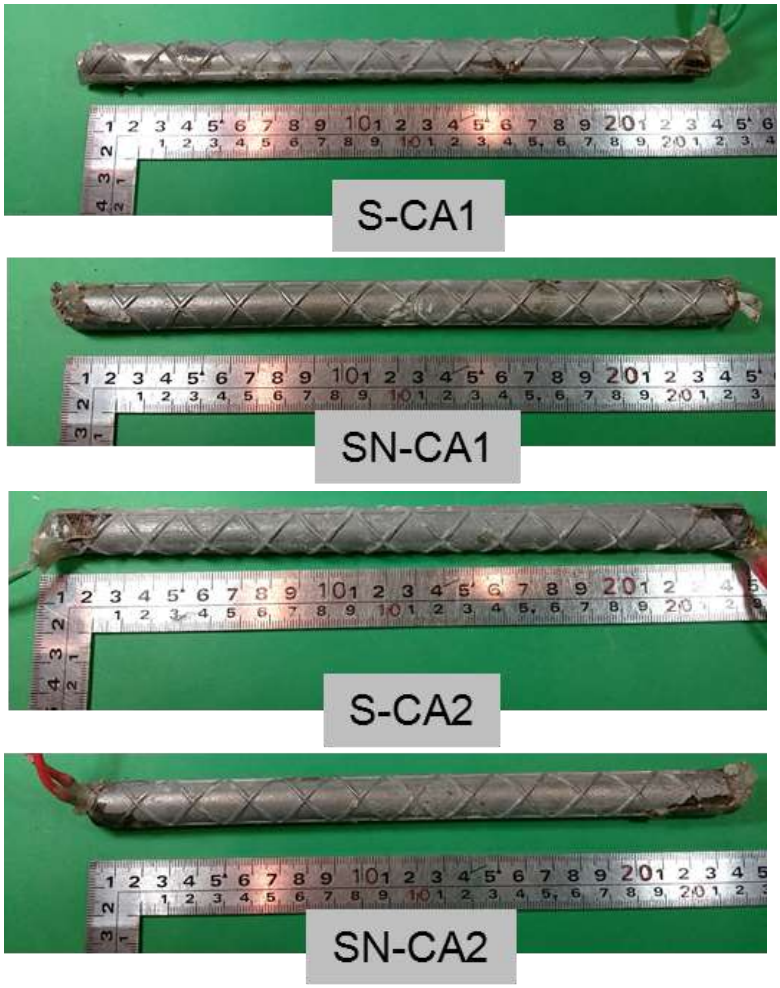

Fig 7.16 Corrosion appearance of steel bar

7.7 Service Life of Zinc Sacrificial Anode

Anode in Current Acceleration Condition

The cathodic protection (CP) system must be designed to provide the required current to every part of the structure for the targeted design life. Anode service life is primarily determined by anode output, anode charge capacity, anode utilization and anode efficiency. In simple terms anode life is given by the useful mA-hours (charge capacity) of the sacrificial metal divided by the average output in mA.

In practice, only a certain percentage of an anode`s mass can be used for current production. As the anodes are used, their surface area getting smaller and the anode resistance increase, because of the non-uniform consumption of anodic mass; thus, anodes can never be fully consumed. Sacrificial CP design requires that

the weight of anode material is sufficient to supply current for the design life of the structure. This is calculated by the following formula:

$$y = \frac{w \; x \; U}{Ano.Eff \; x \; I} \qquad (7.1)$$

Remark:

y	= life of an anode (year)
w	= anodic mass (kg)
U	= usage factor or utilization factor (0.9 for zinc)
$Ano.Eff$	= anode efficiency (kg/A.year)
I	= anodic current demand (A)

Anode Efficiency

The efficiency of a galvanic anode is the ratio of an anode weight sacrificed for CP purposes divided by the total theoretical ampere-hours or capacity of the material used. Galvanic anode materials are subject to self-corrosion which uses some of its energy. This is why the efficiency is less than 100%.

A prospective sacrificial anode must possess a large number of electrons per unit mass and should deliver these electric charges efficiently. Thus the electrical output of an anode is given by current capacity which is expressed in Ah kg^{-1} or kg Amp^{-1} y^{-1}. The value of the current capacity is determined by the electrochemical equivalent, the density and the efficiency of the anodic material. The electrochemical equivalent, which is dependent on the atomic weight and valence, is a characteristic of the anode material.

For example, pure zinc has a theoretical maximum capacity of 820 Ah per kilogram. This means that if a zinc anode were to discharge one ampere continuously, one kilogram would be consumed in 820 hours. If this kilogram was discharging one tenth of an ampere, it would be totally consumed in 8200 hours or 48 weeks. Actually, zinc anodes operate, typically, at about 95 % efficiency. This means that the energy content available for useful current output would be 820 x 0.95, or 780 Ah per kg. Another way of expressing this is in terms of kg per ampere-year. At 780 Ah per kg useful output for zinc, the conversion would be 11.2 kg A^{-1}

year^{-1}. Detail of sacrificial anode properties as described in **Table 7.7**.

Table 7.7 Sacrificial anode properties

Property	**Anode Material Type**
	Zinc
Density,	7130
Electrochem Equiv, g/coulomb	0.339E-3
Theoretical, Ah/Kg	819
Current efficiency, %	0.95
Actual current, Ah/Kg	780
Anode efficiency, Kg/A.year	11.25
Potential V, ref. Ag/AgCl	-1.05

Sacrificial CP design requires that weight of anode material is sufficient to supply current for design life of the structure. Therefore, at the end of test, visual observation to zinc sacrificial anode was carried out as can be seen in **Fig 7.17**. From visual observation, it was found that the weight of zinc decreased from 89 gram to 84.15 gram for anode in CA1 and 83.41 gram for anode in CA2. It means that current acceleration to CP connected to two-steel bar (CA2) accelerate weight loss of zinc higher than connected to one-steel bar. Because the current density provided by anode in CA2 also two-time bigger than CA1 due to consumed by two-steel bar.

Fig 7.17 Visual observation of zinc sacrificial anode

Based on the weight of anode after exposed during 70 days with current acceleration 10 times higher than initial current, service life of anode is calculated using **Eq. 7.1**.

Table 7.8 shows the expecting service life of anode with their own initial output of current, for instance, 0.07 mA for CA1 and 0.056 mA for CA2. With this amount of initial current output and with the initial weight of anode, it is calculated that anode serviceability can reach up to 102 years for CA1 and 128 years for CA2. Afterwards, current of CA1 and CA2 adjusted to 0.07 mA as initial current during acceleration condition.

Meanwhile, during acceleration to throwing power 10 times higher than initial condition, it was observed that service life of anode reduced to 9.7 years for CA1 and 9.6 years for CA2. The remaining service life of anode as can be seen in **Table 7.9**.

Table 7.8 Service life of zinc sacrificial anode with initial condition

Specimen	Anode Material	Type of Anode	Initial weight (gr)	Output of anode (mA)	Life of zinc anode (years)
CA1	Zinc	F	89	0.07	102
CA2	Zinc	F	89	0.056	128

Table 7.9 The remaining service life of zinc sacrificial anode with current acceleration 10 times of initial condition during 70 days

Specimen	Anode Material	Type of Anode	Initial weight (gr)	Output of anode (mA)	Life of zinc anode (years)
CA1	Zinc	F	84.15	0.7	9.7
CA2	Zinc	F	83.41	0.7	9.6

From **Table 7.8** and **Table 7.9** it was observed that by increasing the current demand by 10 times, it makes service life of anode reduced 10 times after 70 days of exposure. It means that the higher current delivery function of anode, the service life of anode become shorter. It can be said that current acceleration method successfully to predict the service life of anode in short time observation.

7.8 Conclusions

This study has presented the service lifetime estimation of zinc sacrificial anode with and without steel embedded in chloride-contaminated concrete and free-chloride concrete exposed to dry and wet-dry condition. In addition, current acceleration method also was carried out in this research in order to observe the service lifetime of anode in shortly. Based on the results from two types of that specimens above, the following conclusion can be drawn as follow:

1. It was observed that moisture and humidity of environment generates protective potential from anode more cathodically polarizes than in dry condition. From this it can be said that the potential value of the sacrificial anode was also affected by the moisture and oxygen content in the concrete.
2. High moisture content in concrete accelerate the zinc sacrificial anode more active to provide large protection current.
3. Service life of zinc sacrificial anode exposed to air curing condition with constant room temperature could predict to reach over 100 years.
4. By increasing the current demand by 10 times, it makes service life of anode reduced 10 times after 70 days of exposure. It means that the higher current delivery function of anode, the service life of anode become shorter.
5. Current acceleration method successfully to observe the service life of anode in short time.

References

7.1 Bennet, J., and McCord, W., “Performance of Zinc Anodes Used to Extend the Life of Concrete Patch Repairs”, Paper No. 06331, *Corrosion/2006, NACE International*, Houston, 2006.

7.2 Dugarte, M., and Sagues, A.A., “Sacrificial Point Anodes for Cathodic Prevention of Reinforcing Steel in Concrete Repairs – Part 1: Polarization Behavior”, *Corrosion*, 2010, Vol. 70, No. 3, pp. 303-317.

7.3 Bertolini, L., Bolzoni, F., and Pedeferri,P., “Cathodic Protection and Cathodic Prevention in Concrete: Principles and Applications”, *Journal of Applied Electrochemistry*, 1998, No. 28, pp. 1321-1331.

7.4 Swain., “Cathodic Protection Design”, Classnotes, 1996, pp. 3-28.

7.5 Christodoulou, C., Glass, G. K., Webb, J., Ngala, V., Beamish, S., and Gilbert, P., “ Evaluation of Galvanic Technologies Available for Bridge Structures”, *A Report for The UK Highways Agency for Area 9, Sacrificial Anodes in Concrete Repair, Document Reference 9-410414-F-RP-0001*, August, 2006.

7.6 American Society of Plumbing Engineers, “Corrosion”, *CEU209*, 2014, pp. 2-21.

7.7 Pedeferri, P., “Cathodic Protection and Cathodic Prevention”, Construction and Building Materials, 1996, Vol. 10, No. 5, pp. 391-402.

7.8 Sergi, G., and Page, C., “Sacrificial Anodes for Cathodic Prevention of Reinforcing Steel Around Patch Repairs Applied to Chloride-contaminated Concrete”, European Federation of Corrosion Publications, 2001, No. 31, pp. 93-100.

7.9 Verma, S. K., Bhadauria, S. S., and Akhtar, S. (2013). "Estimating Residual Service Life of Deteriorated Reinforced Concrete Structures", *American Journal of Civil Engineering and Architechture*, Vol. 1, No. 5, 92-96.

7.10 Bertolini, L., Elsener, B., Pedeferri,P., Redaelli, E., and Polder, R., “Corrosion of Steel in Concrete”, 2013, Wiley-VCH Verlag GmBH & Co KGaA

7.11 Hobbs, D., “Concrete deterioration: causes, diagnosis, and minimizing risk”. In: International Materials Reviews, 2001, 46.3, pp. 117–144.

7.12 ASTM C 876-95, “Standard Test Method for Half-cell Potentials of Uncoated Reinforcing Steel in Concrete,” Philadelphia: American Society of Testing and Materials, 1999.

7.13 Y. Schiegg, M. Büchler, M. Brem, “Potential mapping technique for the detection of corrosion in reinforced concrete structures: Investigation of parameters influencing the measurement and determination of the reliability of the method”, Mat. And Corr. 60, 2009, pp. 79–86.

7.14 G. K. Glass, N. R. Buenfeld, Chloride - induced corrosion of steel in concrete, Prog. Struct. Eng. Mater. 2, 2000, pp. 448–458.

Chapter 8 CATHODIC PROTECTION DESIGN OF ZINC SACRIFICIAL ANODE IN PATCH REPAIR CONCRETE: STUDY CASE OF 40-YEAR-OLD DETERIORATED RC BEAM

8.1 Introduction

In this chapter, performance of zinc sacrificial anode to repair deteriorated RC beam after long-term exposure is studied. Nowadays, a range of systems are available for electrochemical corrosion mitigation including electrochemical treatments, impressed current cathodic protection and galvanic protection. Galvanic systems provide protection using dissimilar metals and operate naturally without the need for an external power source. Galvanic systems can be used for targeted or global corrosion protection. In reinforced concrete, galvanic anodes provide sacrificial protection to the rebar and do not require external power.

Galvanic systems are used to provide low-maintenance protection that can be economically tailored to protect large and small sections of the structure. Anodes used in galvanic protection systems can be surface applied or embedded

into the concrete structure or a new overlay.

For embedded systems, zinc is the most common sacrificial anode used today. Zinc is one of the most evaluated and used anodes in concrete structures, cathodic protection research, and commercialization market. It has been modified and alloyed in the past two decades to enhance its lifetime and efficiency [8.1]. Distributed anode systems utilized to create galvanic encasements have been used to extend the life of concrete structures in extremely corrosive environments [8.2].

The zinc anodes tested, identified as discrete or point anodes, are a new form of cathodic protection system which are placed on patch repairs to protect the surrounding reinforcing steel near the repairs zones where the chloride contamination maintains high [8.1]. These new anodes are made of a zinc nucleus coated with a porous mortar which in some cases has a lithium monohydrated solution to maintain zinc corrosion activation [8.1]. This lithium base solution maintains the zinc surroundings humid and, this, the efficiency of the system is told to be constant during its lifetime [8.1]. The dimensions of these point anodes are variable, depending on the fabricating and distributing company.

The fabricating company defines an effective distance between anodes so the system could be used effectively in large structures [8.1]. This argument, however, is not well presented scientifically by a direct measurement or research to support this information. Therefore an investigation is needed to assist in the effort to answer these questions with well controlled experiments by used full-scale RC elements which already exposed in long-term in order to approaching the real situation .

8.2 Research Objective

Based on the previous explanation, the purpose of this investigation is to determine if these point anodes will work as a cathodic protection system in deteriorated RC beam and to define the protection zone at which point anode is effective. In order to reach the general aim, the following specific objectives have been defined as follow:

1. To observe degradation of concrete after 40 years of exposure

2. To investigate steel corrosion condition before and after anode embedded in patch repair concrete.
3. To develop an implementation design of sacrificial anode cathodic protection of steel bar in concrete

8.3 History of Specimen

8.3.1 Geometry of Deteriorated RC Beam

The RC beams were casted in 1974. The types of specimens used for the exposure tests are presented in **Table 8.1**. The beams were pre-cracked by bending moment until 75% of the ultimate bending moment. All the beams have the identical length of 2400 mm, while their cross-sections and rebar arrangement are varied according to the type of beams. Each cross-section of the beams is shown in **Fig 8.1**. The thickness of concrete cover was 30 mm for S-type and 50 mm for L-type.

Table 8.1 Summary of RC beams

Specimen ID	Cover Depth (mm)	Section/size	Pre-cracked	Initial Exposure Zone
S-Type	30	S (150x300mm)	0.75 Mu	Tidal
L-Type	50	L (200x300mm)	0.75 Mu	Tidal

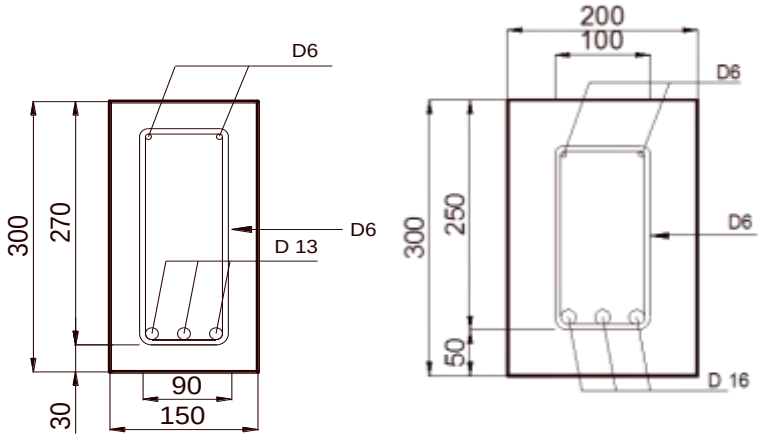

Fig 8.1 Cross-sections of RC beams

The cement used to casted was Ordinary Portland cement. The mix proportion of the concrete is described in **Table 8.2**. The mix proportion of concrete was designed with water/cement ratio (w/c) and sand/total aggregate ratio (s/a) of 65% and 42.5%, respectively. The composition of material in unit weight (kg/m^3) for water, cement, sand and gravel was 170, 260, 796 and 1118 respectively [8.3]. The concrete was designed with a slump target of 4 ± 1 cm and air content about 4 ± 1%. After placing of concrete, the beams were moist cured for one day and demolded. Then the RC beams were cured in air until the start of exposure.

Table 8.2 Mix proportion of 40 year-old concrete

Specimen ID	**Max. size of aggregate (mm)**	**Slump (mm)**	**Air (%)**	**W/C (%)**	**S/a (%)**	**Unit weight (kg/m^3)**			
						W	**C**	**S**	**G**
S and L Type	20	120±20	4±1	65	42.5	170	260	796	1118

8.3.2 Exposure Condition

From 1974 until 1994, all beams have been exposed to real marine environments at the Port of Kagoshima, which is located south-west of Japan, facing the North Pacific Ocean. The annual average temperature is around 17.3°C, the specimens do not experience freezing and thawing action even during winter. A general view of the exposure site is shown in **Photo 8.1**.

After 20 years of exposure, the beams were transferred to the PARI laboratory, stored at a constant temperature and sheltered from the rain over 15 years as shown in **Photo 8.2**. Afterward, from 2009 until now, the RC beams relocated to exposure site of Ito campus in Kyushu University, Fukuoka as shown in **Photo 8.3**. Exposure condition in Ito campus stored at open area and sheltered from the rain by plastic sheet wrapped. Exposure site trajectory of RC beams during 40 years during 40 years is presented in **Fig 8.2**.

Photo 8.1　General view of exposure site at tidal zone in Kagoshima Port

Photo 8.2　RC beams were kept in PARI Laboratory

Photo 8.3　Kyushu University exposure site

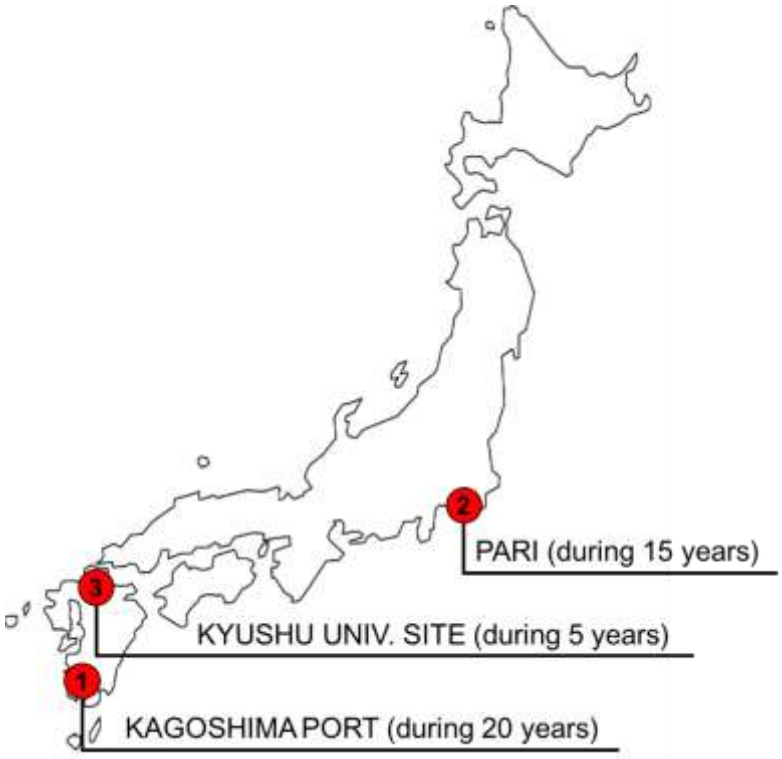

Fig 8.2 Exposure site trajectory of RC beams during 40 years

8.4 Research Scheme

There were three stages conducted in this study as describes in **Fig 8.3**. The first stage was pre-apply of anode (SACP). In this stage, some non-destructive test method to observe degradation of concrete after 40 years of exposure were conducted. Afterwards, repair design and anode apply were established. Then continued by corrosion monitoring during post-apply of SACP.

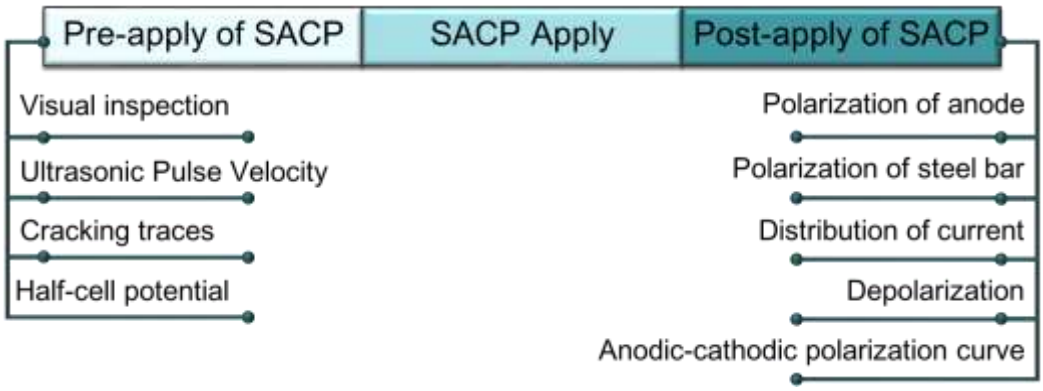

Fig 8.3 Research scheme and method of assessment

8.5 Preliminary Assessment

Basic information about recent condition of RC beams before repair and protect by sacrificial anode cathodic protection (SACP) was obtained by preliminary assessment. Preliminary assessment will discussed with respect to degradation of concrete i.e. appearance of beams, cracking traces, half-cell potential of steel bars and ultrasonic pulse velocity on concrete surface.

8.5.1 Appearance of Beams

Photo 8.1, **Photo 8.2** and **Photo 8.3** show the appearance of all beams before testing. These figures show the side surfaces of the respective beams just after cleaned by steel brush. In addition, from **Photo 8.4** and **Photo 8.5** can be seen that beams exhibited rust stains, uncovered aggregates, air bubbles, rough surface, chips and cracks. Uncovered aggregate were mostly found on the bottom side of beams due to seawater splashing, while rust stains commonly found at the ends of beams and in the vicinity of the cracks. After exposed up to 40 years, all beam surfaces appeared rough surfaces, chips on the edges and a few spalling. Based on visual inspection results in order to check the appearance of beams, it can be concluded that there was no significant degradation for RC beams of concrete with 3cm and 5cm of cover thickness after 40 years of exposure.

Photo 8.4 Appearance of beams over 40 years of exposure

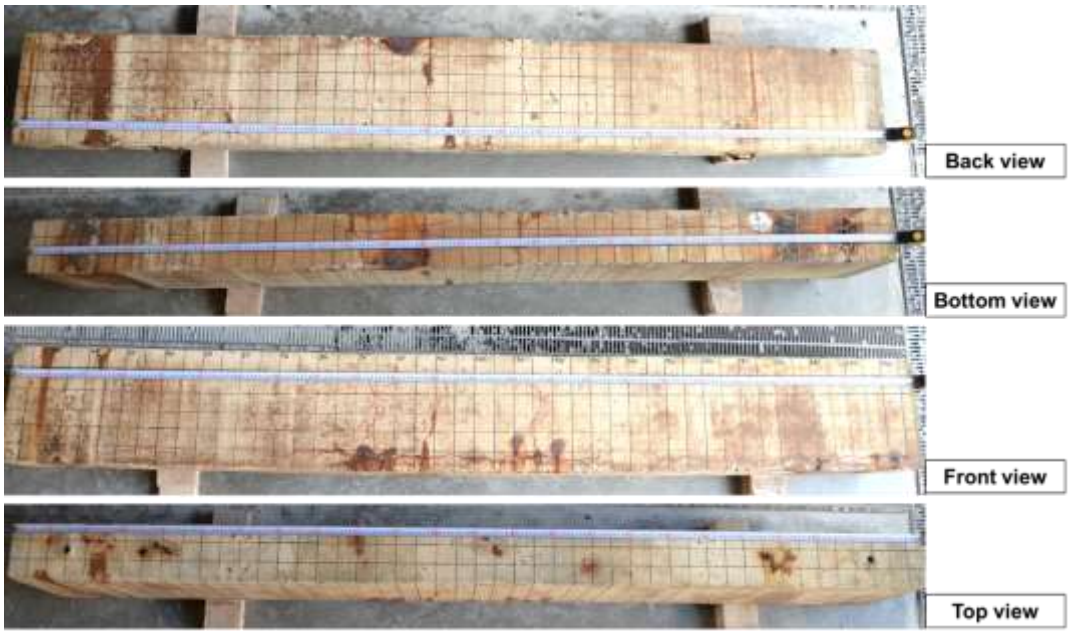

Photo 8.5 Side appearance of S-type beam over 40 years of exposure

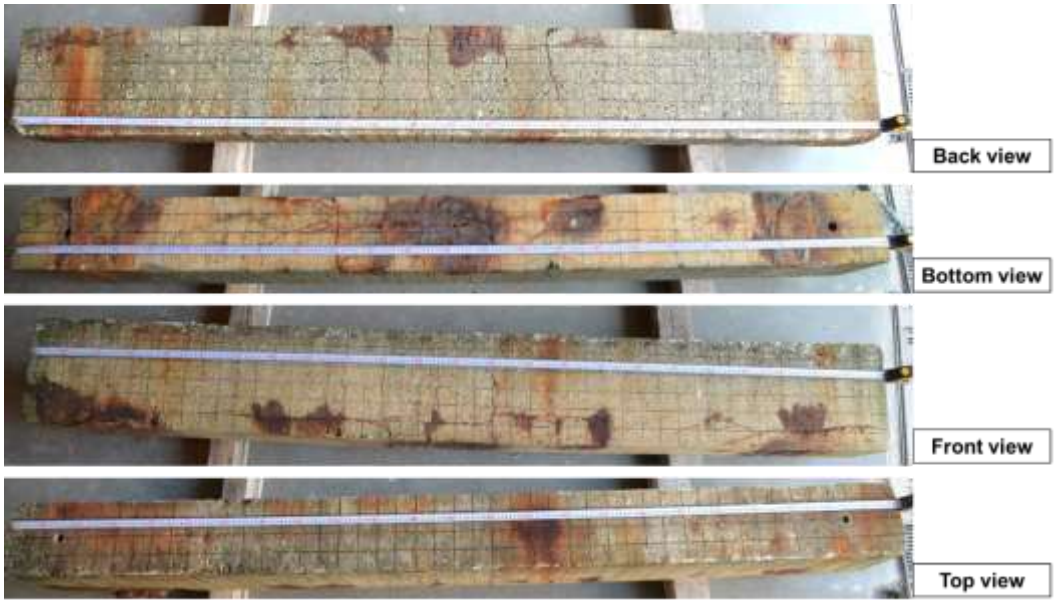

Photo 8.6 Side appearance of L-type beam over 40 years of exposure

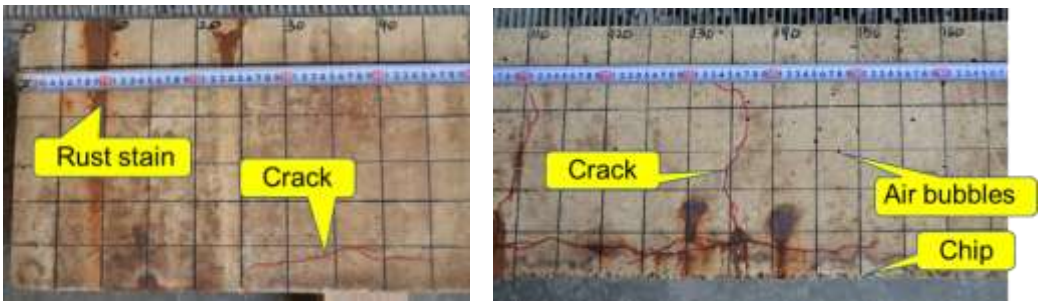

Photo 8.7 Decay appearance of S-type beam after 40 years of exposure

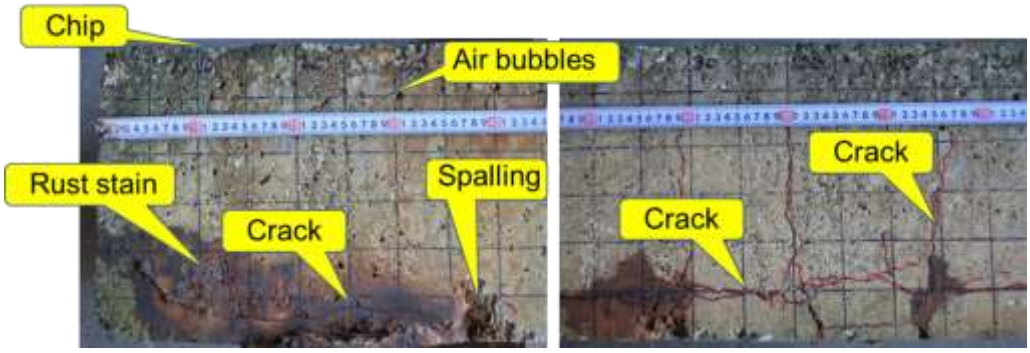

Photo 8.8 Decay appearance of L-type beam after 40 years of exposure

8.5.2 Cracking Traces

Cracking traces of RC beams over 40 years of exposure is shown in **Fig 8.4**. In addition, cracks trajectory of S-type and L-type beam around center line area are presented in **Photo 8.6** and **Photo 8.7** respectively. At the scale area, the maximum cracks width about 1.5 mm for L-type beam and 1.3 mm for S-type beam. Air bubbles of 1-17 mm in diameter also appeared on surfaces of each beams.

Both RC beams presented cracks along the side of beam parallel to the rebar, and most of the cracking occurred in center line area. Longitudinal cracks were found along the bottom of beams. L-type beam had more cracks and rust on the bottom surface, center line area and edge parts of beam than S-type beam. Thus, L-type beam indicates extensive damage visually compared to S-type beams.

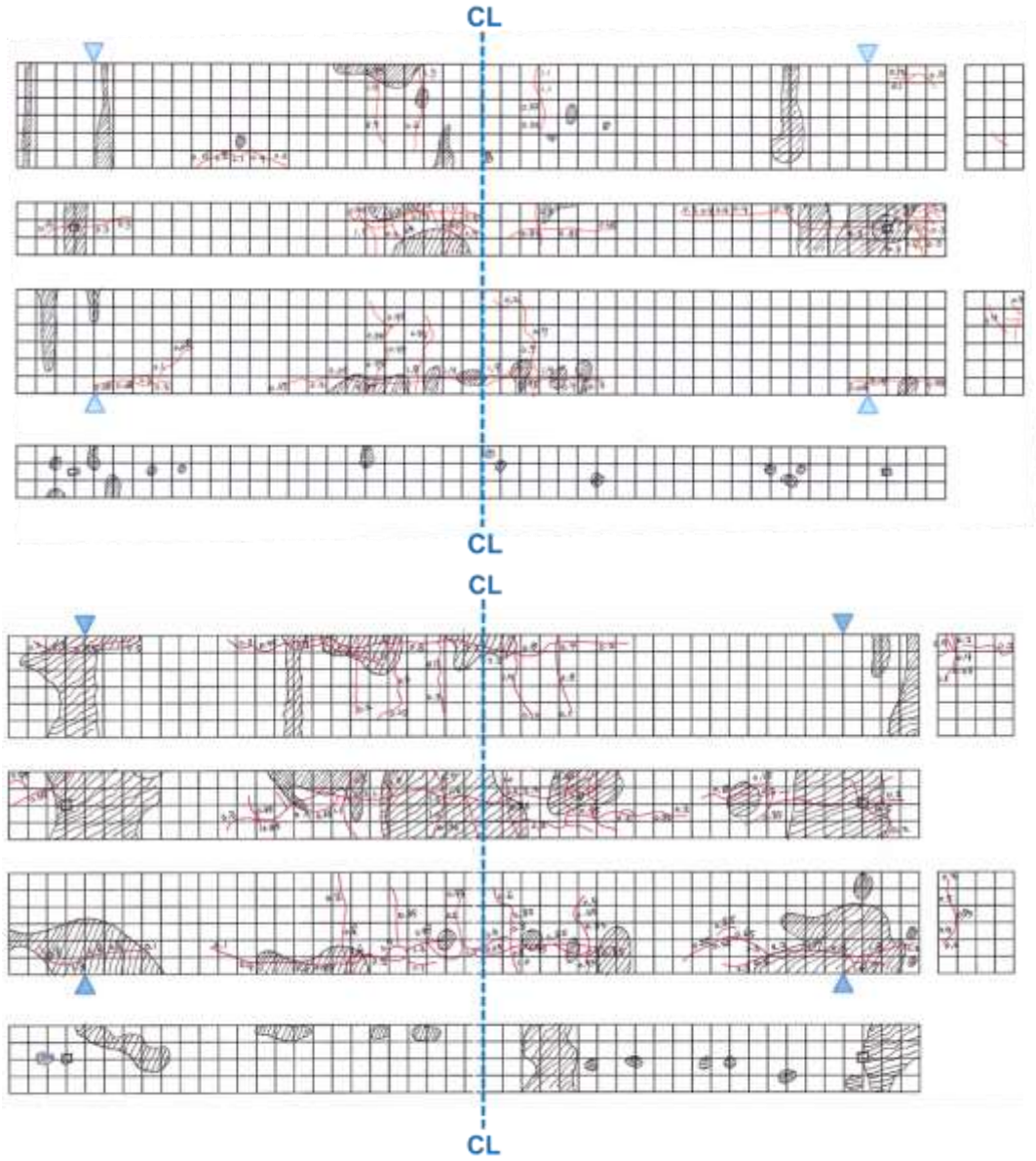

Fig 8.4 Cracking traces of beams over 40 years of exposure

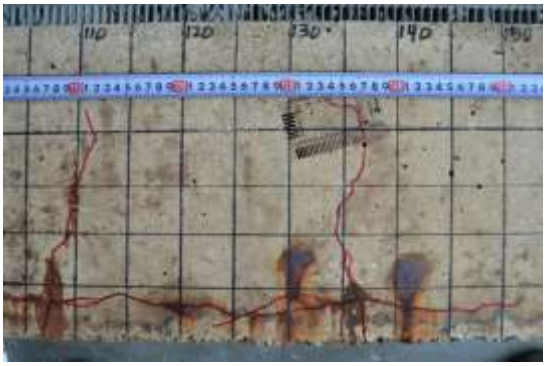

Photo 8.9 Cracks trajectory of S-type beam around center line area

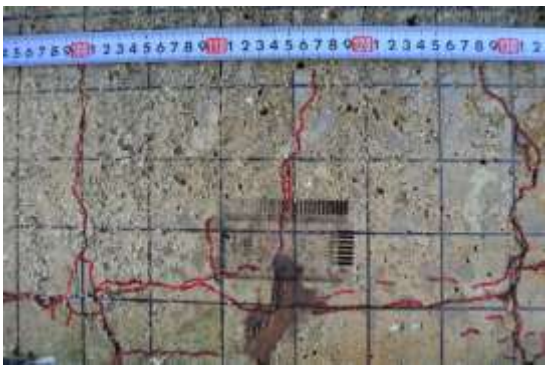

Photo 8.10 Cracks trajectory of L-type beam around center line area

8.5.3 Half-cell Potential of Steel Bar

Potential mapping of steel bar through half-cell potential measurements in S-type and L-type beams according to ASTM C876-91 (1999) are presented in **Fig 8.4** and **Fig 8.5** respectively. The measurement was conducted with silver/silver chloride electrode after 1 hour of pre-wetting. Then measured value was converted to the potential of the copper/copper sulphate electrode (CSE) at 25°C. Measurement point divided every 5 cm from the bottom side of beam (tensile area) to upper side of beam (tension area) and along the beam from 0 cm (the edge of beam) until 240 cm length of beam.

Fig. 8.4 shows the potentials of embedded bars in S-type beam at front and back position measurement dropped to to a value more than -350 mV vs CSE, thereby indicating breakdown of the passive layer and corrosion occurs. It seems that pre-cracking has accelerated the initiation of corrosion. A higher risk of corrosion of steel bar in L-type beam is shown in **Fig 8.5**.

Overall, all steel bars have indicated corroded, because the more negative value of the potential was detected. For corrosion mapping by half-potential value on both of RC beams, the result shown that the potential more positive on tensile rebar position compare than on tension rebar. Perhaps it is because the surface of tensile rebar already cover by rust and difficult to obtain the exact potential of rebar. This rust occurs due to the crack on tensile rebar position.

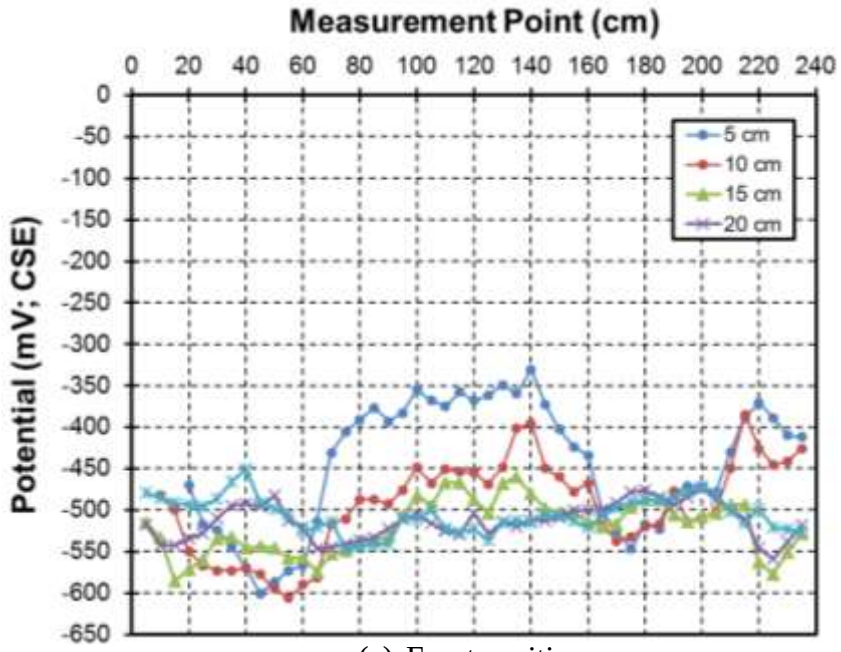

(a) Front position

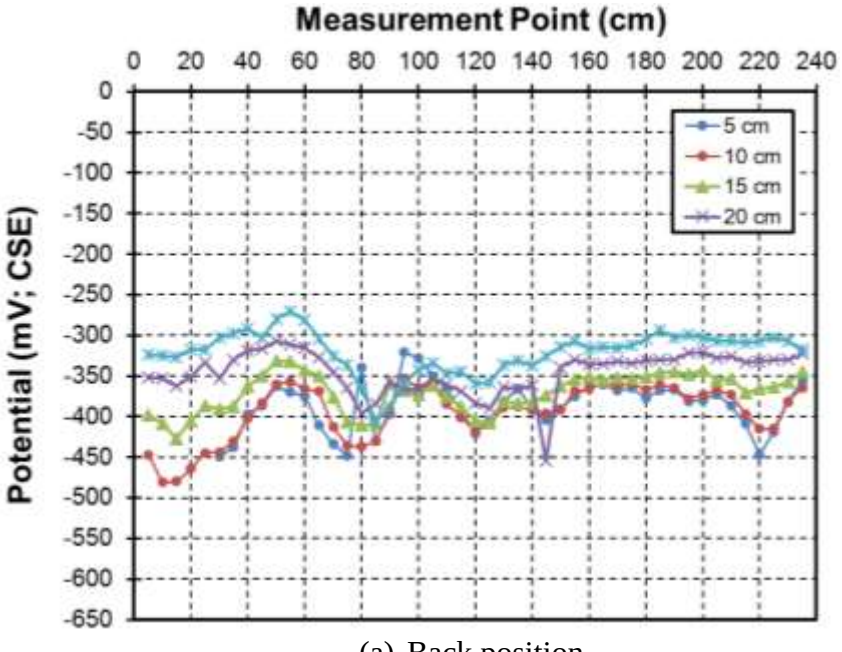

(a) Back position

Fig 8.5 Half-cell potential of S-type beam

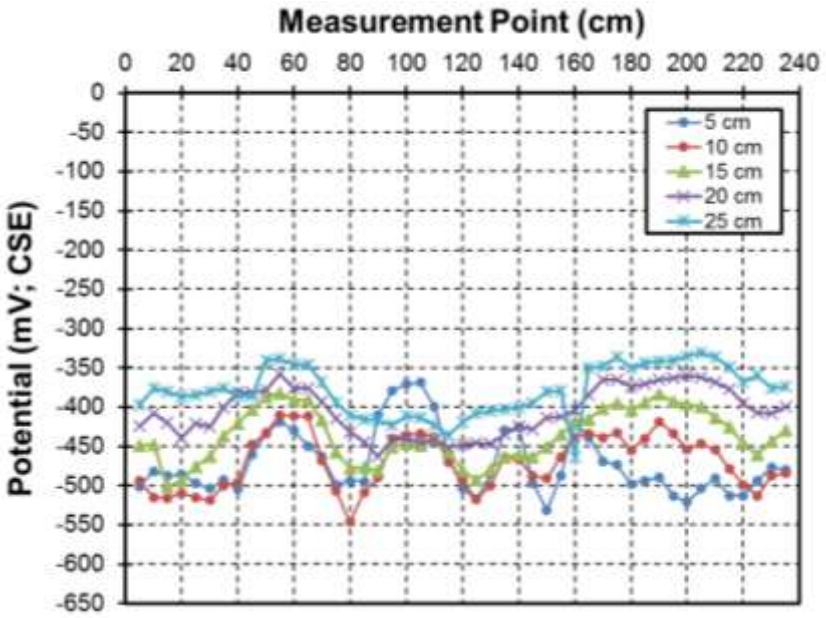

(b) Front position

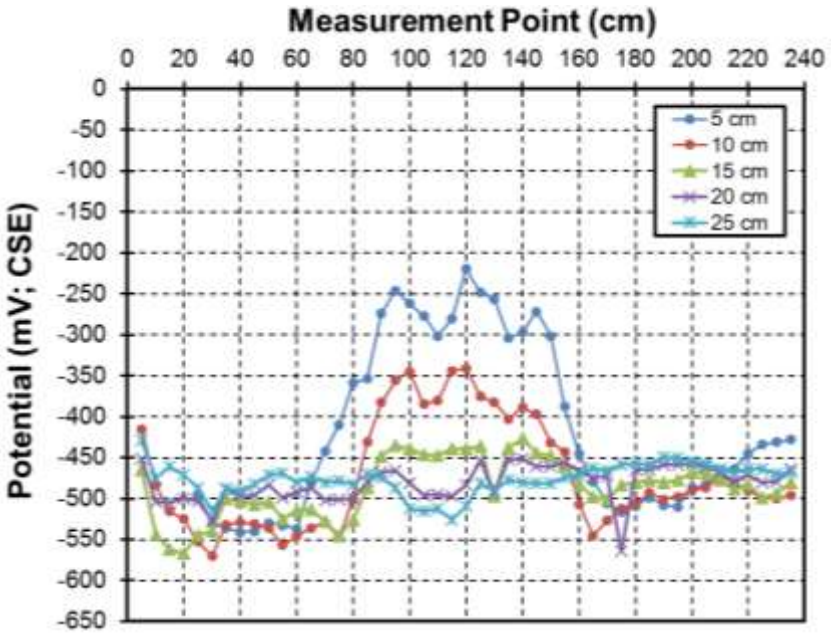

(b) Back position

Fig 8.6 Half-cell potential of L-type beam

8.5.4 Ultrasonic Pulse Velocity

Ultrasonic pulse velocity (UPV) measurement point is illustrated in **Fig 8.7**. The UPV methods have been used in inspect ion operations and monitoring of concrete structures. This test allows to measure and to control a series of basic parameters

to determine the concrete quality. The UPV methods can be considered as one of most promising methods for evaluation the concrete structures, once it makes possible an examination of the material homogeneity.

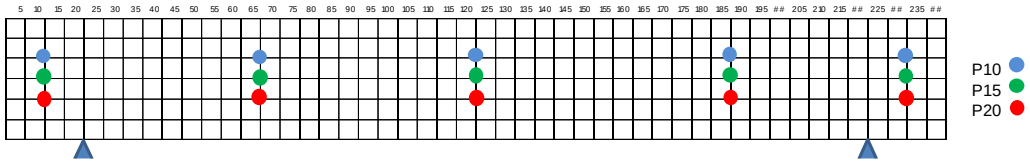

Fig 8.7 UPV measurement point

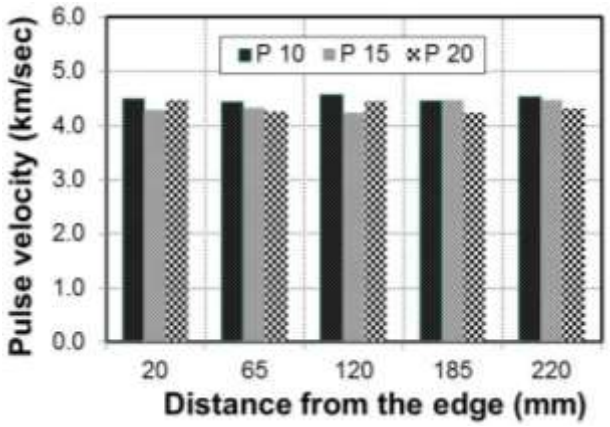

(a) S-type beam

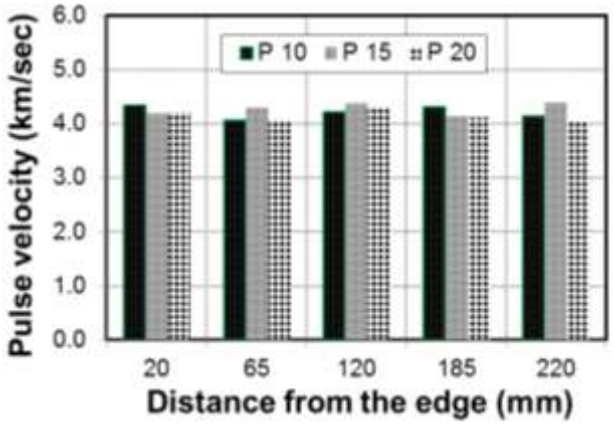

(b) L-type beam

Fig 8.8 UPV measurement point

Fig 8.8 shows the variation data of pulse velocity for S-type and L-type beams. From the UPV testing result, it was observed that velocity of concretes shown less than 4.5 km/sec which means concrete quality is medium quality.

8.6 Repair Broad Outline

In this study, repair method by sacrificial anode cathodic protection system embedded in patch repair is presented.

8.6.1 Materials

Polymer concrete (RIS321), as shown in **Photo 8.8**, and tap water (temperature 20±2°C) were used as mixing water on patch repair in this study. In addition, RIS211E was used as a adhesive between existing concrete and patch repair and also to avoid the absorption of water in patch repair concrete to existing concrete. In addition, a commercial galvanic anode made of zinc as main material was used as sacrificial anode in this study. **Photo 8.9** depicts the F-type anode used in this study with dimension 140 mm in length, 45 mm in width and 13 mm in depth.

Photo 8.11 Polymer concrete (RIS321) appearance

Photo 8.12 Geometry of zinc sacrificial anode F-type

8.6.2 Mix Proportions of Patch Repair Concrete

Mix proportions of patch repair concrete is described in **Table 8.3**. This proportion is based on the guideline from Denka (Denki Kagaku Kogyo Kabushiki Kaisha) as contributor of anode used in this study.

Table 8.3 Mix proportion of patch repair

Material	
RIS321, kg	12.5
RIS211E, kg/m^2	0.15
Water for RIS321, kg	1.8

8.6.3 Patch Repair Design

In order to observe performance of point anode to repair deteriorated RC beam, 2 (two) types of repair design were proposed as illustrated in **Fig 8.9**.

Patch Repair Area

Bottom surface of beam was selected as repair area. The length of patch repair was selected "one third of beam length".

- Length of repair area in S-type beam = 1/3 x 2400 mm = 600 mm
- Length of repair area in S-type beam = 1/3 x 2400 mm = 600 mm

Number of Anode

For S-type beam with concrete cover thickness was 3 cm, one-anode embedded in patch repair concrete. One-anode was chose as extreme number limited number to give protection. Position of anode embedded in the tensile rebar (rebar in middle position). Meanwhile, for L-type beam with concrete cover thickness was 5 cm, incremental number of anode increase to three-anode on each of tensile rebar.

Depth of Patch Repair

Depth of patch repair in this study was design by "two times of concrete cover thickness plus diameter of steel bar". This depth have to design in order to make easy the implementation of anode on the rebar.

- Depth of repair area in S-type beam = (2 x 30 mm) + 13 = 73 mm = 70 mm
- Depth of repair area in S-type beam = (2 x 50 mm) + 16 = 116 mm = 120 mm

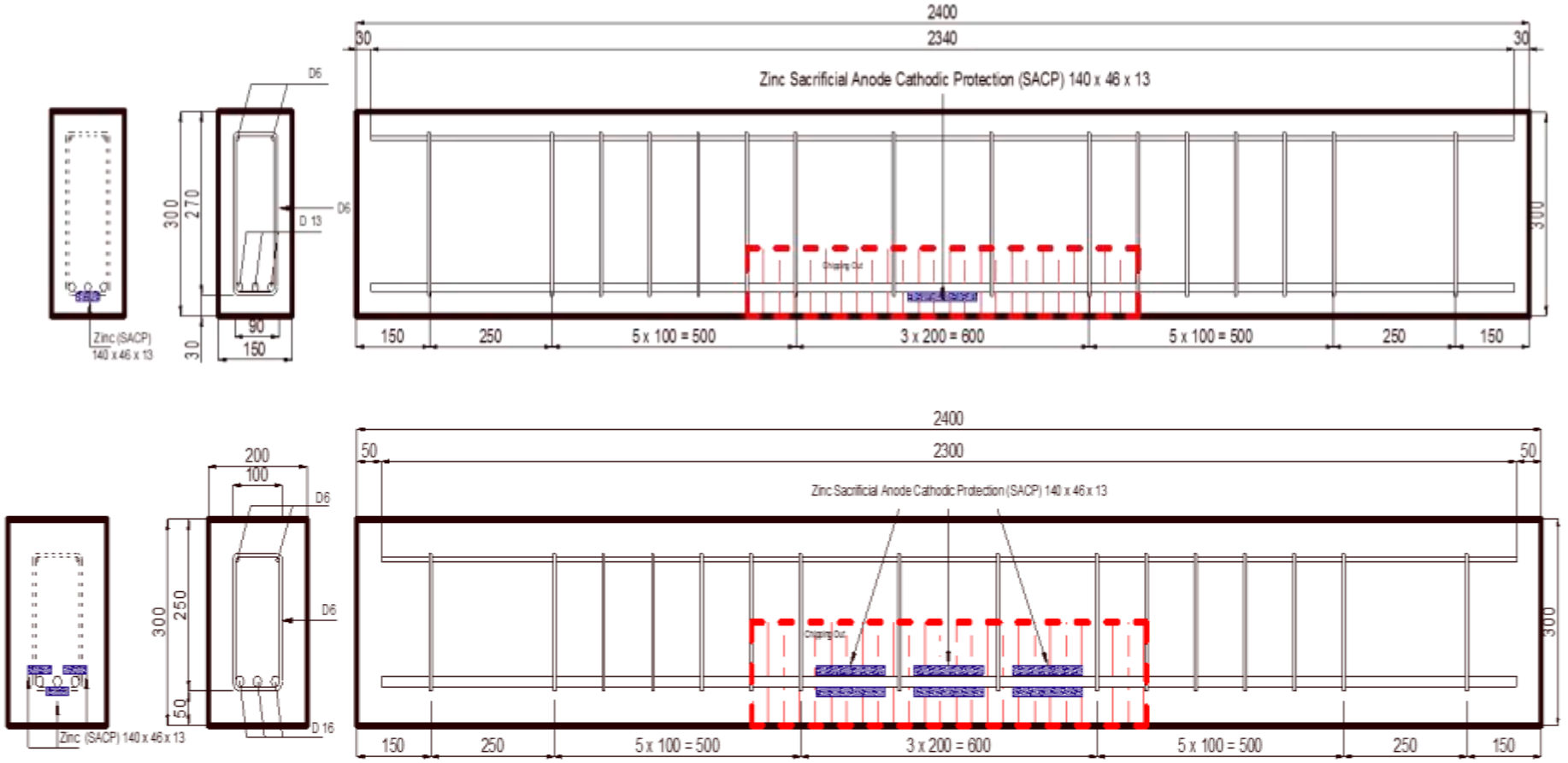

Fig 8.9 Patch repair design for S-type and L-type beams

8.6.4 Casting and Curing

The process of patch repair process with anode embedded in concrete is described in **Fig 8.10**. The first step is by crushing the repair area. Afterwards followed by remove the dust on crush area and clean the rust on the steel surface.

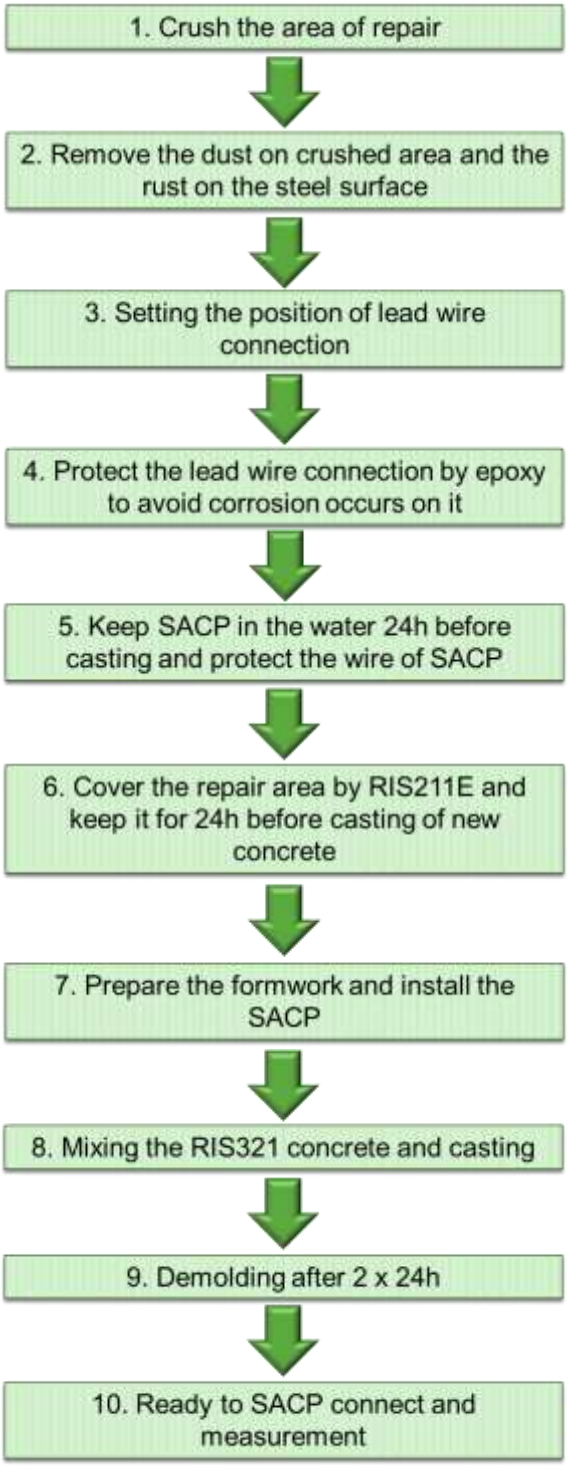

Fig 8.10 Detail of patch repair process

(a) Preparation of S-type beam before crushed

(b) S-type beam after crushed

Photo 8.13 Step 1: crush the area repair of S-type beam

(a) Preparation of L-type beam before crushed

(b) Condition of L-type beam after crushed

Photo 8.14 Step 1: crush the area repair of L-type beam

After remove the dust and clean the rust on steel bar are finish, continued by setting the position of lead wire on the steel bar and protect it by epoxy to avoid corrosion occurs on it. This process as shown in **Photo 8.12**. This lead wire has a function to measure the polarization of steel bar and current distribution from anode to steel bars. For S-type beam, one-anode deliver the current to three-steel bar. However, in L-type beam, one-steel bar protected by throwing power of three-anode.

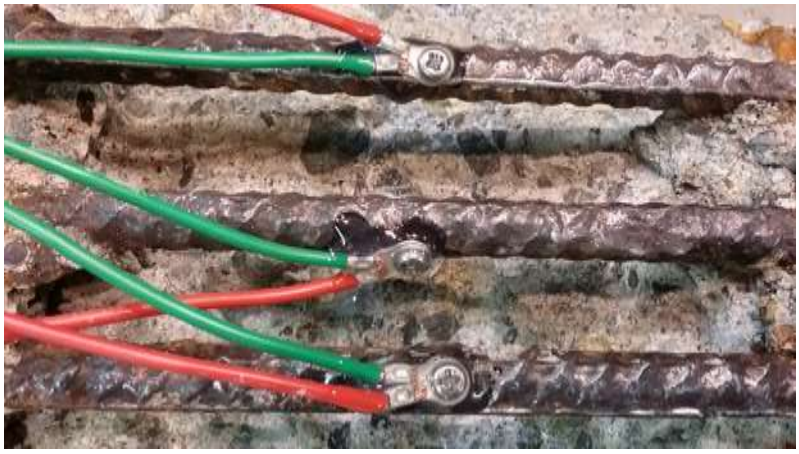

Photo 8.15 Step 4: protect the lead wire connection by epoxy

Before set up the anode in patch repair area, keep point anode in tab water for 24-hour in order to avoid mortar surrounded zinc absorb the water in patch repair concrete mixing. Then covered the wired of anode to evade corrosion on it. This process as depicts in **Photo 8.13**.

Photo 8.16 Step 5: protect the lead wire connection by epoxy

Cover the repair area by RIS211E and keep it for 24h before casting of new concrete. This process is presented in **Photo 8.14**.

(a) Preparation of RIS211E

(b) Cover the repair area by RIS211E

Photo 8.17 Step 5: protect the lead wire connection by epoxy

Finally the last stage is casting the patch repair concrete process. The full of this last step representative by L-type beam in **Photo 8.15**. First, set up the formwork in repair area, and make sure the position of anodes is settle and tight on the steel bars. Afterward, casting the mixing concrete and demolding after 2 x 24-hour. Furthermore, connect the anodes to steel bars as described in **Photo 8.16**.

8.6.5 Exposure Conditions

After the casting finished, all specimens were subjected to exposure conditions, in the air curing under laboratory environmental. Beam surfaces cover by wet towel (**Photo 8.17**) and wetting one time per day. The aim of cover by wet towel in order to give humid condition to concrete surface.

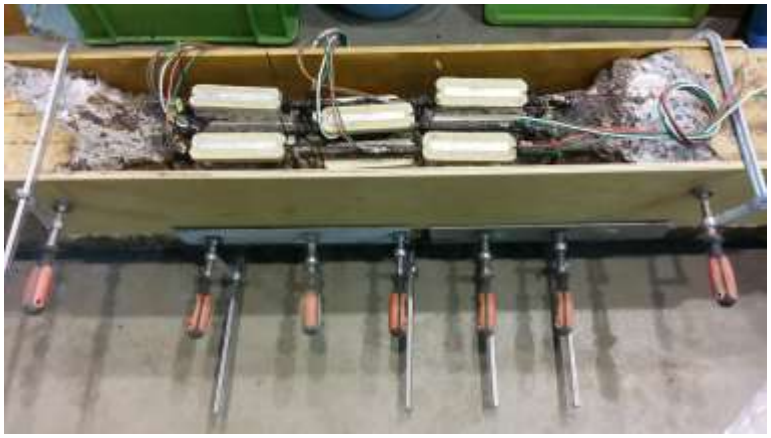

(a) Set up the formwork

(b) Mixing the patch repair concrete

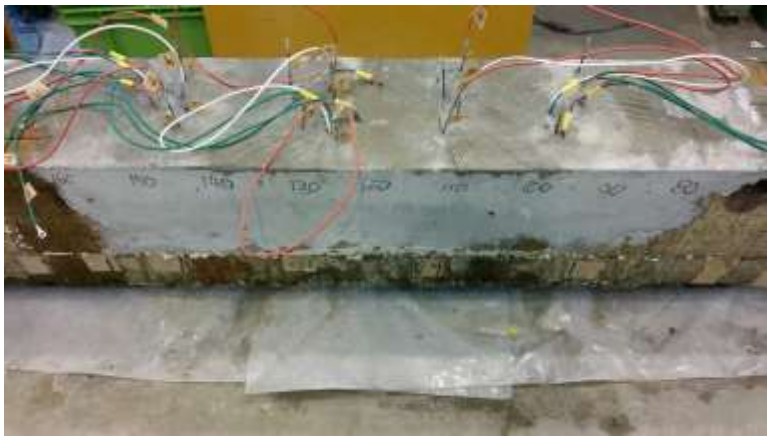

(c) Demold after 2 x 24-hour

Photo 8.18 Casting the patch repair concrete process

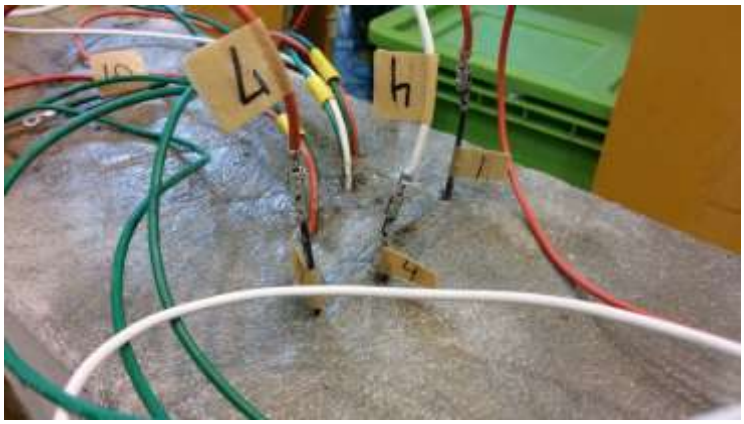

Photo 8.19 Connection of SACP

Photo 8.20 Exposure condition of RC beam under anode protection

8.7 Results

In this section, the most relevant results from the experimental programme carried out within this study are presented. Thereafter, the most important observations are highlighted and discussed. The measurement of potential was conducted with silver/silver chloride electrode after 1 hour of pre-wetting as shown in **Photo 8.18**. Then measured value was converted to the potential of the copper/copper sulphate electrode (CSE) at 25°C. Results from both series of experiments in the RC beams are presented as follows.

Photo 8.21 Pre-wetting before potential measurement

8.7.1 S-Type Beam

A. Polarization of Anode

Potential of Anode

In **Fig 8.11**, the results of potential measurement of anodes embedded in S-type beam during on and instant-off condition is presented. Potential of anode during instant-off condition is more negative than on condition. Initially potentials for anode was quite negative, ~-860 mV. At 28-day of exposure time, potential of anode decreased to ~-960 mV during instant-off and increased slightly to ~-845 mV during on condition. Meanwhile, the potential increased to noble value with polarization time. It was reached ~-500 mV and ~-790 mV during on and instant-off condition respectively. It was observed that during 28-day of polarization time, anode tended to have more negative potential and means protection condition is working.

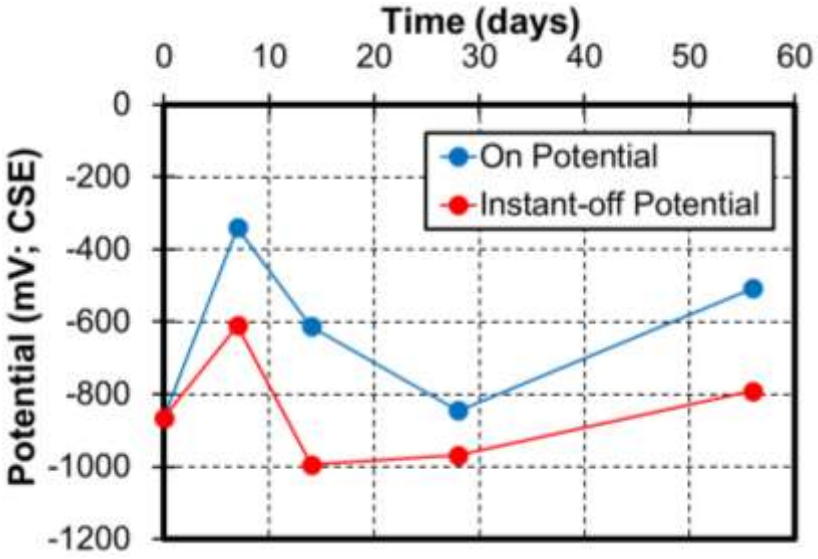

Fig 8.11 Potential of anode embedded in S-type beam with the function of time

Protective Current of Anode

The current delivered by the anodes to the entire rebar assembly as a function of exposure time is shown in **Fig 8.12**. From **Fig 8.12** it can be seen that protective current from anode to steel bar (CP1, CP2 and CP3) in concrete decreased dramatically after 7-day of exposure time. However, after 28-day, current delivery from anode increased gradually to more than 0.4 $\mu A/cm^2$. It was observed that the level of protective current was within the design limit of cathodic protection

between 0.2 - 2 μA/cm^2 as specified in EN 12696 [8.4].

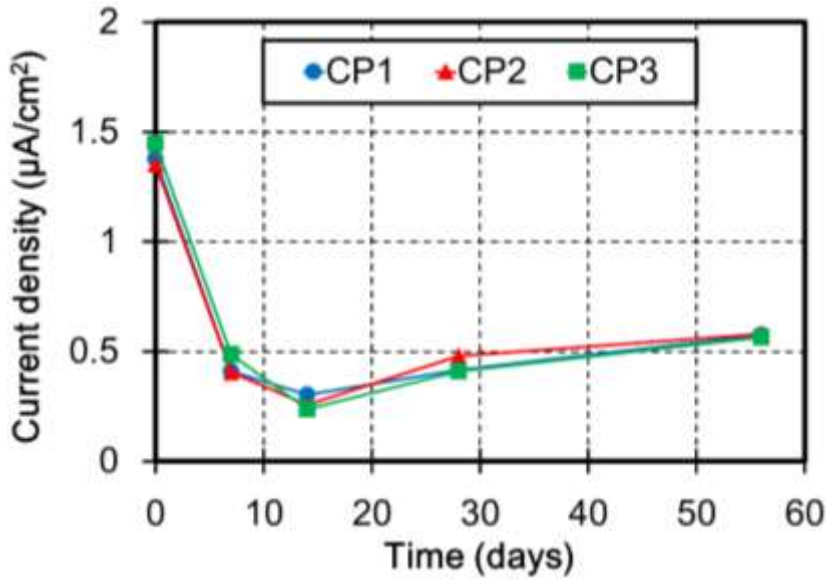

Fig 8.12 Distribution of protective current of anode embedded in S-type beam with the function of time

Anodic Polarization Curve of Anode

The potential-current trajectory of the anodes exposed in frost condition measured after switch-off during 24 hours is presented in **Fig 8.13**. The activity of anode is remarkably decreased, current of anode fell significantly with fluctuations from ~13 μA/cm^2 at 0-day to ~10 μA/cm^2 at 56-day of test period.

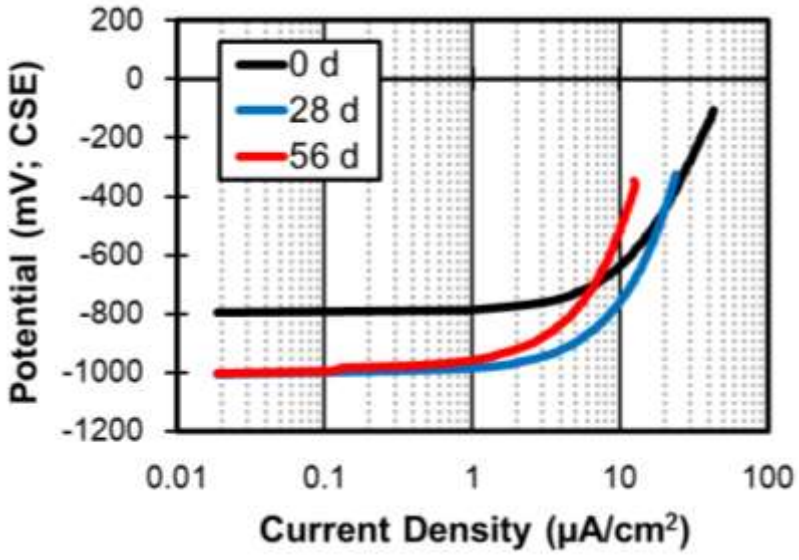

Fig 8.13 Anodic polarization behavior of anode embedded in S-type beam

B. Polarization of Steel Bar

Potential of Steel Bar

Fig 8.14 describes about potential development of steel bar with SACP connected (S-CP) time-dependently during on condition. On potential of steel bar under anode protection in repair area decreased gradually to more negative mainly near the anode position. On potential of steel bars in unrepair area also dropped to more negative time-dependently. However, the potential of steel bar near interfacial zone between repair and unrepair area increased to more positive direction.

Furthermore, **Fig 8.15** shows about potential evolution of steel bar time-dependently during instant-off condition. Potential of steel bar near the anode position decrease to more negative. As well as the steel bar in non-repair area. Same like in on condition, potential of steel bar in interfacial zone increased to more positive direction.

It was observed that anode polarize potential of steel bare to more negative even though not reach protective potential criterion. However, anode seems could not polarize the steel bar near the interfacial zone.

Depolarization Potential

Depolarization tests were regularly carried out by disconnecting the steel bar from the sacrificial anode for 24 hours. The instant-off potentials was measured immediately after disconnection of the sacrificial anodes (E_{off}) and the potential values were measured after 24 hours (E_{off} 24h).

The commonly used criterion for sufficient protection is 100 mV (the difference of E_{off} 24h and E_{off}). The 100 mV polarization shift was introduced in the early 1980s for evaluating the effectiveness of SACP of reinforced concrete. These are the principal criteria currently used in energize cathodic protection systems for reinforced concrete structures [(xx)]. **Fig 8.16** summarized the depolarization measurement results after steel bars disconnecting from the sacrificial anode for 24 hours. It was observed that only S-CP1 and S-CP3 were reached potential decay more than 100 mV at 56-day of exposure time. Moreover, potential decay of S-CP2 increased gradually to more than 50 mV time-dependently but not over the 100 mV anode criterion.

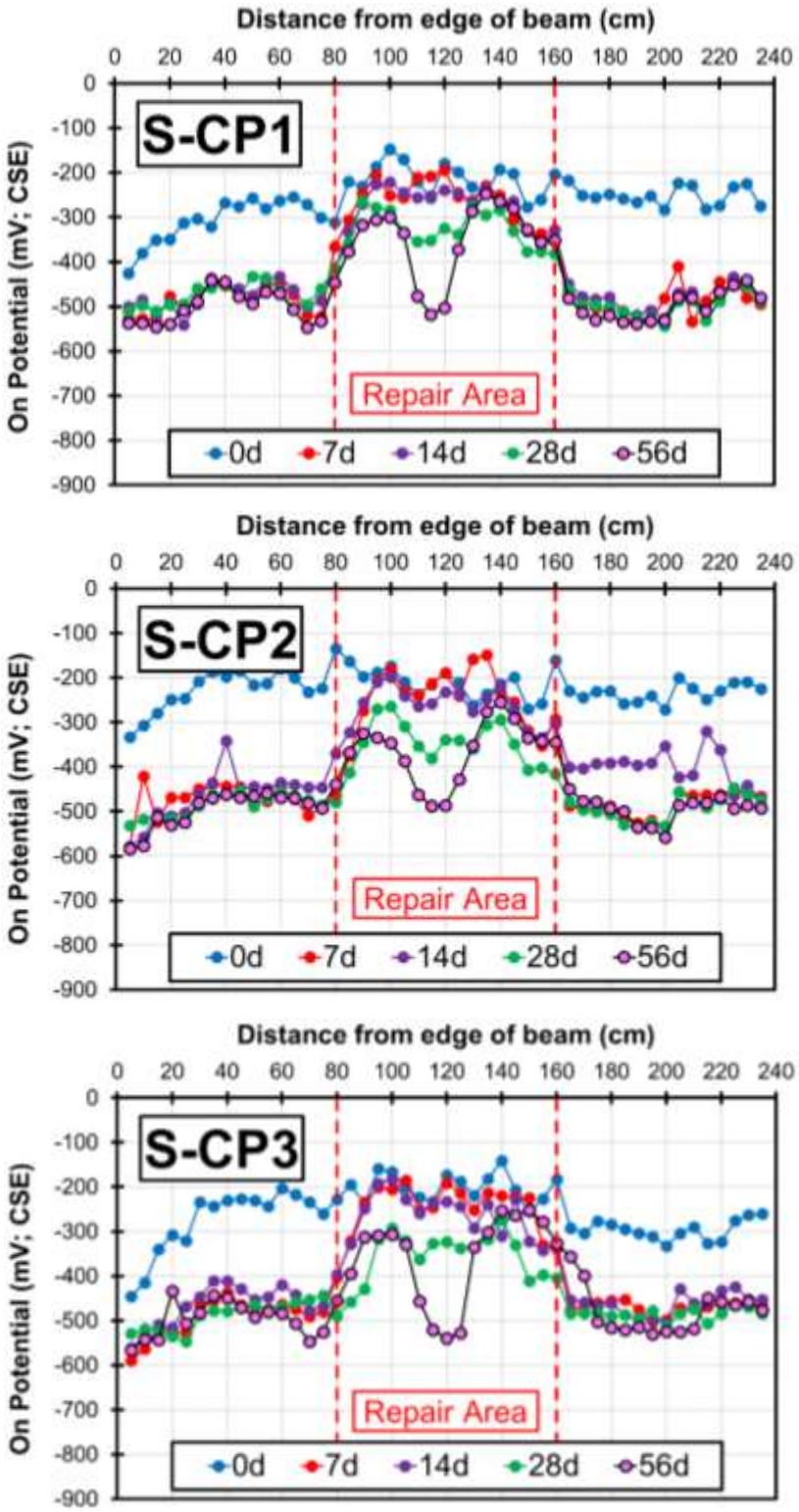

Fig 8.14 On potential evolution of steel bar embedded in S-type beam with polarization time

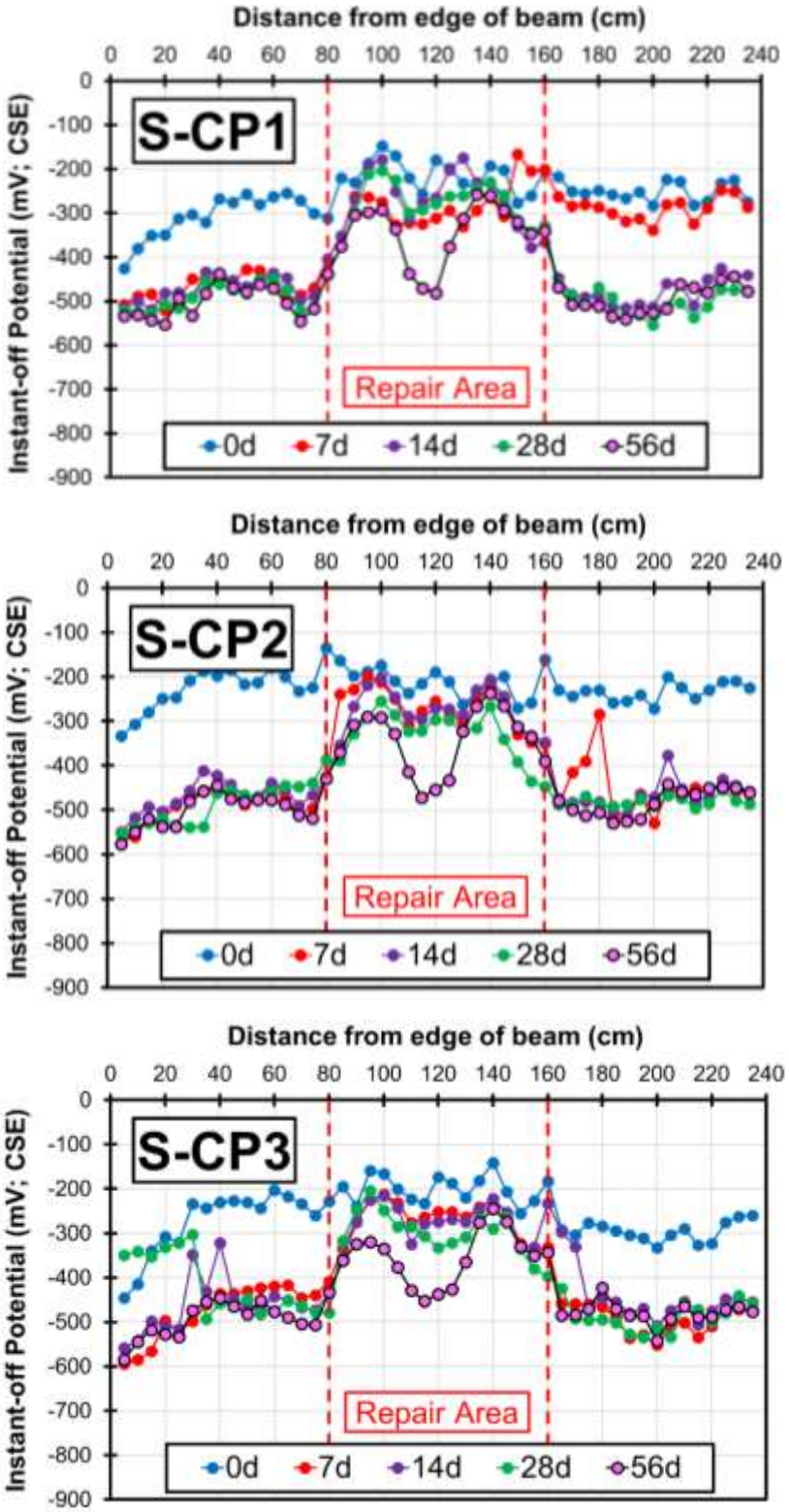

Fig 8.15 Instant-off potential evolution of steel bar embedded in S-type beam with polarization time

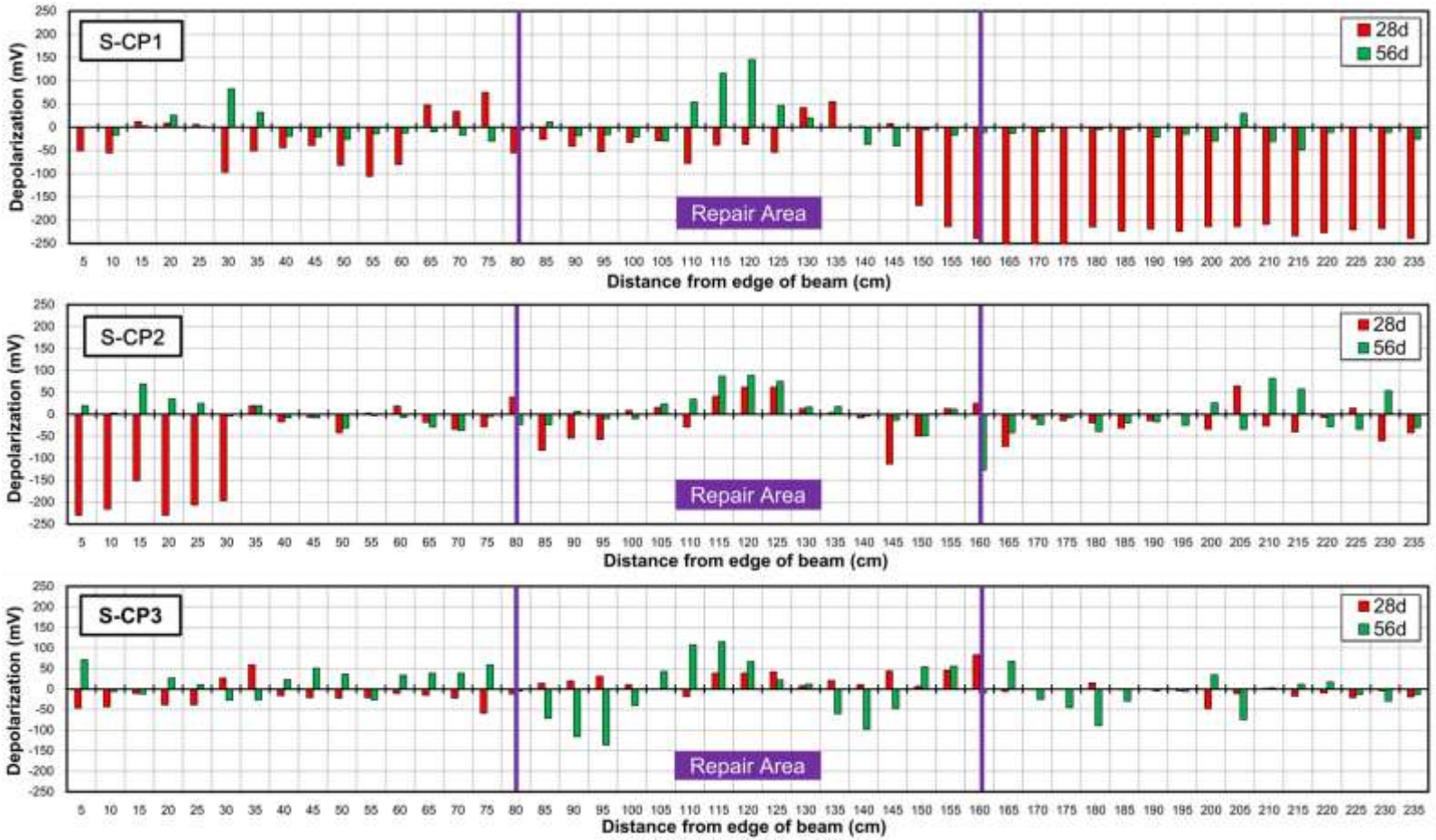

Fig 8.16 Summary of 24-h depolarization test result of steel bar in S-type beam with time

From **Fig 8.16** it can be noticed also that there were fluctuations of potential of steel bar near interfacial zone and non-repaired area to negative directions which means failed polarized by anode.

Rest Potential

The bar charts in **Fig 8.17** illustrates about the rest potential or natural potential of anode embedded in patch repair concrete of S-type beam after disconnected to steel bars by 24-hour. The data shows that natural potential of anode decreased gradually to more than ~-1000 mV vs CSE time-dependently, which is similar to natural potential of Zn alloys [8.5].

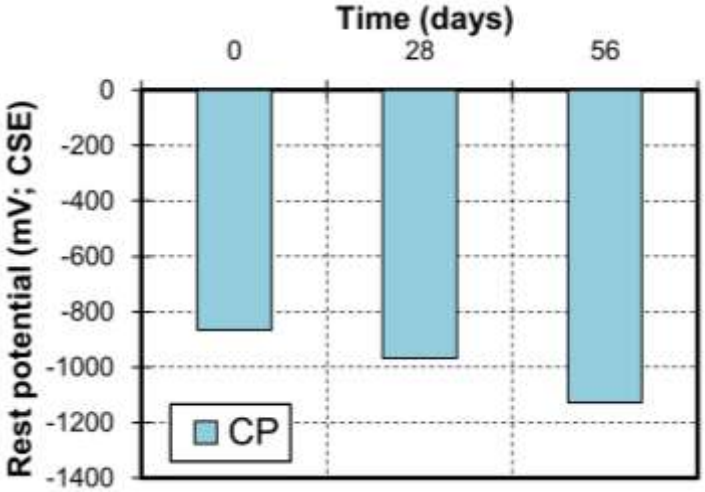

Fig 8.17 Rest potential of anode in S-type beam

Meanwhile, the bar charts in **Fig 8.18** show about rest potential of steel bars after disconnected with anode 24-hour. It was observed that potential of steel bar in patch repair area more positive than in non-repaired area. It means that probability of corrosion in non-repaired area still higher than in repair area. It indicates that anode could effective to protect steel bar only in repair area.

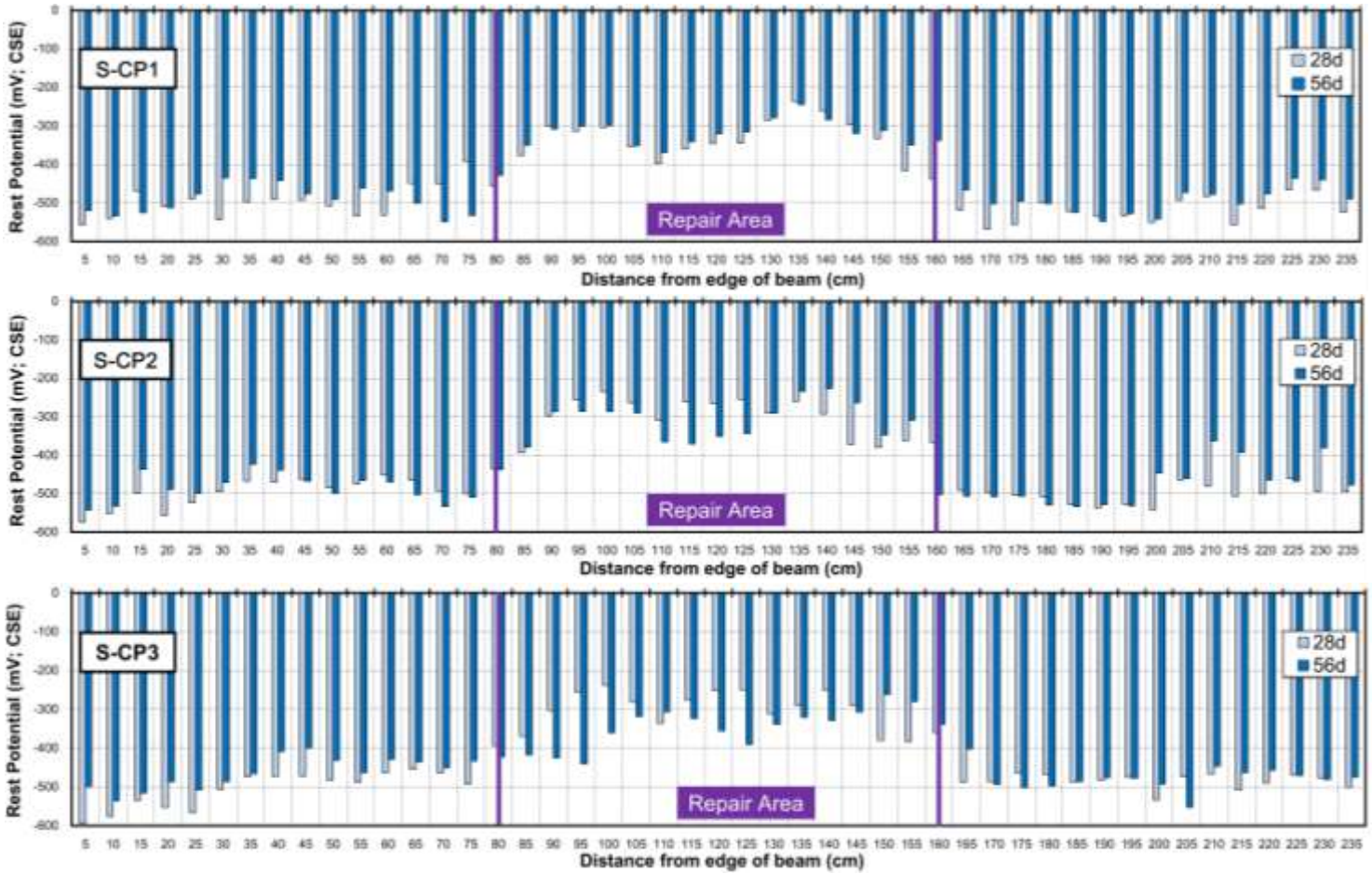

Fig 8.18 Rest potential of steel bars in S-type beam

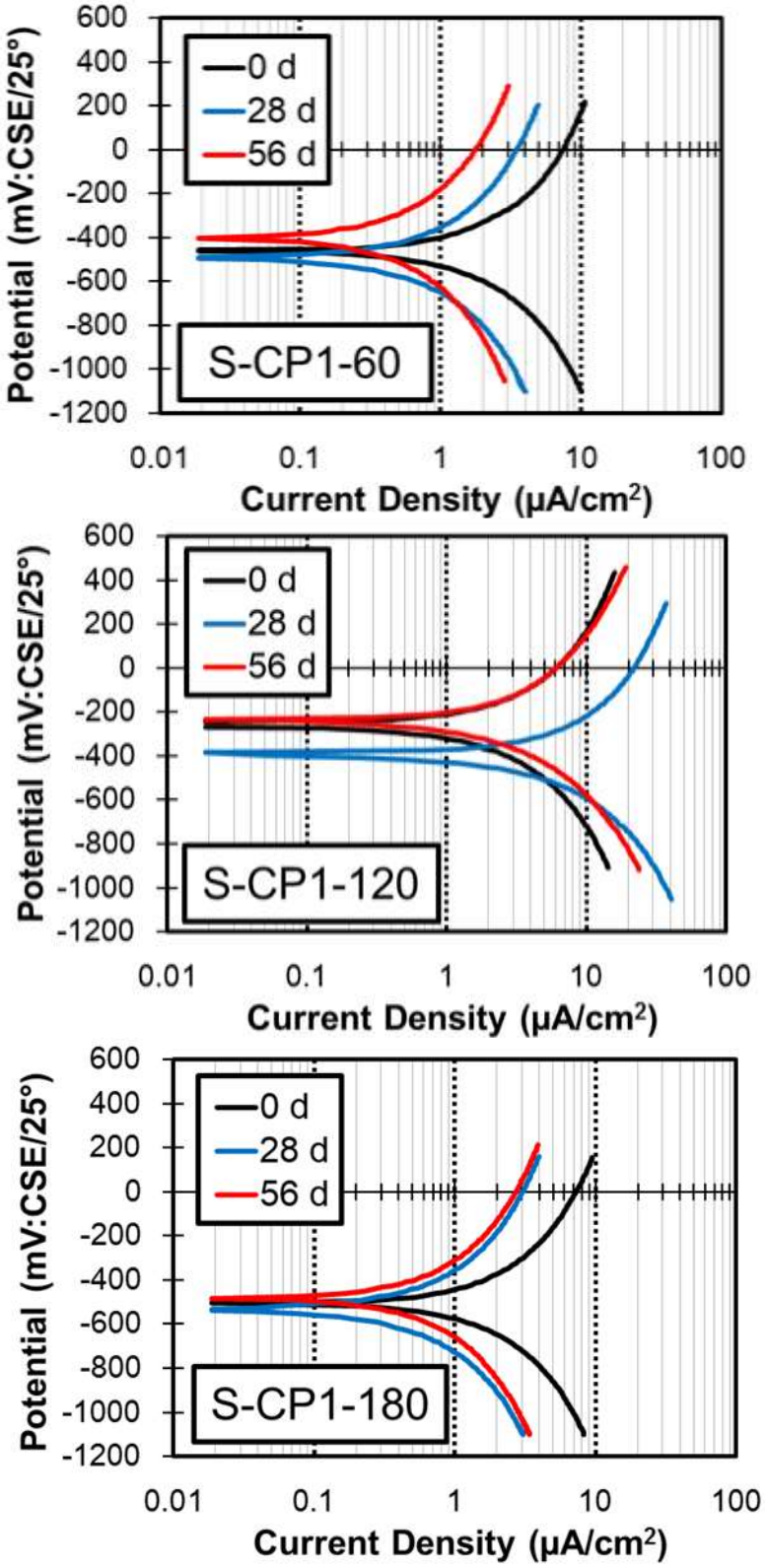

Fig 8.19 Anodic-cathodic polarization curve of S-CP1 at 60, 120 and 180 cm from edge of beam

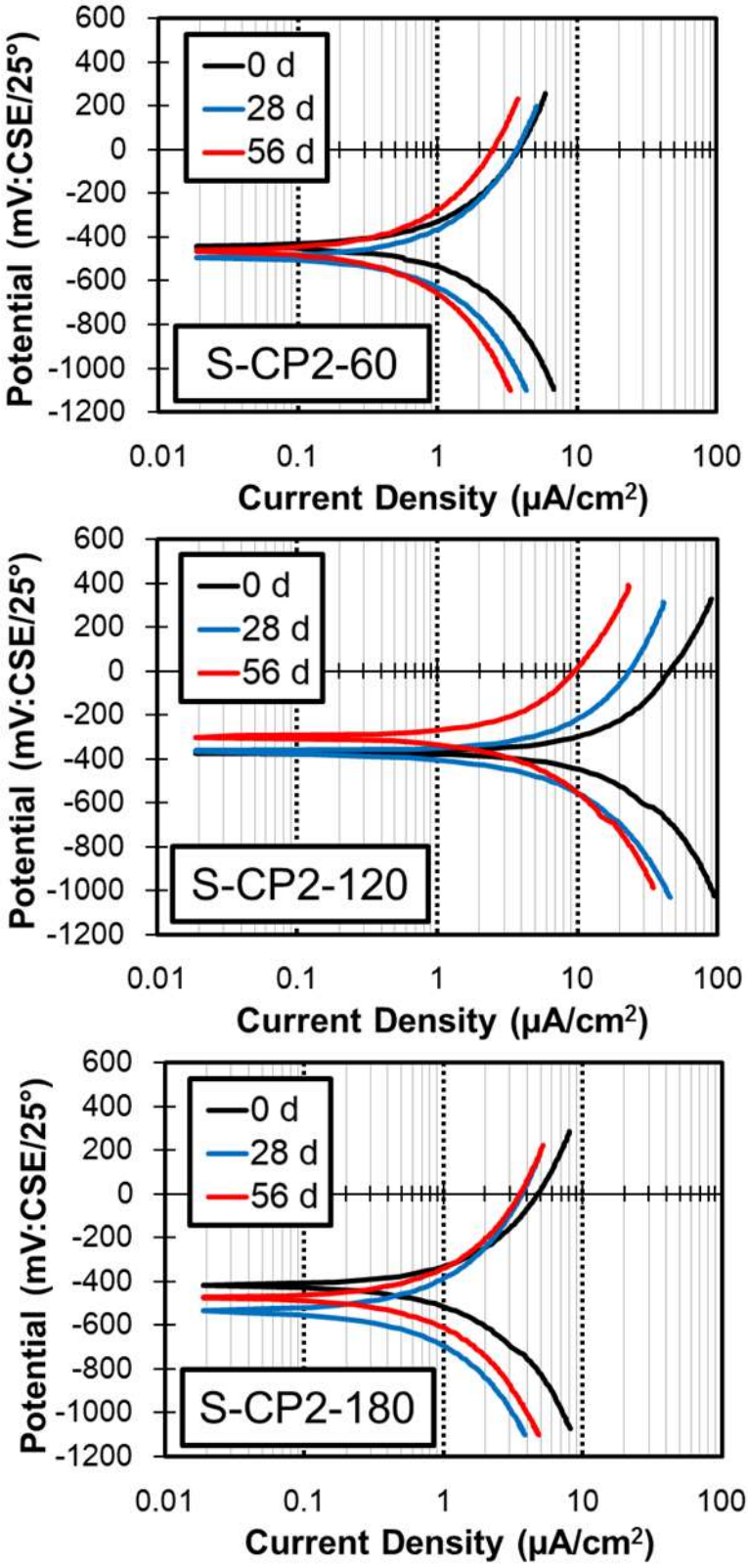

Fig 8.20 Anodic-cathodic polarization curve of S-CP2 at 60, 120 and 180 cm from edge of beam

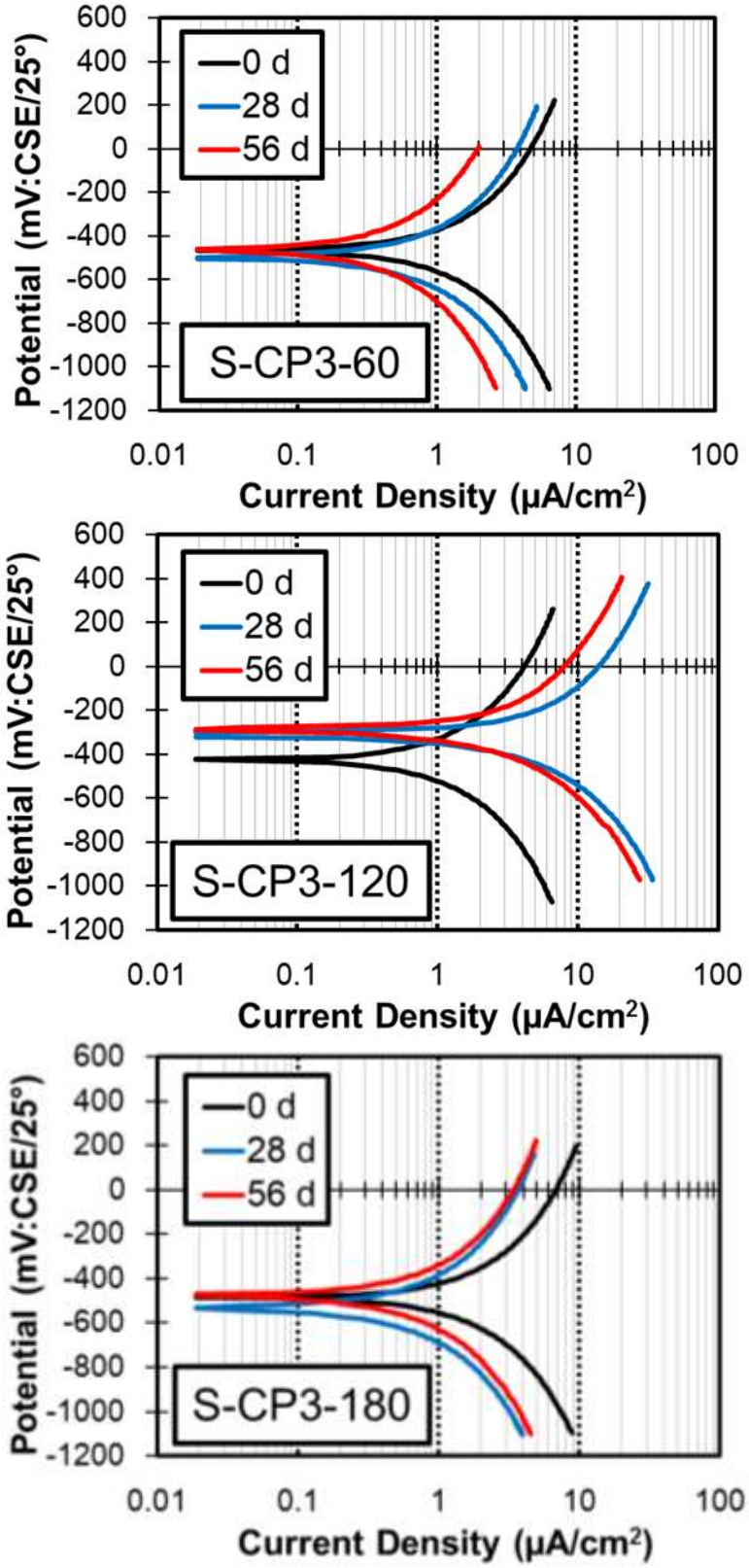

Fig 8.21 Anodic-cathodic polarization curve of S-CP3 at 60, 120 and 180 cm from edge of beam

Anodic-Cathodic Polarization Curve of Steel Bar

The line graphs in **Fig 8.19**, **Fig 8.20** and **Fig 8.21** show about anodic-cathodic polarization curve of S-CP1, S-CP2 and S-CP3 at 60, 120 and 180 cm from edge of beam during 0-day, 28-day and 56-day of exposure time. Based on the grade of the passivity film of steel bar proposed by Otsuki [8.6], the passivity of S-CP1 in repair area tend to worse condition. Meanwhile, passivity grade of S-CP in non-repaired area inclined to more good condition. The same trend was observed for S-CP3. However, passivity condition of S-CP2 in repair area tend to more good condition. It was observed that steel bar close to anode position (S-CP2 at 120 cm from the edge of beam) polarize by anode significantly compare another position.

8.7.2 L-Type Beam

A. Polarization of Anode

Potential of Anode

As mention previously, for L-type beam, incremental number of anode increase to three-anode on each of tensile rebar. It means there 9-anode in total embedded in patch repair area of L-type beam. **Fig 8.22** describes about development of anode potential embedded in patch repair area of L-type beam during on and instant-off condition with the function of time.

The data show that during instant-off condition, potential of anodes tend to more negative ~-1000 mV between 7-day and 56-day of polarization time. However, CP2 and CP3 shown no significance changes time-dependently during on and instant-off condition, even though the potential value both set of condition shown decreased gradually to negative directions. It was observed that anodes embedded in L-type beam reached natural potential of Zn alloys (e.g., ~-1000 mV) time-dependently.

Distribution of Current

The protective current of anodes embedded in patch repair area of L-type beam is shown in **Fig 8.23**. It was observed that the initial of protective current of anodes is between ~1.2 $\mu A/cm^2$ to ~1.3 $\mu A/cm^2$.

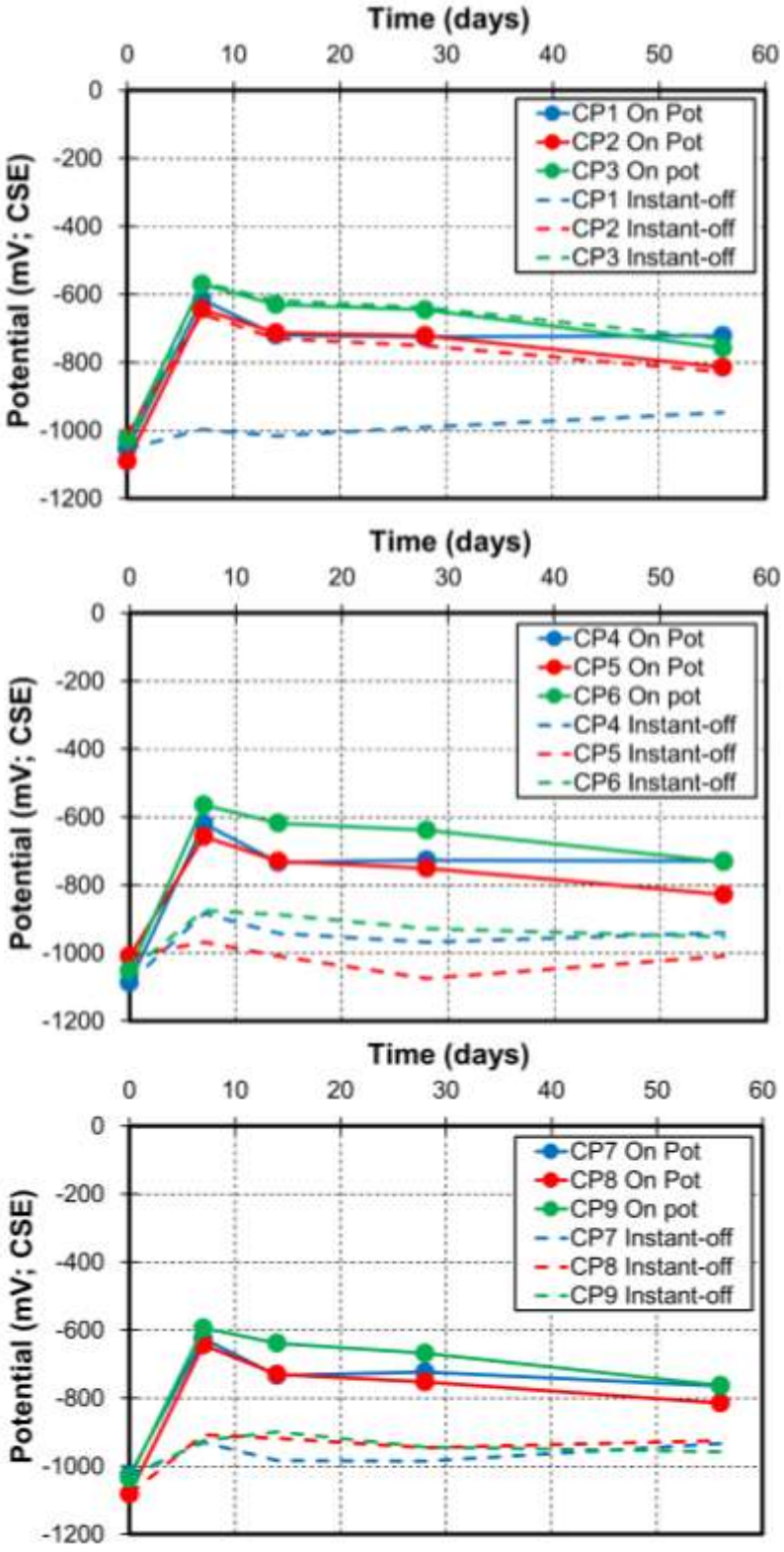

Fig 8.22 Anode potential (on and instant-off potential) evolution embedded in L-type beam with the function of polarization time

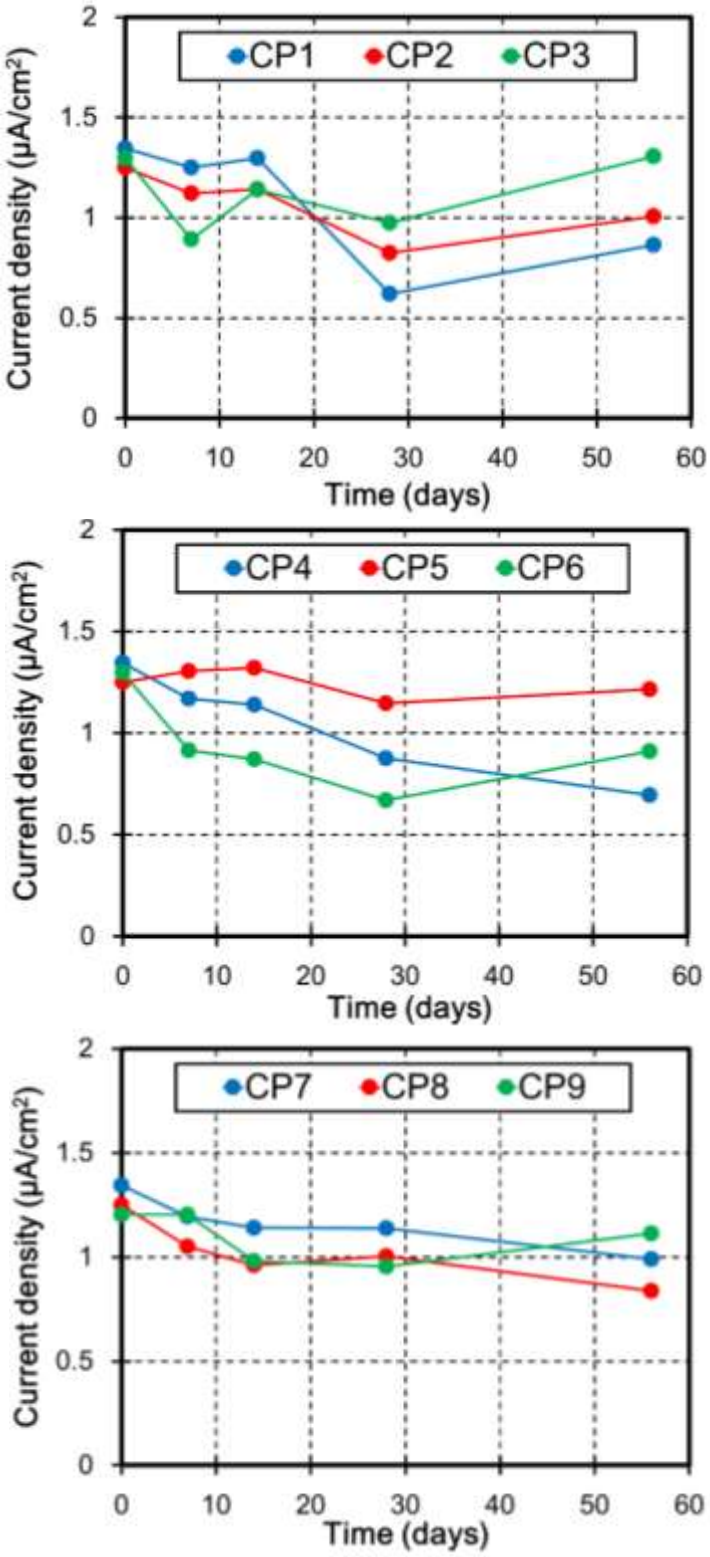

Fig 8.23 Protective current evolution of anodes embedded in L-type beam with the function of polarization time

The data in **Fig 8.23** shows that potential of anodes decreased markedly for anodes notably CP4, CP5, CP6, CP7, CP8 and CP9. But still over the minimum of design limit of cathodic protection between 0.2 - 2 $\mu A/cm^2$ as specified in EN 12696 [8.4]. Meanwhile, protective current of CP1, CP2 and CP3 increased gradually to ~0.8 $\mu A/cm^2$ to ~1.3 $\mu A/cm^2$ at 56-day of polarization time. It means that throwing power of anode keep constant between ~0.6 $\mu A/cm^2$ to ~1.3 $\mu A/cm^2$ with the function of time.

Anodic Polarization Curve of Anode

The potential-current trajectory of the anodes embedded in L-type beam measured at 24 hours after switch off are presented in **Fig 8.24**, **Fig 8.25** and **Fig 8.26**. It was observed that the current density increased gradually time-dependently for all of anodes from 0 day to 28 days of exposure time. It means that anodic polarization increases with increasing of the polarization time between 0-day and 28-day of exposure time. Meanwhile, the activity all of anodes decreased gradually at 56-day of polarization time. This means that although the activity of the sacrificial anode is fell gradually, however, it is still enough to polarize the steel bar to protective levels as current value of anodes shown over the ~10 $\mu A/cm^2$ at the end of test.

B. Polarization of Steel Bar

Potential of Steel Bar

Fig 8.27 describes about potential development of steel bars embedded in L-type beam with SACP connected (S-CP) time-dependently during on condition. On potential of steel bar under anode protection in repair area decreased gradually to more negative ~-800 mV at 56-day of polarization time. On potential of steel bars in non-repaired area also dropped to more negative time-dependently but not more than ~-600 mV at 56-day of polarization time. However, the potential of steel bar near interfacial zone between repair and non-repaired area increased to more positive direction.

Furthermore, **Fig 8.28** shows about potential evolution of steel bar time-

dependently during instant-off condition. Potential of steel bar near the anode position decrease to more negative ~-600 mV at 56-day of exposure time. As well as the steel bar in non-repair area. Same like in on condition, potential of steel bar in interfacial zone increased to more positive direction. It means trans-passive region were occurs in the interfacial zone of L-type beam.

It was observed that anode embedded in L-type beam polarize potential of steel bars in repair to more negative and reach protective potential criterion ~-770 mV. However, anode seems could not polarize the steel bar near the interfacial zone.

Depolarization Potential

Fig 8.29 illustrates the depolarization value of the steel bars in repair and non-repair concrete sections of L-type beam. It was clearly seen that steel bar in patch repair area with achieved "100 mV decay" criterion with fluctuations, which means that a protective condition is achieved on this rebar. On the other hand, steel bars in non-repaired area could not reach potential decay more than 100 mV.

Rest Potential

The bar charts in **Fig 8.30** shows about the rest potential or natural potential of anode embedded in patch repair concrete of L-type beam after disconnected to steel bars by 24-hour. The data shows that natural potential of anode decreased gradually to more than ~-1000 mV vs CSE time-dependently, which is similar to natural potential of Zn alloys.

Meantime, the bar charts in **Fig 8.31** show about rest potential of steel bars in L-type beam after disconnected with anode 24-hour. The data shows that potential of steel within the repair area and non-repaired area depressed to negative direction ~-600 mV at 56-day of exposure time. Based on corrosion probability per ASTM C876-99 [8.7], it indicates that 90% of corrosion occurs in this area. However, rest potential of steel bars in interfacial zone shown increased to positive direction and it means trans-passive region were occurs in the interfacial zone of L-type beam.

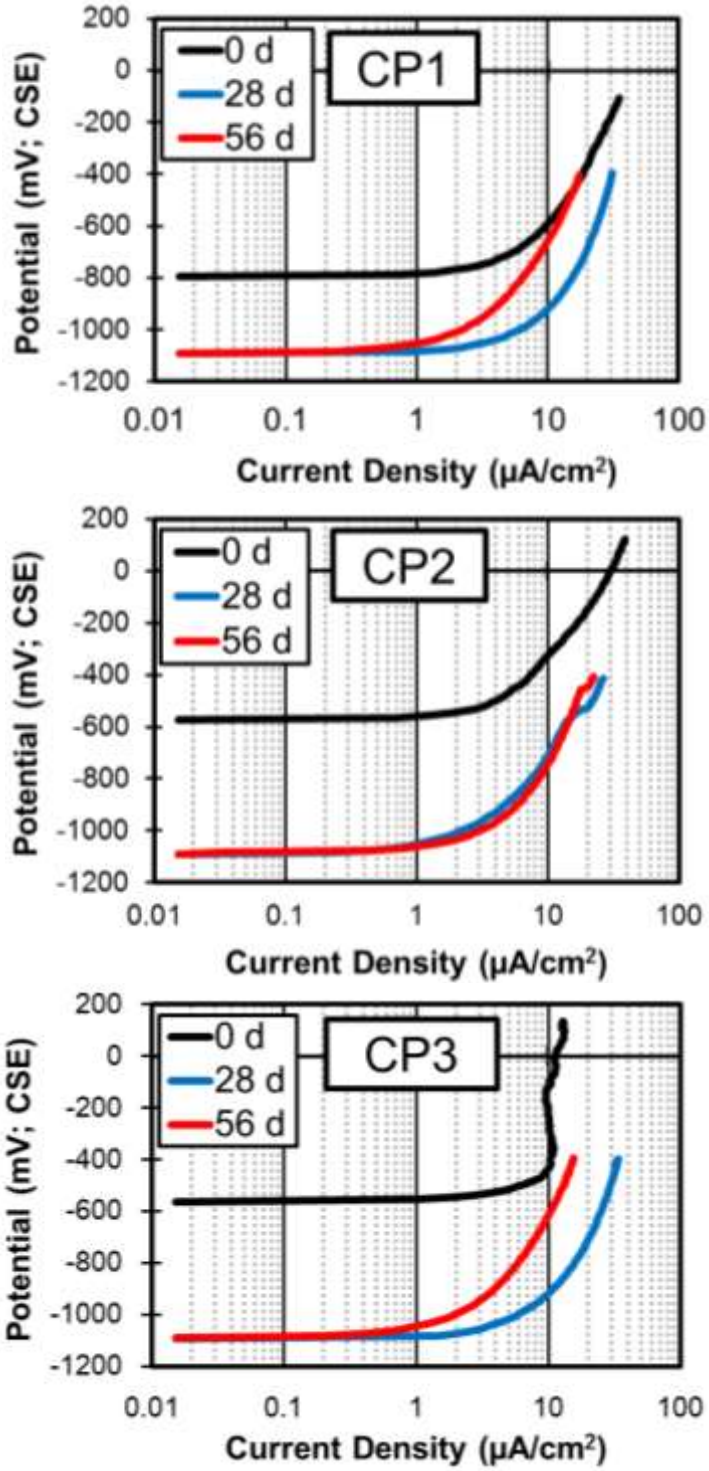

Fig 8.24 Anodic polarization behavior of anode (CP1, CP2 and CP3) embedded in L-type beam

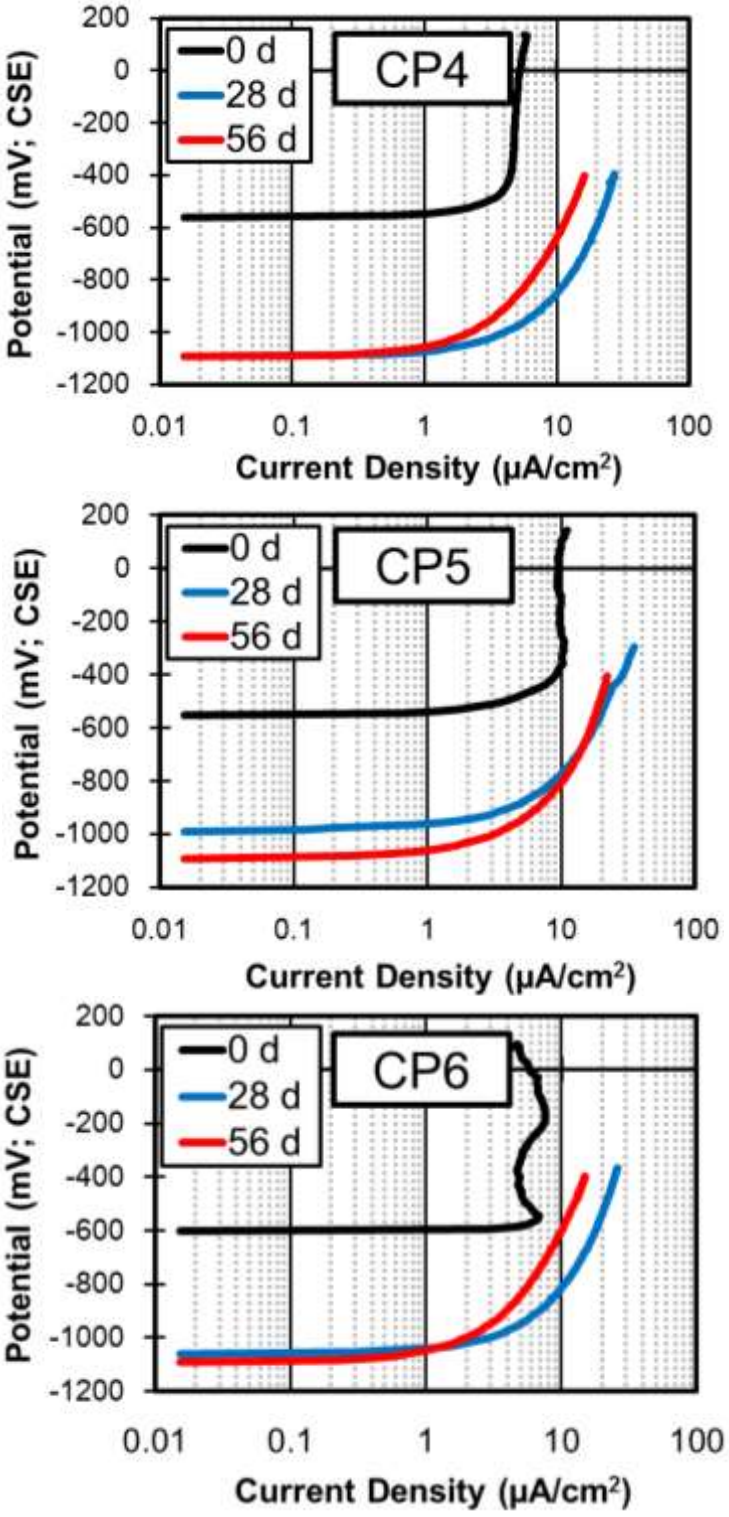

Fig 8.25 Anodic polarization behavior of anode (CP4, CP5 and CP6) embedded in L-type beam

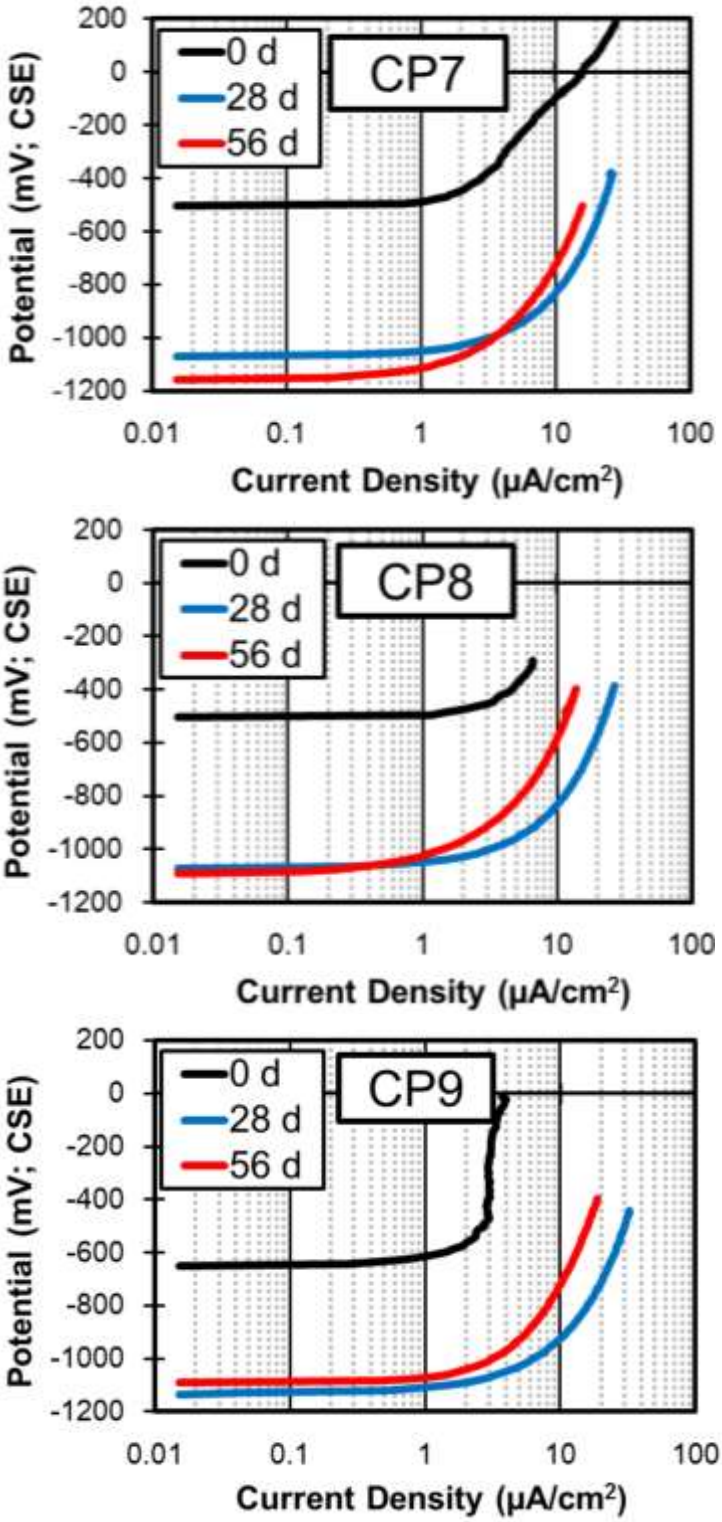

Fig 8.26 Anodic polarization behavior of anode (CP7, CP8 and CP9) embedded in L-type beam

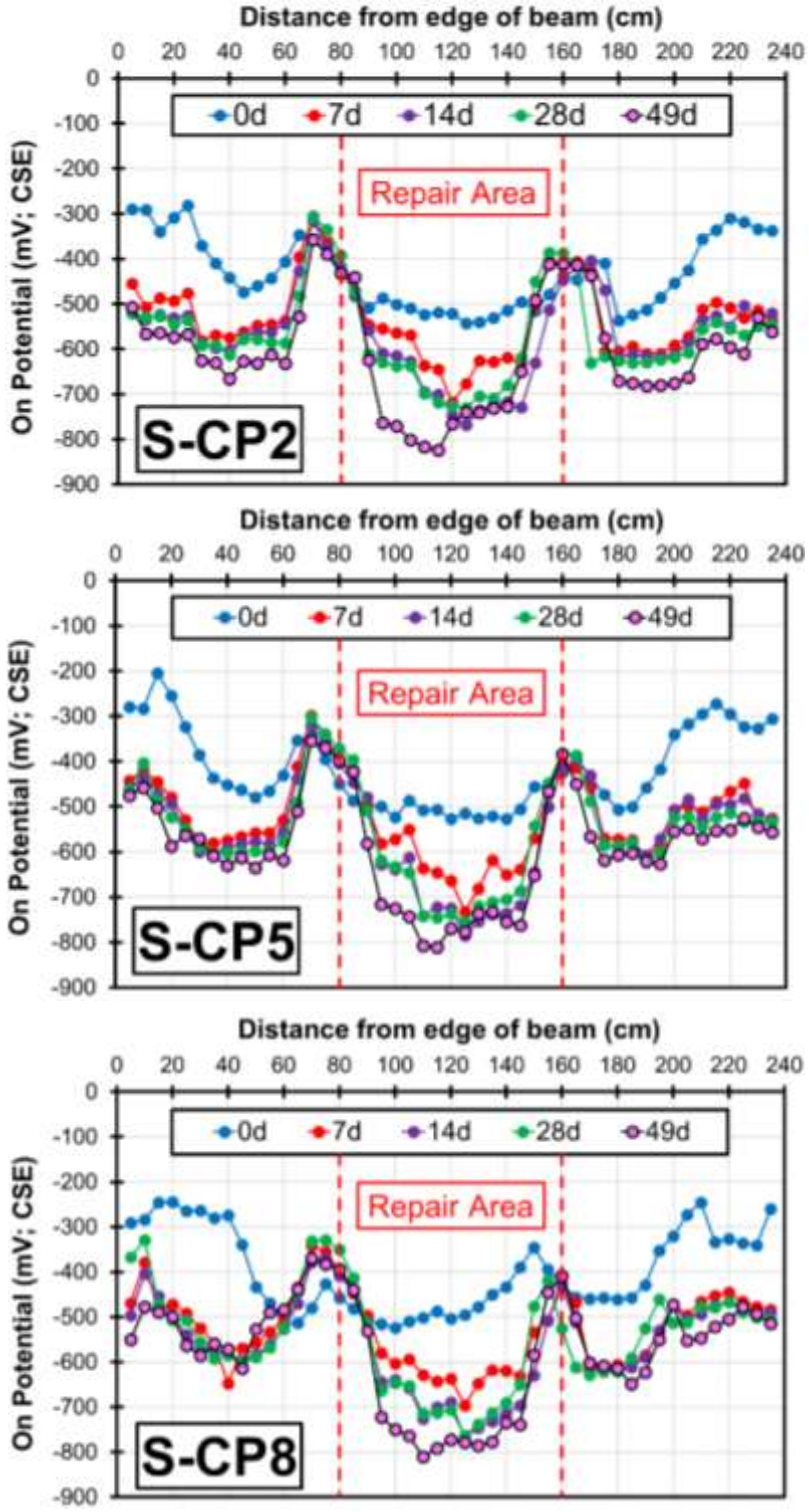

Fig 8.27 On potential evolution of steel bar embedded in L-type beam with

polarization time

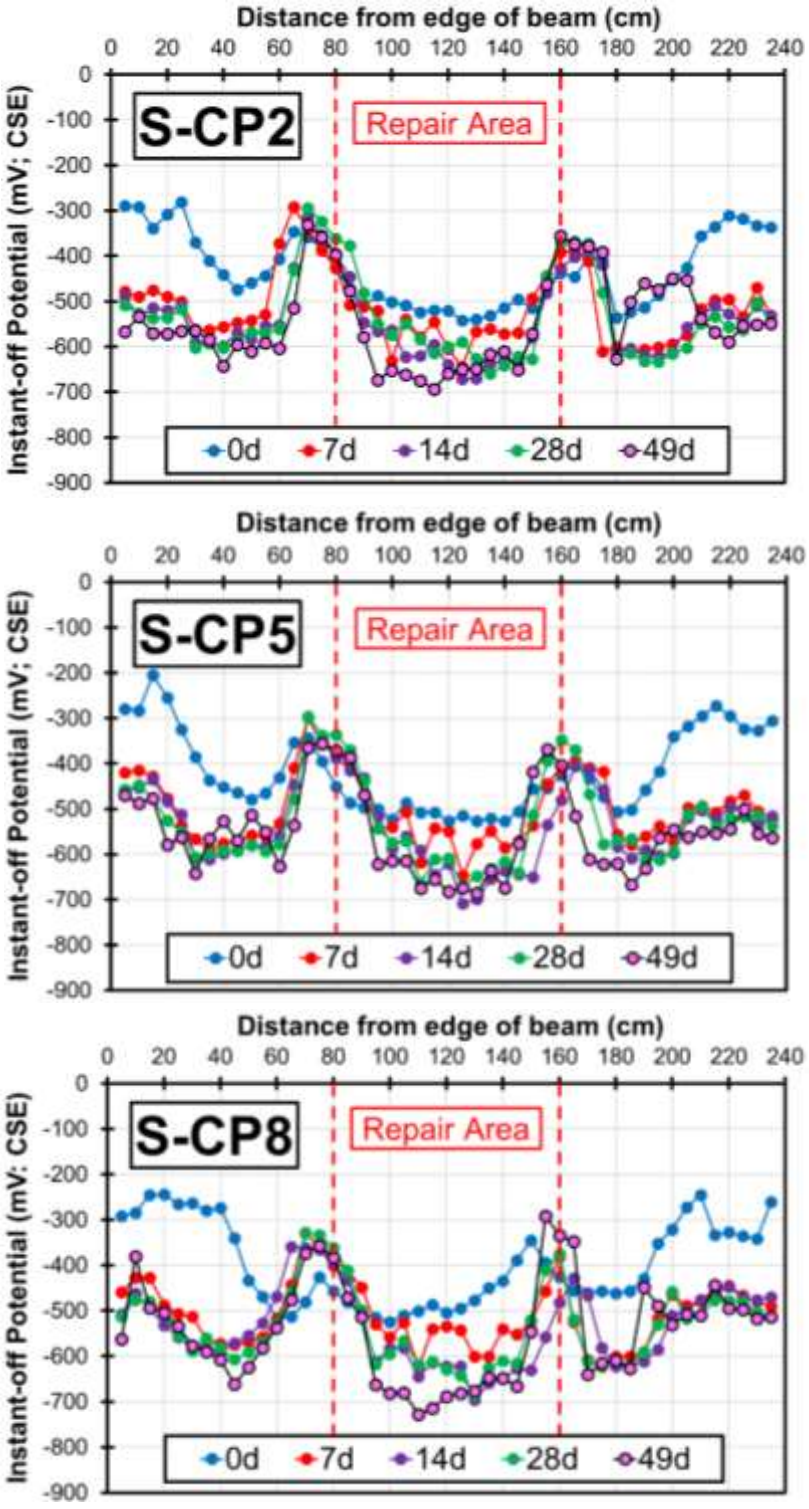

Fig 8.28 On potential evolution of steel bar embedded in L-type beam with polarization time

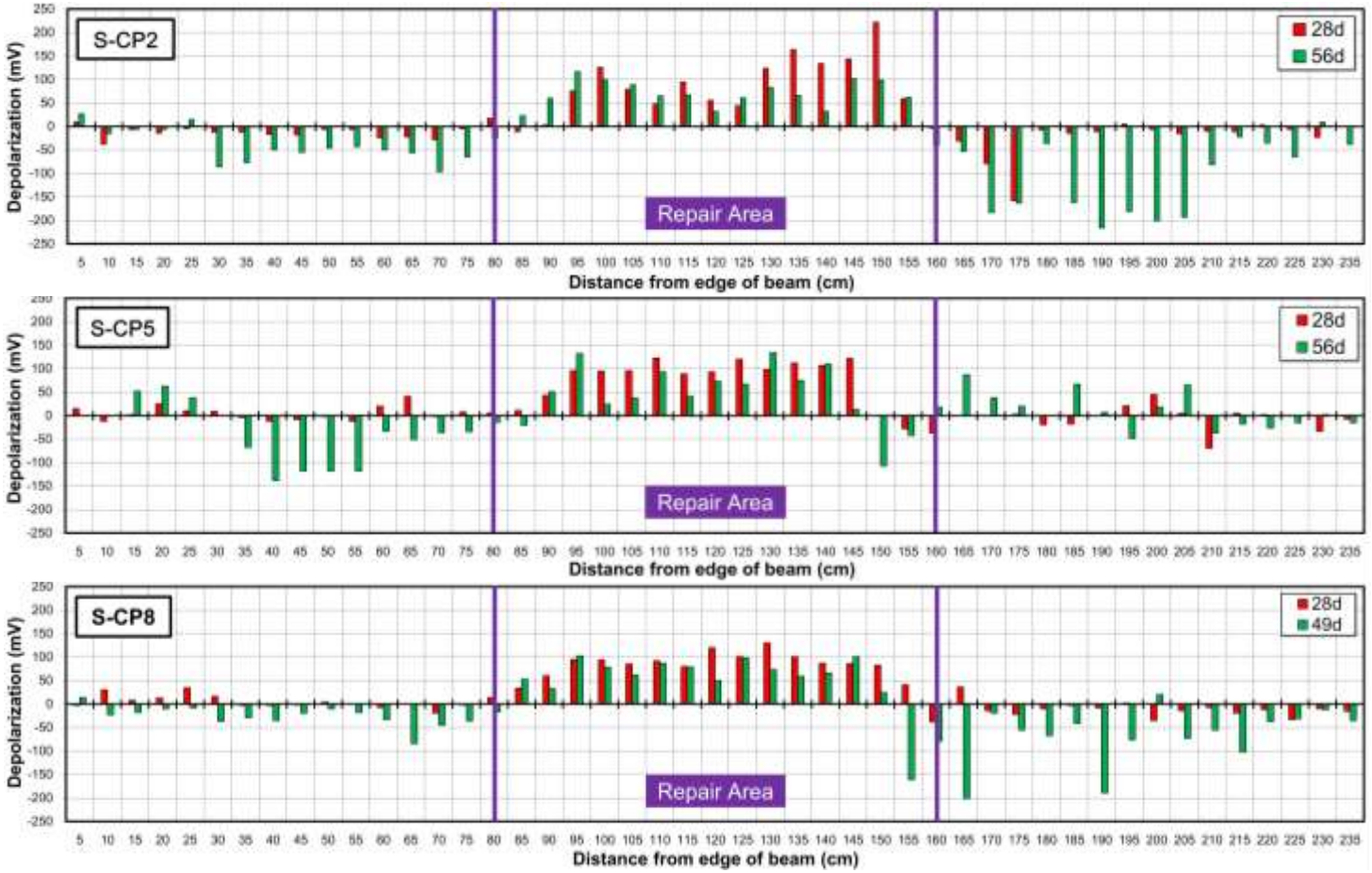

Fig 8.29 Summary of 24-h depolarization test result of steel bar in L-type beam with time

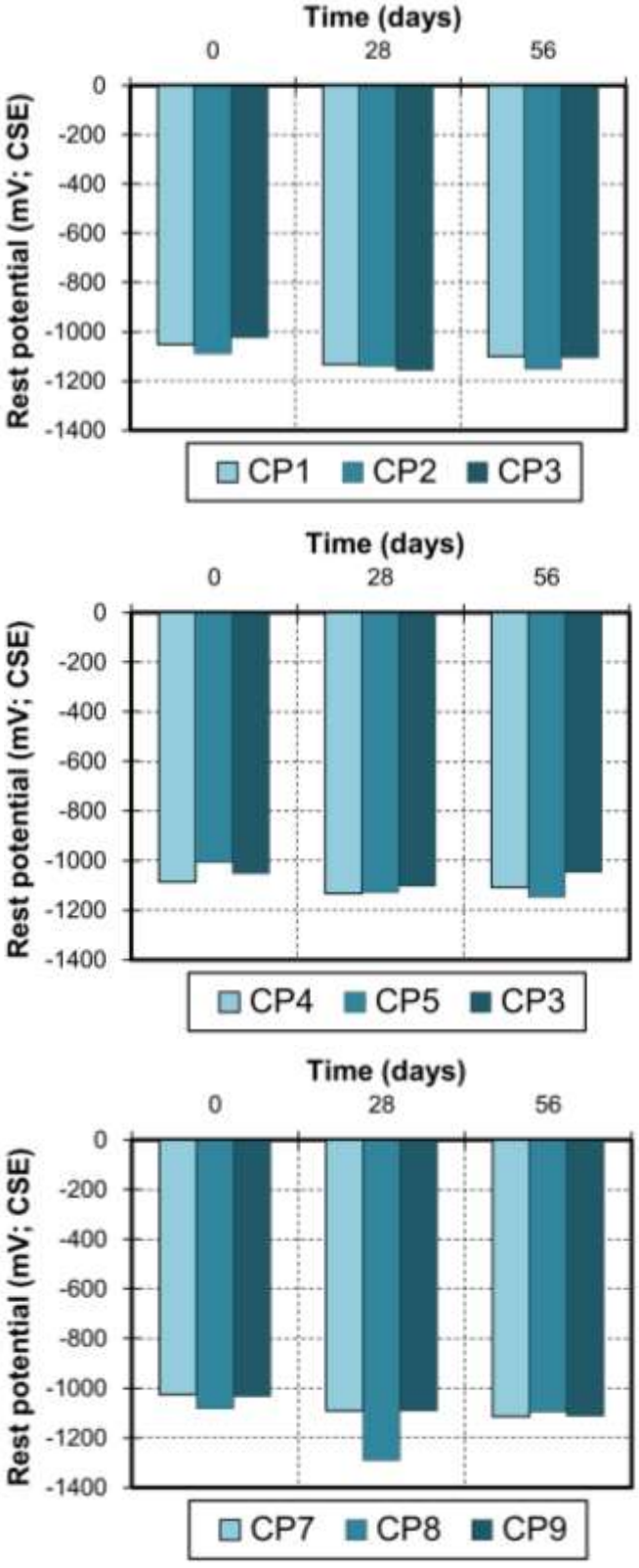

Fig 8.30 Rest potential of anode in L-type beam

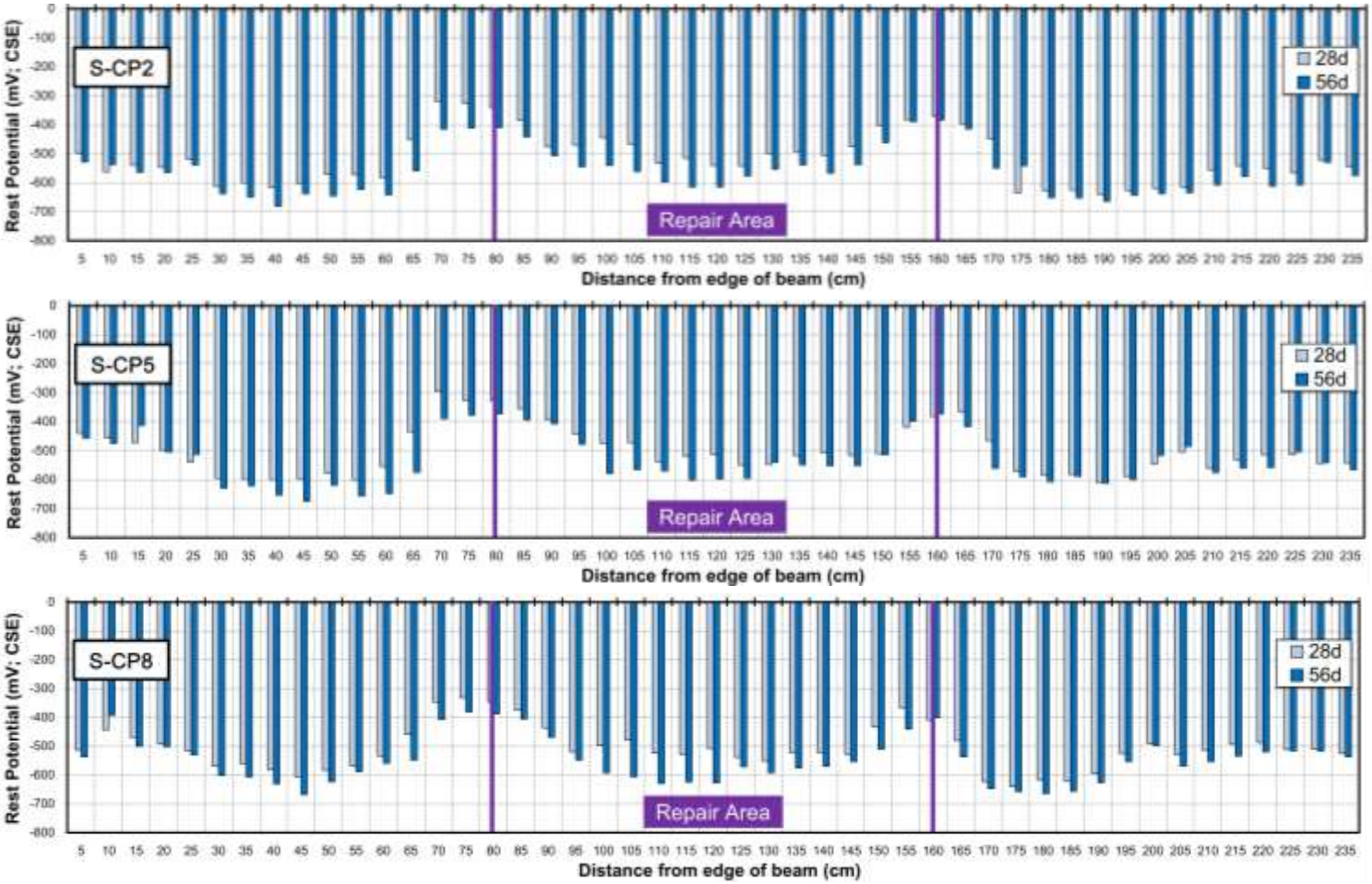

Fig 8.31 Rest potential of steel bars in L-type beam

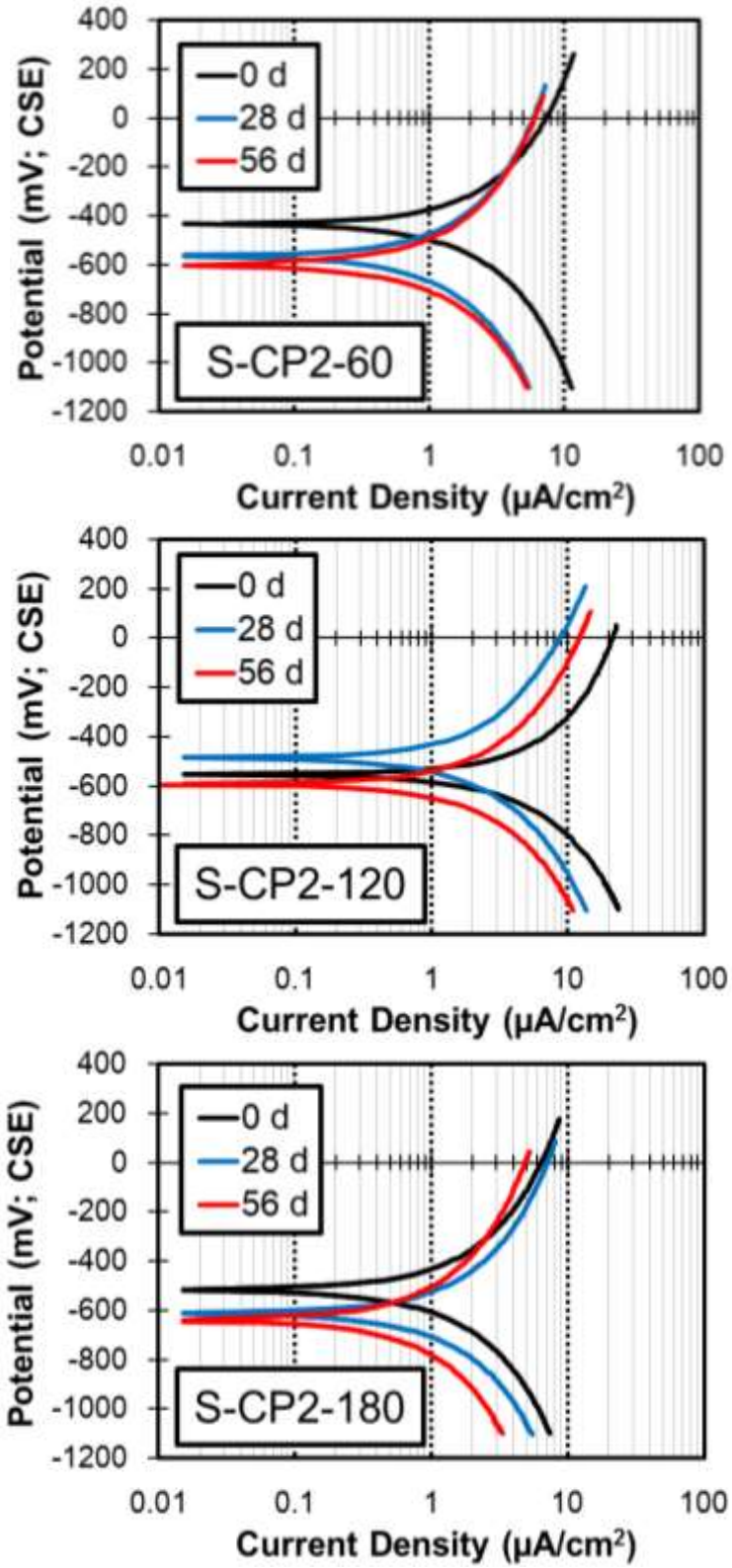

Fig 8.32 Anodic-cathodic polarization curve of S-CP2 at 60, 120 and 180 cm from edge of L-type beam

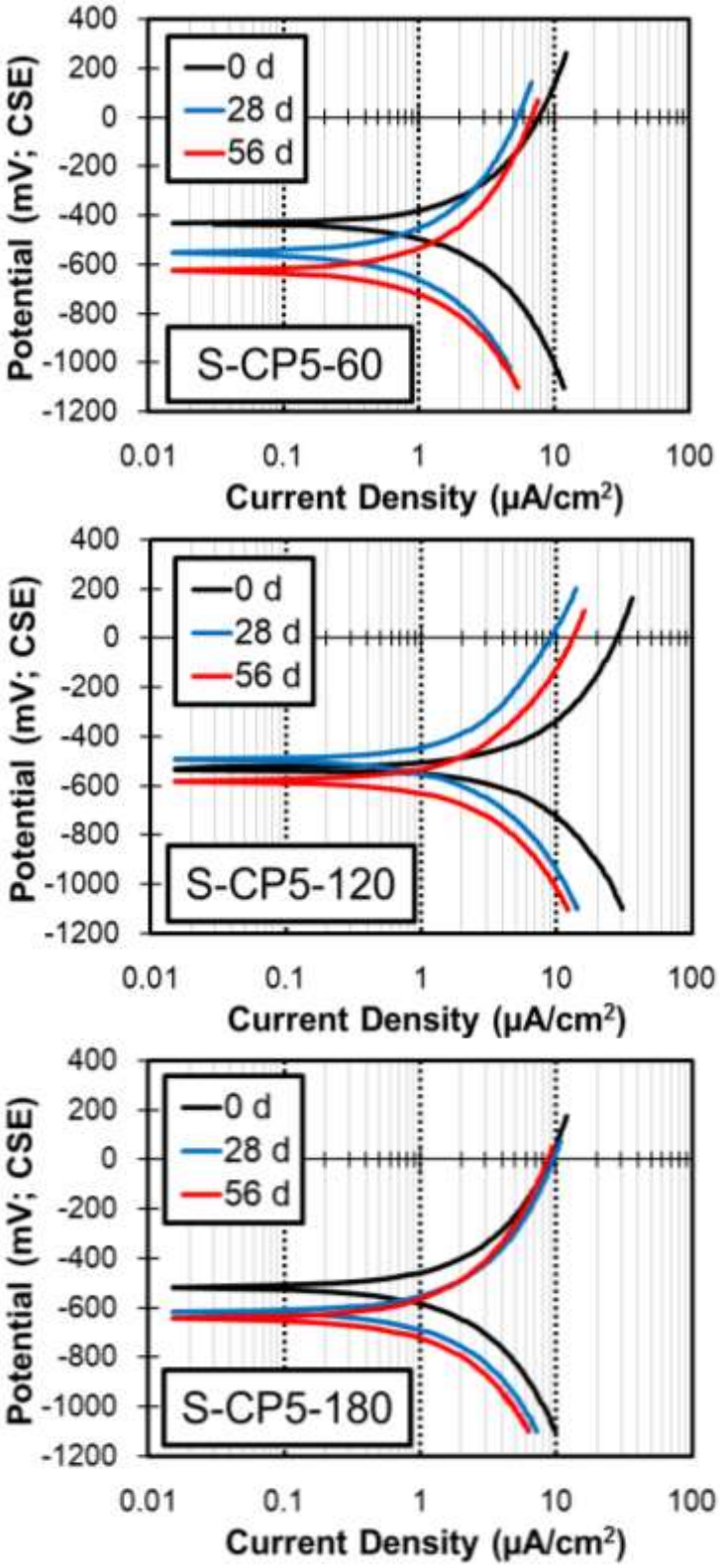

Fig 8.33 Anodic-cathodic polarization curve of S-CP5 at 60, 120 and 180 cm from edge of L-type beam

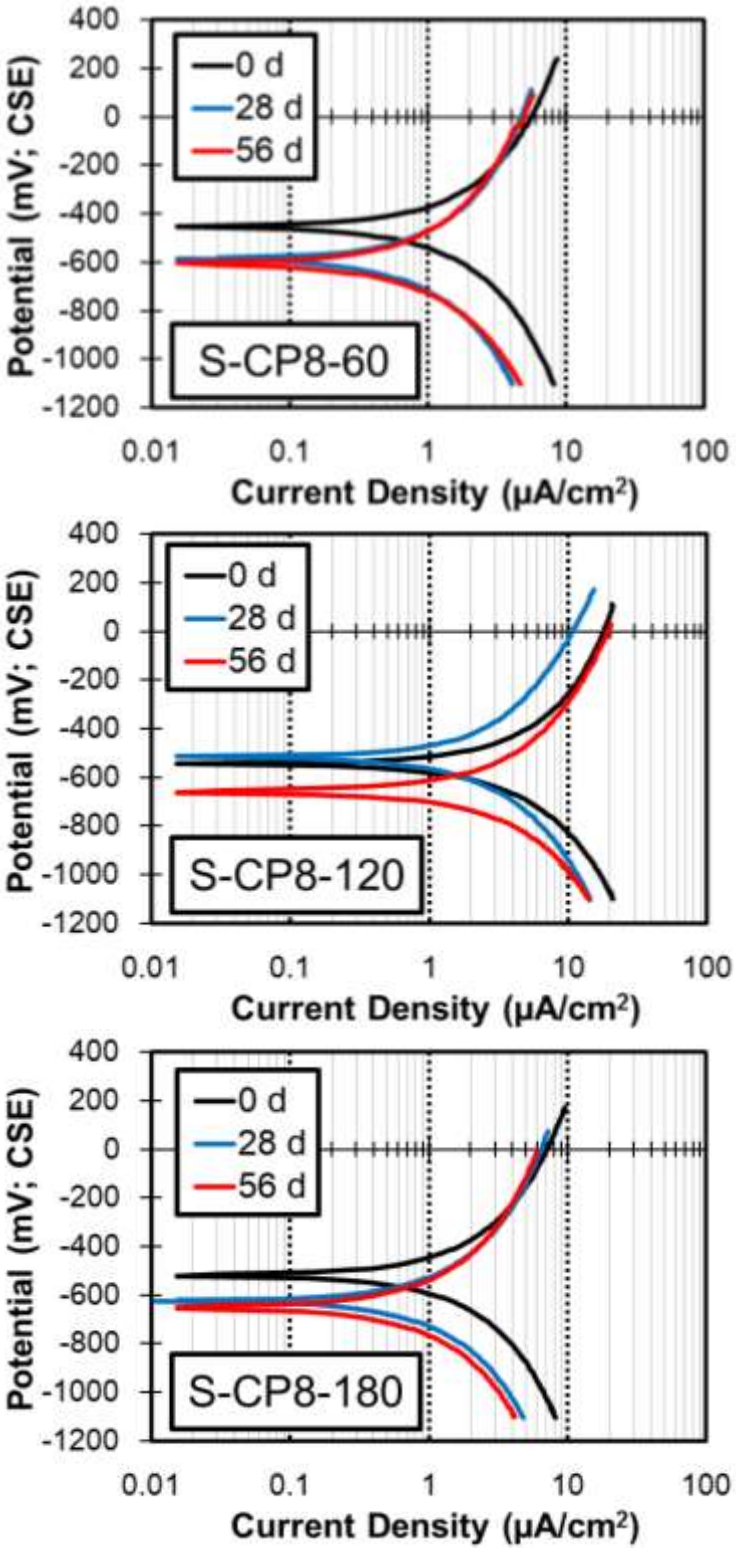

Fig 8.34 Anodic-cathodic polarization curve of S-CP8 at 60, 120 and 180 cm from edge of L-type beam

Anodic-Cathodic Polarization Curve of Steel Bar

The line graphs in **Fig 8.32**, **Fig 8.33**and **Fig 8.34** show about potential-current trajectory of S-CP2, S-CP5 and S-CP8 at 60, 120 and 180 cm from edge of L-type beam during 0-day, 28-day and 56-day of exposure time. Based on the grade of the passivity film of steel bar proposed by Otsuki [8.6], the passivity of S-CP2 and S-CP5 in repair area tend to good condition. Moreover, passivity grade of S-CP in non-repaired area inclined to more good condition with fluctuations. However, passivity condition of S-CP8 in repair area tend to worse condition at 56-day of polarization time. In general, it was observed that anode in patch repair concrete polarize steel bars in this area to good condition.

8.8 Discussions and Recommendations

8.8.1 Anode Potential and Current Functions

Instant-off potential of one-anode embedded in S-type beam increased to noble value at 56-day of polarization time. Meanwhile, instant-off potential of nine-anode embedded in L-type beam keep constant between ~-850 mv and ~-1000 mV at the end of test. A transport limited polarization component could occur due to dynamic accumulation of anode products on its surface, which would effectively shift the equilibrium potential of the anode toward a more positive value as observed in S-type beam.

One-anode deliver protective current to three-tensile rebar in S-type beam, meanwhile three-anode convey current to one-tensile rebar in L-type beam. From this condition it was observed that aging of the anodes by delivering current in service was manifested by the continually decreasing current output in S-type beam which faster than anodes in L-type beam. Protective current density in L-type beam two-time higher than in S-type beam. Potential-current trajectory of anode in anodic-cathodic polarization curve shows that anodes activity in L-type beam increased significantly at 28-day of polarization time and decreased gradually at 56-day of exposure time. However, it is still enough to polarize the steel bar to protective levels, mainly the tensile-rebar in patch repair area at the ranging between 95 cm and 150 cm from the edge of beam.

8.8.2 Factors Affecting Potential of Steel Bar

Anode polarize tensile-steel bars in repair concrete of L-type beam to protection levels but failed to protect the steel bars in non-repair concrete. Meanwhile, anode was failed to polarize the steel bars in patch repair concrete of S-type beam to protection levels as well as in parent concrete.

Factors affecting the measured steel potential in a repaired area include passive film formation, pH, membrane effects and oxygen availability. The steel passive film has to form on the steel in the repaired area and this will take time. However, the formation of the passive oxide film should have been complete after at least some of the periods tested, and should no longer have been affecting the potential within the repaired area.

Thus, the formation of the passive film may only impart some limited time dependence to the potentials within the repaired area. The pH of the environment has a strong impact on equilibrium potentials with a higher pH resulting in more negative equilibrium potentials. Fresh repair concrete may well have a higher pH than aged concrete because the reaction between hydroxide and silica within the concrete or between hydroxide and carbon dioxide in the air will tend to reduce the pore solution pH in aged concrete to that sustained by one of the more abundant solid phases of cement hydration [8.8].

The change in pH between the repair material and the parent concrete can give rise to a membrane (or streaming) potential between the parent and the repair material [8.9]. This is due to diffusion of hydroxide ions from the repair material to the parent concrete and a charge on the walls of the pore system in concrete [8.10].

Passivity and oxygen availability affect the anodic and cathodic kinetics. Oxygen is consumed to passivate the steel in the repaired area. Many proprietary repair materials have a low permeability that restricts oxygen access and increases resistance. Thus Morgan [8.11] concluded that the use of polymer, styrene butadiene or acrylic modified cement mortars with such properties did not affect corrosion of steel in adjacent unrepaired areas. The effects of pH and permeability also suggest that any macrocell activity between parent concrete and proprietary repair materials will have less effect than macrocell activity that resides exclusively

within the parent concrete.

Formation of the passive oxide film probably give rise to some of the time dependence. However, they do not dominate the time dependence to the extent that steel potentials in the repaired areas rise above that in the parent concrete of S-type beam. The data from this study, provided evidence to indicate that macrocell activity is a cause of incipient anode formation in aged concrete structures repaired with patch repair concrete.

8.8.3 Repair Material Interface

Potential of steel bar in the interfacial zone of S-type and L-type beam show increased to positive direction. Passivity is broken when potential is increased in the positive direction, leading to damage in the passive protective films, resulting mostly in pitting-corrosion and this region is called trans-passive region.

Furthermore, cracks may occur at the interface between the parent concrete and the repair material following patch repair. The presence of such cracks can be attributed to drying, or plastic shrinkage, thermal or stiffness incompatibility, poor curing, surface preparation or a combination of the above [8.12, 8.13].

The interface between repair material and parent concrete may provide a path for chlorides to penetrate preferentially into the substrate. The extent of this effect will be dependent on surface preparation, application techniques, curing, material properties and compatibility with the parent concrete. The presence of visible cracks may be obscured by trowel finishing the repair.

8.8.4 Corrosion Risk

From the rest potential testing results, it was observed that corrosion risk of steel bar in parent concrete (non-repair area) of S-type and L-type beam are still high. This analysis has suggested that there is obvious increase in corrosion risk following patch repair of reinforced concrete structures that results from macrocell activity, beyond what would be the case if the steel had remained passive.

Indeed, steel reinforcement in an aged parent concrete may remain cathodic relative to steel in proprietary repair materials for a substantial period

after the repair is undertaken. The results of this study are in line with previously reported findings by Bertolini et al. [8.14] and Qian et al. [8.15] on the corrosion risk presented by a galvanic couple of stainless steel to carbon steel. The damage caused by a corroding steel anode in an unrepaired area probably outweighs any electrochemical protective effects that such a corroding area may deliver [8.16, 8.17].

8.8.5 Cathodic Protection Design

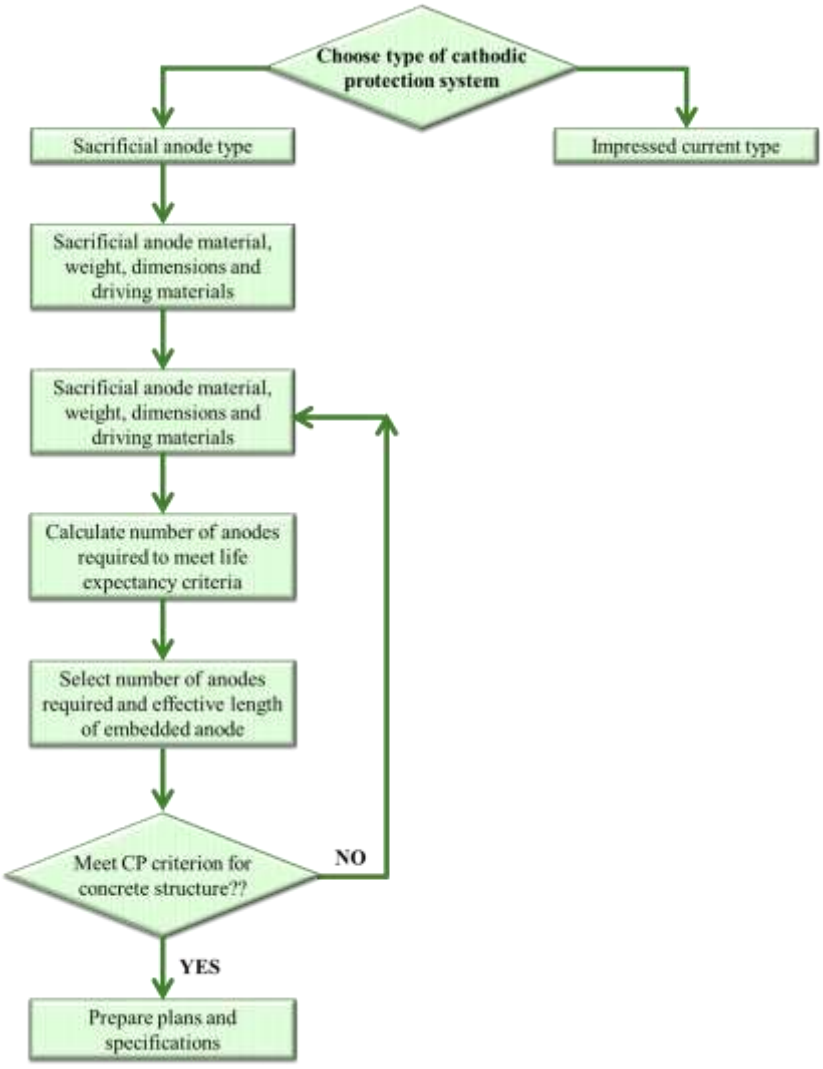

Fig 8.35 Design sequence of sacrificial anode cathodic protection systems for concrete structure

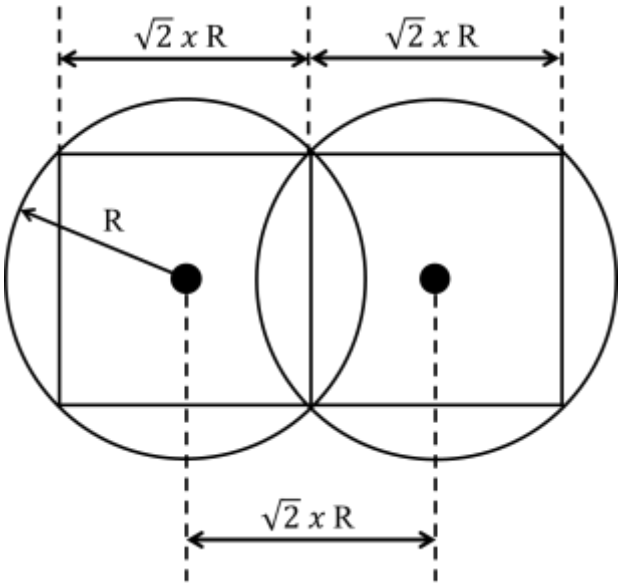

Fig 8.36 Maximum effective length of embedded anode in concrete [8.18]

Based on the results of this research, a design sequence of sacrificial anode cathodic protection systems for concrete structure is proposed as shown in **Fig 8.35**.

Maximum length of embedded anode in concrete as shown in **Fig 8.36** with equation as follow:

$$R = \sqrt{\frac{1}{\left(10\ x\ \frac{SSA}{CSA}\right)}} \qquad (8.1)$$

Where;

R : maximum effective length of embedded anode in concrete (m)

SSA : steel surface area in 1 m^2 of concrete surface (m^2)

CSA : concrete surface area (m^2)

In case of L-type beam, theoretical maximum effective length is 486 mm whereas the actual length is 200 mm. It means the distance between anodes in L-type beam meet the maximum effective length of embedded anode in concrete.

8.8.6 Cathodic Protection Criteria for Concrete Structure

As briefly, if the testing result compared to cathodic protection criteria for concrete structure [8.19], thus;

Current Needed

Since diffusion of oxygen is very low for concrete, 0.2 to 2 $\mu A/cm^2$ current is sufficient for cathodic protection. Based on this criteria, anode embedded in S-type and L-type fulfil the current criteria needed to protect the steel bar from corrosion.

-770 mv Criterion

Generally accepted cathodic protection potential criterion, that is, -850 mV based on copper/copper sulphate (CSE) reference electrode, is taken as -770 mV for protection of reinforced concrete structure. Based on the on potential and instant-off potential of tensile-rebar, anodes polarize the rebar in L-type beam to protection level.

100 mV Polarization Shift

Based on this criterion, concrete steels must be cathodically polarized for at least 100 mV in the negative direction. In other words, the difference between the equilibrium potential and the potential measured right after the current is cut off should be at least 100 mV. Based on the depolarization test results, it was observed that potential of some steel bars in patch repair of L-type beam exceed 100 mV of cathodic protection criteria at 28 day. It means anode effective to protect the steel bar only in the patch repair area.

8.8.7 Service Life of Anode

Fig 8.37 and **Fig 8.38** show about the actual position of anode embedded in S-type beam and L- type beam and service life of anode as well. The figures show that the number of anode in L-type beam are three-anode per each steel bar. Meanwhile, there was one-anode embedded in S-type beam.

Based on the initial mass of zinc anode and initial current flow from anode to steel bar, the service life of anode time-dependently is calculated. There was increasing of anode life which embedded in S-type beam up to 14 days of polarization time. However, it was decreased gradually with the function of time.

Meanwhile, service life of anodes embedded in L-type beam increased gradually with the function of time. In addition, up to 28 days of polarization time, one-anode (CP-5) in L-type beam reached at peak around 10 years of service life. It means, service life of anode is increased by increasing the number of anode embedded in patch repair concrete.

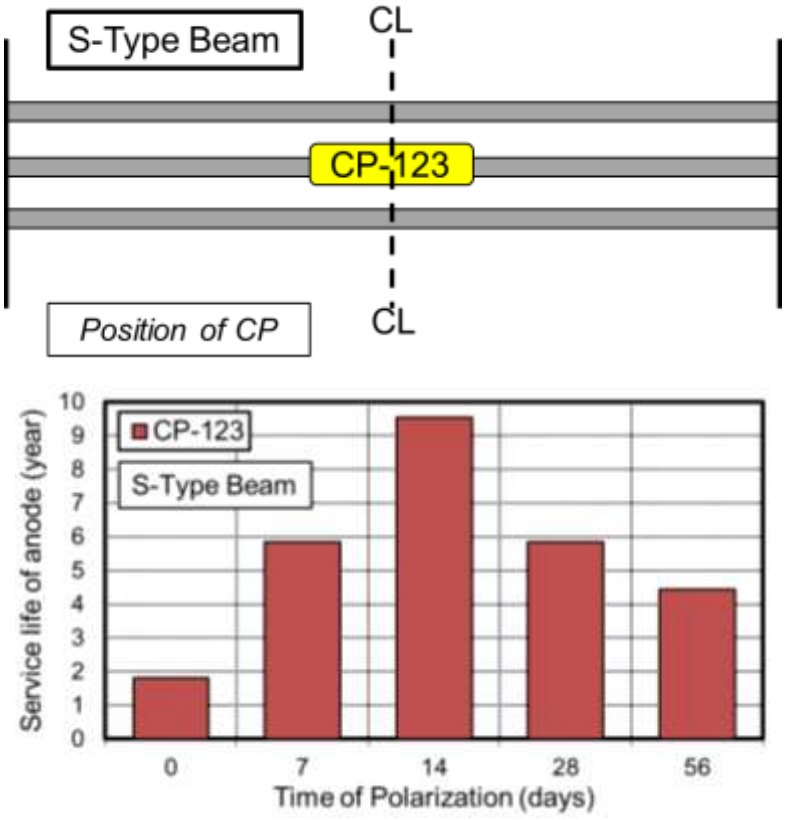

Fig 8.37 Actual position and service life of anode embedded in S-type beam

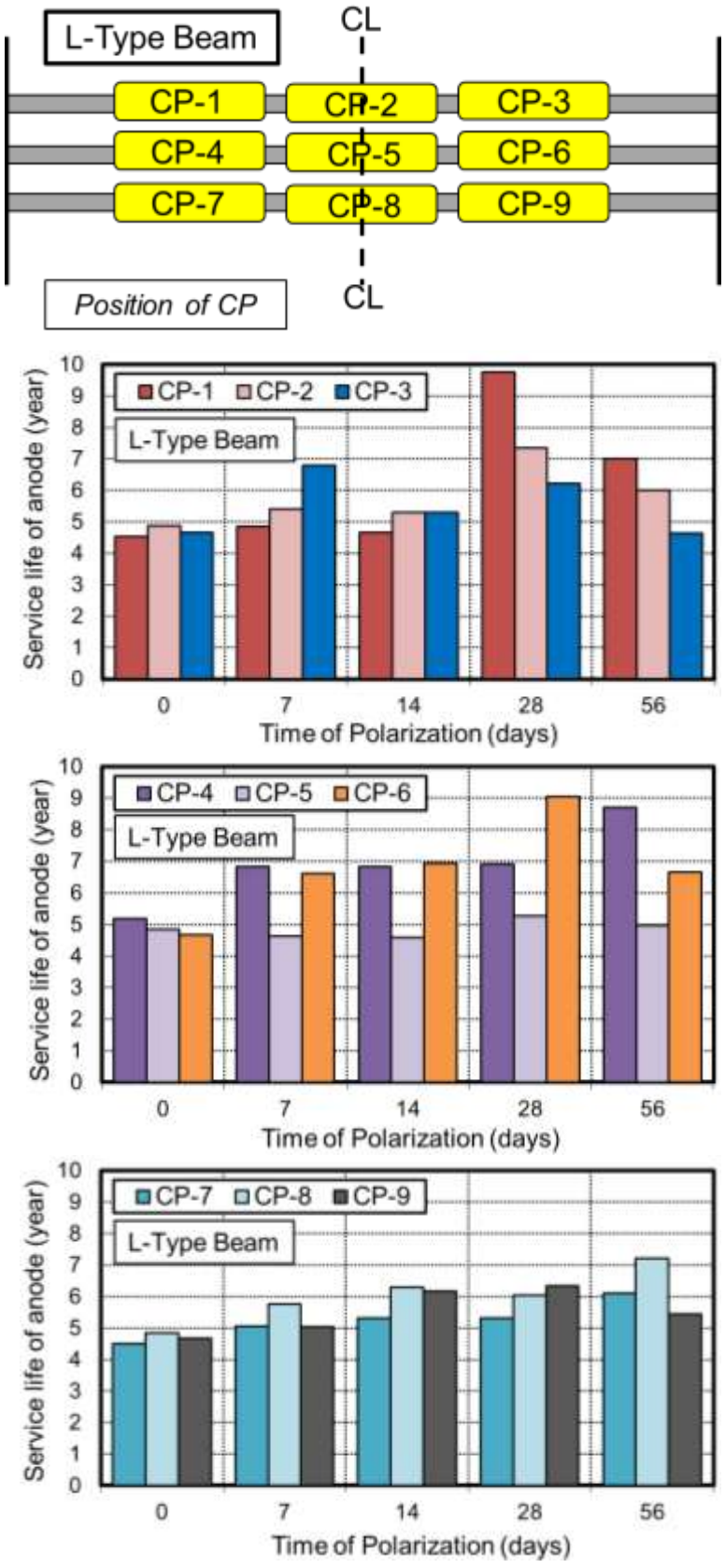

Fig 8.38 Actual position and service life of anode embedded in L-type beam

8.9 Conclusions

This study has presented the application of sacrificial anode to repair 40-year deteriorated RC beam. After around 40 years in exposure site, some conclusions can be drawing regarding corrosion assessment as following:

1. Based on visual inspection results, there was no significant degradation for RC beams of concrete with 3 cm and 5 cm of cover thickness after 40 years of exposure.
2. The concrete of RC beams with 3 cm and 5 cm of cover thickness show medium good condition after 40 years of exposure from the view point of UPV result.
3. For corrosion mapping by half-potential value on both of RC beams, the result shown that the potential more positive on tensile rebar position compare than on tension rebar. It is because the surface of tensile rebar already cover by rust and difficult to obtain the exact potential of rebar. This rust occurs due to the crack on tensile rebar position.

Furthermore, after repair by sacrificial anode cathodic protection during 56-day of polarization time, some conclusions can be drawing regarding corrosion assessment as following:

1. The test results demonstrate that anodes embedded in S-type and L-type beams fulfill the current criteria needed to protect the steel bar from corrosion, 0.2 to 2 $\mu A/cm^2$. However, due to the high resistance in repair concrete, a trans-passive region occurs on the interfacial zone between the patch repair concrete and parent concrete.
2. With respect to the potential value and conditions on the boundary, it was observed that there was no protection at all in the non-repaired section in S-type and L-type beam.
3. Based on 100 mV decay criterion, it was found that applying three anodes at intervals of 200 mm in patch repair concrete is sufficient to polarize one steel bar in the patch repair section only to the protection level.
4. The life-extension of existing structures is enhanced by increasing the

number of anodes embedded in repair concrete.

5. Polymer concrete, casting them in repair sections when anodes are applied inside is less effective.

References

8.1 Troconis de Rincon, O., et al, “Environmental Influence on Point Anode Performance in Reinforced Concrete,” Construction and Building Materials, 22, 2008, pp. 494-503.

8.2 Christodoulou, C., Glass, G. K., Webb., et al, “Evaluation of Galvanic Technologies Available for Bridge Structures”, Structural Faults and Repair, 12th International Conference, Edinburgh, UK, 2008, p.11.

8.3 Watanabe, H., Hamada, H., Yokota, H., and Yamaji, T., “Long Term Performance of Reinforced Concrete under Marine Environment (20 Year of Exposure Test)”, 3rd International Conference on Concrete under Severe Condition, Vancouver, Canada, 2001, pp. 530 – 537.

8.4 EN 12696, “Cathodic Protection of Steel in Concrete,” European Standard, 2000.

8.5 Dugarte, M. J. and Sagues, A. A., “Sacrificial Point Anode for Cathodic Prevention of Reinforcing Steel in Concrete Repairs: Part 1 – Polarization Behavior,” Corrosion, NACE International, Houston, 70(3), 2014, pp. 303-317.

8.6 Otsuki, N., “A Study of Effectiveness of Chloride on Corrosion of Steel Bar in Concrete,” Report of Port and Harbor Research Institute (PHRI), Japan, 1985, pp. 127-134.

8.7 ASTM C 876-95, “Standard Test Method for Half-cell Potentials of Uncoated Reinforcing Steel in Concrete,” Philadelphia: American Society of Testing and Materials, 1999.

8.8 G.K. Glass, B. Reddy L.A. Clark, “Making reinforced concrete immune from chloride corrosion” , Proceedings of the Institution of Civil Engineers, Constr. Mater, 160, 2007, pp. 155‑164.

8.9 Y. Schiegg, M. Büchler, M. Brem, “Potential mapping technique for the detection of corrosion in reinforced concrete structures: Investigation of parameters influencing the measurement and determination of the reliability of the method”, Mat. And Corr. 60, 2009, pp. 79‑86.

8.10 G. K. Glass, N. R. Buenfeld, Chloride - induced corrosion of steel in concrete, Prog. Struct. Eng. Mater. 2, 2000, pp. 448‑458.

8.11 D.R. Morgan, Compatibility of concrete repair materials and systems, Constr. Build. Mater. 10 (1996), pp. 57‑67.

8.12 Concrete Society, Technical Report 22, Non-structural cracks in concrete, Surrey, UK, 2010.

8.13 Concrete Society, Technical Report 54, Diagnosis of deterioration in concrete structures, Surrey, UK, 2000.

8.14 L. Bertolini, M. Gastaldi, M.P. Pedeferri, P. Pedeferri, T. Pastore, Proceedings of the International Conference on Corrosion and Rehabilitation of Reinforced Concrete Structures, Orlando, USA, 1998.

8.15 S. Qian, D. Qu, G. Coates, Galvanic coupling between carbon steel and stainless steel reinforcements, Can. Metall. Q. 45, 2006, pp. 475-484.

8.16 G K Glass, N Davison, A C Roberts, Hybrid corrosion protection of chloride-contaminated concrete, Proceedings of the Institution of Civil Engineers, Constr. Mater. 161, 2008, pp. 163‑172.

8.17 L. Bertolini, M. Gastaldi, M.P. Pedeferri, P. Pedeferri, T. Pastore, Proceedings of the International Conference on Corrosion and Rehabilitation of Reinforced Concrete Structures, Orlando, USA, 1998.

8.18 Denka Guideline for Galvashield XP

8.19 Cicek, V., “Cathodic Protection: Industrial Solutions for Protecting Against Corrosion”, John Willey & Sons, Inc., 2013.

8.20 Hobbs, D. (2001). “3rd Concrete deterioration: causes, diagnosis, and minimising risk”. In: International Materials Reviews 46.3, pp. 117–144.

8.21 Bertolini, L., Elsener, B., Pedeferri,P., Redaelli, E., and Polder, R., “Corrosion of Steel in Concrete”, 2013, Wiley-VCH Verlag GmBH & Co KGaA.

8.22 RILEM Technical Committee 124-SRC, P. Schiessel (ed), “Draft Recommedation for Repair Strategies for Concrete Structures Damaged by Reinforcement Corrosion”, Materials and Structures, 1994, Vol. 27, pp. 415 – 436.

8.23 Bennet, J., and Turk, T., “Criteria for the Cathodic Protection of Reinforced Concrete Bridge Elements”, Technical Alert, SHRP-S-359, 1994.

8.24 Pedeferri, P., “Cathodic Protection and Cathodic Prevention”, Construction and Building Materials, 1996, Vol. 10, No. 5, pp. 391-402.

8.25 Bennet, J., and McCord, W., “Performance of Zinc Anodes Used to Extend the Life of Concrete Patch Repairs”, 2006, Corrosion/2006, NACE International, Paper No. 06331.

8.26 Sergi, G., and Page, C., “Sacrificial Anodes for Cathodic Prevention of Reinforcing Steel around Patch Repairs Applied to Chloride-contaminated Concrete”, European Federation of Corrosion Publications.

Chapter 9 CONCLUSIONS AND FUTURE RESEARCH WORK

9.1 Conclusions

Among the challenges that are still to be taken up in CP system embedded in concrete, some issues were address in this study in order to observe durability and effectiveness of zinc sacrificial anode to increase life-extension of RC structure. Conclusion for each test is concluded in details as follows:

Chapter 3 investigates the deterioration condition of one 77-year-old RC structure, namely an Indonesian port, exposed to severe marine conditions. Field surveys and experimental research by destructive and non-destructive methods were conducted to evaluate the long-term performance of this Indonesian port. Repair strategies for extending the service life of this structure are also presented in this study. The inspection results showed that this Indonesian port's structure, which was exposed to a tropical marine environment over a long period of time, led to serious damage conditions by chloride-induced corrosion. The main damage included broad delamination, spalling, cracking and loss of cross-section of steel reinforcement. The use of a cathodic protection (CP) system as an immediate reactive repair method was proposed as a sustainable long-term remedial option.

Chapter 4 discusses how to identify the effective length of an embedded steel element on partially-repaired concrete protected by sacrificial anodes

against macro-cell corrosion in a non-homogeneous chloride environment. Zinc sacrificial anodes were applied to steel bars embedded in patch repair concrete (non-chloride contamination) in order to deliver protective currents to corroding steel in the parent concrete (with chloride contamination). Based on the criterion of 100 mV CP, zinc sacrificial anode cathodic protection could protect the steel bar at a distance of between 300 mm to 400 mm from the anode's position in the patch repair concrete to the parent concrete with 4 kg/m^3 of chloride content at 350 days of polarization time. Meanwhile, for 10 kg/m^3 chloride content in existing concrete, the applied anode was effective in protecting the steel bar at a distance of up to 260 mm from the patch repair concrete to parent concrete. This means that, for up to one year of exposure time, the higher the chloride content in the existing concrete, the shorter the effective length. Meanwhile, after 2 years of exposure time, commercially available sacrificial anodes are still powerful enough to protect the corroding steel at a distance of up to 260 mm from the anode in the patch repair concrete to the parent concrete.

Chapter 5 presents the effects of steel surface conditions (rusted and non-rusted) on the performance of a zinc sacrificial anode when applied to patch repair concrete (non-chloride contamination). In addition, a study was carried out on how environmental conditions affect the durability of anodes when installed on rusted and non-rusted steel bars. The results of this study show that the protective current of the anode became more active in humid conditions than in dry conditions, due to the high moisture content inside the concrete. Based on the "100 mV decay" CP criterion, protective conditions were achieved on the steel bars connected to a zinc anode with "non-rusted" as an initial condition. Rust on steel surfaces decreases the efficacy of cathodic protection, even if it's embedded in chloride-free concrete, because the rust on the steel bar impedes the current flow from the anode to the steel bar when a zinc anode is applied on it. In conclusion, to protect corroded steel bars in existing concrete (with chloride contamination), a non-rusted rebar condition in the repair concrete (non-chloride contamination) is the most desirable initial condition when a zinc anode is applied.

Chapter 6 investigates the performance of zinc sacrificial anodes to protect steel bars embedded in concrete (chloride and non-chloride contamination) from corrosion under two extreme ambient conditions, namely, freezing temperatures (-17°C, RH 4-5%) and extreme heat (40°C, RH 96-99%). With respect to the protective current density under exposure to high temperatures and after take-out from a hot chamber, it was shown that anodes produce higher levels of current in hot or humid environments, compared to dry and low-temperature conditions. Moreover, anodes age faster in high temperatures than in freezing conditions. It was found that, the higher chloride content in concrete, the higher the possibility of corrosion occurring on steel bars without CP protection which are exposed to freezing temperatures as well as heat. It can be concluded that using anodes in environments of high chloride content with exposure to heat and high humidity is ineffective.

Chapter 7 presents an estimate of the service life of zinc sacrificial anodes (in a short amount of time) by accelerating the current 10 (ten) times higher than initial current of the anode during a polarization time of 70 days. It was possible to predict over 100 years of the service life of zinc sacrificial anodes exposed to air curing conditions at a constant room temperature. By increasing the current demand by 10 times, the service life of anodes is reduced 10 times after 70 days of exposure. This means that the higher the current delivery function of the anode, the shorter the service life becomes. All in all, the current acceleration method enabled us to successfully observe anodic service life in a short time.

Chapter 8 presents the application of zinc sacrificial anodes to repair 40-year old deteriorated RC beams. Two types of deteriorated RC beams, notably the S-type (150x300x2400 mm) and the L-type (200x300x2400 mm), were evaluated in this study.

After around 40 years in exposure site, some conclusions can be drawing regarding preliminary corrosion assessment as following:

1. Based on visual inspection results, there was no significant degradation for

RC beams of concrete with 3 cm and 5 cm of cover thickness after 40 years of exposure.

2. The concrete of RC beams with 3 cm and 5 cm of cover thickness show medium good condition after 40 years of exposure from the view point of UPV result
3. For corrosion mapping by half-potential value on both of RC beams, the result shown that the potential more positive on tensile rebar position compare than on tension rebar. It is because the surface of tensile rebar already cover by rust and difficult to obtain the exact potential of rebar. This rust occurs due to the crack on tensile rebar position.

Furthermore, after repair by sacrificial anode cathodic protection during 56-day of polarization time, the test results demonstrate that anodes embedded in S-type and L-type beams fulfill the current criteria needed to protect the steel bar from corrosion, 0.2 to 2 $\mu A/cm^2$. However, due to the high resistance in repair concrete, a trans-passive region occurs on the interfacial zone between the patch repair concrete and parent concrete. With respect to the potential value and conditions on the boundary, it was observed that there was no protection at all in the non-repaired section. This coincides with the depolarization test result. Based on the "100 mV decay" CP criterion in the depolarization test, it was found that applying three anodes at intervals of 200 mm in patch repair concrete is sufficient to polarize one steel bar in the patch repair section only to the protection level. This means that while the life-extension of existing structures is enhanced by increasing the number of anodes embedded in repair concrete and polymer concrete, casting them in repair sections when anodes are applied inside is less effective.

From the testing results from Chapter 4 to Chapter 8, it can be concluded some repair interventions for increase the service life of structure in Chapter 3, notably:

- Patch concrete can apply to repair the concrete but accelerate macro-cell corrosion and structure damage faster.
- Rust on the steel surface must be clean first before anode applied on it.
- Zinc sacrificial anode can applied to repair deteriorated steel bar by install

the anode per 200 mm in distance.

- By consider the severe condition of embedded steel bar, anode can extending the service life of deteriorated RC structure maximum 8 years.

9.2 Future Research Work

In order to develop the CP system, several future research works are recommended to establish the CP design applicable for steel bar in concrete, notably for zinc sacrificial anode system, as follows:

1. Regarding to the criteria and service life design of these systems in the real structures, is still unclear and need to be undertaken. Thus, advanced research on the anode materials is necessary to ensure the service life extend of structures, notably:
   - Effect of temperature on potential of steel bar by embedded the reference electrode inside the concrete
   - Effect of high temperature, low temperature and wet-dry condition on service life of anode by acceleration current
   - Effect of ordinary Portland cement as patch repair material on RC beam
2. Due to many factors were found in adjusting the protection level, future investigation is necessary on the actual deteriorated structures, as a reference to confirm the research results carried out in the laboratory.